NMR Spectroscopic Investigations

of Transition Metal-Catalyzed Addition Reactions

Dissertation

zur Erlangung des Doktorgrades der Naturwissenschaften

(Dr. rer. Nat)

an der Fakultät für Chemie und Pharmazie

der Universität Regensburg

Vorgelegt von

Felicitas von Rekowski

Aus Füssen

2014

Die vorliegende Dissertation beruht auf Arbeiten, die zwischen Januar 2010 und Mai 2014 im Arbeitskreis von Professor Dr. Ruth M. Gschwind am Institut für Organische Chemie der Universität Regensburg durchgeführt wurden.

Promotionsgesuch eingereicht am: 16.05.2014

Die Arbeit wurde angeleitet von: Prof. Dr. Ruth M. Gschwind

Promotionsausschuss:

    Vorsitzender: Prof. Dr. Alkwin Slenczka

    1. Gutachter: Prof. Dr. Ruth M. Gschwind

    2. Gutachter: Prof. Dr. Axel Jacobi von Wangelin

    3. Gutachter: Prof. Dr. Arno Pfitzner

Des is wia bei jeda Wissenschaft,

am Schluss stellt sich dann heraus,

das alles ganz anders war.

Karl Valentin

1882-1948

In liebevoller Erinnerung an Mounir († 02.09.2013)

Abbrevations

°C	Degree Celsius
1D, 2D	One and two dimensional
AAA	Asymmetric Allylic Alkylation Reaction
ACA	Aasymmetric Copper catalyzed conjugate addition reaction
Ar	Aryl
BINAP	2,2'-Bis(diphenylphosphino)-1,1'-binaphthyl
BINOL	1,1'-Bi-2-naphthol
Bu, ^{t}Bu	Butyl, *tert*-Butyl
CA	Conjugate addition
CA	Conjugate addition
cm	Centimeter
cod	1,5-Cyclooctadiene
COSY	Correlated Spectroscopy
CSA	Chemical shift anisotropy
Cy	Cyclohexenone
DABCO	1,4-diazobiclyclo[2.2.2]octane
DBU	1,8-Diazabicyclo[5.4.0]undec-7-ene
DFT	Density Functional Theory
diob	*O*-Isopropyliden-2,3-dihydroxy-1,4-bis(diphenylphosphino)butane
DMSO	Dimethyl sulfoxide
DOSY	Diffusion Ordered Spectroscopy
dppb	1,4-Bis(diphenylphosphino)butane
dppe	1,2-Bis(dipheynlphosphino)ethane
ee	Enantiomeric excess
eq, equiv.	Equivalents
ESI-MS	Electrospray Ionization Tandem Mass Spectrometry
ESR	Electron Spin Resonance Spectroscopy
Et	Ethyl
et al.	et alii, "and others" (lat.)
GC	Gas chromatography
h	Hour
HMBC	Heteronuclear Multiple Bond Correlation
HSQC	Heteronuclear Single Quantum Coherence

IR	Infrared Spectroscopy
K	Kelvin
kJ	Kilo Joule
Me	Methyl
mg	Milligram
MHz	Megahertz
ml	Milliliter
mm	Millimeter
mM	Millimolar
mmol	Millimol
NMR	Nuclear Magnetic Resonance
NOE	Nuclear Overhauser Effect
NOESY	Nuclear Overhauser Enhancement Spectroscopy
Ph	Phenyl
ppm	Parts per million
RT	Room temperature
S/N	Signal to noise ratio
SI	Supporting Information
T_2	Transversal relaxation time
TADDOL	$\alpha,\alpha,\alpha',\alpha'$-tetraaryl-2,2-dimethyl-1,3-dioxalane-4,5-dimethanol
TC	Thiophenecarboxylate
THF	Tetrahydrofuran
TMS	Trimethylsilane
Tol-BINAP	2,2'-Bis(di-p-tolylphosphino)-1,1'-binapthyl

Table of Contents

1 INTRODUCTION AND OUTLINE

The past decades have brought an increasing demand for enantiopure compounds, not only in the field of fine chemicals, as used for agrochemicals or natural product synthesis, but also in material sciences. In order to cover this increased requirement the use of enantioselective catalysis emerged as a very powerful tool, the main advantage is the use of cheap and prochiral starting materials. Nowadays, modern asymmetric catalysis is based on enzymatic catalysis, metal catalysis and organocatalysis. Thereby the remarkable importance of transition metal catalysis is obvious for the last years, as nine pioneering scientist were awarded the Nobel Prize in Chemistry since 2001 (2001 W. S. Knowles, K. B. Sharpless and R. Noyori for "catalytic asymmetric synthesis", 2005 Y. Chauvin, R. H. Grubbs and R. R. Schrock for the "development of the metathesis method in organic chemistry" and 2010 R. F. Heck, E. Negishi and A. Suzuki for "palladium-catalyzed cross couplings in organic synthesis"). Copper is one of the metals of choice in organometallic chemistry, and also the use in enatioselective reactions increases since the late 1990s. However, only little information of the involved structures and mechanisms is avaiblabe, as the spectroscopic investigation of copper complexes in solution is a very challenging research area. Based on the different magnetic properties of Cu(I)/Cu(III) and Cu(II) various spectroscopic methods are needed. Especially NMR spectroscopic investigations are often limited to the NMR active nuclei of the ligand or substituents of the copper complexes, due to the high quardupole moment of copper. Therefore direct $^{63/65}$Cu NMR spectroscopy is only applicable in highly symmetric complexes, which is usually not given in synthetically relevant copper complexes. Furthermore, copper complexes tend to form self-aggregates, the existence of intra- and interligand exchange processes leading to averaged sets of signals for free and complexed ligands, their chemical shifts differ often not significantly and a high sensitivity to the used synthetic parameters is known. These structural properties reduce the applicability of the classical NMR spectroscopic approach used for small molecules to copper complexes. Nevertheless, some structural insight to precatalytic copper complexes was already observed by the combination of diffusion ordered spectroscopy and the classical NMR approach. The best investigated copper systems are up to now organocuprates, which often represent a model system for mechanistic studies, in contrast for catalytic copper systems only little information is accessible. Upon the variety of possible chemical transformations the enantioselective copper-catalyzed conjugate addition reaction emerges as a very powerful and widely applied method for the formation of highly selective carbon-carbon bonds. Recently, impressive results were

achieved in the expansion of the copper catalytic system, by developing further classes of ligands, testing various copper sources and reaction conditions, and moreover in the applicability of substrates and organometallic reagents. However a detailed understanding of asymmetric transition metal-catalyzed reactions is necessary in order to optimize existing techniques and to create new catalyst systems adjusted to associated conditions and requirements.

Despite the importance of the understanding of the involved structures only few studies addressing the structure elucidation of the precatalytic complexes or the catalytically active species are known. In chapter 2 exemplarily three prominent NMR spectroscopic investigations are described. Thereby the structure of precatalytic phosphoramidite copper complexes and the structure of TADDOL-based thiolate copper complexes are addressed, as well as the reactivity of ferrocenyl-based diphosphine copper complexes in addition reactions of Grignard reagents.

In chapter 3 NMR spectroscopic investigations on the mechanism of the powerful copper-catalyzed conjugate addition reaction of diorganozinc reagents to α,β-unsaturated substrates are described. Thereby phosphoramidite copper complexes were used as model systems, with which in previous investigations a binuclear copper complex with mixed trigonal/tetrahedral coordination on the copper atoms was identified as precatalyst. With these precatalytic structure in hand a unique structural access to the next step in the proposed mechanism – the transmetalation, representing the transfer of the organic residue of the organometallic reagent to the binuclear copper precatalyst – is expected. For the first time a direct experimental evidence for transmetalation intermediates was observed. Therefore modified 1D $^{1}H^{31}P$-HMBC spectra were applied in order to differentiate between transmetalated ethyl groups and unspecific interactions. For the structure identification a special $^{1}H^{31}P$-HMBC approach was used, by comparing the spectra of enantiopure and enantiomeric mixtures of the ligands for complex formation, enabling a differentiation of the species by the number of ligands coordinated. The experimental results reveal that apart from monomeric transmetalation intermediates also a dimeric transmetalation intermediate appears (this deviates from previous results of Feringa and contradicts previous proposals of Woodward), both are below the detection limit of one-dimensional ^{1}H and ^{31}P NMR spectra. Further, in the dimeric transmetalation intermediate retention of the coordination of the copper atoms was observed and this species is supposed to be the catalytically active one.

Chapter 4 deals with the structure elucidation of precatalytic phosphoramidite copper complexes in coordinating solvents, as it is known that the structure of copper complexes is

influenced by the parameters and conditions used. With help of spectra simulations and detailed integral analysis of temperature dependent ligand distributions a polynuclear copper complex with four CuX**L₂** and one CuX**L** fragments is proposed. Interestingly, even in the bigger complex the mixed coordination of the copper atoms is maintained, indicating a preferred formation.

Besides copper rhodium is a commonly used metal for transition metal catalysis. Furthermore rhodium complexes are easier accessible by NMR spectroscopy and might give structural insight, which can then be transferred to the copper complexes. Therefore in chapter 5 first preliminary NMR spectroscopic investigations concerning the mechanism of an unexpected rhodium-catalyzed 1,2-addition reaction of trimethylaluminum to cyclohexenone are described. However, this preliminary NMR experiments reveal several dimeric rhodium complexes, which provide an experimental foundation for further investigations, nevertheless further optimizations of the model system has to be performed.

Apart from asymmetric transition metal catalysis, the past years show tremendous advances in asymmetric organocatalytic reactions, for example in reactions catalyzed by small organic molecules. Thus chapter 6 deals with an unprecedented organocatalytic formation of enynes by the dimerization of nitroalkenes, the substrate scope and partially a mechanism for this reaction was proposed. This reaction can also shed light on processes observed in transition metal catalyzed reactions, as nitroalkenes are also suitable substrates in the copper-catalyzed 1,4-addition reactions of trialkylaluminum reagents.

In general, the direct experimental detection of transmetalation intermediates delivers not only a new NMR spectroscopic approach for the detection of intermediates close to or below the detection limit in one-dimensional spectra, but might also contribute to the broad field of metal catalysis and synthesis with organometallic reagents.

2 NMR SPECTROSCOPIC ASPECTS*

Felicitas von Rekowski, Carina Koch, Ruth M. Gschwind

This chapter was prepared in close cooperation with Carina Koch. The section about copper complexes of ferrocenyl-based ligands (Chapter 2.4) was written by Carina Koch.

2.1   Introduction

The NMR spectroscopic investigation of copper complexes in solution is a challenging research area. Due to the different magnetic properties of Cu(I)/(III) and Cu(II) systems, varying spectroscopic methods are necessary for their structure elucidation. For paramagnetic Cu(II) complexes electron spin resonance (ESR) spectroscopy is applied, while for diamagnetic Cu(I)/(III) complexes high resolution NMR spectroscopy is the method of choice.[1]

Though the two NMR spectroscopic active Cu isotopes ([63/65]Cu) have a quite high natural abundance and gyromagnetic ratios similar to ^{13}C, the scope of [63/65]Cu NMR spectroscopy is limited by their high quadrupole moment.[2] Due to this magnetic property of copper, it is only possible to detect a copper signal if very small electric field gradients are present at the copper nucleus, which occur mainly in highly symmetric complexes with a tetrahedral coordination on Cu.[3,4] In such symmetric complexes it is possible to get structural information about the π-acceptor properties of the ligand, the complex geometry or ligand exchange processes. The π-acceptor properties of copper bound ligands or vice versa the electron donating effects of copper to these ligands can be measured by [63]Cu NMR. This is possible, because the [63]Cu chemical shifts are mainly determined by the back-donation of electrons of the copper *d* orbitals to the ligands.[5,6] Information on the symmetry of the complex and also ligand exchange processes are obtainable from the line widths of the [63]Cu signal and its temperature dependency. In contrast the [63/65]Cu signals of complexes with reduced symmetry appear extremely broad or even undetectable due to fast relaxation processes. The synthetically relevant copper complexes are normally less symmetrical and therefore to the best of our knowledge direct [63/65]Cu spectroscopy have not been used for the structure elucidation in asymmetric copper catalyzed reactions. Therefore, NMR structural investigations are limited to NMR active nuclei of the ligands or substituents. In addition common structural properties of copper complexes are challenging features for NMR spectroscopists. For example copper complexes are known to tend to self-aggregation, resulting in dimeric, oligomeric or polymeric supramolecular complexes, which hampers the application of classical NMR spectroscopic methods. Additionally, in such partially highly symmetric complexes ligand exchange processes exist, which could either be intramolecular between the ligands themselves, or intermolecular between different complex species leading to averaged sets of signals. Furthermore often very similar ^{1}H chemical shifts occur for the free ligands and their complexes. From synthetic and spectroscopic studies it is known, that these complex structures are very sensitive towards the solvent, salt effects and the used ligand. Due to this sensitivity it is difficult to propose a general structural model for all reactions; thereby the structure among various experimental conditions

has to be examined separately. All these structural properties of the copper complexes are limitations for the applicability of the classical NMR spectroscopic approach for small molecules, especially for the structure elucidation of the precatalytic complexes in copper catalyzed reactions. Moreover for such sensitive structural equilibriums as known for the copper complexes, the structures in solution are not necessarily identical with the crystal structures. Therefore a structure determination in solution, including aggregation numbers and aggregate size, is necessary for each of these variable systems.[1] Despite all these limitations it is possible to get some insight into the structures of copper complexes especially with a combination of classical NMR spectroscopic methods and diffusion ordered spectroscopy (DOSY).[1,7]

Due to the spectroscopic properties of copper and the difficulties in the investigation of copper complexes only few studies dealing with structure elucidation are known. Investigations concerning the mechanism or catalytic cycle are often based on organocuprates as model system, which are the best investigated copper systems so far. However, these systems are already described in several reviews[1,8–13] and therefore are not addressed. In this chapter we concentrate on NMR spectroscopic investigations of Cu complexes used in enantioselective catalysis. We selected exemplarily three prominent NMR spectroscopic investigations out of the few available studies dealing with the structure elucidation of the catalytically active species or the precatalytic complexes. Firstly we report about a catalytic system consisting of phosphoramidite ligands and a copper(I) salt. On the one hand this systems represents the most extensive investigation on the precatalytic system, on the other hand the use of a monodentate class of ligands is described. Furthermore the structural NMR spectroscopic approach is presented. For this system a binuclear mixed trigonal/tetrahedral complex structure was identified as new structural motif for the precatalytic complexes. Next, a study using TADDOL-based thiolate ligands in combination with CuCl is presented. There the first study based on diffusion ordered spectroscopy (DOSY) was performed and in contrast to the phosphoramidite ligands a bidentate class of ligands is used. With this system a tetranuclear complex structure was identified as active catalyst. In this case the normally bidentate TADDOL-derived ligands act as monodentate ligands. At least the application of ferrocenyl-based ligands in the copper catalyzed conjugate addition reaction with Grignard reagents is described. With this system the first detailed transmetalation study until now has been presented and in contrast to the other studies, which combine mainly NMR spectroscopy and X-Ray analysis, a variety of analytical methods was used. In this study a mononuclear complex structure was identified as the active transmetalation intermediate. In addition, a brief insight into the occurring structures of the asymmetric allylic alkylation with ferrocenyl-based ligands and Grignard reagents is given. Beside

this three structure elucidations also further investigations were done by ESR spectroscopy,[14] theoretically calculations,[15] kinetic studies with an early observation of non-linear effects[16] and also on further classes of ligands.[17,18] But a comprehensive coverage of all these methods is far beyond the scope of this chapter.

2.2 Copper Complexes with Phosphoramidite Ligands

The enantioselective C-C-bond formation is one of the most important reaction types among the high number of organic transformations. A very powerful method for this reaction is the asymmetric copper catalyzed conjugate addition (ACA) reaction. The advantages of this reaction are the high compatibility with many functional groups, low costs of the copper salts and excellent regio- and enantioselectivities. Recent efforts enable to enlarge the scope of substrates and nucleophiles, in order to increase the synthetic application for more complex molecules, like biologically active and natural compounds (for recent reviews see [19–22]). A very powerful class of ligands, not only in the ACA, but also for many other reactions,[23] are phosphoramidite ligands, because they are a low-priced and easily accessible class of ligands which enables high yields and *ee* values. Their electronic properties can be controlled by different substituents on the oxygen or nitrogen atom, therefore a fine-tuning for specific catalytic applications is possible. Furthermore the chiral diol or amine moiety can be used as source for stereodiscrimination of the desired catalytic system, like matched or missmatched effects.[23] In contrast to the broad application range of the ACA in synthesis, structural and mechanistic information on the copper complexes and their intermediates a very rare.[24–26] Although these information are essential prerequisites for further developments on this types of reactions.[19,21,23] Therefore this chapter provides a literature survey of known NMR studies dealing with this topic.

2.2.1 Precatalytic Copper Complexes

2.2.1.1 Structure Determination

The first and very important step of each structural investigation is to select a system among the synthetically applied one, which is suitable for NMR spectroscopic investigations. In synthetic applications Cu(I) and Cu(II) salts are appropriate copper sources, because the Cu(II) salts are completely reduced during the reaction by the organometallic reagent.[14] In contrast to synthesis only Cu(I) salts are suitable for NMR spectroscopic investigation of the precatalytic system, because Cu(II) is paramagnetic and no reducing agent is present in the precatalytic system. A further prerequisite for successful structure elucidation are sharp and well separated signals of the examined system.

In 2006 Gschwind *et al.* were able to identify a binuclear Cu(I) complex with mixed trigonal/tetrahedral stereochemistry as new structural motif for the precatalytic copper complex **C2** (Figure 2.1 a).[27]
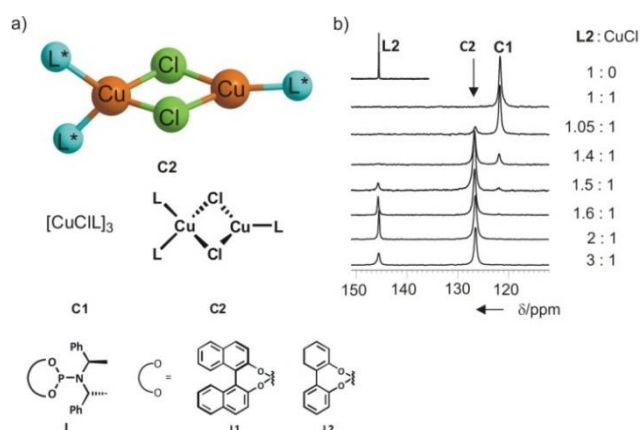
Figure 2.1: a) Schematic drawing of the binuclear copper complex **C2** with mixed trigonal/tetrahedral coordination site on copper and of the 1:1 complex **C1**[28] and the highly selective phosphoramidite ligands **L1** and **L2**; b) ^{31}P NMR spectra of **L2** and mixtures with CuCl at varying ratios in CDCl$_3$ at 220 K.[27]

For this study **L1** and **L2** were selected (see Figure 2.1a), because they give high selectivities and represent the binaphthol- and biphenol-based ligands introduced by Feringa and Alexakis.[16,29] They were spectroscopically investigated with different copper salts, ligand to salt ratios and solvents.[27,28] As described above sufficient signal distribution is necessary, here about 20 ppm for free ligand and complexes, which was obtained in dichloromethane with a ligand to salt ratio of 2:1,[27] corresponding well to synthetic applications.[16,30,31] Also in chloroform, it is possible to receive relatively sharp, separated signals for complexes **C1** and **C2** at 230 K. For **C2** only one averaged ^{31}P signal is observed for all three ligands, because of a fast ligand exchange within the complex at 230 K. Using other solvents like THF or toluene in combination with CuCl, broad signals occur, which indicate the existence of further complexes beside **C1** and **C2** and higher aggregates.[27] By variation of the ligand to salt ratio it was possible to determine how many ligands are involved in the complex structures of **C1** and **C2** and also the amount of each was controllable (schematic drawings shown in 2.1a). In Figure 2.1b the ^{31}P NMR spectra of **L2** and CuCl at varying ratios in CDCl$_3$ at 220 K are shown. For a 1:1 ratio or lower only **C1** occurs, while at ratios higher than 1.05:1 the signal intensity for **C2** starts to increase, while the signal for **C1** decreases. At ratios higher than 1.5:1 mainly **C2** and an increasing amount of free ligand as well as a small amount of **C1** is observed, indicating a 1.5:1 ratio of ligand to copper salt in **C2**. Unfortunately, no proton chemical shift differences were observed for nearly all proton signals of the free ligand and the complexes. Therefore the classical NMR spectroscopic approach is not applicable and it is necessary to switch to further NMR methods, like diffusion ordered spectroscopy (DOSY), which provides further information about the molecular size of the complexes. Although the signals in the ^{31}P NMR spectra are well separated it is not possible to measure ^{31}P DOSY spectra, due to rapid relaxation of the phosphorous atoms in the copper complexes, so ^{1}H DOSY experiments were performed. But the problem is that due to the

chemical shift overlap of **C1**, **C2** and free ligand only diffusion coefficients with contributions of all three species can be measured. The solution of this problem is to take advantage of the effect of dynamic NMR at temperatures close to the synthetic application. There, the difference in the internal dynamic processes within the ligand and the complexes - especially **C2** - are big enough to cause different line widths of the methine signals. By choosing a suitable pulse sequence it is possible to separate the methine signal of **C2** by eliminating the exchange broadened signals of free ligand and **C1** through a T_2 filter (here the longish convection compensating pulse sequence of Müller and Jerschow).[1,27] Thus, it was possible to determine, that in the precatalytic complex three ligands are involved. In combination with the 1.5:1 ratio it was possible to identify a binuclear mixed trigonal/tetrahedral structure for **C2**.

Because of the known sensitivity towards salt effects, the dependency of the precatalytic complex structure on the used salt was also addressed in the elucidation. Therefore Gschwind *et al.* tested four different Cu(I) salts (CuX, X = Cl, Br, I, TC). In all cases the binuclear mixed trigonal/tetrahedral structure could be identified as basic structural motif and therefore it is not an exclusive effect of chloride.[28]

2.2.1.2 Temperature Dependence

Since temperature plays a crucial role for high *ee* values, as well as for the reaction yield in copper catalyzed reactions,[24,32–36] it is essential to get an insight into temperature-dependent interconversion mechanisms of the complexes. For that reason Gschwind *et al.* prepared low-temperature NMR spectroscopic investigations. Reducing the temperature decelerates the exchange processes. At low-temperatures two ^{31}P signals are expected for the two different kinds of ligands in **C2**, which would allow confirming the structure of **C2** by classical NMR methods. In Scheme 2.1b the temperature-dependent ^{31}P NMR spectra of **L1**:CuCl and **L2**:CuI, each in a 2:1 ratio, are shown. At 180 K it was possible to identify a further complex structure **C3**, which arise from addition of free ligand **L** to **C2** (Scheme 2.1a). Furthermore, the low-temperature ^{31}P NMR spectra shows an AA'BB' scalar coupling pattern for **C3**, which is typical for slightly distorted L_2Cu fragments. In a ^{31}P,^{31}P COSY spectra the observed coupling pattern was confirmed as result of scalar coupling between the two ligands. The existence of two L_2CuX units in the dimeric complex **C3** was shown by DOSY experiments. Beside the signal for **C3** a signal splitting for **C2** at 180 K in a 2:1 ratio can be observed, which represents a slow intraligand exchange on the NMR timescale for the two different ligand groups in the mixed trigonal/tetrahedral precatalytic complex structure at low temperatures. In order to confirm the existence of these two complexes, the ^{31}P NMR spectra of **C2** and **C3** have been simulated

(Scheme 2.1c and 2.1d), superimposed (Scheme 2.1e) and compared with the experimental spectrum at 180 K (Scheme 2.1f).[37] Thus the temperature-dependent conversion of **C2** into **C3** was observed. As expected the low-temperature structures in solution approximates the solid state structure. However at reaction temperature exclusively **C2** exists, which is in in good agreement with the crucial role of the temperature on the outcome of the reaction.[24,32–36]
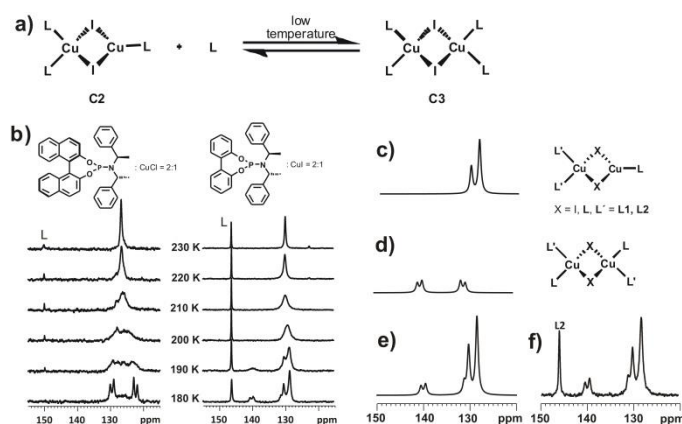
Scheme 2.1: a) Intermolecular interaction between **C2** and **L** generating **C3** at low temperatures; b) ^{31}P NMR spectra of **L1**:CuCl (left) and **L2**:CuI (right) in a 2:1 ratio at varying temperatures in CD$_2$Cl$_2$. Simulated ^{31}P NMR spectra of binuclear copper complexes with c) mixed trigonal/tetrahedral and d) tetrahedral coordination on copper, e) superposition of c and d for comparison with f) experimental spectra of **L2**:CuI (2:1) in CD$_2$Cl$_2$ at 180 K.[37]

The presented NMR study describes the first direct experimental proof for the precatalytic complex structure **C2,** which was previously only identified by DOSY NMR measurements.[37] In a DFT study of Woodward, investigating the reaction mechanism of the ACA, a mononuclear copper complex was detected as ground state of the transmetalation intermediate using a phosphoramidite ligand, copper(I) salt and ZnMe$_2$. Interestingly, after the addition of a dienone a binuclear copper complex was identified as the energetically most accessible, which enables the postulation of a possible favored reaction pathway. This binuclear complex structure is essentially identical with the determined structure of the Gschwind group.[15]

2.2.1.3 Ligand Specific Aggregation Trends

The temperature-dependent interconversion of copper complexes described above raised the question, whether this structure variation is mediated by the general properties of the phosphoramidites as ligands or if it is a particular effect of the copper complexes due to their high structural variability. Therefore, a temperature-dependent aggregation study of different phosphoramidite ligands and their transition metal complexes was performed (Figure 2.2). The ligands **L1** and **L2** were selected to represent the binaphthol- and biphenol-based ligand families introduced by Feringa and Alexakis.[16,29] For the investigation of the influence of steric effects and rotary motion on the catalysis, the smaller ligand **L3** was the ligand of choice. In order to

check the influence of different transition metals and coordination spheres in terms of complex structures and stoichiometries, transition metal complexes bearing different copper, palladium and iridium salts have been tested.
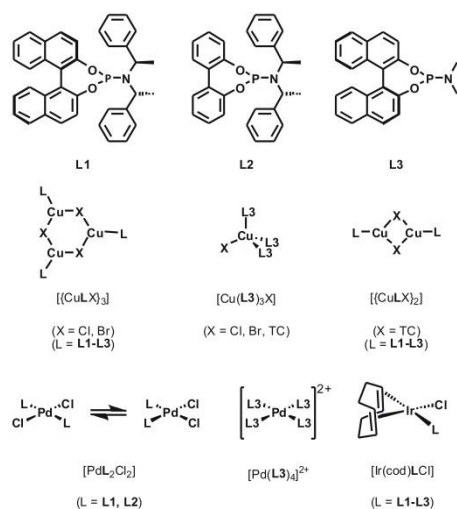
Figure 2.2: Phosphoramidite ligands **L1-L3** and different transition metal complexes investigated concerning their aggregation trends (TC = 2-thiophenecarboxylate, cod = 1,5-cyclooctadiene).[38]

The method of choice to gain an insight into the aggregation behavior of all these systems was to use temperature-dependent ^{1}H DOSY NMR spectra and to calculate the viscosity- and temperature-corrected diffusion coefficients. For all ligands and complexes used in this study baseline separated specific signals were used for the DOSY analysis. Therefore, out of the whole series of copper complexes only $[CuLX]_n$, $[Cu(\mathbf{L3})_3X]$ and two $[Cu_2L_3X_2]$ were appropriate for this study. First the aggregation trends of the free ligands were determined. At 270 K all three ligands exist as monomers and all of them show threshold temperatures, where aggregation starts. As expected the individual threshold temperatures and the slopes of the aggregation curves depend on the ligand structures.[38]

Interestingly, the aggregation trends of all transition metal complexes with the highly stereoselective ligands **L1** and **L2** show very similar behavior as the corresponding free ligands. This was found to be independent of the used transition metal, the complex structure or the complex stoichiometry. Only in the case of the smaller ligand **L3**, which shows only moderate *ee* values in catalytic application, significant different aggregation trends were observed. In conclusion a fast and simple ^{1}H DOSY NMR screening method was presented on the example of phosphoramidite ligands to predict the aggregation behavior of ligands and their transition metal complexes. Furthermore this offers a great opportunity to apply a fast and simple method for the optimization of catalytic reaction conditions - especially temperature - via ^{1}H DOSY NMR spectroscopy.[38] This shows, that in case of the highly stereoselective phosphoramidite ligands

the aggregation trend of the copper complexes as well as other transition metal complexes is mainly influenced by the ligand properties.

2.2.2 Phosphoramidite Trialkylaluminum Interactions

The first step in the proposed mechanism of the ACA is the transmetalation step, where an alkyl or aryl moiety from the organometallic reagent is transferred to the precatalytic complex.[28] The spectroscopic proof for such a transmetalation product is very difficult to achieve. The only extensive example for a detected transmetalation product via NMR spectroscopy is published by Feringa with ferrocenyl-based ligands in the addition reaction of Grignard reagents (Chapter 2.4.1).[25] For the ACA with phosphoramidite ligands no transmetalation studies are published until now, potential organometallic reagents are ZnR_2 and AlR_3. The only NMR spectroscopic study about interactions of phosphoramidite ligands with $AlMe_3$ was published by Alexakis *et al.* in 2006 with dichloromethane as solvent.[39] After the addition of $AlMe_3$ the ligand signal for **L1** disappears in the ^{31}P NMR spectra and a new signal at 35 ppm appears. The workup of the mixture and purification via column chromatography provides two substances, which could be identified as BINOL and oxidized aminophosphine ligand **L4$_{ox}$**, so the signal at 35 ppm is the result of a complexation of diaminophosphine ligand **L4** by $AlMe_3$ (Scheme 2.2).[39]
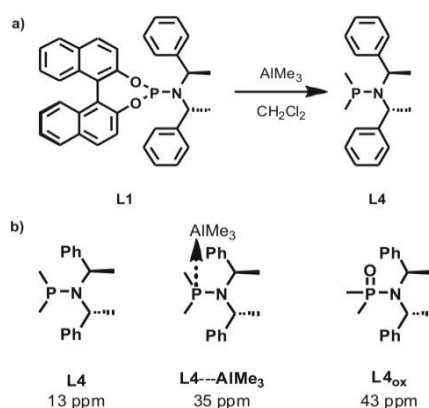
Scheme 2.2: a) Reaction between **L1** and $AlMe_3$ yielding **L4**; b) ^{31}P NMR chemical shift of aminophosphine **L4**, complexation of aminophosphine by $AlMe_3$ **L4**---**AlMe$_3$** and oxidized aminophosphine **L4$_{ox}$**.

The modification of the phosphoramidite ligands is also visible in toluene, but is not observed in coordinating solvents, like THF or diethyl ether.[39] With other transmetalation reagents, e. g. ZnR_2 these ligand transformation reaction was also not observed.

2.3 Copper Complexes with TADDOL-based Thiolate Ligands

The first NMR based study, to our knowledge, about structure elucidation of precatalytic copper complexes in enantioselective catalysis, was published in 2000 by the groups of Pregosin and Seebach. As model system the 1,4-addition reaction of Grignard reagents to enones with a combination of CuCl and the TADDOL-based thiolate ligands **L5-L7** as catalysts was selected (Scheme 2.3).[7]
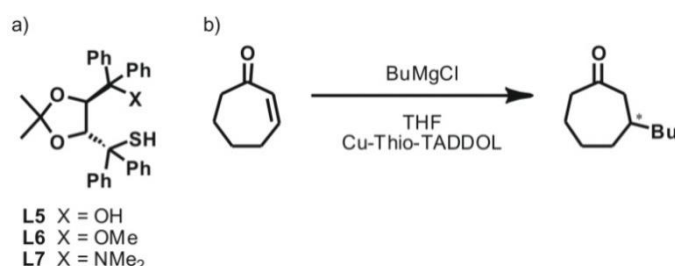
Scheme 2.3: a) TADDOL-based thiolate ligands **L5-L7**; b) copper catalyzed conjugate addition of BuMgCl to cycloheptenone (TADDOL = $\alpha,\alpha,\alpha',\alpha'$-tetraaryl-2,2-dimethyl-1,3-dioxolane-4,5-dimethanol).[7]

Modest positive nonlinear effects suggested that more than one ligand (and perhaps several metals) might be involved in the catalysis.[40–42] In accordance with this result the crystal structure of **C4** showed a tetranuclear complex structure. Surprisingly is that the normally bidenate[43] thiolate ligand act in this crystal structure as a monodenate ligand, in which the oxygen atom of the hydroxyl group is not complexed. In order to investigate whether these structural features are also present in solution NMR spectroscopic investigations, especially ^{1}H DOSY and NOESY experiments were performed on the copper complexes with the thiolate ligands **L5-L7**. With diffusion NMR measurements it was possible to confirm the tetranuclear complex structure also in solution. In addition the ^{1}H low field shift of the hydroxyl proton (about 8.7 ppm) proved the monodentate coordination of **L5** in solution. For the complexes **C5** and **C6** similar results were accessible via NMR studies.[7]
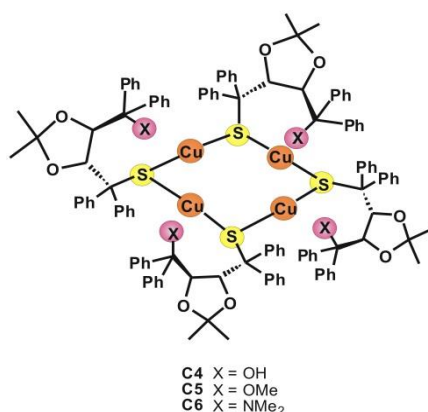
Figure 2.3: Schematic presentation of the tetranuclear copper thiolate complexes **C4-C6**.[7]

In order to prepare further model systems related to the copper chemistry in the copper catalyzed 1,4-addition reactions of Grignard reagents, the complexes **C4-C6** were treated with an excess of *tert*-butylisocyanide in THF-*d8*, which was assumed as additional donor ligand in order to get the corresponding isocyanide complexes. With diffusion NMR measurements it was possible to confirm the tetranuclear complex structure of these systems also in solution, i.e. no deaggregation to mononuclear species of **C4-C6** occurs, even in presence of additional donor ligands. In the ^{1}H,^{1}H NOESY spectra various cross-peaks were observed for the basic ligands, this suggests different structures of the complexes based on the used ligand and so the structural differences generate other chiral environments on the copper atom. With this, a hint for the stereoselective inversion was achieved.[1,7] In conclusion they were able to identify a tetranuclear copper thiolate complex, which uses an unprecedented monodentate complexation mode, in solution, as well as in solid state. Furthermore they present the first example for an application of diffusion measurements for the determination of aggregation behavior of organocopper complexes in solution.[7]

2.4 Copper Complexes with Ferrocenyl-based Ligands

Another prominent example of the structure elucidation of catalytically active copper complexes and their intermediates is an extensive study of Feringa and co-workers, regarding the mechanism of the asymmetric copper catalyzed conjugate addition reaction of Grignard reagents to α,β-unsaturated carbonyl compounds.[25] In this study they selected the ferrocenyl-based ligands **L8** and **L9** (Scheme 2.4b) which are known to catalyze the ACA of Grignard reagents to α,β-unsaturated enones with high yields and enantioselectivities (Scheme 2.4a).[44]
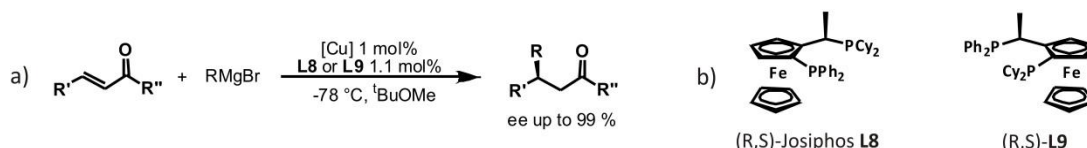
Scheme 2.4: a) Enantioselective conjugate addition reaction of Grignard reagents to acyclic α,β-unsaturated enones; b) ferrocenyl-based ligands **L8** and **L9**.[25]

2.4.1 Structural Studies of Asymmetric Conjugate Addition Reactions

2.4.1.1 Precatalytic Copper Complexes

The precatalytic complexes were identified either as mononuclear (**C8**) or binuclear (**C7**) complex by X-ray diffraction analysis (Scheme 2.5).[25,45]
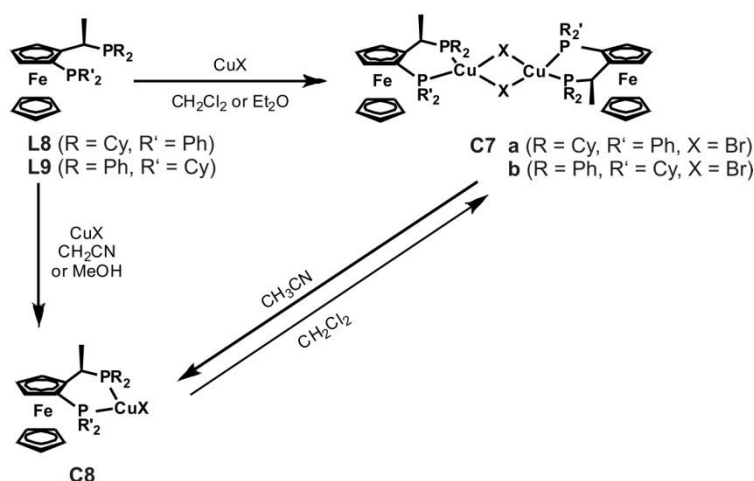
Scheme 2.5: Formation of the precatalytic, solvent dependent, copper complexes **C7** and **C8** (CuX; X = Cl, Br, I).[25]

Due to the fact that the structures in solution may differ from these crystal structures, Feringa and co-workers investigated the existence of the precatalytic structures also in solution. Because the ^{1}H and ^{31}P NMR spectra of the mononuclear and the binuclear complexes are nearly identical, classical NMR spectroscopic methods could not be applied for their differentiation. Compared to the above described phosphoramidite copper complexes, this is a second example

of indistinguishable signals in the ^{1}H spectrum of the precatalytic complexes. Due to this fact no ^{1}H DOSY measurements[1,7,27,28,38] would be possible, because this requires a specific, baseline separated signal in the corresponding 1D spectrum. Feringa and co-workers surrounded this problem using a combination of ESI-MS, IR spectroscopy and electrochemical studies, to examine the behavior of the complexes by changes of the solvent.[25] They were able to show, that the solvent dependent equilibrium between the mono- and binuclear complex structures **C8** and **C7** (Scheme 2.5) also exists in solution. Especially electrochemical studies confirmed the existence of a binuclear halide bridged copper complex **C7** in CH_2Cl_2, which is the thermodynamically most favored complex in halogenated solvents. In addition, this voltammetry investigation showed, that the electron density on the copper(I) centers in several binuclear complexes varies despite a high structural similarity. Interestingly these differences are caused by the ligand involved, and not on the bridging halide.[25] This study reveals, that severe signal overlap preventing the application of DOSY experiments, can be circumvented by the use of elaborated combinations of various analytical methods.

2.4.1.2 Transmetalation Intermediates with Grignard Reagents

2.4.1.2.1   Transmetalation Studies by NMR

As first step in the copper catalyzed 1,4-addition, a transmetalation step beween the organometallic reagent and the copper complex is postulated. For this generally assumed transmetalation intermediate, some hypothetical structures have been proposed for the enantioselective CA[16,31] and a number of studies about non chiral transmetalated copper salts are known.[10,46–52] Experimental reports about the transmetalated intermediate species under catalytic conditions are very rare and to our knowledge only two reports have been published so far. In a very short report about the addition of $ZnEt_2$ to copper complexes with a chiral diphosphate ligand, an extremely large upfield shift in the ^{31}P spectrum was detected and attributed to an Et-Cu transmetalation intermediate.[53] The second report of Feringa about the transmetalation intermediates in the ACA of Grignard reagents to α,β-unsaturated carbonyl compounds is very detailed and interestingly there very small ^{31}P chemical shift differences between the precatalytic and the transmetalated species were found.[25] Due to the fact that reliable structural information about the transmetalation intermediates are very important for the mechanistic understanding, the study about the occurring transmetalation intermediates is explained in detail. However, we would like to remind the known sensitivity of copper catalyzed reactions to variation in the ligand structures, copper salts, solvents, temperatures and organometallic reagents. Thus, it might not be possible to propose one general mechanism and one common transmetalation intermediate for all copper catalyzed reactions.
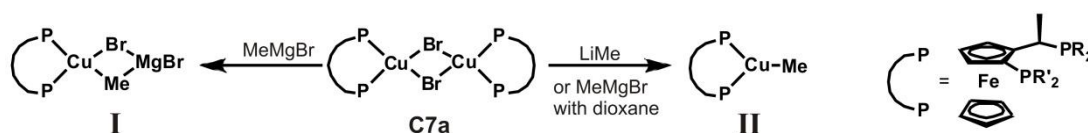
Scheme 2.6: Transmetalated complexes **I** and **II**, after the addition of organometallic reagents or dioxane to the precatalytic complex **C7a**.[25]

Feringa and co-workers were able to elucidate the structure of the transmetalation complex, based on classical 1D NMR spectroscopic experiments, such as changes of the ^{1}H and ^{31}P chemical shifts, scalar coupling pattern and integrals upon the variation of reaction parameters. The reactive intermediate species was then identified by connecting the appearance of different compounds with known reactivities.
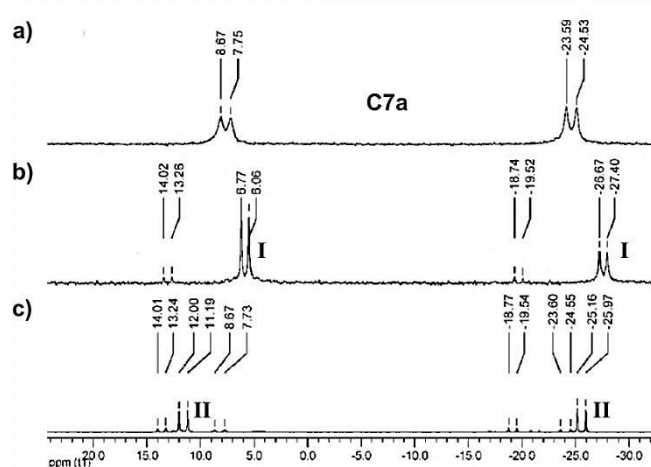
Figure 2.4: ^{31}P NMR spectra in CD_2Cl_2 at 213 K: a) complex **C7a**; b) complex **C7a** with 3 equiv. of MeMgBr; c) complex **C7a** with 3 equiv. of MeMgBr followed by addition of 3 equiv. of dioxane. Reprinted with permission from ref [25]. Copyright 2006 American Chemical Society.

Upon addition of an excess of MeMgBr to the precatalytic complex **C7a** a main new species appeared in the ^{31}P spectrum (see **I** in Figure 2.4b). The chemical shift values and the integral ratio of the corresponding new methyl-signal in the ^{1}H spectrum indicated a transmetalated species with a ratio of one methyl group at the copper per ligand attached. To test whether $MgBr_2$ is part of this intermediate dioxane was added, which is known to coordinate strongly to $MgBr_2$ and removes it from the solution. As a result it drives the Schlenk equilibrium towards the formation of R_2Mg. Under these conditions a new transmetalated species **II** is detected (Figure 2.4c). The identical intermediate can be created upon addition of MeLi with and without crown ether. This set of experiments allow to assign species **I** to a transmetalated intermediate with $MgBr_2$ attached, whereas in **II** $MgBr_2$ or LiBr is not part of the intermediate (see Scheme 2.6 for structures).

Next, Feringa and coworkers performed stoichiometric addition reactions with **I** and **II** to identify the catalytically active species. The outcome of these reactions and subsequent studies of the solvent and salt dependence of the intermediate and the synthetic outcome are all in agreement "that species **I** rather than species **II** is essential to obtain high levels of regio- and enantioselectivity in the catalytic CA of Grignard reagents to unsaturated carbonyl compounds."[25] With this experimental setup the composition of **I** was clearly defined. However it remained to clarify whether **I** is a mono- or a binuclear copper complex.

2.4.1.2.2   Kinetic Studies

Additional evidence for the mononuclearity of the catalytically active species was obtained by kinetic studies. Therefore, the catalytic activity of heterocomplex **C7ab** compared with that of the homocomplexes **C7a** and **C7b**, in the CA of EtMgBr to methyl cinnamate was determined (Scheme 2.7a).
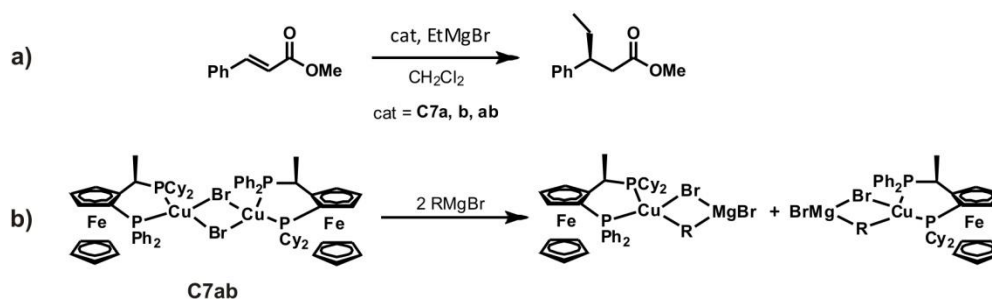
Scheme 2.7: a) Analyzed reaction in the kinetic study; b) Dissociation of the heterocomplex **C7ab**.[25]

For the reaction performed with the homodimeric precatalyst **C7a** a low yield (4 %) was reached, in contrast for **C7b** a high conversion of 69 % was observed (**C7a** and **C7b** see Scheme 2.5). Then the heterocomplex **C7ab** was applied as precatalytic complex in the identical reaction, resulting in halved conversion (32 %) corresponding to the reaction with **C7b**. In accordance, double the amount of the precatalyst **C7ab** resulted in the same yield compared with **C7b** (65 %). Thus, the catalytically active species could be identified to be the mononuclear complex **I**.

2.4.2   Structural Studies of Asymmetric Allylic Alkylation

In 2011 Feringa *et al.* developed the first asymmetric allylic alkylation (AAA) of allylic halides with high yields and enantioselectivities, despite the high reactivity of the organolithium compounds (Scheme 2.8a).[54] Moreover, they performed a further NMR spectroscopic study, dealing with this reaction. In contrast to other organometallic reagents (ZnR_2, AlR_3, RMgX), in the case of organolithium compounds further structural information can be collected using the NMR active nuclei $^{6/7}$Li. Based on the above described experience, 1D NMR spectra were used to identify the

precatalytic complex **C9** and complex **II** as transmetalated species in solution. Thereby an incorporation of lithium ions can be excluded directly by $^{6/7}$Li NMR spectra.[54]
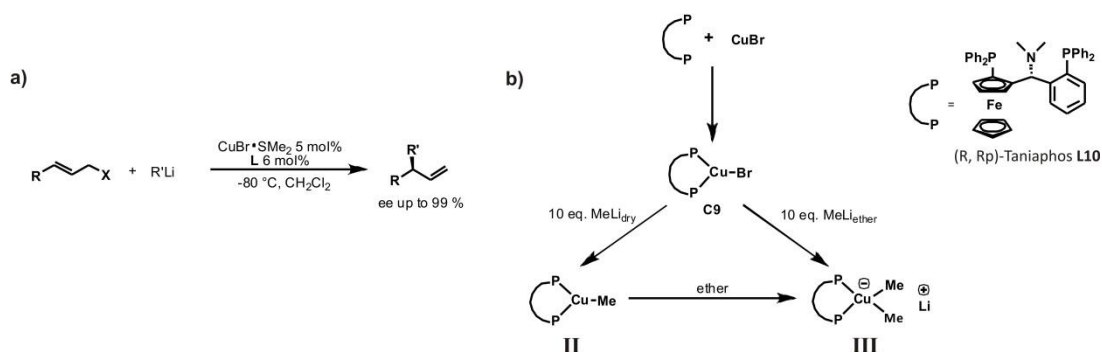
Scheme 2.8: a) Asymmetric allylic alkylation reaction with organolithium reagents (X = Br, Cl); b) By NMR spectroscopy identified structures: precatalytic complex **C9** and the transmetalated species **II** and **III** in CD$_2$Cl$_2$ at 200 K.[54]

The chemical shifts in the ^{1}H, ^{31}P and $^{6/7}$Li NMR spectra were used to identify the complex structures present in solution. Thereby, the spectra of different combinations of copper salts, solvents and quantities of MeLi over a range of temperatures were analyzed. Relevant was also the investigation on the influence of ethereal solvents on the structure in the reaction mixture. In the presence of Et$_2$O a drastic decrease in yield and enantioselectivity is observed (for instance, if Et$_2$O is used as co-solvent e.g. to delute *n*-BuLi).[54] When MeLi without Et$_2$O was added, complex **II** was observed exclusively in the ^{31}P spectrum. In contrast, by adding Et$_2$O subsequently to this reaction mixture or using MeLi containing Et$_2$O, the occurrence of complex **III** was observed (Scheme 2.8). Hence it is concluded, that complex **II** is responsible for the unique activity and selectivity in the copper catalyzed allylic alkylation with organolithium reagents. A further proof for the postulated structure of species **II** was the absence of a peak in the $^{6/7}$Li NMR spectra, when complex **II** is prepared exclusively. This shows that there is no lithium ion incorporated in this structure.[54]

This study clearly shows the before mentioned problem, that the structures of the transmetalation intermediates differ significantly, depending on the respective reaction. In the present case the use of MeLi instead of a Grignard reagent and a small change of the ligand structure are responsible for the formation of species **II** during the transmetalation step, which was found to be the less reactive species in the above describe reaction with Grignard reagents. Great care is recommended for proposing a general transmetalation intermediate, since each reaction has to be investigated for its own.

2.5   Conclusion

In conclusion this chapter provides a literature survey of the performed NMR spectroscopic investigations, dealing with the elucidation of the mechanism of asymmetric copper catalyzed conjugate addition (ACA) and allylic alkylation (AAA) reaction. This research area is a quite challenging field, due to the magnetic properties of copper (e.g. high quadrupol moment). Out of the few studies concerning the mechanism elucidation, three prominent examples were selected and presented here in detail. For phosphoramidite copper complexes Gschwind *et al.* were able to identify a binuclear Cu(I) complex with a mixed trigonal/tetrahedral stereochemistry as new structural motif for the precatalytic complex structure by diffusion NMR measurements (DOSY) and confirmed this structure also by classical NMR methods. This structural motif is independent of the halide used, but can be interconverted into other complex structures dependent on the temperature. For the investigation of the origin of the structure variations a fast and simple ^{1}H DOSY NMR screening method was developed on the example of phosphoramidite ligands to predict the aggregation behavior of ligands and their transition metal complexes. For transition metal complexes with highly stereoselective phosphoramidite ligands aggregation trends were determined, which are mainly dependent on the ligand properties. With TADDOL-based ligands Pregosin and Seebach identified a tetranuclear thiolate complex with an unprecedented monodentate complexation mode both in the solid state and in solution. This was the first study applying NMR diffusion measurements for the determination of aggregation trends of organocopper complexes. Although various organometallic reagents ($RMgX$, ZnR_2, AlR_3) are already introduced to synthetic applications, only one extensive NMR spectroscopic investigation concerning the proposed transmetalation intermediates was published by Feringa for the ACA of Grignard reagents with ferrocenyl-based ligands. By combination of various analytical methods (NMR spectroscopic, electrochemical and kinetic investigations, X-ray diffraction) they were able to identify equilibrium between mono- and binuclear precatalytic complexes, depending on the solvent properties. In synthetically applied solvents, the binuclear structure is present. Upon the addition of an excess of MeMgBr, one major new species could be identified. Based on chemical shift values, integral ratios and variation of the reaction conditions it was possible to determine, that the transmetalation intermediate obtain one attached methyl group at the copper per ligand and include $MgBr_2$. The mononuclearity of this intermediate was confirmed by kinetic studies. Also the transmetalation intermediate structures in the AAA with a ferrocenyl-based ligand and CuBr as catalyst and MeLi as transmetalation reagent were investigated by Feringa, for this reaction they assigned a diphosphine copper monoalkyl species, without included lithium, as the active one.

In summary, from the very few detailed structural studies in solution it is still difficult to conclude a structural trend and for that purpose a lot of more studies will be required. However, some common trends and deviations are already visible. Under experimental conditions all precatalytic complexes known so far in ACA are not mononuclear, but dimer, tetramer or mixed aggregates. Thus, self-aggregation of precatalytic copper complexes has to be considered as important property also in catalytically active enantioselective systems. For the transmetalation intermediates, interestingly the structural outcome of the two studies with a bidentate ferrocenyl-based ligand shows the identical monomethylation of the copper complexes. However the transmetalation intermediates differ in the inclusion or exclusion of the metal atom of the transmetalation reagent. This is a strong reminder to the sensitivity of copper reactions and also of their intermediates to the reaction conditions used. Therefore, in case of copper catalyzed enantioselective reactions great care has to be taken to transfer structural information from one system to another without structural studies in solution and most probably more than one mechanistic pathway is possible in enatioselective copper catalyzed reactions.

2.6   References

[1]   R. M. Gschwind, *Chemical Reviews* **2008**, *108*, 3029–3053.

[2]   R. K. Harris, E. D. Becker, S. M. Cabral de Menezes, R. Goodfellow, P. Granger, *Pure and Applied Chemistry* **2001**, *73*, 1795–1818.

[3]   P. Kroneck, J. Kodweiss, O. Lutz, A. Nolle, D. Zepf, *Z. Naturforsch., Teil A* **1982**, *37A*, 186–190.

[4]   T. Gärtner, R. M. Gschwind, in *The Chemistry of Organocopper Compounds*, John Wiley & Sons Ltd., **2009**.

[5]   M. Kujime, T. Kurahashi, M. Tomura, H. Fujii, *Inorganic Chemistry* **2006**, *46*, 541–551.

[6]   H. Nakatsuji, K. Kand, K. Endo, T. Yonezawa, *Journal of the American Chemical Society* **1984**, *106*, 4653–4660.

[7]   A. Pichota, P. S. Pregosin, M. Valentini, M. Wörle, D. Seebach, *Angewandte Chemie International Edition* **2000**, *39*, 153–156.

[8]   N. Yoshikai, E. Nakamura, *Chemical Reviews* **2011**, *112*, 2339–2372.

[9]   E. Nakamura, S. Mori, *Angewandte Chemie International Edition* **2000**, *39*, 3750–3771.

[10]   S. Woodward, *Chem. Soc. Rev.* **2000**, *29*, 393–401.

[11]   B. H. Lipshutz, S. Sengupta, *Organic Reactions*, Wiley-VCH, **1992**.

[12]   E. Nakamura, in *Modern Organocopper Chemistry*, Wiley-VCH, **2002**.

[13]   B. L. Feringa, R. Naasz, R. Imbos, L. A. Arnold, in *Modern Organocopper Chemistry*, Wiley-VCH, **2002**.

[14]   T. Pfretzschner, L. Kleemann, B. Janza, K. Harms, T. Schrader, *Chemistry – A European Journal* **2004**, *10*, 6048–6057.

[15]   M. Welker, S. Woodward, L. F. Veiros, M. J. Calhorda, *Chemistry – A European Journal* **2010**, *16*, 5620–5629.

[16]   L. A. Arnold, R. Imbos, A. Mandoli, A. H. M. de Vries, R. Naasz, B. L. Feringa, *Tetrahedron* **2000**, *56*, 2865–2878.

[17]   K. Nakano, Y. Bessho, M. Kitamura, *Chem Lett.* **2004**, *32*, 224–225.

[18]   E. Gallo, F. Ragaini, L. Bilello, S. Cenini, C. Gennari, U. Piarulli, *Journal of Organometallic Chemistry* **2004**, *689*, 2169–2176.

[19]   A. Alexakis, J. E. Bäckvall, N. Krause, O. Pàmies, M. Diéguez, *Chemical Reviews* **2008**, *108*, 2796–2823.

[20] S. R. Harutyunyan, T. den Hartog, K. Geurts, A. J. Minnaard, B. L. Feringa, *Chemical Reviews* **2008**, *108*, 2824–2852.

[21] T. Jerphagnon, M. G. Pizzuti, A. J. Minnaard, B. L. Feringa, *Chem. Soc. Rev.* **2009**, *38*, 1039–1075.

[22] J. Christoffers, G. Koripelly, A. Rosiak, M. Rössle, *Synthesis* **2007**, *9*, 1279–1300.

[23] J. F. Teichert, B. L. Feringa, *Angewandte Chemie International Edition* **2010**, *49*, 2486–2528.

[24] N. Krause, *Modern Organocopper Chemistry*, WILEY-VCH Verlag GmbH, Weinheim, **2002**.

[25] S. R. Harutyunyan, F. López, W. R. Browne, A. Correa, D. Peña, R. Badorrey, A. Meetsma, A. J. Minnaard, B. L. Feringa, *Journal of the American Chemical Society* **2006**, *128*, 9103–9118.

[26] M. D. Murphy, C. A. Ogle, S. H. Bertz, *Chem. Commun.* **2005**, 854–856.

[27] H. Zhang, R. M. Gschwind, *Angewandte Chemie International Edition* **2006**, *45*, 6391–6394.

[28] H. Zhang, R. M. Gschwind, *Chemistry – A European Journal* **2007**, *13*, 6691–6700.

[29] A. Alexakis, S. Rosset, J. Allamand, S. March, F. Guillen, C. Benhaim, *Synlett* **2001**, *2001*, 1375–1378.

[30] A. H. M. de Vries, A. Meetsma, B. L. Feringa, *Angewandte Chemie International Edition in English* **1996**, *35*, 2374–2376.

[31] A. Alexakis, C. Benhaim, S. Rosset, M. Humam, *Journal of the American Chemical Society* **2002**, *124*, 5262–5263.

[32] A. Alexakis, C. Benhaim, *Organic Letters* **2000**, *2*, 2579–2581.

[33] H. Malda, A. W. van Zijl, L. A. Arnold, B. L. Feringa, *Organic Letters* **2001**, *3*, 1169–1171.

[34] D. Pena, F. Lopez, S. R. Harutyunyan, A. J. Minnaard, B. L. Feringa, *Chem. Commun.* **2004**, 1836–1837.

[35] W. Zhang, C.-J. Wang, W. Gao, X. Zhang, *Tetrahedron Letters* **2005**, *46*, 6087–6090.

[36] A. H. Hoveyda, A. W. Hird, M. A. Kacprzynski, *Chem. Commun.* **2004**, 1779–1785.

[37] K. Schober, H. Zhang, R. M. Gschwind, *Journal of the American Chemical Society* **2008**, *130*, 12310–12317.

[38] K. Schober, E. Hartmann, H. Zhang, R. M. Gschwind, *Angewandte Chemie International Edition* **2010**, *49*, 2794–2797.

[39] C. Bournaud, C. Falciola, T. Lecourt, S. Rosset, A. Alexakis, L. Micouin, *Organic Letters* **2006**, *8*, 3581–3584.

[40] D. Guillaneux, S.-H. Zhao, O. Samuel, D. Rainford, H. B. Kagan, *Journal of the American Chemical Society* **1994**, *116*, 9430–9439.

[41] M. Reggelin, *Nach. Chem. Tech. Lab.* **1997**, *45*, 392–396.

[42] C. Girard, H. B. Kagan, *Angewandte Chemie International Edition* **1998**, *37*, 2922–2959.

[43] D. Seebach, A. K. Beck, A. Heckel, *Angewandte Chemie International Edition* **2001**, *40*, 92–138.

[44] F. López, S. R. Harutyunyan, A. J. Minnaard, B. L. Feringa, *Journal of the American Chemical Society* **2004**, *126*, 12784–12785.

[45] F. López, S. R. Harutyunyan, A. Meetsma, A. J. Minnaard, B. L. Feringa, *Angewandte Chemie International Edition* **2005**, *44*, 2752–2756.

[46] B. Christenson, T. Olsson, C. Ullenius, *Tetrahedron* **1989**, *45*, 523–534.

[47] S. H. Bertz, R. A. J. Smith, *Journal of the American Chemical Society* **1989**, *111*, 8276–8277.

[48] S. H. Bertz, C. M. Carlin, D. A. Deadwyler, M. D. Murphy, C. A. Ogle, P. H. Seagle, *Journal of the American Chemical Society* **2002**, *124*, 13650–13651.

[49] N. Krause, R. Wagner, A. Gerold, *Journal of the American Chemical Society* **1994**, *116*, 381–382.

[50] K. Nilsson, C. Ullenius, N. Krause, *Journal of the American Chemical Society* **1996**, *118*, 4194–4195.

[51] A. Alexakis, A. Commercon, C. Coulentianos, J. F. Normant, *Pure and Applied Chemistry* **1983**, *55*, 1759–1766.

[52] B. H. Lipshutz, C. Hackmann, *The Journal of Organic Chemistry* **1994**, *59*, 7437–7444.

[53] M. Yan, L.-W. Yang, K.-Y. Wong, A. S. C. Chan, *Chem. Commun.* **1999**, 11–12.

[54] M. Pérez, M. Fananás-Mastral, P. H. Bos, A. Rudolph, Syuzanna R. Harutyunyan, B. L. Feringa, *Nat. Chem.* **2011**, *3*, 377–381.

3 STRUCTURE ELUCIDATION OF TRANSMETALATION INTERMEDIATES IN COPPER-CATALYZED 1,4-ADDITION REACTIONS OF ORGANOZINC REAGENTS
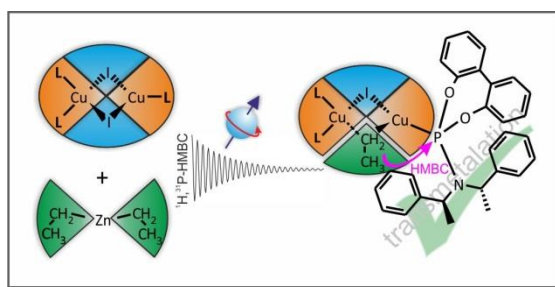
3.1 Abstract

The enantioselective copper-catalyzed 1,4-addition reaction is a very powerful tool in synthetic applications, nevertheless only little information concerning the mechanism and involved structures is accessible. We present here for the very first time a direct experimental proof for the commonly accepted transmetalation intermediate. Thereby NMR spectroscopic investigations on the reaction of phosphoramidite copper complexes and diethyl zinc were performed, by using a special approach of samples with enantiopure phosphoramidite ligands and an enantiomeric mixture of the phosphoramidite ligands. The detection of the highly elusive transmetalation intermediate was exclusively possible by 1D and 2D ^{1}H^{31}P-HMBC spectra, due to the missing of signals in the ^{1}H and ^{31}P NMR spectra. Nevertheless identification of several mono- and dimeric transmetalation intermediates was feasible. All of the monomeric species have one ligand bound to the copper atom, whereas the dimeric transmetalation species is the first example of retention of the precatalytic copper complex structure with a mixed trigonal/tetrahedral coordination of the copper atoms. With this first direct experimental evidence it is assumed that the mechanistic and theoretical understanding as well as further synthetic developments are supported.

3.2 Introduction

The asymmetric copper-catalyzed conjugated addition (ACA) reaction of organometallic reagents to α,β-unsaturated substrates is one of the most important organic transformations.[1] The ACA reaction enables the formation of highly enantioselective C-C bonds. The versatile applicability of this reaction is described in several reviews and publications[1–4] and represents the basis for further progress in the synthesis of complex natural products, pharmaceuticals or biologically active compounds.[5–8] Also in the field of supramolecular chemistry and molecular nanoscience chiral compounds are of increasing importance.[1] A further advantage of the asymmetric catalysis is the selective synthesis of products from cheap and commercial available prochiral starting materials, low costs of the copper salt and a high compatibility with functional groups.[3] Chiral phosphoramidite ligands emerge as a very powerful ligand class, not only in ACA but also for many other reactions. These are cheap and easily accessible ligands providing high yields and *ee*-values. Furthermore their electronic properties can be fine-tuned to several catalytic applications by substitutions at the oxygen or nitrogen atom and the chiral diol or amine side chain can be used directly as stereodiscrimination source, due to matched or mismatched effects.[9] For the organometallic reagent, apart from diorganozinc[10–12] also Grignard[4,13] reagents and triorganoaluminum[14–16] compounds are applicable. Thereby the addition of soft nucleophiles leads to 1,4-addition adducts, while hard nucleophiles favors the 1,2-addition

product.[1] Although a lot of information concerning the synthetic applicability of ACA reactions is available only few information addressing the involved structures and mechanisms is accessible.[17–19] Especially this informations are of utmost importance for further developments of this reaction type. The transmetalation of the organic moiety of the organometallic reagent to the copper catalyst is a commonly accepted step in the mechanism of ACA reactions, but a direct experimental proof for a transmetalated species is still missing.[1,3] Feringa and co-workers identified in an experimental study of binuclear copper complexes with ferrocenyl-based diphosphine ligands a monomerization of this precatalyst upon the addition of MeMgX (X = Cl, Br, I) by changes in the ^{1}H and ^{31}P NMR spectra, scalar coupling pattern and integrals upon variation of the reaction parameters (see Scheme 3.1 a).[17] In our previous investigations concerning the structure of precatalytic copper complexes with phosphoramidite ligands similar binuclear copper complexes were observed. Thereby the binuclear copper complex **C2** with a mixed trigonal/tetrahedral coordination of the copper atoms was identified as main species in solution (see Scheme 3.1 b).[20-22] Both studies were recently supported by DFT-calculations performed by Woodward and co-workers. Therein they identified a lowest energy zinc cuprate, which is mononuclear in copper but bimetallic (see Scheme 3.1 c, left). Based on this structure docking experiments with substrate were performed and the only energetic suitable pathway is observed for dimeric copper-π-complexes with mixed trigonal/tetrahedral stereochemistry (see Scheme 3.1 c, right).[23]
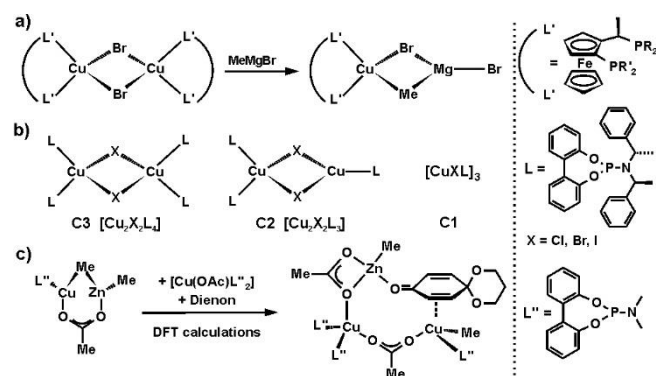
Scheme 3.1: Proposed structures of precatalytic copper complexes and transmetalation intermediates: a) Monomerization and formation of a bimetallic transmetalation intermediate upon MeMgBr addition,[17] b) Interconversion and coexistence of phosphoramidite copper complexes **C1**, **C2** and **C3**, thereby **C2** was proposed as precatalyst for ACA reactions,[20] c) Bimetallic transmetalation intermediate and a theoretically calculated π-complex, which essentially is in accordance with **C2**.[23]

The investigation of the transmetalation intermediates is a very challenging field of research, due to the high sensitivity of the system towards the applied reaction parameters (e. g. dependence on the copper salt, ligand, ligand to salt ratio and solvents used,[20,21] temperature dependent complex interconversion, ligand and complex aggregation,[22] as well as ligand

acceleration and non-linear effects[17,24]). Therefore we present here a structural elucidation of the transmetalation step between phosphoramidite copper complexes and diorganozinc reagents by multidimensional NMR spectroscopy. For the very first time a direct experimental proof for transmetalation intermediates was accessible by NMR spectroscopic measurements, using a precatalytic system of phosphoramidite ligands and either copper iodide or chloride. Furthermore a probable explanation for the lower activity of CuI compared to CuCl in synthesis was found. For CuI a plenty of monomeric and dimeric transmetalation intermediates exists. In contrast, with CuCl only one dimeric species and no monomeric species were suggested, apart from some side reactions of the free ligand. Thereby a retention of the structure of the precatalyst for the dimeric transmetalation intermediate was observed. Also the amount of free ligand present in the investigated sample plays a decisive role for the formation of transmetalated species, which can be an indication for the detrimental performance of the reaction if a ligand to salt ratio below 1.5:1 is used. Beside the transmetalation intermediates unspecific interactions between free and complexed ligands with the organometallic reagents were identified, based on strong π,π- or CH,π-interactions.

3.3   Investigations with Diethylzinc

3.3.1   Investigations of a 2:1 mixture of L2 and CuI and their transmetalation intermediates with ZnEt$_2$

Among the synthetically applied diorganozinc reagents diethylzinc is by far the most commonly used one, providing high yields and enantioselectivities.[3] Nevertheless only few information concerning the mechanism of the 1,4-addition reaction is available.[1,3] Due to the high reactivity of diethylzinc we decided to use it for our NMR spectroscopic investigations of the copper-catalyzed 1,4-addition reaction.

With ZnEt$_2$ a first direct experimental proof of the elusive transmetalation intermediate in 1D and 2D NMR experiments was detected using a precatalytic system consisting of copper iodide and phosphoramidite ligands. Furthermore we were able to identify these transmetalation intermediates partially as monomeric species. Monomerization of dimeric precatalytic species, due to the addition of organometallic reagents, was already described by Feringa and co-workers for investigations with a precatalytic system of ferrocenyl-based diphosphine ligands and copper salts after addition of Grignard reagents.[17] Despite the monomeric transmetalation intermediates also a dimeric intermediate was detected, in which the binuclear structure and the corresponding coordination of the copper atoms of the precatalyst remains intact.

For our NMR spectroscopic investigations a 2:1 ratio of a chiral, highly stereoselective phosphoramidite ligand **L2** and a Cu(I) salt was used as model system, because with this catalytic system high *ee*-values and quantitive yields are accessible.[3,11] Furthermore this combination enables the detection of well separated and sharp signals in the ^{31}P NMR spectrum and moreover in the low temperature spectrum (180 K) a signal splitting into a 2:1 signal for the two different ligand groups of **C2** is observed.[20] As solvent we used CD$_2$Cl$_2$, because in other solvents like toluene broad signals appear indicating the existence of several complex species.[21] For synthetic applications Cu(I) and Cu(II) salts are suitable copper sources, due to a complete reduction of the Cu(II) salt by the organometallic reagent.[5] In contrast we are limited to Cu(I) salts for our investigations, even if they are not as reactive as Cu(II) salts in synthetic application, but Cu(II) salts are paramagnetic and thus structure elucidation of the precatalytic system is not possible by NMR spectroscopy. Previous studies showed, that with a 1.5:1 ligand to salt ratio the reaction works quite well, ratios below are detrimental for the outcome of the reaction and the best results are obtained with a 2:1 ratio.[10,25] Therefore we chose the 2:1 ratio as the traditional ratio which is mostly effective in synthetic protocols. Furthermore, in earlier investigations with this combination we were able to identify a binuclear copper complex with a mixed

trigonal/tetrahedral coordination on the copper atoms as a new structural motif for precatalytic copper complexes, which is stabilized by a 2:1 ligand to salt ratio.[21,22] Besides this precatalytic structure **C2** ([$Cu_2X_2L_3$]) also an additional complex **C1** ([$CuXL$]$_3$) is observed at temperatures above 220 K (see Scheme 3.2). The appearance of these two complexes, besides free ligand and further copper complexes, e. g. the thermodynamic stable complex **C3** (present at temperatures lower than 180 K) is dependent of the solvent, copper salt, temperature and the ligand to salt ratio used.[20,22] Furthermore in a study which set out to determine the structure of precatalytic phosphoramidite copper complexes, Gschwind *et al.* found that the ligand to copper ratio in the complexes influences the phosphorous chemical shift. A higher amount of ligand in the complex, is accompanied with a stronger lowfield shift of the signals in the ^{31}P NMR spectrum.[20,21]
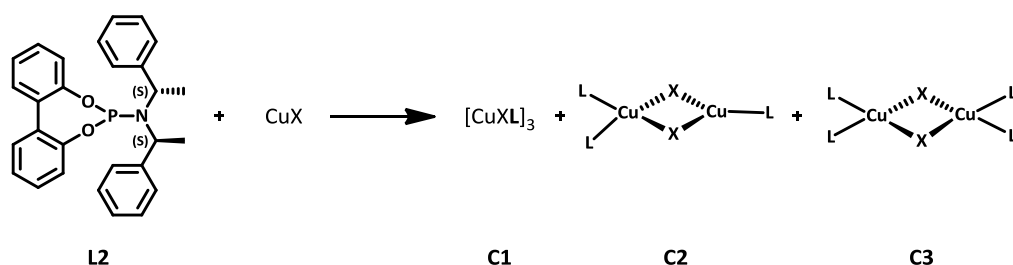
Scheme 3.2: Used phosphoramidite ligand **L2** and possible complexes **C1** ([$CuXL$]$_3$), **C2** ([$Cu_2X_2L_3$]) and **C3** ([$CuXL_2$]$_2$) depending on the temperature used (CuX, X = I, Br, Cl, thiophene carboxylate TC).[20]

After preparation of the complex mixture $ZnEt_2$ was added. In order to avoid big residual solvent signals of the organometallic reagent, which are detrimental for the spectra quality, we decided to use freshly prepared solutions of neat $ZnEt_2$ in the corresponding deuterated solvent. Otherwise it is not possible to detect any transmetalation intermediates, because they occur in tiny amounts close to the detection limit. The improved spectra quality using neat $ZnEt_2$ in CD_2Cl_2 (freshly prepared) instead of a toluene solution (commercial available) of $ZnEt_2$ is presented in the supporting information (Chapter 3.7). In synthetic applications typically a high excess of $ZnEt_2$ (60-70 eq) compared to the copper complex is used.[26] Such a high excess would be detrimental for spectra quality and so is not applicable for our NMR spectroscopic investigations. Therefore we use only a reduced excess (4-20 eq $ZnEt_2$ with regard to **C2**) in order to improve the signal to noise ratio (S/N) and to enable the detection of further upstream intermediates, which might be of interest for the mechanism.

However, after the addition of $ZnEt_2$ no striking changes occur in the ^{1}H NMR spectrum, apart from the $ZnEt_2$ signals. The use of standard proton based 2D NMR experiments, like [1]H[1]H-COSY or [1]H[1]H-NOESY spectra, for structure elucidation of the transmetalated species failed due to the missing of new signals. Also in the ^{31}P NMR spectrum no new signals appear (data not shown).

Next we tested $^1H^{31}P$-HMBC spectra, as they act as a spectroscopic filter for free ZnEt$_2$. This means, that all signals from free ZnEt$_2$ not bound to the complex are eliminated. Therefore they are very sensitive for transmetalation intermediates. In case of an ethyl group is transmetalated to one of the copper atoms of the precatalyst **C2** a magnetization transfer from the protons of the ethyl group to the phosphorous atom of the ligand via copper should become possible (see Scheme 3.3), revealing a cross signal in the 2D $^1H^{31}P$-HMBC spectrum.
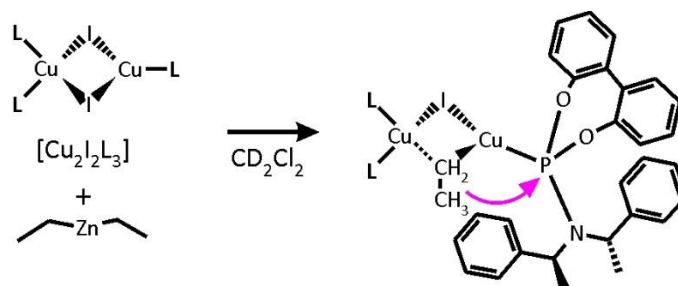
Scheme 3.3: Proposed transmetalation step of an ethyl group of ZnEt$_2$ to one of the copper atoms in **C2**. The direct connection of both the ethyl group and the phosphoramidite ligand to one copper atom should enable a magnetization transfer via the copper atom (purple arrow).

With the use of $^1H^{31}P$-HMBC spectra we already got promising results by the detection of a key intermediate of a palladium-catalyzed Negishi coupling reaction.[27] Due to the high quadrupole moment of copper the magnetization transfer via copper is more difficult than via palladium and is in general exclusively possible in highly symmetric copper complexes with very small electric field gradients.[28,29] Consequently only few examples of successful magnetization transfer via copper are reported, e. g. in $^1H^{13}C$-HMBC spectra of ^{13}C-labelled organocuprates,[30] in $^1H^{31}P$-HMBC spectra of Me$_3$Cu(PPh)$_2$Li[31] or in $^{31}P^{31}P$-COSY spectra of precatalyst **C2** (with CuBr or CuCl and **L2**).[9,20] Despite the obstacles and difficulties in observing magnetization transfers via copper we were able to detect some new cross signals for transmetalated species in the 2D $^1H^{31}P$-HMBC spectra, neither detectable in the ^1H nor in the ^{31}P NMR spectra. In Figure 3.1 the 2D $^1H^{31}P$-HMBC spectra of a mixture with 2 eq **L2**, 1 eq CuI and 20 eq ZnEt$_2$[1] at 250 and 170 K are presented. At 250 K two classes of signals are present in the spectra. On the one hand cross signals appear which remain on the chemical shift of **L2** (146.4 ppm) or **C2** (129.0 ppm) to ZnEt$_2$ (1.10 and 0.21 ppm, dashed red boxes) and on the other hand signals with different chemical shifts in the proton, as well as in the phosphorous dimension (red boxes) are detected. At low

---

[1] Equivalent determination of ZnEt$_2$: first step: integration of the complete methine area and the CH$_3$ signal of ZnEt$_2$ in the ^1H NMR spectrum, the intensity of the latter one was set to 6 (corresponding to 1 eq ZnEt$_2$); second step: integration of the ^{31}P NMR and normalization of the sum of all integrals to 100 (corresponding to the percentage distribution of free and complexed ligand); third step: with the percentage of **C2** of the ^{31}P NMR spectrum calculation of the methine integral corresponding to **C2**, hence calculation of the equivalents by comparing the integral and the six methine protons of **C2**.

temperature the cross signals with no change in the chemical shifts are only detected between **L2** and $ZnEt_2$. This is the result of line broadening effects for the precatalytic complex, due to remaining ligand exchange contributions even at low temperatures, compared to free ligand (see the line widths of the signals for **C2** compared to **L2** in Figure 3.1 below).[22] Therefore signal intensity is reduced for the complex. Furthermore the temperature dependent complex **C3** appears as a broad signal at 139.2 ppm. For two of the new signals (purple and green line 121.4 and 123.9 ppm respectively in Figure 3.1) also the splitting of the methine signals is visible at 170 K (for the latter one the second methine group is beyond the threshold of the selected presentation). This signal splitting effect is known from the phosphoramidite ligands, due to decelerated rotation of the C-N bonds in the amine side chain at low temperatures[32] and therefore gives proof for an intact amine side chain in the corresponding structures. The assignment of the cross signals is based on the fact, that the $^3J_{(H,P)}$ coupling is much bigger than the $^2J_{(H,P)}$ coupling for ethyl groups directly bound to a phosphorous atom (e. g. PEt_3: $^2J_{(H,P)} =$ 0.5 Hz, $^3J_{(H,P)} = 13.7$ Hz).[33] Therefore for structures with an ethyl group directly bound to a phosphorous atom the CH_3 group is detected, whereas for transmetalated ethyl groups the detected cross signal belongs to the CH_2 group. The proton chemical shifts of the new signals (0.90-0.40ppm) are in agreement with the expected peak range for a transmetalated CH_2 group to Cu(I) (e. g. proton chemical shifts for the CH_2 group of $Et_2CuLi \cdot LiI$ and $Et_2CuLi \cdot LiCn$ -0.53 and -0.54 ppm, respectively[34]; Me_3EtCu 0.54 ppm[35]; of course ethyl groups bound to Cu(III) show higher ppm values $Me_2EtCuPMe_3$ 1.89 ppm, $Me_2EtCuP(OMe)_3$ 2.07 ppm, $Me_2EtCu(PPh_3)$ 2.31 ppm[36]).
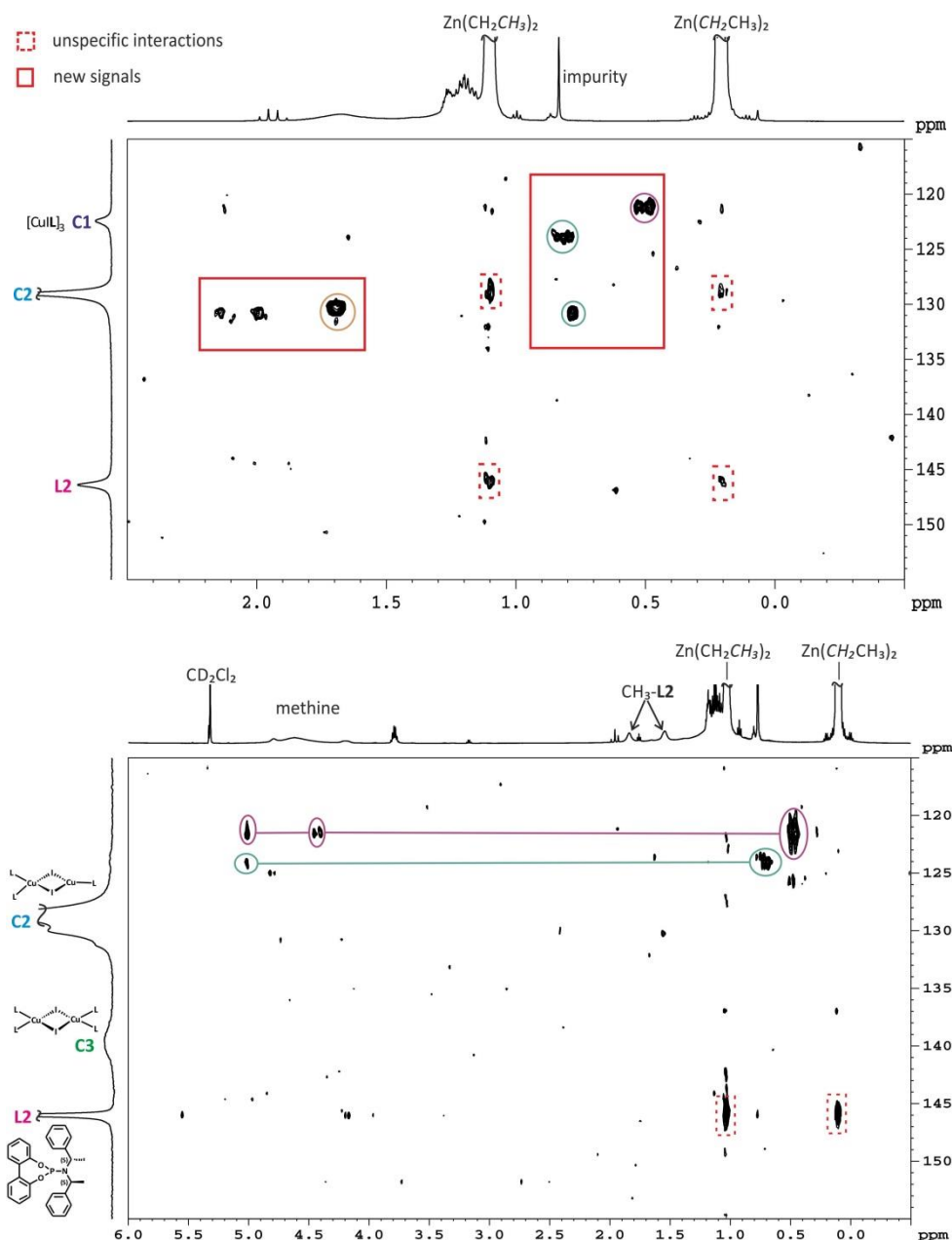
Figure 3.1: 2D ^{1}H^{31}P-HMBC spectra of 2 eq **L2,** 1 eq CuI and 20 eq ZnEt$_2$ at 250 (top) and 170 K (below) in CD$_2$Cl$_2$. The red boxes represent new signals after addition of ZnEt$_2$ with changes in the chemical shift in the ^{1}H and the ^{31}P NMR spectra, while the dashed red boxes highlight signals without chemical shift variation compared to **C2** or **L2** and ZnEt$_2$. For the purple (121.4 ppm) and green (123.9 ppm) line two separated signals for the methine groups at 170 K are visible, based on slower rotation in the amine side chain of the ligand (the signal of the second methine group of the latter signal is beyond the threshold of the presentation used).

To determine whether the magnetization transfer occurs via chemical bonds (scalar coupling) or through space (cross correlation, as combination of chemical shift anisotropy and dipolar interaction pathways) various modified 1D ^{1}H^{31}P-HMBC spectra were measured (pulse sequences see Figure 3.2 a). In the following for simplification called magnetization transfer via scalar coupling or cross correlation. Applying simultaneously 180° pulses on protons and phosphorous atoms enables the suppression of cross correlation and therefore only magnetization transfers via scalar couplings are detected. In contrast applying a 180° pulse only

on the protons permits refocussing of scalar coupling and reveals the solely detection of magnetization transfers via cross correlation, which is the combination of chemical shift anisotropy (CSA) and dipolar interaction (see Figure 3.2 a). These pulse sequences were already applied successfully in elucidations of the H-bond network in acylguanidine complexes and of a flavoprotein.[37–39] With these measurements the signals without change neither in the phosphorous nor in the proton dimension compared to **C2**, **L2** and ZnEt$_2$ were identified as unspecific interactions. For such unspecific interactions signals in all three modified ^{1}H^{31}P-HMBC spectra – with both of the interaction pathways, only scalar coupling pathway and solely cross correlation pathway – are expected and thus make it impossible to clearly assign one of the magnetization transfer pathways. Furthermore such unspecific interactions were also detected to the solvent, if the organometallic reagent is used as a commercial available solution, where scalar coupling can be excluded. These interactions are based on very strong π,π- or CH,π-interactions between free ligand and the solvent (here toluene) that beside cross correlation also signals for scalar coupling are detected (for details see supporting information, Chapter 3.7). For the detection of these unspecific interactions a minimum amount of ZnEt$_2$ is needed, in a sample with only 3.7 eq they are not detectable, while in a sample with 7.7 eq they exist. In a further investigation with CuCl as copper source (see Chapter 3.3.3) a similar behavior was observed, in a sample with only 1 eq of ZnEt$_2$ no unspecific interactions were detected, while with 10 eq these interactions were observed.
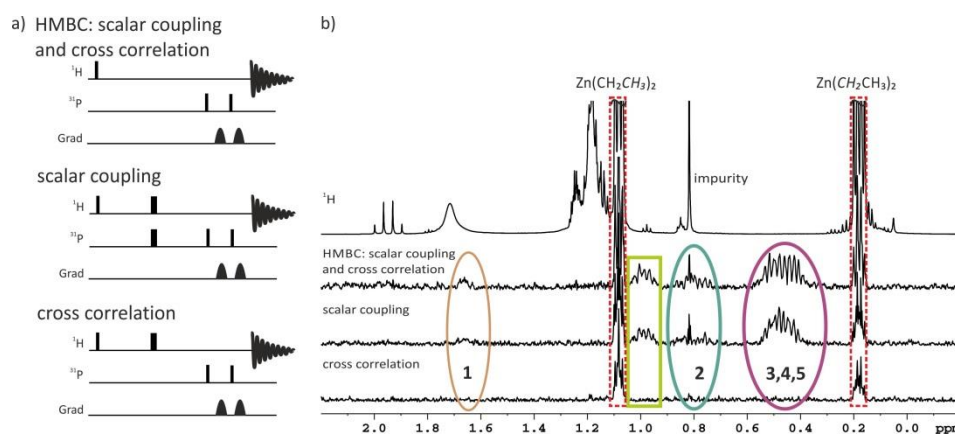
Figure 3.2: a) Pulse sequences for standard (scalar coupling and cross correlation), as well as for the modified 1D ^{1}H^{31}P-HMBC spectra, with magnetization transfers solely via scalar coupling and for cross correlation (combination of chemical shift anisotropy and dipolar interactions). b) Comparison of ^{1}H NMR and 1D ^{1}H^{31}P-HMBC spectra of 2 eq **L2**, 1 eq CuI and 7 eq ZnEt$_2$ at 230 K in CD$_2$Cl$_2$ (red dashed boxes represent unspecific interactions).

In Figure 3.2 b a comparison of the ^{1}H NMR and the 1D ^{1}H^{31}P-HMBC spectra of a sample with 2 eq **L2**, 1 eq CuI and 7 eq of ZnEt$_2$ is shown. A transmetalated ethyl group would only lead to a signal in the scalar coupling spectrum and none in the cross correlation spectrum. Obviously four signals fulfill this condition (see colored signals in Figure 3.2 b) and therefore belong to directly

coupled protons. By comparison of the 1D and 2D spectra it becomes clear, that the signals with solely magnetization transfer via scalar coupling are the new cross signals with changed chemical shifts in the ^{1}H and ^{31}P dimension in the two dimensional spectra. Furthermore, these species are stable in a temperature range of 250-170 K and detectable with different amounts of $ZnEt_2$. Samples were prepared with 4, 7, 12, 15 and 20 eq (see below). In order to determine interactions between free ligand and $ZnEt_2$, a copper free sample was prepared (see supporting information, Chapter 3.7). With this copper free sample the signal at 0.95 ppm (light green box) was determined as ligand-$ZnEt_2$ interaction, which is not yet identified. Based on the existence of the signal at 0.95 ppm (light green) also in copper free samples, we assume that this species plays a non-decisive role in the catalytic cycle. At 0.82 ppm an impurity of $ZnEt_2$ appears, but high- and lowfield shifted scalar coupling proportions occur (green, signal 2). The signal between 0.58 and 0.37 ppm (purple, superposition of signals 3-5) is in agreement with the expected peak range of a transmetalated ethyl group (CH_2 of ethyl groups bound directly to Cu(I)/Cu(III) appear at 2.31-(-0.54) ppm[34-36]). In the ^{31}P NMR spectra a highfield shift of 7.8 ppm relative to the averaged signal of **C2** is detected (see purple ellipse in Figure 3.1). This shift is in agreement with an investigation of the addition of Grignard reagents done by Feringa and co-workers. They determine a binuclear bromide bridged copper complex with ferrocenyl-based diphosphine ligands, as precursor, which splits into monomeric species after addition of the organometallic reagent. Thereby an highfield shift of the dicylcohexyl and diphenylphosphine moieties of the ligand by 1.8 and 3.1 ppm respectively in the ^{31}P NMR spectrum compared to the precursor complex was observed and new monomeric transmetalated species occur.[17]

Due to the fact, that no signals for the transmetalated intermediates were observed in the ^{1}H and ^{31}P NMR spectra, the complete identification and structural characterization is based exclusively on ^{1}H^{31}P-HMBC spectra. In principle several transmetalation intermediates are possible, which are either mono- or dimeric in copper with one, two or three ligands and contain varying amounts of $ZnEt^+$ and I^- moieties. In Scheme 3.4 a proposed structures for the monomeric transmetalation intermediates with one (**A**-**C**) and two (**D**) ligands coordinated to copper and dimeric structures with three ligands (**E**-**G**) are presented. To address the structural assignment under the assumption that exclusively ^{1}H^{31}P-HMBC spectra can be used a special approach had to be applied. In general a differentiation of the number of ligands coordinated to the copper atoms is possible by the comparison of ^{1}H^{31}P-HMBC spectra of transmetalation intermediates with enantiopure phosphoramidite ligand (**L2**) and such with equal amounts of enantiomeric phosphoramidite ligands (50 % **L2** and 50 % **L2***).

a)

C2 $\xrightarrow{\text{ZnEt}_2}$ A or B or C or D

E or F or G

L = L2   L2*

b)

	2 eq L + 1 eq CuI	1 eq L + 1 eq L* + 1 eq CuI		
A	100.0 %	100.0 %		
B	100.0 %	100.0 %		
C	100.0 %	100.0 %		
D	100.0 %	50.0 %	25.0 %	25.0 %

c)

	2 eq L + 1 eq CuI	1 eq L + 1 eq L* + 1 eq CuI			
E	100.0 %	25.0 %	25.0 %	25.0 %	25.0 %
F	100.0 %	25.0 %	25.0 %	25.0 %	25.0 %
G	100.0 %	25.0 %	25.0 %	25.0 %	25.0 %
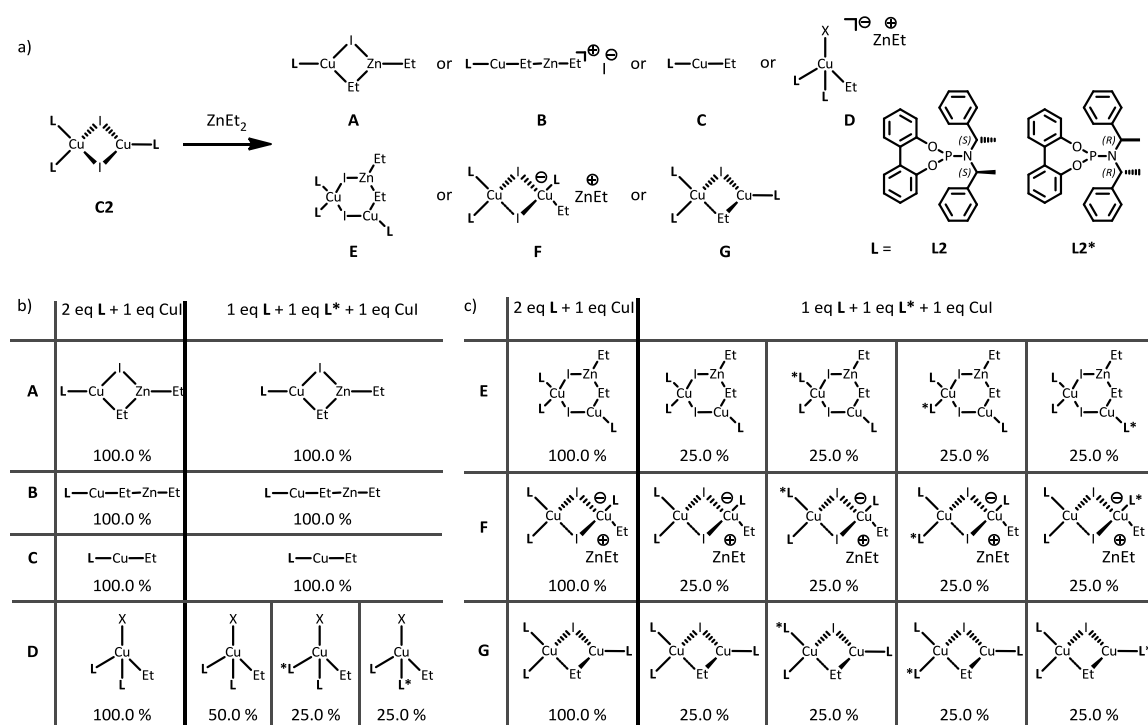
Scheme 3.4: a) Proposed monomeric transmetalation intermediates **A**-**C** with one ligand and **D** with two ligands coordinated to the copper atom and proposed dimeric transmetalation species **E**-**G** with three ligands coordinated to the copper atoms after addition of ZnEt$_2$ to the precatalytic complex **C2**. Statistical structure distribution in % is given below each structure for the enantiopure and enantiomeric mixture for b) monomeric (for structures **B** and **D** charge is omitted) and c) dimeric transmetalation intermediates.

Structures with only one ligand coordinated to the copper atom are not influenced by the use of an enantiopure or a 1:1 mixture of the enantiomeric ligands; since the structures (either with **L2** or **L2*** coordinated) represent enantiomers, which are not distinguishable by NMR spectroscopy, so the signal arises with the same integral (see Scheme 3.4 b structures **A**-**C**). In **A** an iodine bridged bimetallic copper-zinc structure occurs with an ethyl group as second bridge. Woodward and co-workers were able to identify a similar structure to the proposed structure **A** by a computational combination of a simplified phosphoramidite ligand, Cu(OAc) and ZnMe$_2$ as lowest energy zinc cuprate by DFT-calculations.[23] While structure **B** represents a Cu**L** fragment with a ZnEt$_2$ moiety attached, structure **C** presents a transmetalation intermediate without any zinc atom. Structures **A** and **C** represent the organozinc structures comparable with the monomeric transmetalation intermediates with Grignard reagents described by Feringa and co-workers.[17] In contrast, if two ligands are coordinated to the copper atom always the possibility of formation of diastereomers with mixed ligand coordination occurs, resulting in a reduction of the signal integral for the same ligand coordination, while one or two new signals appear for the possible mixed coordination (assuming that the different ligand orientations appear with the same probability, see Scheme 3.4 b structure **D**). Beside monomerization of the precatalytic complex structure also dimeric transmetalation intermediates are possible due to the free

coordination site on the trigonal coordinated copper atom in **C2**. The use of the 1:1 enantiomeric mixture of the ligands enables the formation of four possible diastereomers for **C2**, as well as for the dimeric transmetalation intermediates with three ligands (each with 25 % probability, see Scheme 3.4 c structures **E**-**G**). Therefore one diastereomer appears with three times the same ligand enantiomer (identical with the enantiopure sample), while the others represent the mixed diastereomers, in which at least one ligand occurs as the other enantiomer. Overall three different mixed transmetalation intermediates are possible; therefore the probability to get a mixed ligand arrangement is three times higher than for one with enantiopure ligands (see Scheme 3.4 c structures **E**-**G** for the 1:1 mixture of the enantiomeric ligands). This means that in the spectrum of the enantiomeric mixture the signal for the intermediate with the same ligand enantiomer coordinated decreases, while new signals appear for mixed ligand arrangements. For the dimeric transmetalation intermediates three possible structures **E**-**G** occur. Structure **E** represents **C2** with an incorporated $ZnEt_2$ unit, while structure **F** gives the structure for a dimeric species, which only has one ethyl group transferred to the copper atom and the corresponding residue of $ZnEt_2$ as counter ion. In the dimeric structure **G** one of the bridging iodine atoms of **C2** is exchanged by an ethyl group. The existence of transmetalation intermediates with more than three ligands can be excluded, as for them a more sophisticated signal pattern for the possible diastereomers in the enantiomeric mixture would occur, which is not detected in the recorded spectra. Scheme 3.5 gives an overview of the possible "final" monomeric transmetalation intermediates with one or two ligands and of the "final" dimeric transmetalation intermediate with three ligands. Obviously monomeric species with one and two ligands reveal only one phosphorous chemical shift. At first glance it can be expected that for the dimeric species different ^{31}P chemical shifts appear, due to the different position of the ligands in the complex. But the coupling between a phosphorous atom and a further nuclei depends in general on the electronegativity of the coupling partners, the coordination sphere and the corresponding dihedral angel.[40] These properties are identical in the four diastereomers of the dimeric transmetalation intermediate with three ligands. But the strength of the coupling between the ethyl group and the three ligands would be different, due to their dihedral angle and the coordination sphere, beyond them one would be preferred and thus the phosphorous chemical shift of the ligand with the highest value for the coupling detected.
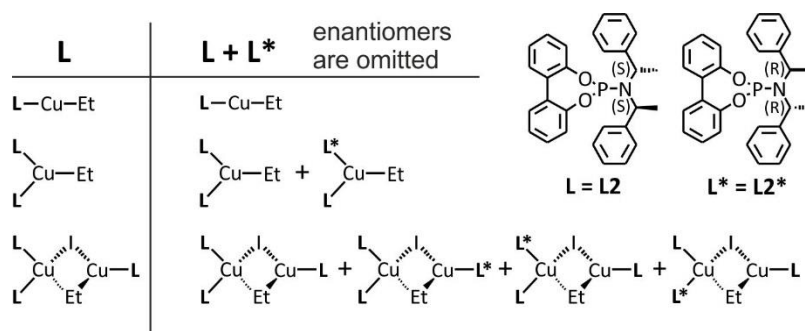
Scheme 3.5: Possible momomeric transmetalation products with one and two ligands and dimeric transmetalation intermediate with three ligands as well as corresponding signal distribution for enantiopure phosphoramidite ligand (**L2**) and enantiomeric mixture of phosphoramidite ligands (**L2** + **L2***). The possible enantiomers are omitted.

In Figure 3.3 a and c the comparison of the 2D $^1H^{31}P$-HMBC spectra of a sample with 2 eq **L2**, 1 eq CuI (a) and of 1 eq **L2**, 1 eq **L2***, 1 eq CuI (c) each with about 15 eq ZnEt$_2$ at low temperature (170 K) is presented. The presence of nearly the same amount of organometallic reagent is important to avoid equivalent dependent formation of intermediates and therefore ensure comparability of the two samples. Indeed, in the 1:1 enantiomeric mixture sample identical cross signal pattern occur with variation in the integrals and some new signals appear.
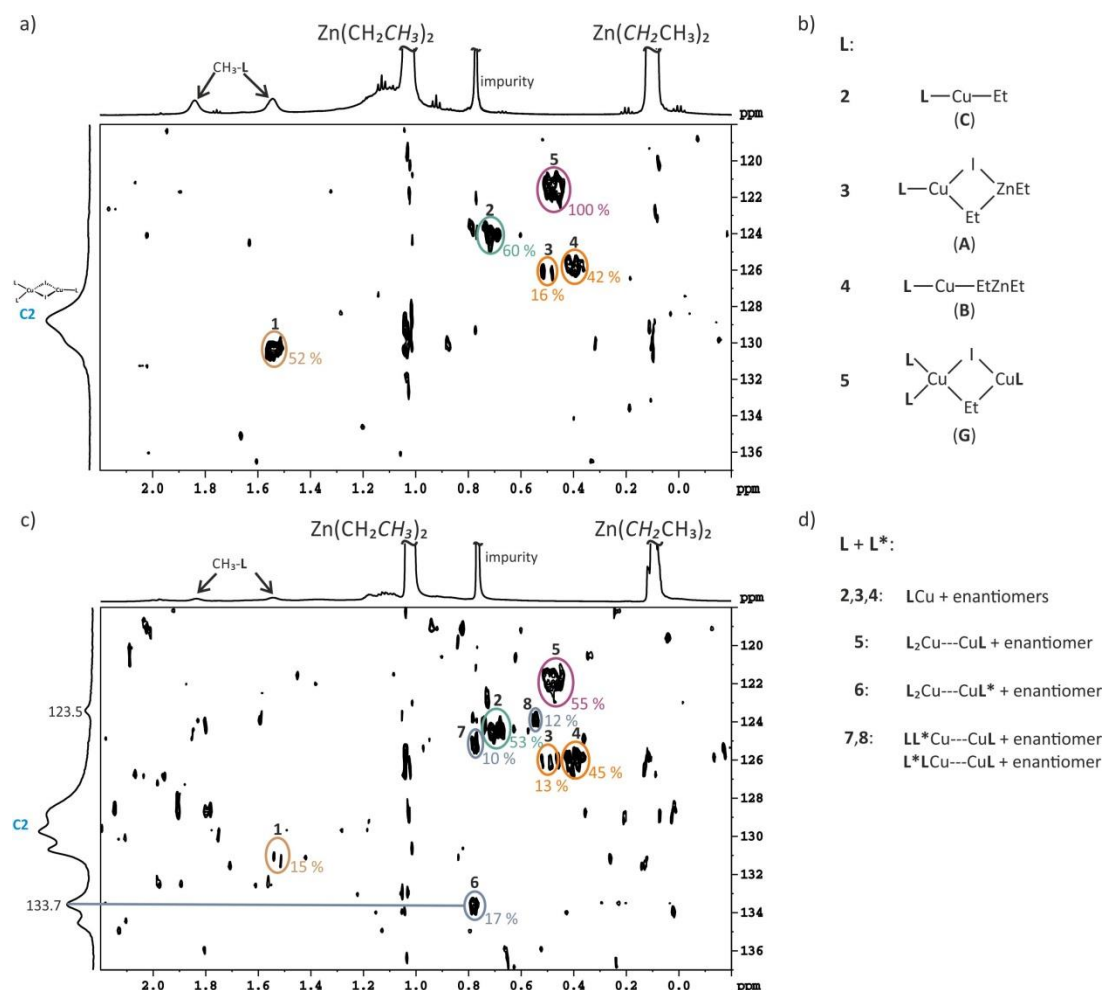
Figure 3.3: 2D $^1H^{31}P$-HMBC spectra of 2 eq **L2**, 1 eq CuI and 14.7 eq ZnEt$_2$ (a) and of 1 eq **L2**, 1 eq **L2***, 1 eq CuI and 14.5 eq ZnEt$_2$ (c) at 170 K in CD$_2$Cl$_2$. The signal intensities referenced to signal 5 of the enantiopure sample are written beside the corresponding signal. Therefore the intensity of signals 2-4 is nearly identical, while signals 1 and 5 diminishes and signals 6-8 appear new in the enantiomeric mixture. For structure assignment (b and d) see below.

Three classes of signals occur in the spectra of the 1:1 enantiomeric mixture. Already detected ones with comparable integrals within the experimental error (signals 2-4), some with diminished intensities (signal 1 and 5) and completely new ones (signals 6-8) appear, which were a priori proposed as structures with a mixed arrangement of the ligand enantiomers. Based on this intensity patterns signals 2-4 were identified as structures with one ligand, while the others either have two or three ligands coordinated to the copper atom. Therefore for signal 2 (0.72 to 124.2 ppm), signal 3 (0.50 to 126.0 ppm) and signal 4 (0.41 to 125.6 ppm) the monomeric structures **A**-**C** were proposed. For signal 5 (0.48 to 121.5 ppm) the intensity is reduced by a factor of two compared to the enantiopure sample, this is only possible if at least two ligands are coordinated to the copper atom. Hence the monomeric structure **D** with two ligands, as well as the dimeric structures **E**-**G** with three ligands bound to the copper atoms are supposed. A differentiation between these possible structures is only feasible by the new appearing signals in the enantiomeric mixture. Furthermore the sum of the integrals for signal 5 and the new

appearing ones should achieve almost 100 %, due to the separation of one of the dimeric species **E**-**G** into different signals for the four possible diastereomers. Structure **D** was excluded for signal 5, as either one or two new signals are expected for the mixed ligand arrangement diastereomers, depending if the mixed arrangements can be distinguished by NMR spectroscopy or not. Therefore an integral pattern of 50:50 or 50:25:25 is expected, which are both not observed, even if the spectra quality enables it. In contrast the appearing signal pattern of one reduced and three new appearing signals fits exactly to a dimeric transmetalation intermediate with three ligands (see structures **E**-**G** in Scheme 3.4). At first glance the integral distribution of signals 5-8 is puzzling, because a statistical structure distribution of 25 % for all four diastereomers is expected under the assumption of identical interligand interactions for **LL** and **LL*** (see Scheme 3.4). In previous and ongoing investigations we already detected a general affinity of the phosphoramidite ligands to create noncovalent interligand interactions in transition metal complexes[32,41,42] and a distinct preference for special ligand combinations.[41–43] Signal 5 appears over statistically with 55 % in the enantiomeric mixture, representing strong preference for the formation of structures with enantiopure ligand coordinated at one copper atom. Due to the fact, that the signal occurs in both samples it is assigned to one of the dimeric structures **E**-**G** with three times the same enantiomeric ligand. Such a preferred formation of intermediates with the same ligand enantiomer coordinated at one copper atom is also expected, but on a lower level for the possible diastereomers of **E**-**G** with mixed ligand arrangement. This is in agreement with the integrals of new appearing signal 6 (0.78 to 133.5 ppm), signal 7 (0.78 to 124.9 ppm) and signal 8 (0.54 to 123.7 ppm), which occur with 17 %, 10 % and 12 % and were assigned to the corresponding diastereomers of the dimeric structures **E**-**G** with a mixed coordination of the ligand enantiomers. Furthermore it is supposed that signal 6 represents the dimeric structure with Cu**L$_2$** bound to the tetragonal coordinated copper atom, while signal 7 and 8 present the mixed coordination of **L** and **L*** at the tetragonal coordinated copper atom. In addition the sum of the integrals of signals 5-8 is with 94 % a strong evidence that these four intermediates in the enantiomeric mixture indeed originate from intermediate 5 in the enantiopure sample (100 %). Among the dimeric structures **E**-**G** we assume that most likely **G** is formed, because a separation of ZnEtI seems to be more probable, due to the big difference of the enthalpy of formation (CuI: -67.8 kJ, ZnI$_2$: -208 kJ).[44] The spectra quality and signal separation of the ^{1}H NMR spectra are too low to differentiate between signals for ZnEt$_2$ and ZnEtI, because both compounds have quite similar proton chemical shift values ($\Delta\delta$ = 0.2 ppm)[45] therefore also a formation of ZnEtI is not detectable. In addition to signal 5 also signal 1 shows a decreased intensity in the enantiomeric mixture sample. The proton and

phosphorous chemical shifts of signal 1 (1.54 and 130.3 ppm respectively) are assigned to a ligand-ZnEt$_2$ interaction product in which one P-O bond of the biphenol backbone is cleaved and an ethyl group directly transferred to the phosphorous atom (structure **L4** see Scheme 3.6), this is in analogy to investigations on interactions of ZnMe$_2$ and parts of structural characteristics of the ligand (see Chapter 3.5). A signal reduction for the enantiomeric mixture is only possible if the decomposed ligand **L4** is involved in a copper complex, otherwise according to the Cu**L** containing structures no intensity loss occurs. On this account we assume that signal 1 refers to a copper complex of **L4**, probably with three ligands. Using the enantiomeric mixture of the phosphoramidite ligand **L2** and **L2*** and this new occurring ligand **L4** seven ligand arrangements are possible, one with three times **L4**, three with two times **L4** and one of the phosphoramidite enantiomers and three for complexes with **L4**, **L2** and **L2***, each with about 14 % probability (for possible ligand arrangements see supporting information, Chapter 3.7).
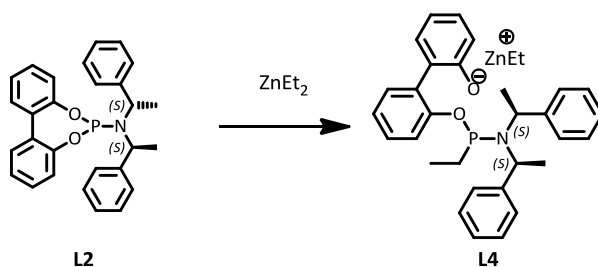
Scheme 3.6: Decomposition product **L4** after addition of ZnEt$_2$ to **L2**, one P-O bond of the biphenol backbone is cleaved and one ethyl group directly transferred to the phosphorous atom.

Next, further information concerning the structure of the transmetalation intermediates was collected. Until now we were able to identify signals 2-4 as monomeric species **A**-**C** with one ligand coordinated to the copper atom, while signal 5 represents one of the dimeric structures **E**-**G** with three ligands. Still the question arises if a ZnEtI unit is involved in the structure of the transmetalation intermediates or not. Basically a CuI bond has a distinctly lower energy than a ZnI bond, this is due to the different enthalpies of formation.[44] In contrast to other organometallic reagents diorganozinc reagents are monomeric, while the corresponding ZnRX compounds build dimeric, trimeric or tetrameric structures with M-X-M bonds.[46] Contrary to other organometallic reagents, a selective removal of zinc in the presence of copper is not possible, due to the missing of a selective additive (e. g. MeLi, removal of lithium by addition of 12-crown-4 ether, MeMgBr, removal of magnesium by addition of dioxane[17]). Therefore the equilibrium is forced towards structures with a zinc iodide unit involved by the addition of an excess of ZnI$_2$. The expected effect is an increase of the signal intensity for transmetalation intermediates having a zinc iodide unit included, while a decrease occurs for those without. In the ^{31}P NMR spectra slight changes occur after ZnI$_2$ addition in the intensities. The amount of

ligand decreases little bit, while the signals for **C2** and the signal at 125.1 ppm increases little bit (data not shown).
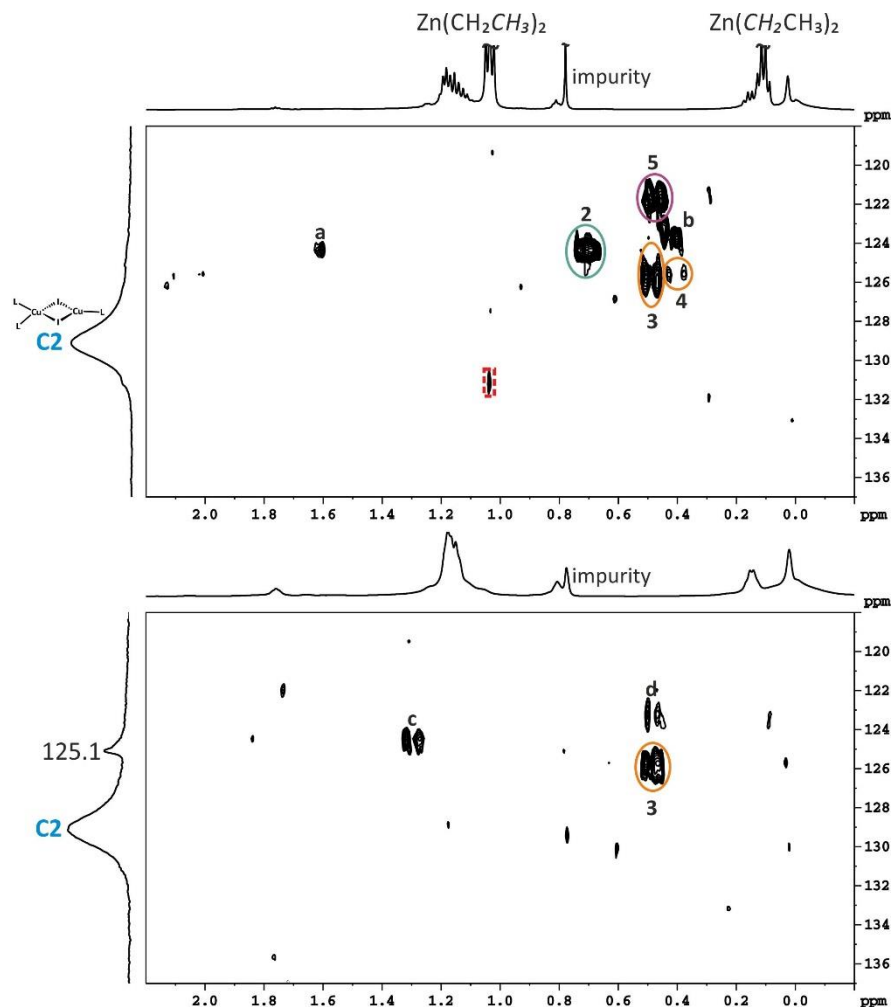
Figure 3.4: 2D ^{1}H^{31}P-HMBC spectra of 2 eq **L2**, 1 eq CuI and 7.7 eq ZnEt$_2$ before (top) and after (below) addition of an excess of a ZnI$_2$ solution at 180 K in CD$_2$Cl$_2$. After addition of the zinc salt solution only signal 3 remains and two new signals c and d appear.

In Figure 3.4 the 2D ^{1}H^{31}P-HMBC spectra of a sample with 2 eq **L2**, 1 eq CuI and 7.7 eq ZnEt$_2$ are shown before (top) and after (below) addition of an excess of a ZnI$_2$ solution. After the addition of ZnI$_2$ only signal 3 remains, implying that signal 3 is the only transmetalation intermediate with a ZnI unit incorporated. Therefore signal 3 was assigned to monomeric structure **A**, with an iodine and an ethyl bridge between the copper and zinc atoms. Conversely signals 2, 4 and 5 are without a ZnI unit. For signals 2 and 4 monomeric structures **B** and **C** are supposed. An assignment is feasible by the proton chemical shift, because for structures including a zinc atom a highfield shifted signal for the CH$_2$ group is expected, due to the second metal atom increasing the electron density on the CH$_2$ group. Signal 2 is shifted 0.3 ppm lowfield compared to signal 4. Therefore signal 2 is assumed as structure **C**, while signal 4 as structure **B**. After addition of ZnI$_2$

signal 5 vanishes, therefore no ZnI unit is incorporated. This excludes dimeric structure **E**. The existence of a halogen bridge in the dimeric structure was proven by further investigations with CuCl as salt. Therein no identical signal as for CuI was observed in the 2D $^1H^{31}P$-HMBC spectra (see Chapter 3.3.1). Furthermore the CuCl investigations enables to exclude two ethyl groups bound to the copper atom, as they would appear with a distinct highfield shift (see Chapter 3.3.4). The differentiation between the proposed structures **F** and **G** for signal 5 is possible by the formation trends of the transmetalation intermediates, depending on the equivalents of $ZnEt_2$ added (see Figure 3.5). The formation trends of the monomeric species reveal, that structures **A** and **B** containing ZnEt units are formed preferred with small amounts of $ZnEt_2$. While the "final" transmetalated species **C** without a ZnEt moiety accumulates with higher amounts of $ZnEt_2$. Provided that the same formation trends appear also for the dimeric transmetalation species, as similar intensity trends occur for signal 2 and 5, signal 5 was assigned to the "final" transmetalation intermediate **G** without a ZnEt unit. This structural assignment confirms the previous assumption of most likely formation of **G**, due to the bond energies. In structure **G** the typical structural characteristics of the binuclear precatalytic system with mixed trigonal/tetrahedral coordination of the copper atoms is preserved. Thus the new appearing signals 6-8 of the enantiomeric mixture represent the corresponding diastereomers of **G** with mixed ligand arrangements.
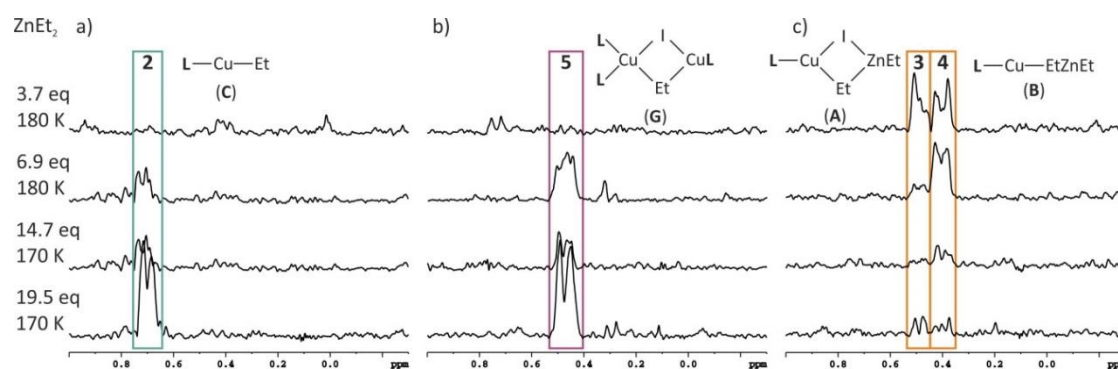
Figure 3.5: 1D rows of the 2D $^1H^{31}P$-HMBC spectrum of 2 eq **L2** and 1 eq CuI for signal 2 at 124.2 ppm (a), signal 5 at 121.5 ppm (b) and for signal 4 at 125.6 ppm (c) with 3.7, 6.9, 14.7 and 19.5 eq $ZnEt_2$ at 170 and 180 K respectively in CD_2Cl_2. The formation trends of the transmetalation intermediates reveal intermediates 3 and 4 as precursors, whereas 2 and 5 build the final transmetalation intermediates.

This study has shown that with a 2:1 mixture of either enantiopure or enantiomeric mixture of phosphoramidite ligands **L2/L2*** and CuI a direct experimental detection of various transmetalation intermediates is possible with 1D and 2D $^1H^{31}P$-HMBC experiments, even if no signal is observed in the 1D ^1H and ^{31}P NMR spectra. Two monomeric transmetalation intermediates were identified without a zinc iodide unit involved and one monomeric species with a zinc iodide unit. All three structures have only one ligand coordinated to the copper atom.

The existence of monomeric species with one ligand is in agreement with results of Feringa and co-workers, investigating the addition reaction of Grignard reagents to copper diphosphine complexes and the structure of the corresponding transmetalation intermediates.[17] Their obtained structures are in accordance with structures **A** and **C** observed in this structure elucidation study. Interestingly, neither in the here presented study nor in the previous study of Feringa a monomeric transmetalation intermediate with two ligands bound to the copper atom was detected, even if such structures are often proposed in mechanistic schemes.[1,5,26] For the first time a direct spectroscopic proof of a dimeric transmetalation intermediate, which maintains the mixed trigonal/tetrahedral coordination of the precatalytic complex **C2** upon substitution of one of the iodine bridges by an ethyl bridge, was observed. The mono- and dimeric transmetalation intermediates appear in similar amounts. The facts that, typically a ligand to salt ratio of 2:1 is used in synthetic protocols, the stabilization of **C2** by an excess of ligand and DFT-calculations, performed by Woodward, pointing out that solely dimeric copper complexes revealing a suitable energetic pathway, indicating all that the dimeric transmetalation intermediate, acts as the reactive one beyond the detected ones.

3.3.2 Investigation of a 1:1 mixture of L2 and CuI and their transmetalation intermediates with ZnEt$_2$

Previous studies of the Gschwind group showed the dependence of the different complex species on the solvent, temperature and ligand to salt ratio.[20] In order to investigate the influence of the ligand to salt ratio on the formed transmetalation intermediates and to control if one is built preferably with lower ligand to salt ratios, a sample with 1 eq **L2** and 1 eq CuI was prepared.

Figure 3.6 represents a comparison of the temperature dependent ^{31}P NMR spectra. At 145.6 ppm a small signal for free ligand **L2** occurs. At 129.2 and 122.6 ppm complexes **C2** and **C1** respectively are detected. While the amount of free ligand is nearly constant, the intensities of **C2** and **C1** vary with different temperatures. At 230 K nearly a 1:1 ratio of them occur, this indicates a poorer solubility of **C1** with CuI as copper source compared to CuBr or CuCl.[20,47] Further reducing of the ligand to salt ratio,[20] longer reaction times and even the warming of the sample to 20 °C during synthesis achieved not the desired success of changing the complex ratio completely to **C1** and therefore exclusive formation of transmetalation intermediates with one ligand coordinated to the copper atom. Even if these reaction conditions influence the complex ratio, it is not possible to detect with the NMR parameters used, because at 230 K the 1:1 ratio of **C1** and **C2** is reset. This is an example for the high sensitivity of these systems towards the

used conditions.[17,20–22,24] In order to shift the ratio towards the **C1** complex, to get mainly Cu**L** containing transmetalation intermediates, temperature was increased. At 240 K the ratio of **C2**:**C1** already raises to 1:1.7 for **C1**, further increase of 10 K yield in a 1:2.3 ratio for **C1**. Apart from free ligand and the complexes a further signal arises at 104.5 ppm with lowering amount at higher temperatures. For the addition of ZnEt$_2$ 250 K was chosen, because there the highest amount of **C1** occurs, and in former studies we were already able to detect transmetalation intermediates in a 2:1 ligand to salt sample of the precatalytic system and ZnEt$_2$ (see Figure 3.1).
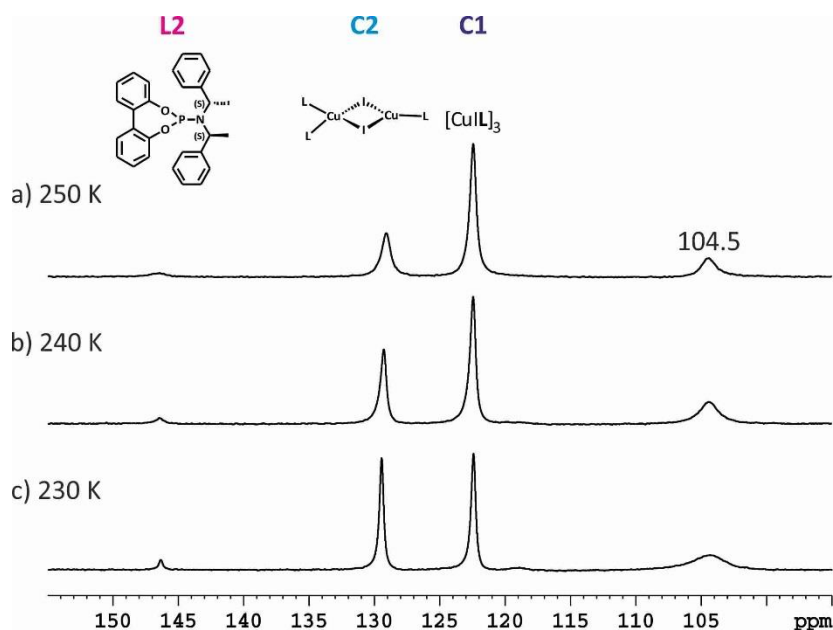
Figure 3.6: Temperature dependent ^{31}P NMR spectra of a 1:1 mixture of **L2** and CuI at a) 250 K, b) 240 K and c) 230 K in CD$_2$Cl$_2$. Resonances occur at 145.6 ppm for **L2**, 129.2 ppm for **C2**, 122.6 ppm for **C1** and a new signal at 104.5 ppm.

After the addition of 11.7 eq ZnEt$_2$ compared to **C1**, no significant changes occur in the [31]P (see Figure 3.7 a and b) and ^{1}H NMR spectra, beside the signals for ZnEt$_2$, also in the 2D [1]H[31]P-HMBC spectra no cross signals were accessible at 250 K. In the 1D [1]H[31]P-HMBC spectra for the differentiation of magnetization transfer via scalar coupled groups and cross correlation, only signals for unspecific interactions of ZnEt$_2$ were observed. The missing of cross signals with the 1:1 ligand to salt ratio directly after addition of ZnEt$_2$ is a further proof for the detrimental reaction of ligand to salt ratios lower than 1.5:1. Therefore the sample was stored at -80 °C, in order to extend the reaction time and measured again three weeks later. Indeed, in the ^{31}P NMR spectrum two new signals appear at 125.0 and 118.5 ppm at 250 K (Figure 3.7 c). In addition low temperature measurements were performed at 180 K (Figure 3.7 d). Therefore some changes in the ^{31}P NMR spectra are visible, the signal for **L2** becomes sharper, while the signal for **C2** broadens and is getting bigger, due to remaining ligand exchange contributions and temperature dependent complex interconversion processes. In contrast the signal for **C1** decreases, due to

the temperature dependent existence of the complex only above 220 K.[22] Furthermore the signal at 104.5 ppm becomes broader and splits into two signals at low temperature.
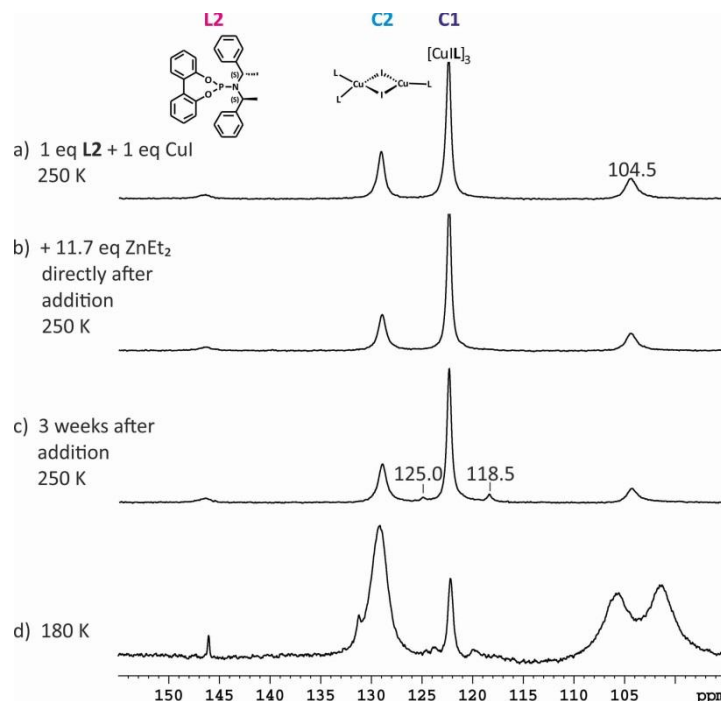
Figure 3.7: Comparison of ^{31}P NMR spectra of a mixture containing a) 1 eq of **L2** and 1 eq of CuI, b) directly after addition of 11.7 eq ZnEt$_2$ compared to **C1** or 27.5 eq compared to **C2**, c) after storage for three weeks in the freezer (-80 °C) at 250 K in CD$_2$Cl$_2$ and d) the spectra of the stored sample at 180 K.

In the 2D [1]H[31]P-HMBC spectrum at 180 K cross signal 2 occurs from 0.71 to 124.1 ppm (see Figure 3.8 below green circle), which also generates a signal in the 1D [1]H[31]P-HMBC spectra for the detection of magnetization transfer via scalar coupling. This cross signal also appearing in a 1:1 ligand to salt sample, confirmed the identification as monomeric structure **C** with one ligand and an ethyl group at the copper atom in the 2:1 mixture of **L2** and CuI.
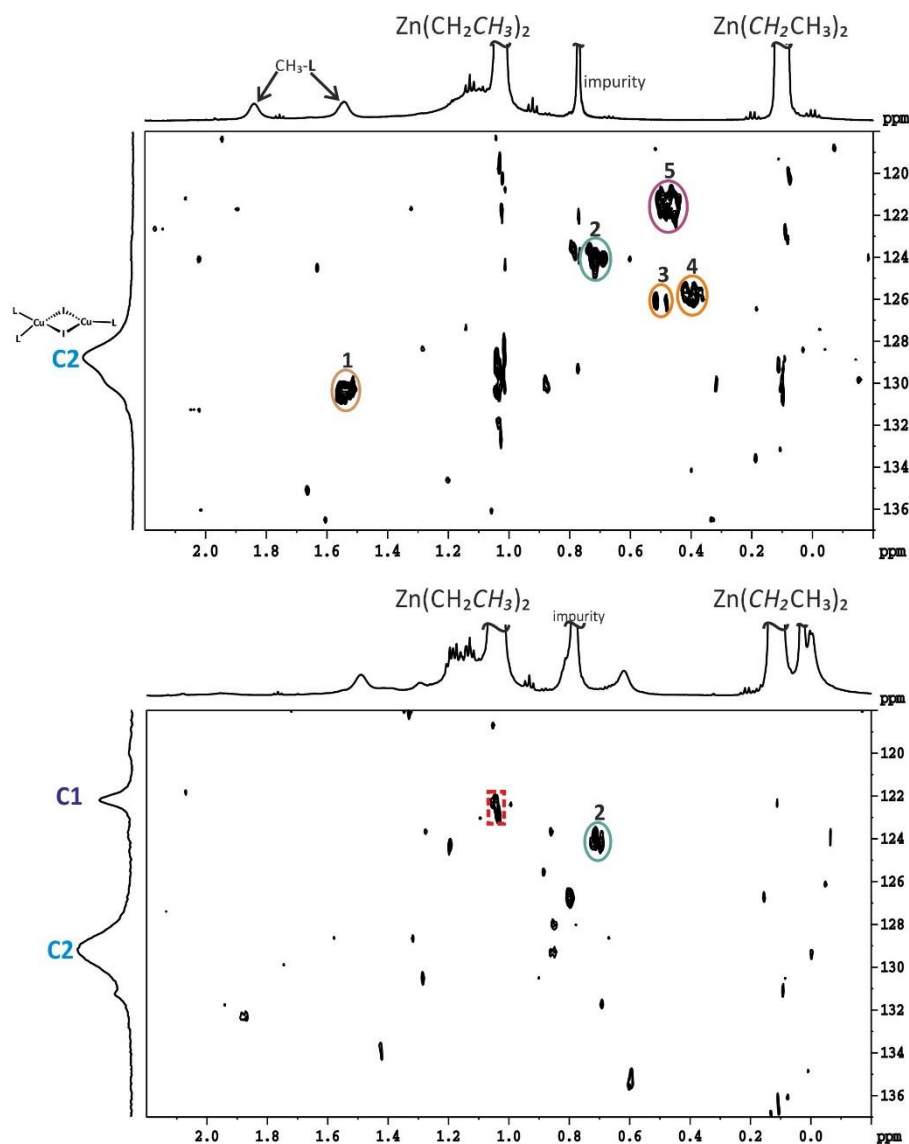
Figure 3.8: 2D $^1H^{31}P$-HMBC spectra of 2 eq **L2**, 1 eq CuI and 14.7 eq ZnEt$_2$ at 170 K (top) and with 1 eq **L2**, 1 eq CuI and 27.5 eq ZnEt$_2$ compared to **C2**, which represents 11.7 eq ZnEt$_2$ compared to **C1** at 180 K (below), both in CD$_2$Cl$_2$.

This chapter has demonstrated that with 1 eq **L2** and 1 eq CuI also the monomeric transmetalation species **C** with one ligand and an ethyl group coordinated to copper is detected. The existence of this intermediate also in a 1:1 sample, which is known to be detrimental for the outcome of the reaction, suggests, that the appearance of this monomeric species results in a reduced activity. Due to the low solubility of the 1:1 complex with CuI it is not possible to investigate **C1** separately and therefore corresponding transmetalation intermediates.

3.3.3 Investigation of a 2:1 mixture of L2 and CuCl and their transmetalation intermediates with ZnEt$_2$

In 2002 Alexakis and co-workers showed that the enantiomeric excess of the investigated conjugate addition reaction is highly sensitive towards the nature of the used copper salt.[26] Therefore in a previous study Gschwind *et al.* investigated the influence of the copper salt on the structure of the precatalytic complex.[20] Among other salts CuCl was chosen, due to high *ee*-values and excellent conversions obtainable in different solvents in combination with phosphoramidite ligand **L2**.[26] With CuCl it is possible to detect either **C1** or **C2** with a 1:1 and 2:1 ligand to salt ratio respectively.[20] In order to investigate if this sensitivity towards the used copper salt influences the structure of the transmetalation intermediates or to get an explanation for different reactivities, samples with CuCl as copper source, phosphoaramidite ligand **L2** and ZnEt$_2$ were prepared. Figure 3.9 compares the ^{31}P NMR spectra of a 2:1 mixture of **L2** and CuCl at 230 (top), 180 (middle) and 170 K (below). At 230 K relatively broad signals occur for **L2** (146.3 ppm), **C2** (127.1-126.1 ppm) and a further small signal appears at 121.6 ppm. By cooling the sample, line width is narrower for the free ligand and becomes broader for the complexes, due to still existing ligand exchange processes.[22] At 170 K three small signals appear lowfield shifted to **C2** (130.9, 129.8 and 128.1 ppm). In previous investigations we found, that the best resolved spectrum at low temperatures are obtained with CuI in combination with **L2**, due to the identification of two separated low temperature species (**C2** and **C3**). The signal pattern of the Cu**LL'** unit with CuI is also partially but in different resolution detected in the low temperature ^{31}P NMR spectrum of the CuCl sample.[22]
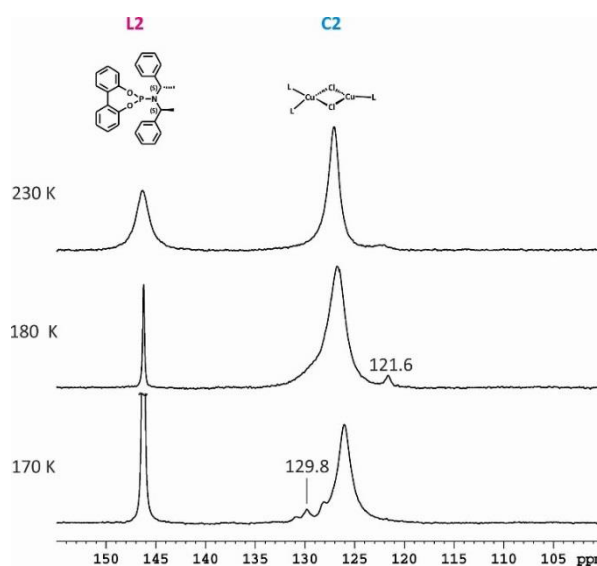

Figure 3.9: ^{31}P NMR spectra of 2 eq **L2** and 1 eq CuCl at 230 (top), 180 (middle) and 170 K (below) in CD$_2$Cl$_2$. Signals appear at 146.3 ppm for **L2** and 127.1-126.1 ppm for complex **C2**. Beside them occurs a small signal at 121.6 ppm at 180 and 230 K. At 170 K three small signals arises lowfield shifted to **C2** (130.9, 129.8 and 128.1 ppm).

After addition of $ZnEt_2$ only slight changes occur in the ^{31}P NMR spectra. In Figure 3.10 two samples are represented, one with a stoichiometric amount of $ZnEt_2$ (b) and one with 10 eq of $ZnEt_2$ (d). In both samples a new signal arises at 131.2 ppm. In the latter sample a further signal appears at 121.6 ppm in the complex mixture, after $ZnEt_2$ addition this signal decreases and a new one arises at 119.9 ppm. In contrast the ^{31}P NMR spectra of CuI samples show no further signals after $ZnEt_2$ addition besides the complexes and free ligand. In a previous investigation with CuCl and $ZnMe_2$ release of the ligand was observed,[48] in contrast only a minimal contribution is observed here, due to only slight increase in the signal intensity of **L2** within the experimental error (plus 6 % for 1 eq $ZnEt_2$ and plus 3 % for 10 eq $ZnEt_2$).
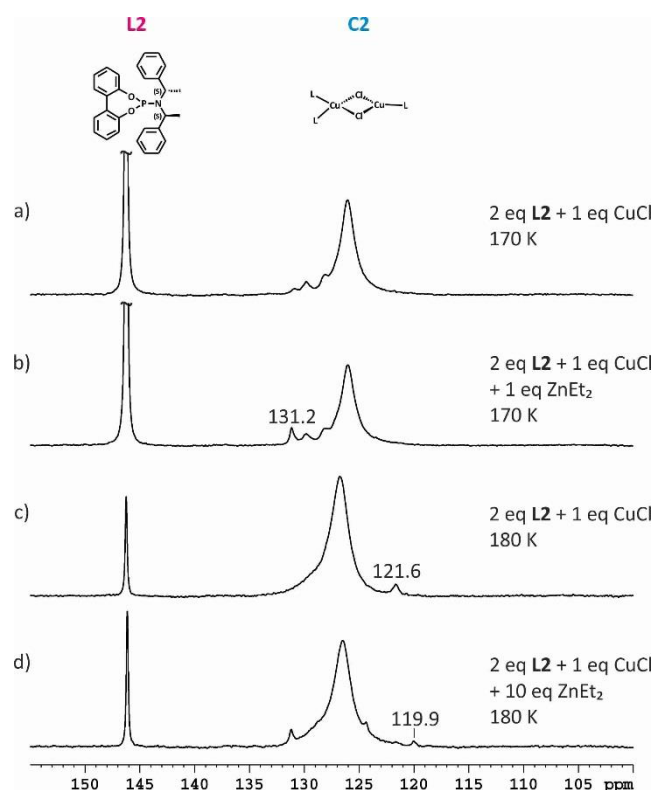
Figure 3.10: ^{31}P NMR spectra of a 2:1 mixture of **L2** and CuCl before (a) and after (b) addition of 1 eq $ZnEt_2$ at 170 K and before (c) and after (d) addition of 10 eq $ZnEt_2$ at 180 K in CD_2Cl_2. In both samples only slight changes are visible after addition of the organometallic reagent.

Nevertheless in the 2D $^{1}H^{31}P$-HMBC spectra of both samples at low temperature (170 and 180 K) some new cross signals were detected (Figure 3.11 and Figure 3.12), even if no signal is visible in the 1D ^{31}P and ^{1}H NMR spectra. Four signals occur in the expected peak range of transmetalated ethyl groups, see signals I-IV (red box in Figure 3.11), e. g. literature known chemical shifts for CH_2 of ethyl groups bound directly to a Cu(I)/Cu(III) atom are between 2.31 and -0.54 ppm.[34–36] In contrast the phosphorous chemical shift of signal V only possess cross signals to splitted methine groups, due to low temperature and therefore reduced rotation of the C-N bonds in the amine side chain.[32] Furthermore unspecific interactions to $ZnEt_2$ as described in Chapter 3.3.1

only occur in the sample with higher amount of ZnEt$_2$ to free ligand (see Figure 3.12 red dashed box). Indeed, the proton and phosphorous chemical shift range of the proposed transmetalation intermediates are in a comparable shift range as in the CuI samples. It seems plausible to assume that no identical transmetalation intermediates are formed, due to the missing of identical cross signals for both copper salt samples. Furthermore we can suppose that with CuCl the tendency for the formation of dimeric transmetalation intermediates is higher than with CuI, because the enthalpy of formation for CuCl with -137 kJ is almost double that of CuI (-67.8 kJ).[44] Therefore breakup of the chloride bridges would be more difficult and the existence of monomeric species with one or two ligands coordinated to copper, as described for CuI (structures **A**-**D** in Scheme 3.4 a) would not be preferred. Consequently the dimeric species **E**-**G** are more likely for CuCl (see Scheme 3.7) compared to monomeric species. Among them structure **G** is supposed to be the most probable one, because similar to the CuI sample, the ZnCl bond is more stable than the CuCl bond, and therefore an involvement of a ZnCl unit in the transmetalation intermediate structure is unfavored (enthalpy of formation for CuCl -137 kJ and for ZnCl -415 kJ[44]).
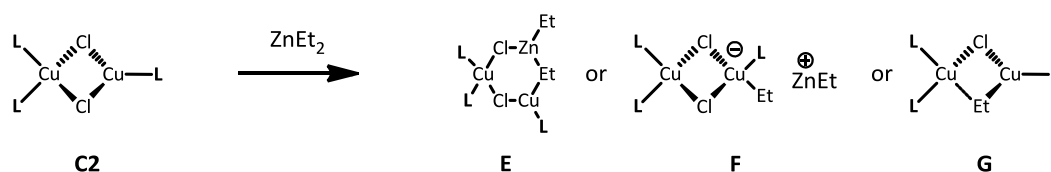
Scheme 3.7: Proposed dimeric transmetalation intermediates **E**-**G** with three ligands coordinated to the copper atoms, formed by transmetalation of **C2** with ZnEt$_2$.

In the 2D ^{1}H^{31}P-HMBC spectra, with 1 eq and 10 eq ZnEt$_2$ respectively, the phosphorous chemical shifts of signals I and II (0.90 to 114.6 ppm and 0.29 to 118.3 ppm respectively) possess no further cross signals. These two signals will be discussed later. Signal III represents a cross signal between 0.43 and 123.6 ppm. Also a signal in the 1D ^{1}H^{31}P-HMBC spectrum for the detection of magnetization transfer via scalar coupling and none in the spectrum for cross correlation is observed (see Figure 3.13 a and c). As this is expected for transmetalated ethyl groups, it was assigned to the CH$_2$ of a directly bound ethyl group. At the ^{31}P chemical shift of signal III further cross signals to 5.03 and 4.38 ppm were detected. These two signals represent the methine protons of the amine side chain, typically separated into two signals at low temperature, so also an intact amine side chain of the ligand is involved in the structure of signal III. Signal IV represents a cross signal between 0.80 and 122.4 ppm, which also gives a signal in the spectrum for detection of scalar coupling (beyond the threshold of the presentation in Figure 3.13). In contrast with a higher amount of ZnEt$_2$ signal VI arises (0.03 to 119.9 ppm). Further cross signals

appear at 4.99 and 4.57 ppm and to some aromatic protons. The phosphorous chemical shift of 119.9 ppm represents the new emerging signal in the ^{31}P NMR spectrum. Also for VI a signal in the 1D [1]H[31]P-HMBC spectrum for magnetization transfer via scalar coupling was identified at 0.03 ppm (see Figure 3.13 c), which is compared to signal III 0.40 ppm shifted to highfield. Based on these signals for VI a transmetalated ethyl group and a complete ligand, due to cross signals to the methine groups (4.57 and 4.99 ppm) as well as to aromatic protons were identified as structural characteristics. For signal V (4.18 to 131.2 ppm) one further cross signal was detected at 4.76 ppm, the ^{1}H chemical shifts belong to methine groups and are quite similar to those of free ligand (4.79 and 4.21 ppm). Whereas signals I, II and V occur in both samples, for signals III, IV and VI significant differences arise. Besides varying quantities of $ZnEt_2$ also various amounts of free ligand appear in the two samples, although identical sample preparation was applied. Previous studies have reported that ligand to salt ratios below 1.5:1 are detrimental for the reaction outcome and the best to use is a 2:1 ratio.[10,25] This is in agreement with investigations of Gschwind *et al.* which show the ligand to salt dependent existence of the copper complexes **C1** and **C2**, while the first one decreases with a higher amount of ligand, the latter one increases at ratios higher 1.5:1, representing the active precatalyst. As consequence also an increased amount of free ligand occurs, with a kind of stabilizing effect for the precatalytic system.[21] In the sample with 1 eq $ZnEt_2$ a quite high amount of free ligand (51 %) occurs, resulting in the appearance of signals III and IV. In contrast the sample with 10 eq $ZnEt_2$ contains only a small amount of free ligand (11 %), giving signal VI and a reduced amount of III and IV (actually not detectable). The percentage refers to the ligand distribution in the ^{31}P NMR spectrum in the range of 160.0-100.0 ppm and is just slightly varied after $ZnEt_2$ addition with regard to the precatalytic complex mixture (see above). Taking the ligand to salt dependence into account for the existence of the transmetalation intermediates a stabilization of III and IV by high amounts of free ligand can be assumed, while a destabilization occurs with small amounts of free **L2**. For signal VI it is the other way around, stabilization through small and destabilization through high ligand amounts respectively.
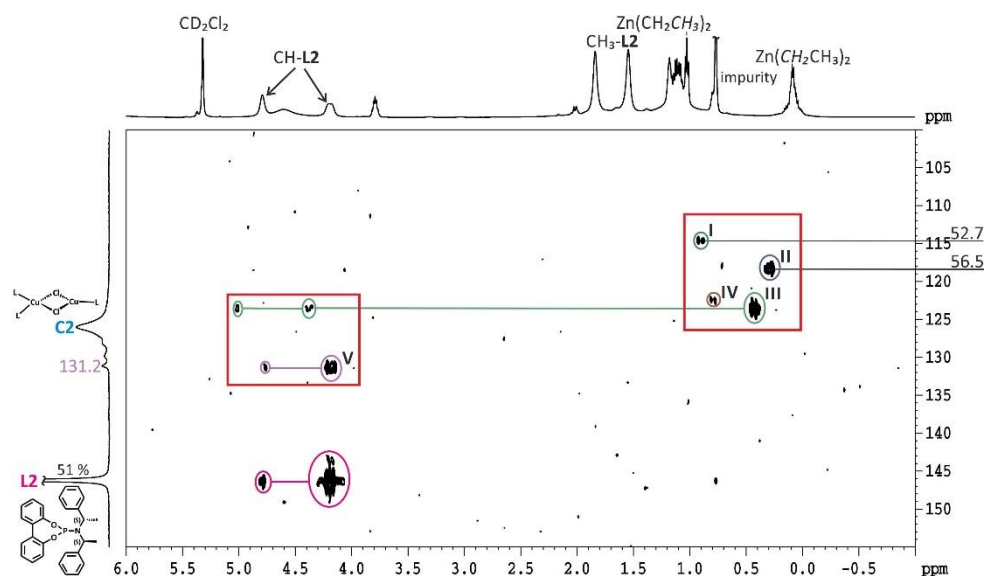
Figure 3.11: 2D ^{1}H^{31}P-HMBC spectrum of 2 eq **L2**, 1 eq CuCl and 1 eq ZnEt$_2$ at 170 K in CD$_2$Cl$_2$. The red boxes highlight new arising signals I-V after the addition of ZnEt$_2$. The low temperature splitting of the methine signals is detected for free ligand **L2** (pink, 146.2 ppm), signal V (light purple, 131.2 ppm) and signal III (green, 123.5 ppm). The signals between 0.20 and 1.00 ppm are in the expected peak range of transmetalated ethyl groups.[34–36] Signals I and II are folded back, therefore the correct phosphorous chemical shift is indicated. The percentage in the ^{31}P NMR refers to the ligand distribution in the range of 160.0-100.0 ppm.
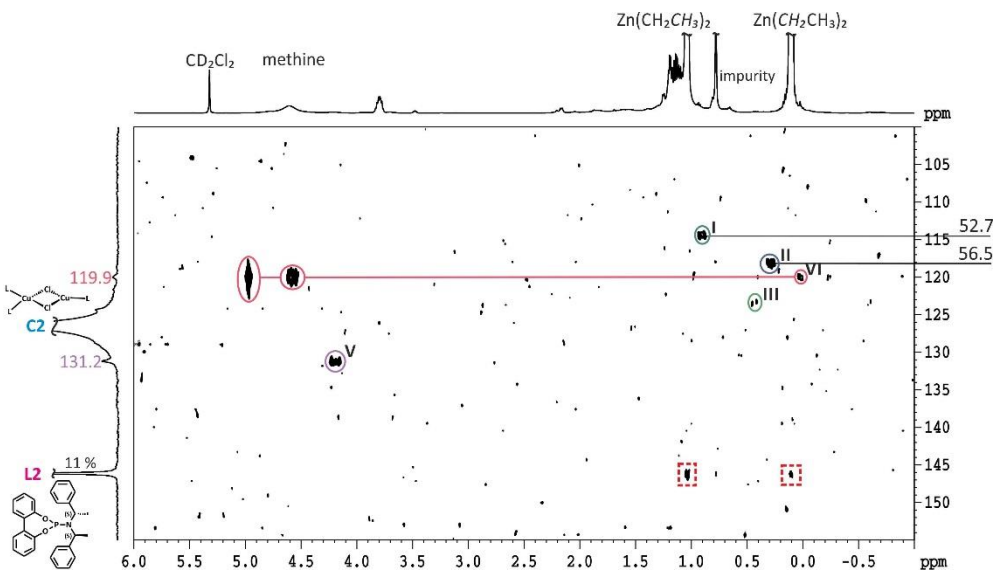
Figure 3.12: 2D ^{1}H^{31}P-HMBC spectrum of 2 eq **L2**, 1 eq CuCl and 10 eq ZnEt$_2$ at 180 K in CD$_2$Cl$_2$. Signals I-III and V were already detected with a smaller amount of ZnEt$_2$. Signal VI arises only with the higher amount of ZnEt$_2$ at a phosphorous chemical shift of 119.9 ppm, where a new signal in the ^{31}P NMR spectrum is detected (light rose). Furthermore for 119.9 ppm signal splitting of the methine groups is detected and unspecific interactions occur between free ligand and ZnEt$_2$ (red dashed boxes). The percentage in the ^{31}P NMR refers to the ligand distribution in the range of 160.0-100.0 ppm.

Figure 3.13: 1D ^{1}H^{31}P-HMBC spectra of 2 eq **L2**, 1 eq CuCl and 1 eq ZnEt$_2$ with magnetization transfer via scalar coupling (a) and cross correlation (b) at 170 K and of 2 eq **L2**, 1 eq CuCl and 10 eq ZnEt$_2$ with magnetization transfer via scalar coupling (c) and cross correlation (d) at 180 K, both in CD$_2$Cl$_2$. With 1 eq ZnEt$_2$ no unspecific interactions to ZnEt$_2$ (d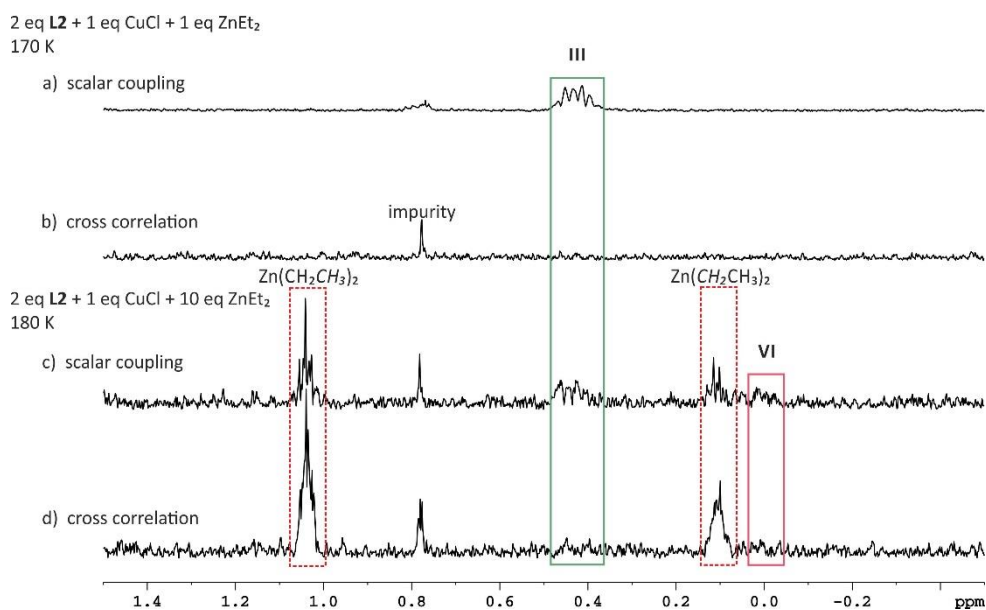ashed red boxes) were detected. In both samples a scalar coupling signal for signal III of the corresponding 2D spectra is detectable (0.43 ppm). In the second sample, with higher amounts of ZnEt$_2$, also scalar coupling is visible for signal VI (0.03 ppm). For signals I and II spectra with scalar coupling signals are presented in the supporting information.

In order to get further insight into the structure of the detected transmetalation intermediates the previous described special approach of using enantiopure and 1:1 enantiomeric mixtures of the phosphoramidite ligands was used for the differentiation between species having varying numbers of ligands coordinated. Due to the missing of signals in the ^{1}H NMR spectrum for the transmetalation intermediates and therefore no application of standard proton based 2D NMR measurements, assignments are exclusively based on 1D and 2D ^{1}H^{31}P-HMBC spectra. For sample preparation an enantiomeric mixture of 1 eq **L2**, 1 eq **L2*** and 1 eq CuCl was used, in order to maintain the overall ligand to salt ratio of 2:1, which achieves the best results in synthetic applications.[10] In Figure 3.14 a the 180 K ^{31}P NMR spectrum of this mixture is shown. Nearly a 1:1 ratio between free ligand and complex **C2** occurs, furthermore compared to the corresponding CuI spectra no low temperature signal splitting for the different ligand groups in **C2**, as well as for the mixed ligand coordination occurs. Directly after the addition of 11 eq ZnEt$_2$ nearly no change emerges in the spectrum (Figure 3.14 b). Measuring the sample after one or two weeks, while storing it in the freezer (-80 °C) results in a slightly decrease of **C2**, an increase of free ligand and the appearance of a resonance at 131.2 ppm, which pertains to signal V of the 2:1 mixture (see Figure 3.14 c and d).
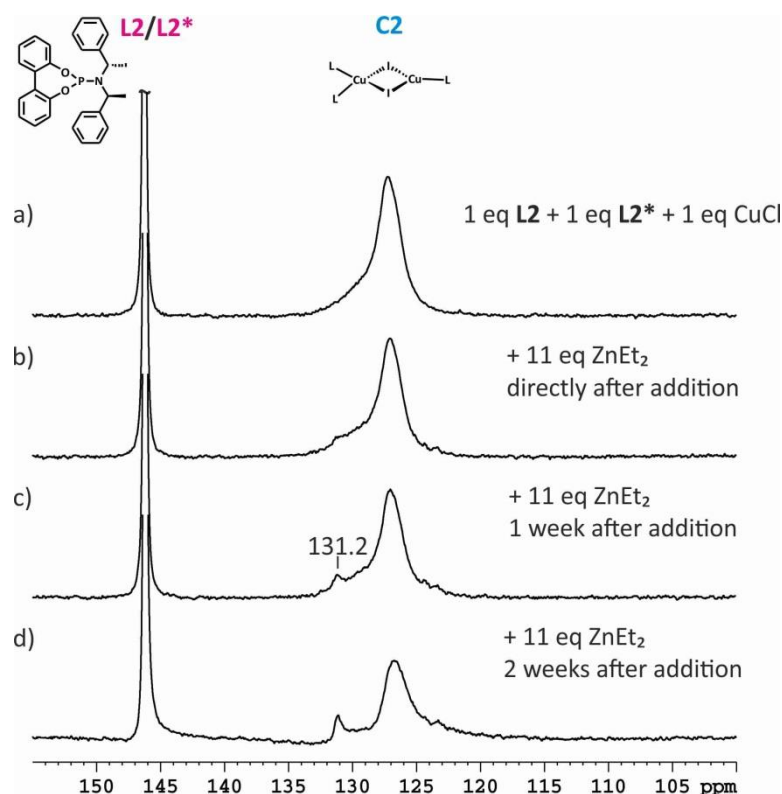
Figure 3.14: ^{31}P NMR spectra of a) 1 eq **L2**, 1 eq **L2*** and 1 eq CuCl, b) directly after addition of 11 eq ZnEt$_2$, c) one week after ZnEt$_2$ addition and d) two weeks after ZnEt$_2$ addition at 180 K in CD$_2$Cl$_2$. At 146 ppm free ligand **L2/L2*** and at 130.0-124.8 ppm **C2** appear. In c) a new signal arise at 131.2 ppm.

Nevertheless some cross signals were detectable in the 2D [1]H[31]P-HMBC spectrum directly after ZnEt$_2$ addition (Figure 3.15). Beside the already observed signals I-IV, a new cross signal VII appears at 0.33 to 119.8 ppm, which is a hint for a mixed coordination of the ligand enantiomers. The chemical shift difference of the ^{31}P signals of I and II compared to the 2:1 mixture is based on a too small chosen spectral window. In order to get better resolution a relative small spectral window (80 ppm) was chosen, signals which lie outside of this range are folded back. This means, that they occur at a different phosphorous chemical shift than their real value. The variation of the spectral window enables identification of back folded signals, because they differ in their chemical shift in the indirect dimension, while real signals remain unchanged. Therefore signals I and II are folded back. By a retrograde calculation the wright spectral window was determined and a second spectrum measured (Figure 3.16). Therein the ^{31}P chemical shift for signal I was revealed at 52.7 ppm and for signal II at 56.5 ppm (anticipated in Figure 3.11, Figure 3.12 and Figure 3.15). For the ^{1}H chemical shifts of signal I (0.91 ppm) and signal II (0.30 ppm) respectively signals in the 1D [1]H[31]P-HMBC spectra for the detection of magnetization transfer via scalar coupling are observed (spectra see supporting information, Chapter 3.7). In addition for both phosphorous chemical shifts further cross signals were detected (signal I: 52.7 to 4.80, 4.56, 2.61 and 1.32 ppm; signal II: 56.5 to 4.83, 4.06, 1.55 and 0.80 ppm). The [31]P

chemical shift range is in agreement with the more electron rich dialkylaminephosphine ligands investigated by Alexakis and co-workers in combination with copper salts and organoaluminum reagents (δ^{31}P for diethylaminephosphine ligand 40.1 ppm in C_6D_6).[49] This ligand class consists of the same amine side chain, as the phosphoramidite ligands and instead of the biphenol backbone two alkyl groups bound to the phosphorous atom. In a further study we also investigate AlMe$_3$ as potential organometallic reagent for copper-catalyzed 1,4-addition reactions with phosphoramidite copper complexes (see Chapter 4.4). Therefore we performed test reactions with dimethylaminephosphine ligands and obtained a lowfield shift for their copper complexes compared to free ligand. This contrary effect to phosphoramidite ligands (complexes appear highfield shifted to free ligand) are based on different electronic properties of the phosphorous atom. Therefore signal I and II were identified as different complex species of diethylaminephosphine ligands, resulting in a side reaction. Hence no signal is observed in the 1D ^{31}P NMR spectrum, we assume, that these structures only occur in very small amounts beyond the NMR detection limit and therefore has no big influence on the reactions outcome. A detailed integral analysis in order to differentiate between structures with one, two or three ligands coordinated to the copper atom was not possible, due to different amounts of free ligand in the enatiopure and enantiomeric mixture. This means that an exclusion of ligand dependent formation of the different species was not possible. However signal VII appear as a new one, indicating a mixed ligand arrangement.

Figure 3.15: 2D ^{1}H^{31}P-HMBC spectrum of 1 eq **L2**, 1 eq **L2***, 1 eq CuCl and 11 eq ZnEt$_2$ at 180 K in CD$_2$Cl$_2$. The red dashed boxes represent unspecific interactions of **L2/L2*** and ZnEt$_2$. The other marked signals I-IV were already detect in a 2:1 ligand to salt mixture with 1 and 10 eq ZnEt$_2$, just signal VII (119.8 ppm light blue) appears as a new signal. In comparison to the 2:1 sample the ^{1}H chemical shift of signals I and II is identical, while the ^{31}P chemical shift differs.
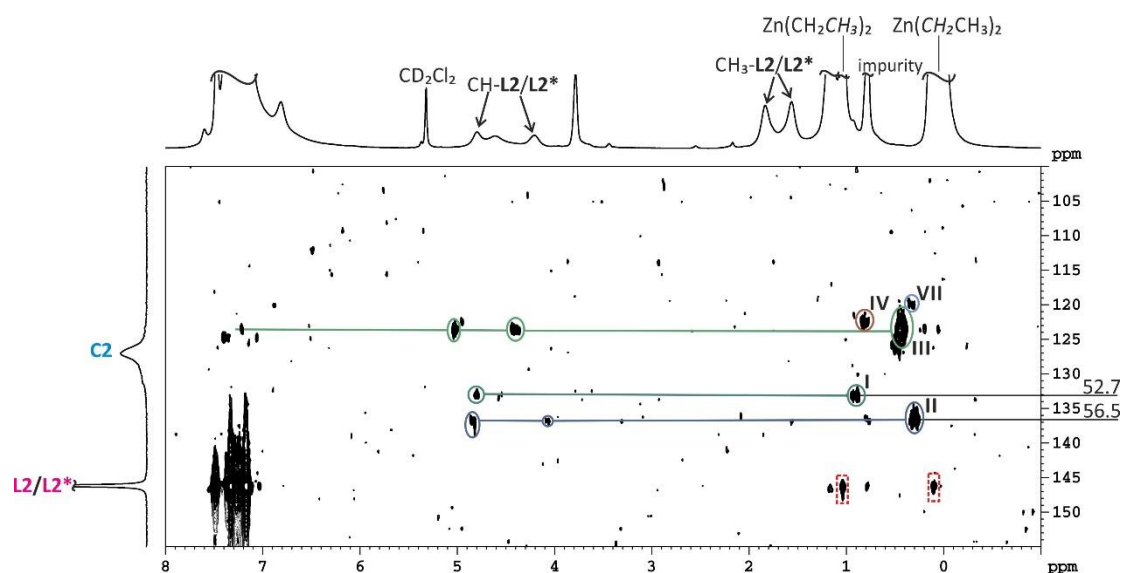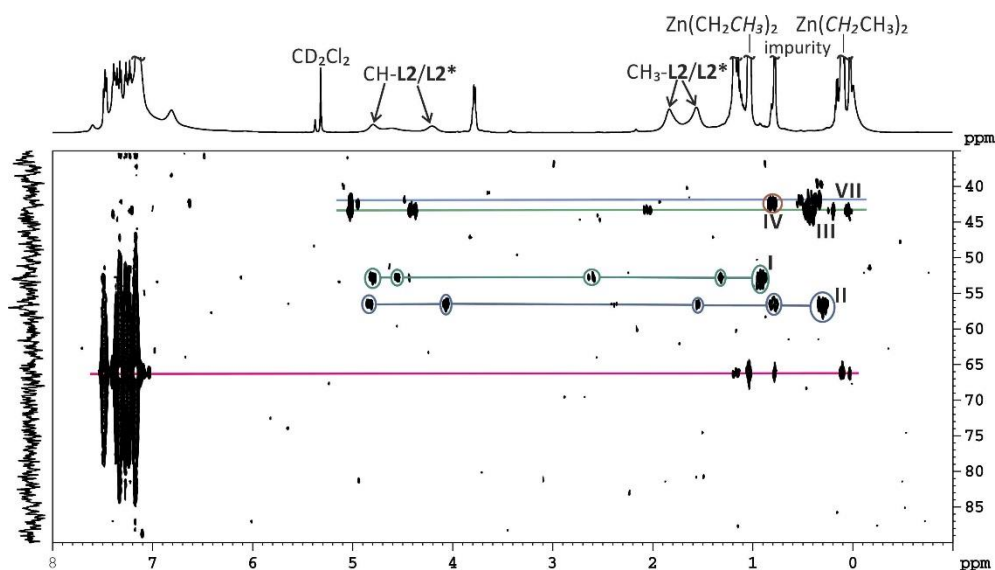
Figure 3.16: 2D $^1H^{31}P$-HMBC spectrum of 1 eq **L2**, 1 eq **L2***, 1 eq CuCl and 11 eq ZnEt$_2$ at 180 K in CD$_2$Cl$_2$. Free ligand **L2** (pink) and signal III (green) are folded back. Signal I and II appear at their real phosphorous chemical shift (52.7 and 56.5 ppm respectively).

In order to determine if the structures have a zinc chloride unit coordinated or not, ZnCl$_2$ was added to the reaction mixture. With this we force the structures towards zinc chloride coordination, because the other way around of removing zinc is not accessible, due to the missing of a selective additive for removal of zinc at simultaneous presence of copper (see Chapter 3.3.1). Therefore signals for structures with a zinc chloride unit incorporated are expected to increase, while signals without are expected to decrease. Obviously after addition of ZnCl$_2$ complex **C2** is nearly completely decomposed (2 %), while the signals for free ligand (91 %) and 131.2 ppm (7 %) increases (Figure 3.17, the percentage is referred to the ligand distribution in the ^{31}P NMR spectrum in the range of 160.0-100.0 ppm). The integration of the 2D $^1H^{31}P$-HMBC cross signals before and after addition of ZnCl$_2$ indicates no changes for signal I and II, so they are not influenced by the presence of zinc chloride. In contrast a new signal VIII appears (black line in Figure 3.18), while signal III decreases (light green ellipse) and signals IV and VII vanishes completely. Therefore, signal III, IV and VII were identified as structures without zinc chloride. The new appearing signal VIII at 0.37 to 42.1 ppm is attributable to the free diethylaminephosphine ligand with further cross signals to 5.03, 4.47, 1.91 and 0.54 ppm.
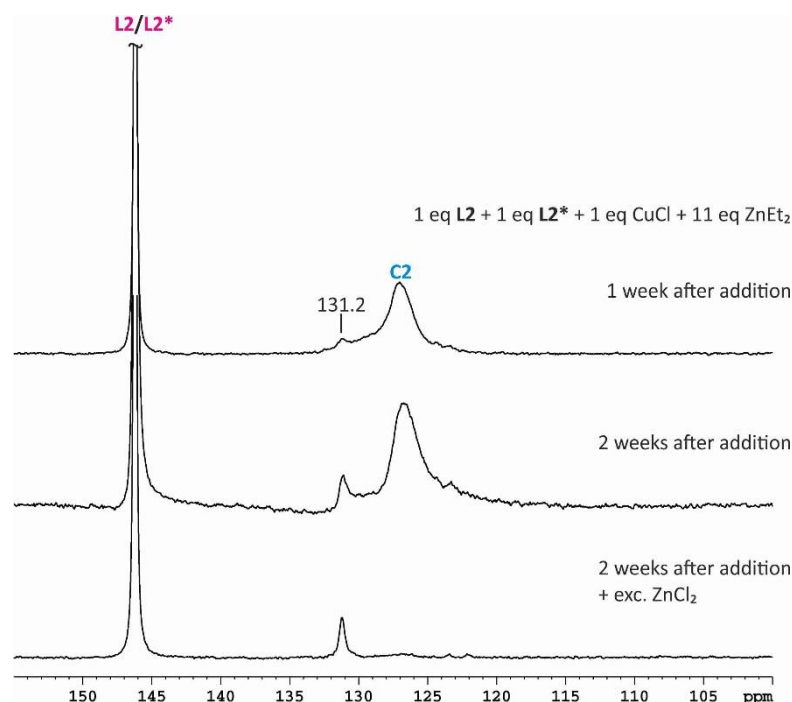
Figure 3.17: ^{31}P NMR spectra of 1 eq **L2**, 1 eq **L2***, 1 eq CuI and 11 eq ZnEt₂ one week after ZnEt₂ addition (top), two weeks after addition (middle) and after addition of an excess ZnCl₂ at 180 K in CD₂Cl₂. Complex **C2** is decomposed by the addition of ZnCl₂, and the amount of free ligand rises extremely (up to 91 %). The signal at 131.2 ppm remains after addition. The percentage is referred to the ligand distribution in the ^{31}P NMR spectrum in the range of 160.0-100.0 ppm.
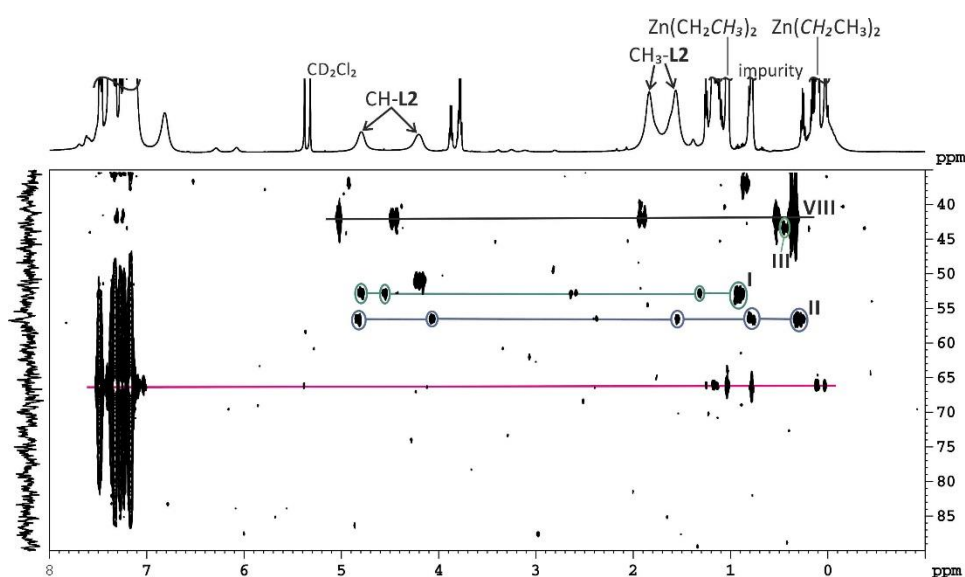
Figure 3.18: 2D [1]H[31]P-HMBC spectrum of 1 eq **L2**, 1 eq **L2***, 1 eq CuI, 11 eq ZnEt₂ and an excess of ZnCl₂ at 180 K in CD₂Cl₂. Signal VIII (black line) arises after ZnCl₂ addition, signals I and II remain unchanged, while signal III is decreased and the cross signals IV and VII vanishes completely.

With a 2:1 ligand to salt ratio, either as enantiopure or 1:1 mixture of the enantiomeric phosphoramidite ligands, we were able to identify signal VIII as diethylaminephosphine ligand and signals I and II as corresponding copper complexes of this ligand. Furthermore we can assume that signal III has a Cu**L₂** fragment, because the signal is missing in a 1:1 ligand to salt sample (see below) and that no zinc chloride unit is involved in the structure, due to the

decreasing intensity by addition of $ZnCl_2$. The involvement of the halogen in the structure is proven by no identical signals appearing for CuCl and CuI. Furthermore similar ^{1}H and ^{31}P chemical shifts of III with CuCl and signal 5 of the CuI sample appear, whereby the involvement of the halogen atom gives a probable explanation for the difference. For the other signals IV, V, VI and VII until now no clear assignment is possible.

3.3.4 Investigation of a 1:1 mixture of L2 and CuCl and their transmetalation intermediates with ZnEt$_2$

In order to enable a differentiation between structures containing a Cu**L** or Cu**L$_2$** fragment of the detected transmetalation intermediates a 1:1 sample of **L2** and CuCl was prepared. With this ratio it is possible to selectively prepare the trinuclear complex **C1** ([CuCl**L**]$_3$), and therefore after addition of the organometallic species only structures with one ligand coordinated to the copper atom are expected. Figure 3.19 presents the corresponding ^{31}P NMR spectra before (top) and after (below) addition of 33 eq ZnEt$_2$. In the spectra of the precatalytic mixture besides **C1** (122.0 ppm) a signal for **C2** (127.0 ppm) is visible, which is the result of an inaccurate 1:1 ligand to salt ratio. After the addition of ZnEt$_2$ the signal for **C1** decreases drastically, while the amount of **C2** increases and new signals arises at 124.3 and 118.4 ppm. Also a small amount of ligand is released after addition of the organometallic reagent. Therefore we assume that only Cu**L** containing transmetalation intermediates occur.
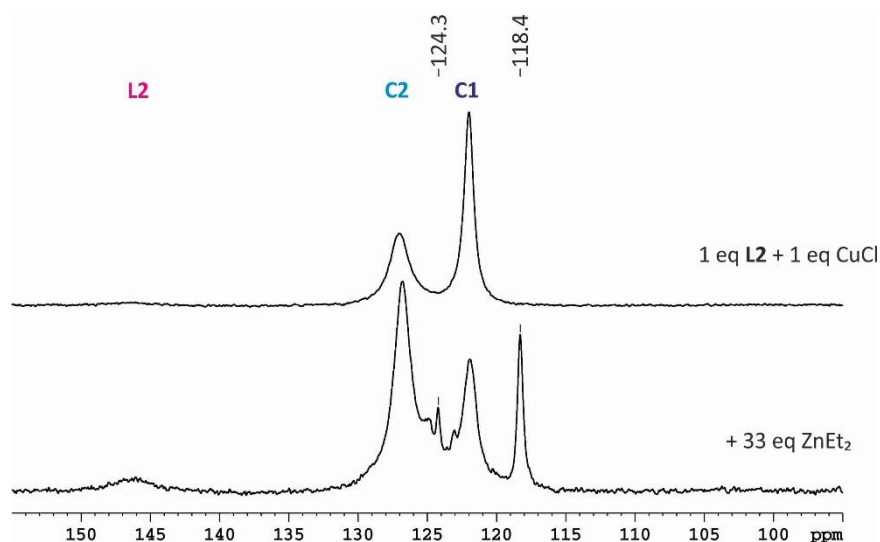
Figure 3.19: ^{31}P NMR spectra of 1 eq **L2** and 1 eq CuCl before (top) and after (below) addition of 33 eq ZnEt$_2$ at 230 K in CD$_2$Cl$_2$. Before ZnEt$_2$ addition nearly no free ligand is observed, and despite **C1** (122.0 ppm) also a broad signal for **C2** (127.0 ppm) is visible. After the addition of ZnEt$_2$ the signal for **C1** drops drastically and new signals arise at 124.3 and 118.4 ppm.

Another investigation, concerning the time as well as temperature dependency was performed. Figure 3.20 shows a comparison of the ^{31}P NMR spectra of the sample three weeks after addition

of $ZnEt_2$ at 230 (a) and 200 K (b), as well as two month after addition at 200 (c) and 180 K (d). Obviously in the aged 180 K spectra (d) the amount of free ligand increases with time and decreasing temperature. The same behavior applies to the signal at 131.3 ppm. Of course the amount of **C1** decreases too, due to the temperature dependent existence of the various complexes. In contrast a new signal appears at 119.9 ppm in the low temperature spectra while the signal at 118.4 ppm disappears.
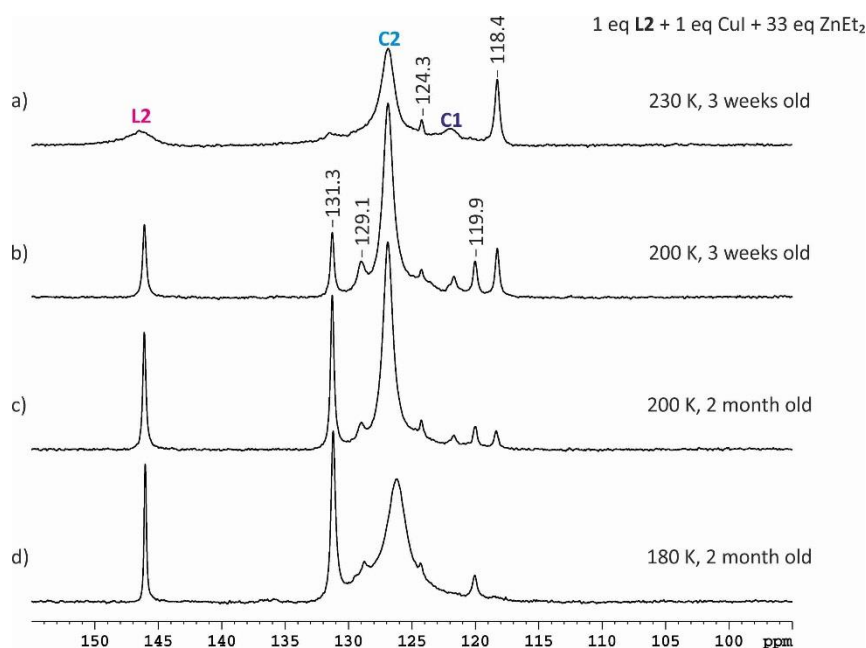
Figure 3.20: Comparison of ^{31}P NMR spectra of 1 eq **L2**, 1 eq CuI and 33 eq $ZnEt_2$ at 230 K (a) and at 200 K (b) three weeks after addition of $ZnEt_2$ as well as at 200 K (c) and at 180 K (d) two months after addition of $ZnEt_2$ in CD_2Cl_2. Obviously the signal at 118.4 ppm decreases, while a new signal occurs at 119.9 ppm in the low temperature spectra. Furthermore at 131.3 ppm a signal rises and the amount of free ligand increases.

Figure 3.21 and Figure 3.22 represent the 2D [1]H[31]P-HMBC spectra of the sample at 200 K after three weeks and 180 K after two months respectively. The red dashed boxes represent unspecific interactions of $ZnEt_2$ and **L2**, **C2** and for the first time detected also with the signal at 131.3 ppm. The cross signal IX (light blue) at 0.39 to 118.4 ppm has also cross signals to aromatic signals (7.28 and 7.21 ppm) on the corresponding ^{31}P chemical shift. Due to the missing of cross signals to methine protons signal IX was assigned as a ligand side product, in which the amine side chain is substituted by an ethyl group. The phosphorous chemical shift value is in agreement with literature known values (δ^{31}P for ethylnaptholdioxaphosphepin 121.2 ppm in $CDCl_3$).[50,51] In contrast for signal VI (0.05 to 119.9 ppm) further cross signals were detected to some aromatic signals, to methine groups (4.98 and 4.62 ppm) and to -0.81 ppm. The ^{1}H chemical shifts of the ethyl group are in good agreement with iodo and cyano ethyl cuprates investigated by Bertz *et al.* ($Et_2CuLi \cdot LiI$: 1.08 and -0.53 ppm, $Et_2CuLi \cdot LiCN$: 1.08 and -0.54 ppm).[34] Therefore signal VI was proposed to be a cuprate-like structure with a phosphoramidite ligand coordinated on the

copper atom (**L**CuEt$_2^-$). Again only a small amount of free ligand is present in this sample, due to the 1:1 ligand to salt ratio used for sample preparation. This is a probable explanation for the detrimental outcome of the reaction for ratios below 1.5:1, because the existence of a cuprate-like species results in an unspecific reaction and therefore no highly selective reaction in asymmetric synthesis.[52] For the phosphorous chemical shift of signal V (131.3 ppm, light purple) at 200 K only signals to some aromatic protons (7.63, 7.52, 7.45 and 7.15 ppm) were detected, while at 180 K signals to methine groups (4.77 and 4.18 ppm) as well as a signal to 3.27 ppm were observed. The chemical shift of 3.27 ppm is in good agreement with values for compounds containing P-OEt groups, e. g. P(OEt)$_3$ has a proton chemical shift of 3.88 ppm for the CH$_2$ group and 1.27 ppm for the CH$_3$ group.[53] Based on the missing signal for a transmetalated ethyl group and the similarity of the proton chemical shift of the methine groups to that of the free ligand, signal V is proposed to be a side product of the ligand with a P-OEt group.
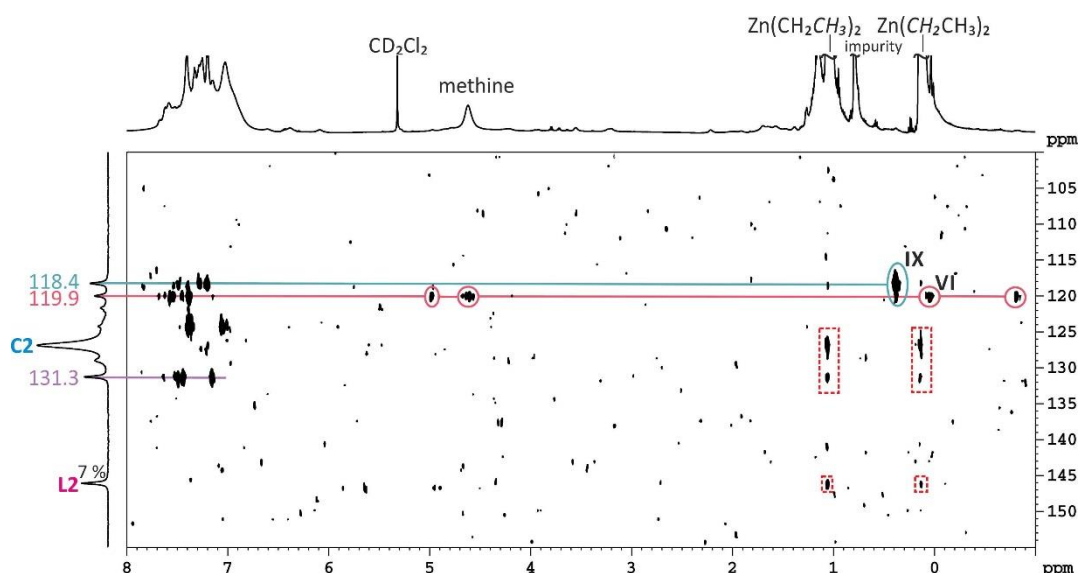
Figure 3.21: 2D ^{1}H^{31}P-HMBC spectrum of 1 eq **L2**, 1 eq CuCl and 33 eq ZnEt$_2$ after three weeks at 200 K in CD$_2$Cl$_2$. Signal VI was already detected in a sample with a 2:1 ligand to salt ratio with 11 eq of ZnEt$_2$, while signal IX appears as a new signal in the 1:1 mixture. Due to the excess of ZnEt$_2$ unspecific interactions occur to free ligand **L2**, **C2** and to the signal at 131.3 ppm (red dashed boxes). The percentage in the ^{31}P NMR refers to the ligand distribution in the range of 160.0-100.0 ppm.
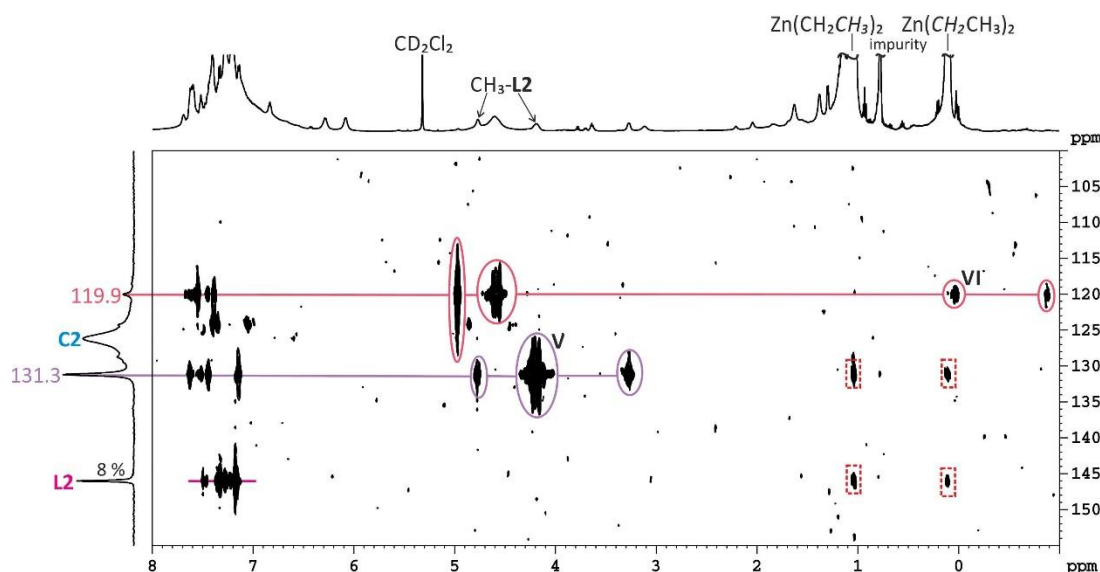
Figure 3.22: 2D $^1H^{31}P$-HMBC spectrum of 1 eq **L2**, 1 eq CuCl and 33 eq $ZnEt_2$ after two month at 180 K in CD_2Cl_2. The red dashed boxes represent unspecific interactions between the signals of $ZnEt_2$, free ligand and 131.3 ppm. The signals V and VI were already detected in a 2:1 ligand to salt ratio sample. The percentage in the ^{31}P NMR refers to the ligand distribution in the range of 160.0-100.0 ppm.

In the 1:1 ligand to salt sample neither signal III nor signal VII were observed, from the already known signals only V and VI were detected and a new signal IX appears at 200 K. The differences probably are the result of the high quantity of $ZnEt_2$ used, or due to the time and temperature shifts. Nevertheless signal VI was identified as a cuprate-like structure. Signal V and IX as side products of the ligand, in contrast to the already detected signals I, II and VIII, representing free and complexed diethylaminophosphine ligands, signal IX has an intact biphenol backbone, but the amine side chain is released, assumption due to the missing signals for the methine groups and signal V can be assigned to structures with a P-OEt group involved.

In addition to the NMR spectroscopic investigations of the transmetalation intermediates either with copper iodide or chloride, we also tried to identify them by mass spectrometry.[2] Therein only signals for **C1** and **C2** and their decomposition products and no for transmetalation intermediates were detected. So the occurring transmetalation intermediates are not ionizable, neither for iodine nor for chloride as halogen atom in the copper source.

---

[2] Measurements were performed in cooperation with Dr. A. Putau former member of the Koszinowski group at the Georg-August-University Göttingen.

3.3.5 Summary for investigations with ZnEt$_2$

This study gives the first direct experimental proof, by 1D and 2D ^{1}H^{31}P-HMBC spectra, for the elusive transmetalation intermediate in copper-catalyzed 1,4-addition reactions with diethylzinc and phosphoramidite copper complexes. Therefore investigations with CuI and CuCl were performed. Due to the fact that no signals are detected for the transmetalated species in the 1D ^{1}H and ^{31}P NMR spectra and so exclusively ^{1}H^{31}P-HMBC spectra are accessible for the detection of these signals a special approach has to be used in order to get further information on the structure. Therefore enantiopure and 1:1 enantiomeric mixtures of the phosphoramidite ligands were prepared for the differentiation between structures with one, two or three ligands coordinated to copper. For CuI besides monomeric transmetalation intermediates also a dimeric species was identified, in which for the first time the mixed trigonal/tetrahedral coordination of the copper atoms remains. The involvement of a zinc iodide unit in the structure of the transmetalation intermediates was determined by the addition of ZnI$_2$. With these different samples and approaches three monomeric species were identified with one ligand coordinated to the copper atom, one with a zinc iodine unit involved (**A**) and two without (**B** and **C**). The monomerization of dimeric precatalytic complexes is in agreement with investigations of the addition of Grignard reagents, performed by Feringa and co-workers.[17] Their observed structures are in conformity with structures **A** and **C** observed here. Although monomeric species with two ligands coordinated to the copper atom are often proposed in mechanistic presentations,[1,5,26] neither in the here presented study, nor in the previous investigation of Feringa such structures were detected. For the first time a direct experimental proof of a dimeric transmetalation intermediate with no zinc iodine unit, but retention of the basically precatalytic complex structure with mixed trigonal/tetrahedral coordination of the copper atoms was observed (this deviates from Feringa's results and contradict previous proposals of Woodward). The amount of monomeric and dimeric transmetalation intermediates are in the same order of magnitude. The typical 2:1 ligand to salt ratio in synthetic applications,[10,25] the stabilization of the precatalytic complex by an excess of ligand,[21] as well as Woodward's DFT-calculations,[23] revealing a dimeric copper complex as only suitable energetic pathway, indicating all that the dimeric transmetalation intermediate act as the reactive one. Furthermore, we assume that monomeric transmetalation intermediates are not preferable with CuCl, because of the stronger CuCl bond compared to CuI, therefore cleavage of the chloride bridges in the precatalytic complex will be more difficult. Due to the missing of identical signals for CuI and CuCl the involvement of the halogen atom was proven. Furthermore, in samples with a too small amount of free ligand, and therefore ligand to salt ratios below 1.5:1, cuprate-like structures with a

phosphoramidite ligand coordinated to the copper atom were detected, which led to no highly selective reaction and therefore can be an explanation for the detrimental effect of ratios below 1.5:1 for the outcome of the reaction in asymmetric catalysis. This first structural insight into the transmetalation intermediates, by direct experimental detection, are supposed to support the mechanistic understanding and to promote further synthetic developments on this important class of reactions.

3.4 Investigation of other organometallic reagents

In order to cover a broader scope of organometallic reagents further transmetalation reagents were investigated. Therefore we used $ZnPh_2$[3], because it is known that aryl groups are transferred easier as alkyl groups.[52,54–57] Furthermore the transmetalation of methyl groups was adressed with $ZnMe_2$ and the more reactive MeLi.[4] Furthermore we want to determine similarities or differences in the structure of the transmetalation intermediates.

Diphenylzinc was successfully introduced to ACA reactions with selectivities up to 94 % *ee* and excellent conversions.[9,58] Furthermore aryl groups are expected to be more readily transferred then alkyl groups.[52,54–57] In addition our recent aggregation studies of phosphoramidite ligands and their transition metal complexes reveal that π,π-interactions contribute to the stabilization of their aggregates,[32] this can similarly be assumed for transmetalation complexes. Nevertheless only unspecific interactions were observed in the 2D $^1H^{31}P$-HMBC spectrum indicated through cross signals between **C2** and the proton chemical shifts of $ZnPh_2$ (data not shown).[59] In addition interactions between free ligand and $ZnPh_2$ were observed, which are reversible by the addition of copper (data not shown).[59] Therefore these interactions are negligible in copper containing samples.

In a further study the transmetalation of methyl groups was investigated. Therefore $ZnMe_2$ was used, as it is the most interesting dialkylzinc derivative for synthetic purpose. A stabilization of the transmetalation intermediate was assumed, due to the size and the lower reactivity of $ZnMe_2$ compared to $ZnEt_2$. The lower reactivity is based on higher bond energy values compared to the higher homologs.[52,60] Nonetheless in contrast to $ZnEt_2$ we were not able to detect signals for a transmetalation intermediate with $ZnMe_2$, just signals for unspecific interactions and a ligand decomposition product occurs with CuI as copper salt (see supporting information, Chapter 3.7). By the use of CuCl decomposition of complex **C2** occurs besides the formation of cuprate species (data not shown). Next the more reactive MeLi was tested as potential transmetalation reagent, in order to get an idea about the associated chemical shift values of methylated transmetalation intermediates.[52] By generating a transmetalated species with this reagent, further information e. g. if the metal of the organometallic reagent is involved in the structure, can be gained by adding 12-crown-4 ether as a selective additive to the solution and therefore removing the lithium atom from the structure. Such a selective removing is not possible for zinc in the presence of copper, due to the missing of a zinc selective additive besides

---

[3] Investigations with $ZnPh_2$ were performed by Dr. Katrin Schober.[59]
[4] Investigations with $ZnEt_2$ and MeLi were performed by Carina Koch.

copper, as already described above. With MeLi a transmetalation intermediate was detected, but only if a shortage and low temperatures (230-200 K) are used (data not shown). Higher amounts of MeLi produce cuprate species and the decomposition of **C2**, whereas higher temperatures reveal carbenes, as a reaction product of MeLi and CD_2Cl_2 (data not shown).

In conclusion, until now no direct experimental evidence for a transmetalation intermediate was found neither for $ZnPh_2$ nor for $ZnMe_2$. With the more reactive MeLi it is possible to detect a signal for a transmetalated methyl group, if a shortage of MeLi is used. This transmetalated methyl group enables us to estimate the chemical shift range of other transmetalated species. In contrast using a higher amount of MeLi the precatalytic complex **C2** is destroyed with accompanied formation of $LiCuMe_2$.

3.5 Investigation of interactions between structural characteristics of the ligand and ZnMe$_2$[5]

To assess more information about the unspecific interaction between the organometallic reagent and the phosphoramidite ligand or corresponding copper complexes, the binding of the organometallic reagent to the ligand was investigated. Therefore different structural characteristics of the ligand were combined with ZnMe$_2$. If ZnMe$_2$ is added to **L2** or the precatalytic system new signals, which show scalar coupling, appear in the 1D ^{1}H^{31}P-HMBC spectra. Due to the chemical shift region (2.00-1.00 ppm) it could be excluded that these signals derive from transmetalated species but from an interaction between **L2** and ZnMe$_2$. These interactions might not matter for the transmetalation itself, but can be expected to be important for the mechanism and can be taken into consideration for the design of new ligands.
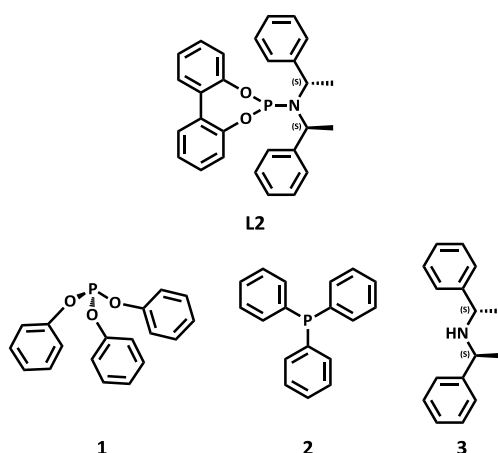
Figure 3.23: Structure of **L2** and substructures P(OPh)$_3$ **1**, PPh$_3$ **2** and the amine side chain **3** of **L2** used as model systems for investigations of interactions with dimethylzinc.

Figure 3.23 presents the three chosen model systems for the determination of these interactions. P(OPh)$_3$ **1** was used due to a comparable binding structure as the biphenol backbone of **L2**, PPh$_3$ **2** for comparison with **1**, to determine whether the oxygen is involved in these interactions or not. Conversely the amine side chain **3** of **L2**, without any oxygen or phosphorous atom, enables the investigation of the impact of the nitrogen atom on these interactions.

---

[5] Interactions between structural characteristics of the phosphoramidite ligand **L2** and ZnMe$_2$ were elucidated by Carina Koch.
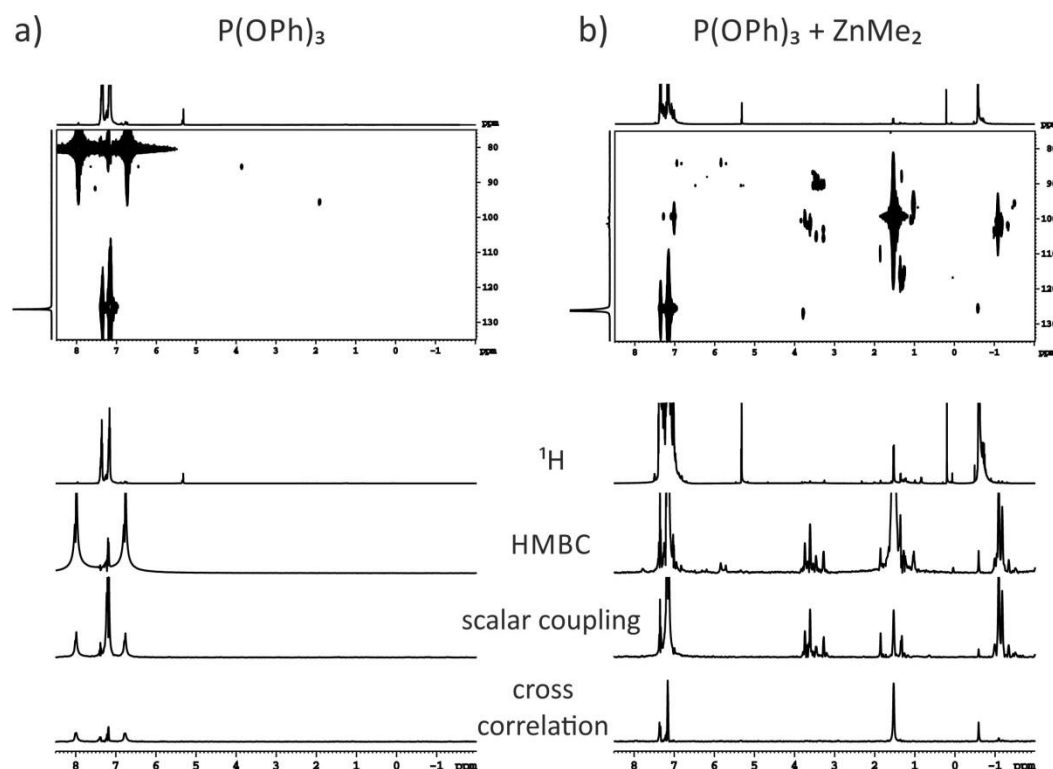
Figure 3.24: 2D (top) and 1D (below) $^1H^{31}P$-HMBC spectra of P(OPh)$_3$ **1** a) before and b) after addition of ZnMe$_2$ at 230 K in CD$_2$Cl$_2$.

In Figure 3.24 the 2D and 1D $^1H^{31}P$-HMBC spectra before (a) and after (b) addition of ZnMe$_2$ to **1** are represented. Obviously new signals occur after the addition of the organometallic reagent, for most of them also signals in the 1D $^1H^{31}P$-HMBC spectra for the detection of magnetization transfer via scalar coupling occur (Figure 3.24 b below). Compared to the corresponding spectra with free and complexed phosphoramidite ligand, the signals in the chemical shift range of 2.00-1.00 ppm are quite similar. We propose that these signals belong to species with a methyl group directly bound to the phosphorous atom and one P-O bond of the biphenol backbone cleaved, because for PMe$_3$ a chemical shift of 0.97 ppm is literature known.[61] Beside the main cross signal at 1.53 to 99.4 ppm further smaller signals occur, which probably represent different coordinations of Zn-clusters. The signals between 4.00 and 3.00 ppm were assigned to species with a P-OMe group, as a comparable compound P(OMe)$_3$ is mentioned (3.39 ppm).[61] Whereas signals with lower chemical shifts than ZnMe$_2$ (-0.59 ppm) are assigned to species with P-Zn-Me groups.
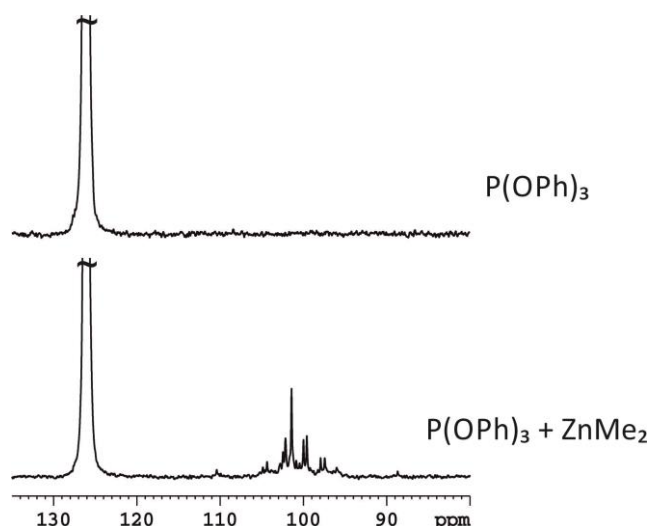
Figure 3.25: ^{31}P NMR spectra of P(OPh)$_3$ **1** before (top) and after (below) addition of ZnMe$_2$ at 230 K in CD$_2$Cl$_2$.

After the addition of ZnMe$_2$ to **1** new signals (111.0-94.0 ppm) were detected in the ^{31}P NMR spectrum highfield shifted to free P(OPh)$_3$ (Figure 3.25). This means that the concentration of the species is higher than in samples with **L2**. The chemical shift difference lies with 15 ppm in the same range of the difference between free **L2** and the precatalytic complex **C2**.

In contrast with **2** none of the above mentioned signals compared to **1** were detected (spectra not shown). Therefore it is proven that the oxygen atom is needed for the observation of interactions with the ligand.

In order to elucidate the impact of the nitrogen atom on the interactions samples of the amine side chain **3** and ZnMe$_2$ were prepared. In the ^{1}H NMR spectrum a lowfield shift for the protons of **3** and a strong highfield shift ($\Delta\delta$ = -0.2 ppm) of the methyl groups of ZnMe$_2$ is visible (spectra not shown). This would be expected for a species with a zinc atom coordinated to the nitrogen atom, but in our investigations of either the free or the complexed ligand **L2** no corresponding signals were observed. Therefore a coordination of the organozinc reagent to the nitrogen of the phosphoramidite ligand can be excluded, although it might be expected due to literature known species.

As the experiments with P(OPh)$_3$ and ZnMe$_2$ showed very similar results to our initial phosphoramidite ligand system, we added CuI to P(OPh)$_3$ (Figure 3.26).
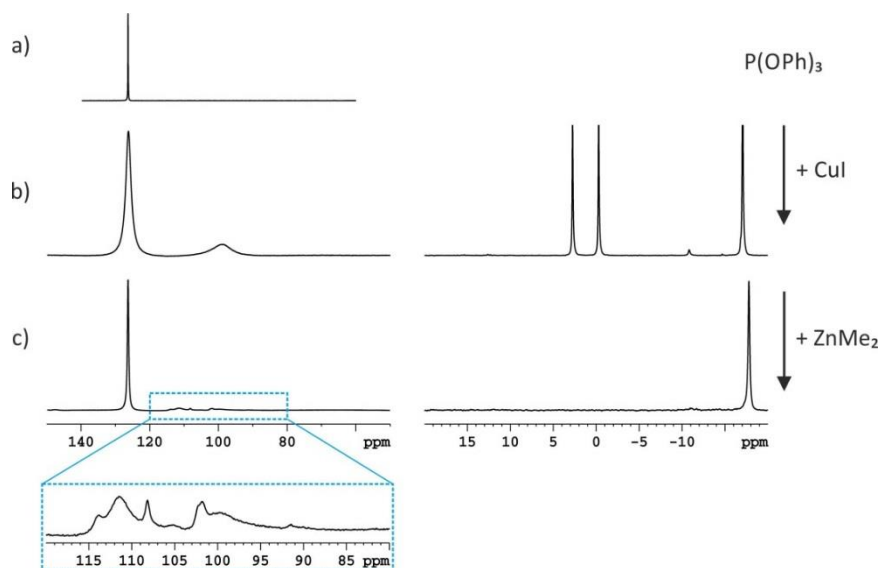
Figure 3.26: ^{31}P NMR spectra of P(OPh)$_3$ at 230 K in CD$_2$Cl$_2$ a) before and b) after addition of CuI, c) with CuI and ZnMe$_2$ and enlargement of spectra c) (blue box).

The mixture of CuI and P(OPh)$_3$ shows similar behavior like CuI and ligand **L2**. A complex species arises at 98.9 ppm, the chemical shift difference between free and complexed P(OPh)$_3$ (27 ppm highfield) is in the chemical shift range as for **L2** and **C2** (16 ppm highfield). Therefore we assume a comparable complex structure to **C2**. After the addition of ZnMe$_2$ the broad signal at 98.9 ppm disappears and several new signals arise in this chemical shift range of 115.0 to 90.0 ppm, which point to a multitude of complex structures (Figure 3.26).
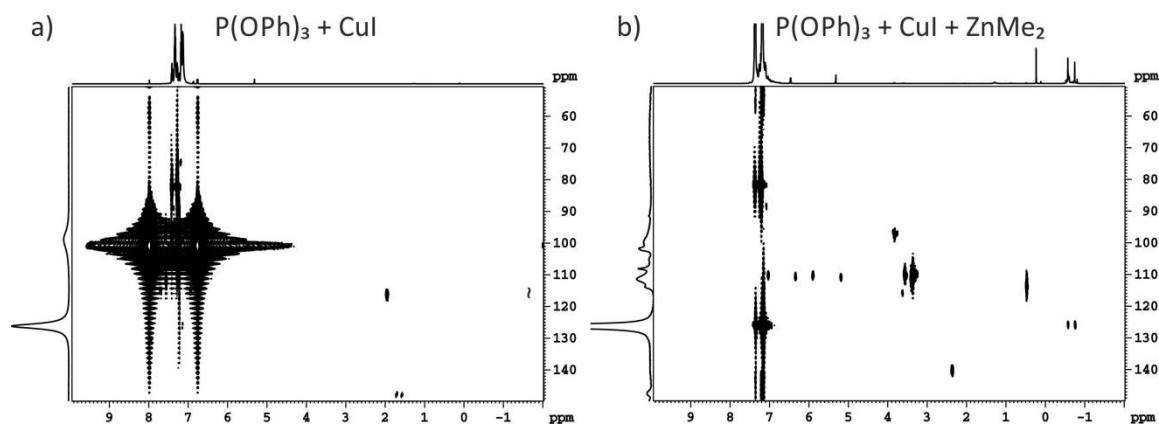
Figure 3.27: 2D ^{1}H^{31}P-HMBC spectra of P(OPh)$_3$ and CuI a) before and b) after addition of ZnMe$_2$ at 230 K in CD$_2$Cl$_2$.

In Figure 3.27 the 2D ^{1}H^{31}P-HMBC spectra of the P(OPh)$_3$ and CuI mixture before (a) and after (b) addition of ZnMe$_2$ are shown. Obviously none of the detected signals can be assigned to familiar species like in the spectra above with pure P(OPh)$_3$ or with **L2**, due to the missing of signals between 2.00 and 1.00 ppm. Furthermore no indications for transmetalated species are identified in this system. The signal at 1.90 ppm in the left spectra is assigned to a H-P bond, based on a impurity in P(OPh)$_3$ (e.g. P(OPh)$_2$H).

In conclusion, the investigation of the structural characteristics of the phosphoramidite ligand **L2** determines that for the interaction with organozinc reagents the oxygen atom of the backbone is indispensable. Only with $P(OPh)_3$ signals with similar proton chemical shifts were detected, compared to the initial system. In contrast with PPh_3 no interactions were detected. The elucidation of the amine side chain resulted in interactions, but they were not comparable with the phosphoramidite system, and therefore coordination of the zinc reagent via the nitrogen atom was excluded.

3.6 Conclusion

In this NMR spectroscopic study on transmetalation intermediates in the asymmetric conjugate addition (ACA) reaction for the very first time a direct experimental proof for the commonly accepted transmetalation step is observed. Different transmetalation intermediates were identified for reactions of binuclear phosphoramidite copper complexes. Thereby the identification and structural assignment of the transmetalation intermediates is exclusively based on ^{1}H^{31}P-HMBC spectra, due to the missing of signals in the ^{1}H and ^{31}P NMR spectra. Using CuI as copper salt results in the existence of a plenty of different transmetalation intermediates, either monomeric (with one ligand coordinated to the copper atom) or dimeric with the mixed trigonal/tetrahedral coordination on the copper atoms of the precatalyst still intact, but one of the iodine bridges substituted by an ethyl group (with three ligands involved). The assignment of the structures is based on a special approach using either enantiopure or 1:1 enantiomeric mixtures of the phosphoramidite ligands. Therefore different signal intensities in the 2D ^{1}H^{31}P-HMBC spectra occur, depending on the number of ligands (one, two or three) involved in the transmetalation species. The existence of transmetalation species with more than three ligands was excluded, as they appear with a more sophisticated signal pattern for possible diastereomers in the enantiomeric mixture, which were not detected in the recorded spectra. Due to the existence of the transmetalated species only in very tiny amounts in solution no signals were detected in the ^{1}H and ^{31}P NMR spectra, but nevertheless cross signals were obtained in the 2D ^{1}H^{31}P-HMBC spectra, even if magnetization transfer via copper is challenging in not highly symmetric copper complexes, due to the high quadrupole moment of copper. Measuring several modified 1D ^{1}H^{31}P-HMBC spectra enables the differentiation of magnetization transfers via chemical bond (scalar coupling) and through space (cross correlation, as a combination of chemical shift anisotropy and dipolar interactions). For the assumed transmetalation intermediates only signals in the scalar coupling spectra were detected. The monomeric and dimeric transmetalation intermediates observed with CuI appear in the same order of magnitude. The exclusive detection of monomeric species with one ligand coordinated to the copper atom is in agreement with investigations performed by Feringa concerning the structures of transmetalated species with Grignard reagents. However, neither his nor our investigations indicating a monomeric species with two ligands coordinated on the copper atoms, although it is often proposed in reaction mechanisms. Nevertheless, the simultaneous observation of monomeric and dimeric transmetalation intermediates differs from previous results of Feringa and contradicts proposals of Woodward. This represents a further example of the high sensitivity of thes reactions to the synthetic conditions used and reaveal that it is not

possible to determine one general structure for transmetalation intermediates. The standard 2:1 ligand to salt ratio used in synthetic applications, the stabilization of the dimeric precatalytic complex by excess of ligand and DFT-calculations performed by Woodward, revealing a dimeric copper complex as solely suitable energetic pathway, all indicating that the dimeric transmetalation intermediate reacts as the active one. Furthermore, we assume that monomeric species are unfavored with CuCl, due to the high energy of the CuCl bond, and therefore it is more difficult to break up the chloride bridges in the precatalytic copper complex. Therefore we suggest one dimeric transmetalated species and no monomeric species with CuCl. Apart from the transmetalation intermediate some side products occur, due to reactions of free ligand and $ZnEt_2$, both substitutions at the amine side chain and partial or complete cleavage of the biphenol backbone were observed, which can be assigned by comparison with literature known values and comparative measurements. Furthermore the existence of the detected species depends also on the present amount of free ligand in the sample. With small amounts of free ligand cuprate-like species appear which might be an indication for the detrimental effect of ligand to salt ratios below 1.5:1, because with cuprate species a highly selective reaction is not possible. In addition unspecific interactions were identified between free and complexed ligands to the transmetalation reagents. These interactions are based on strong π,π- or CH,π-interactions, and were also detected in samples using commercial available solutions of organometallic reagents to the solvent and are more pronounced in copper free samples, which was proven by investigations with diphenylzinc. Nevertheless, the first direct experimental detection of transmetalation intermediates is expected to improve the mechanistic understanding and to support further synthetic development of copper-catalyzed ACA reactions. Furthermore this special approach for the observation of intermediate signals beyond the detection limit of 1D ^{1}H and ^{31}P spectra can also be applied to further catalytic systems. These results are the basis for further investigations on this research area addressing the next step of the mechanism – the addition of the substrate. Due to the proximity of the transmetalation signals to the detection limit, first a suitable model system of precatalytic complex and substrate with optimized interaction sites, based on our experiences with inter- and intraligand interactions in palladium phosphoramidite complexes and simplified DFT-calculations, has to be found. This is now ongoing work in our group as subject of a further PhD thesis.

Beside the addition of diethylzinc also diphenyl- and dimethylzinc were tested as they were also widely used as transmetalation reagents, in order to investigate similarities and differences in the transmetalation intermediates. Until now it was not possible to detect transmetalated species with these two reagents. Using the more reactive MeLi for the investigation results in a

transmetalation intermediate, but only if a shortage of MeLi and temperatures below 200 K are used. Investigations of various structural characteristics of the ligand with $ZnMe_2$ determine that the oxygen atom is indispensable for observed interactions.

3.7   Supporting information

3.7.1   Experimental Part

3.7.1.1   General Considerations

All sample preparations were performed under standard Schlenk technique under argon atmosphere and in dry solvents. CD_2Cl_2 was dried with CaH_2 and freshly distilled before use. The phosphoramidite ligands were either prepared according to reported protocols[62] or purchased by ABCR. Copper iodide was used as commercially available from Sigma Aldrich (99.999 %). Copper chloride was used as commercially available from Alfa Aesar (97 %). The solutions of the neat dialkylzinc reagents were freshly prepared in deuterated solvents (diethyl- and dimethylzinc in CD_2Cl_2). Therefore the organometallic reagent (0.5 mL) was solved in 2 mL solvent. Neat $ZnEt_2$ was purchased by Sigma-Aldrich ($\geq$ 95 %) and used without further purification. $ZnMe_2$ was purchased either by ABCR (neat, 95 %) or as 2M solution in toluene by Sigma-Aldrich and used without further purification. $ZnPh_2$ was used as commercially available from Strem Chemicals or it was used as synthesized by Dipl.-Chem. Fabian Mutzbauer (AK Korber).[63] The synthesis of $ZnPh_2$ was performed from a reaction of $ZnCl_2$ and PhLi in Et_2O at 0 °C. $ZnPh_2$ was purified via distillation at 120 °C under vacuum ($5*10^{-2}$ mbar) and obtained as pure white solid. $ZnCl_2$ was recrystallized from 1,4-dioxane and dried before use. PhLi was synthesized from PhBr and Li in Et_2O under reflux. All manipulations with $ZnPh_2$ were performed in a glove box under argon atmosphere and exclusion of daylight. In the commercially available source of $ZnPh_2$ traces of benzene were detected. MeLi was purchased as a 1.6M solution in diethyl ether by Sigma-Aldrich. Investigations were performed in CD_2Cl_2.

3.7.1.2   Sample Preparation

3.7.1.2.1   Preparation of the phosphoramidite copper complexes

An argon flushed Schlenk tube equipped with magnetic stirring bar and septum was charged with 2 eq ligand (0.036 mmol, 15.81 mg) and 1 eq copper iodide (0.018 mmol, 3.43 mg) or copper chloride (0.018 mmol, 1.78 mg), freshly distilled solvent CD_2Cl_2 (0.6 ml) was added and the mixture stirred for 1-2 h at room temperature until a clear solution was obtained. Subsequently the samples were transferred to an argon flushed NMR tube. The samples were stored at -85 °C.

3.7.1.2.2   Preparation of the phosphoarmidite copper complexes – MR_x samples

To the freshly prepared phosphoramidite copper complex solution the corresponding amount of freshly prepared $ZnEt_2$ or $ZnMe_2$ solution was added at room temperature.

ZnPh₂: Complex preparation as describe above. A second argon flushed Schlenk tube with magnetic stirring bar and septum was charged with $ZnPh_2$ and CD_2Cl_2 (0.4 mL) was added ($ZnPh_2$: 0.09 mmol, 22.04 mg; 5-fold excess to CuI, 10-fold excess to **C2**). After stirring for 2 h, the cloudy solution of $ZnPh_2$ was transferred to the solution of the phosphoramidite copper complexes. A slightly exothermic reaction was observed upon by the condensation of CD_2Cl_2 at the upper part of the Schlenk tube. The mixture was stirred for 25 min and transferred into an argon flushed NMR tube.

MeLi: To the freshly prepared phosphoramidite copper complex solution the corresponding amount of MeLi was added to the cooled complex mixture (at least 200 K).

3.7.1.3   NMR Data Collection and Processing

NMR spectra were recorded on a Bruker Avance DRX 600 (600.13 MHz) spectrometer equipped with a 5 mm broadband triple resonance z-gradient probe (maximum gradient strength 53.5 Gauss/cm). The temperature for all low temperature measurements were controlled by a BVTE 3000 unit. The ^1H chemical shifts were referenced to the residual solvent signal of CD_2Cl_2 or TMS, for the ^{31}P chemical shifts the Ξ value was applied. NMR data were processed and evaluated with Bruker Topspin 3.1.

2D $^1H^{31}P$-HMBC spectra: pulse program = inv4gplrndqf, relaxation delay = 6 s, mixing time = 0.05 s, NS = 128, DS = 8, TD = 16k F2 and 64 F1. 1D $^1H^{31}P$-HMBC spectra: pulse program = gs_hmbc1D27.gf for HMBC, gs_hmbc1D25.gf for scalar coupling and gs_hmbc1D26.gf for chemical shift anisotropy/dipolar interaction, relaxation delay = 6 s, NS = 1k, DS = 16, TD = 64k.

3.7.2   Additional NMR spectra and Information

3.7.2.1   Solvent influence of the organometallic reagent

The solvent used for the $ZnEt_2$ solution has a quite big influence on the spectra resolution. In the ^1H NMR spectra of $ZnEt_2$ dissolved in different solvents, and the associated complex spectra it becomes obvious that spectra resolution is explicitly better, if no further solvent is applied as the deuterated one (here CD_2Cl_2, data not shown). All in all the spectra are little bit shifted, depending on the used solvent, while the shift of free $ZnEt_2$ in CD_2Cl_2 is not as big as in the toluene solution, which can depend on shielding effects of the solvents. Furthermore the readily bought solution contains more impurities, as the freshly prepared one. A more substantial influence is observed in the 2D $^1H^{31}P$-HMBC spectra. In a sample with about 10 eq $ZnEt_2$ as toluene solution (Figure SI 3.1 top) it is not possible to detect any cross signals of transmetalation intermediates, in contrast in a sample with 6.5 eq $ZnEt_2$ in pure CD_2Cl_2 (Figure SI 3.1 below) detection of cross signals for transmetalated ethyl groups (red box) is possible.
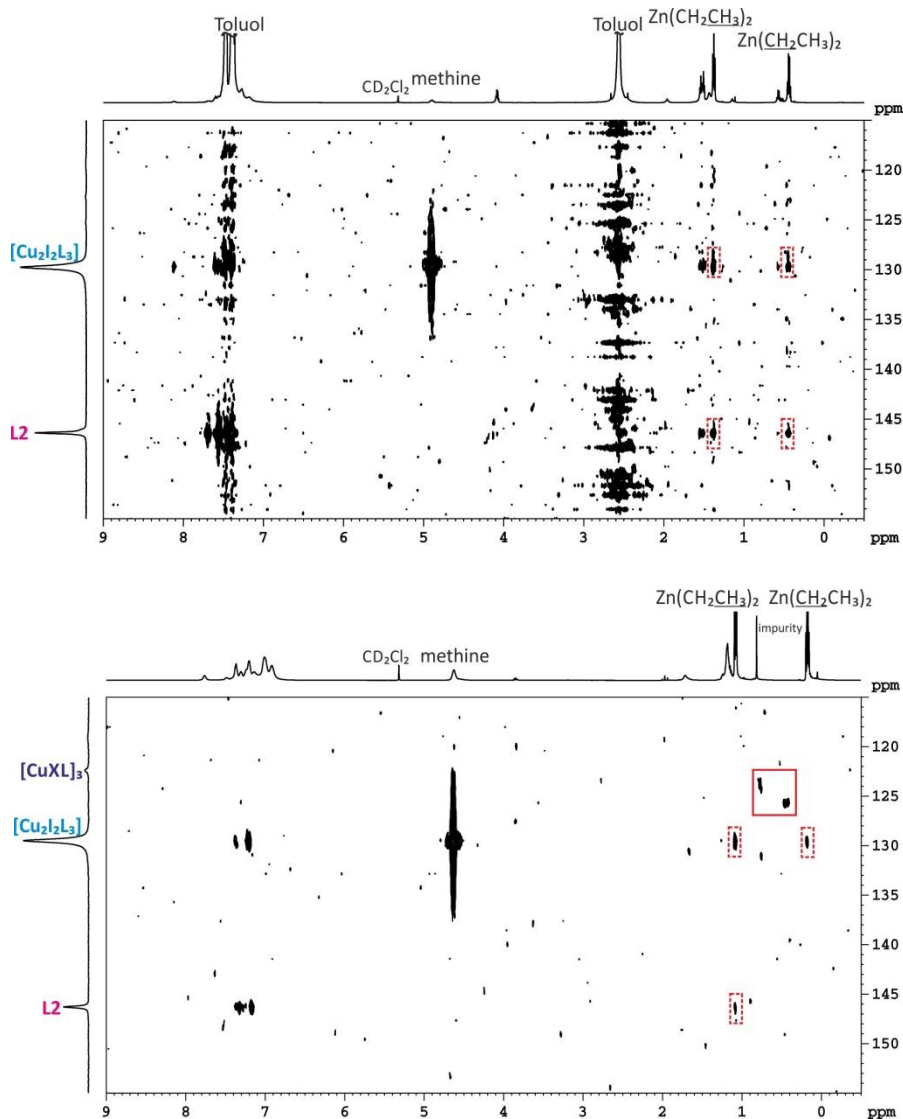
Figure SI 3.1: 2D ^{1}H^{31}P-HMBC spectra of 2 eq **L2**, 1 eq CuI and 10 eq ZnEt$_2$ (1M in toluene, top) and of 2 eq **L2**, 1 eq CuI and 6.5 eq ZnEt$_2$ (circa 2M in CD$_2$Cl$_2$, below) at 230 K in CD$_2$Cl$_2$. The red boxes represent new appearing signals for transmetalation intermediates (below), whereas the red dashed boxes represent unspecific interactions between ZnEt$_2$ and **C2** or **L2**.

The red dashed boxes represent unspecific interactions. The assignment as unspecific interactions is based on further investigation using ZnMe$_2$ as organometallic reagent.[6] Therefore ZnMe$_2$ was used as a 2M solution in toluene. In the 1D ^{1}H^{31}P-HMBC spectra for the differentiation of magnetization transfer, either via scalar coupling (Figure SI 3.2 c) or via cross correlation, representing the combination of chemical shift anisotropy and dipolar interaction (Figure SI 3.2 d), in both spectra a signal occur at the chemical shifts of residual toluene (7.24, 7.15 and 2.34 ppm) therefore no clear identification of the pathway is possible. Such a signal without clear assignment to one transfer pathway also occurs at -0.59 ppm, the chemical shift of free ZnMe$_2$. We assume that signals occurring in spectra for both magnetization transfer

---

[6] Investigations with ZnMe$_2$ were performed by Carina Koch.

pathways belong to unspecific interactions, based on strong π,π- or CH,π-interactions. From investigations with $ZnEt_2$ we knew, that a distinct amount of $ZnEt_2$ is needed before such interactions occur. In contrast for $ZnMe_2$ these interactions already occur with one equivalent. We assume that these unspecific interactions have no influence on the reaction.
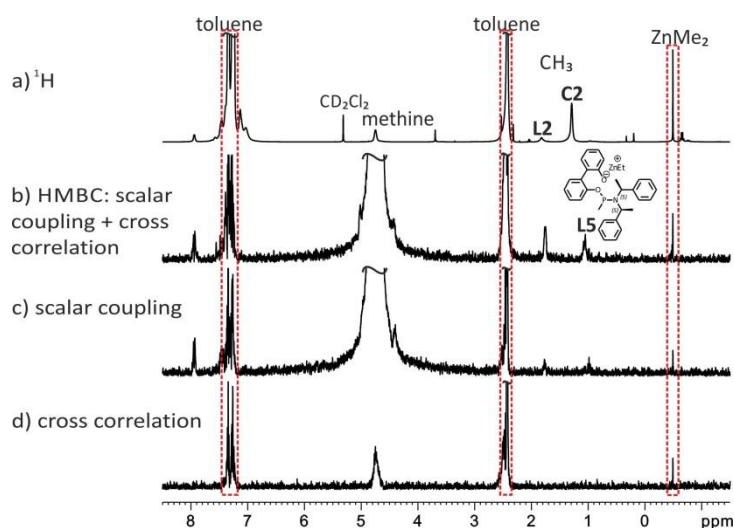

Figure SI 3.2: Comparison of ^{1}H NMR spectrum (a) and 1D [1]H[31]P-HMBC spectra with both magnetization transfer pathways (b), solely scalar coupling (s) and with cross coupling (chemical shift anisotropy (CSA) and dipolar interaction) of 2 eq **L2**, 1 eq CuI and 1 eq $ZnMe_2$ at 230 K in CD_2Cl_2.

Apart from the unspecific interactions in the 1D [1]H[31]P-HMBC spectra of 2 eq **L2**, 1 eq CuI and $ZnMe_2$ a signal appear at 1.76 and 1.06 ppm in the spectra for magnetization transfer via scalar coupling. The first one corresponds to the methyl group of the free ligand, while the latter one was identified as a ligand side product, in which one half of the biphenol backbone is cleaved and a methyl group directly transferred to the phosphorous atom (**L5**).

3.7.2.2 Additional findings with CuI as copper salt

3.7.2.2.1 Identification of side products in CuI sample

In order to determine interactions between free ligand and $ZnEt_2$ a copper free sample was prepared. Therefore 2 eq of ligand **L2** were dissolved in 0.7 ml CD_2Cl_2 and 4.5 eq $ZnEt_2$ added. Figure SI 3.3 presents the comparison of the ^{1}H NMR spectrum (a) and the 1D [1]H[31]P-HMBC spectra (b) magnetization transfer via scalar coupling and cross correlation, c) magnetization transfer via scalar coupling, d) magnetization via cross correlation – combination of chemical shift anisotropy and dipolar interactions; the red dashed boxes represent unspecific interactions).
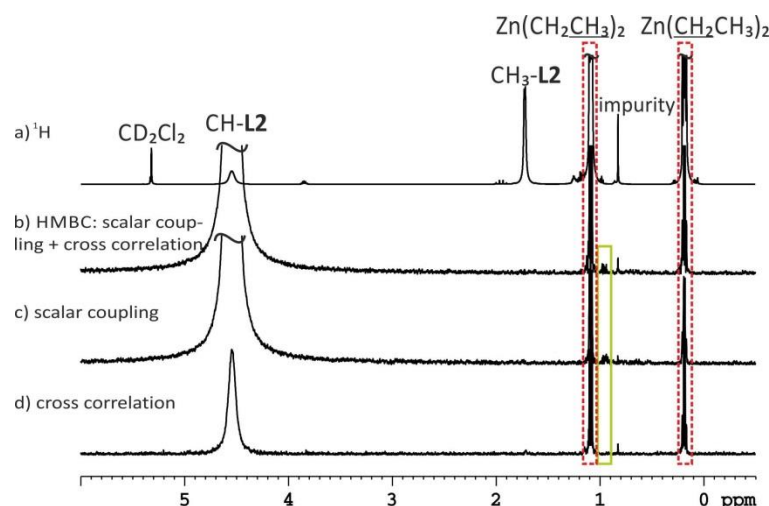
Figure SI 3.3: Comparison of ^{1}H NMR spectrum (a) and the 1D [1]H[31]P-HMBC spectra with both magnetization transfer pathways (b), solely scalar coupling (c) and with cross coupling (d, chemical shift anisotropy (CSA) and dipolar interaction) of 2 eq **L2** and 4.5 eq ZnEt$_2$ at 230 K in CD$_2$Cl$_2$.

Obviously unspecific interactions with ZnEt$_2$ occur, due to the existence of the signals in all three spectra (red dashed boxes). In contrast the signal at 0.95 ppm (light green) appears only in the scalar coupling spectra, so it corresponds to a directly transferred ethyl group. The occurrence of the signal in a copper free sample permits the assumption, that this structure plays a non-decisive role in the catalytic cycle and is a ligand-ZnEt$_2$ interaction product.

In contrast signal 1, observed in the 2D [1]H[31]P-HMBC spectra of 2 eq **L2**, 1 eq CuI with 7 or 15 eq ZnEt$_2$ respectively (see main part), does not appear in the copper free sample. However it was assigned to a copper complex with a ligand derivative, which has one half of the biphenold backbone opened and substituted by an ethyl group. This assignment to decomposed ligand **L4** is in analogy to the above described investigations with ZnMe$_2$ (see **L5** Figure SI 3.2 b). The missing in copper free samples and the reduction of the signal intensity in the enantiomeric mixture (see main part) is a probable explanation for complex formation with decomposed ligand **L4**. With additional **L4** present in solution, apart from the both enantiomeric phosphoramdite ligands **L2** and **L2*** for the complex **C2** seven possible mixed arrangements of the ligands are possible. These possible arrangements appear also for dimeric transmetalation species **E**-**G** (see Scheme 3.4) with three ligands coordinated to the copper atoms (each also can occur in the corresponding enantiomeric form).
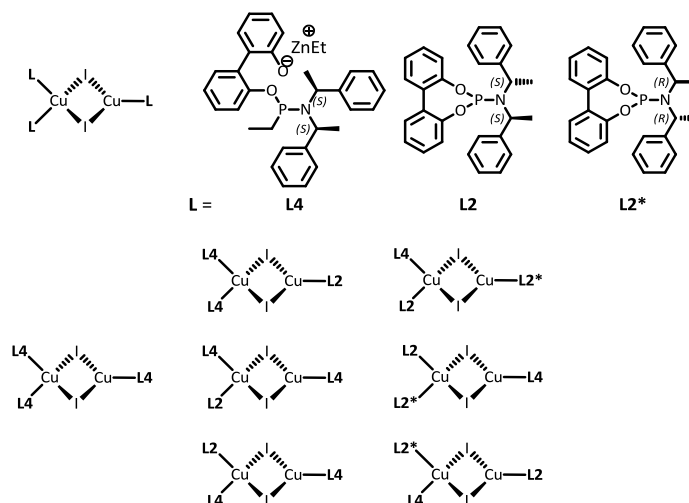
Scheme SI 3.1: Possible ligand arrangements for **C2** with decomposed ligand **L4** and the two enantiomeric forms of phosphoramidite ligand **L2** and **L2***. These ligand arrangements are also possible for dimeric transmetalation intermediates, providing reduced signal intensity.

3.7.2.2.2 ^{31}P NMR spectra of a 1:1 enantiomeric mixture sample with CuI and ZnEt$_2$

In the ^{31}P NMR spectra of the ligand mixture a large singlet occurs at 133.5 ppm and a smaller one at 134.6 ppm with an integral ratio close to 2:1. Such a signal splitting is known for the **C2** complex at low temperatures, due to decelerated intermolecular ligand exchange processes, and therefore differentiation between the two ligand groups in the complex is possible.[22] With the ligand mixture four possible arrangements for the ligands occur, each of them can in turn exist in two enantiomeric forms, which are not distinguishable by NMR spectroscopy. Therefore even for the precatalytic copper complex a more sophisticated low temperature ^{31}P NMR spectrum appears as for a sample with only one enantiomer of the ligand used. In Figure SI 3.4 a comparison of the ^{31}P NMR spectra of a sample with 1 eq **L2**, 1 eq **L2*** and 1 eq CuI (top), after addition of about 15 eq (middle) and an excess of ZnEt$_2$ (below) at 170 K is presented. Besides free ligand (146.3 ppm) also a small amount of the temperature dependent complex **C3** (139.3 ppm) has a presentiment (beyond the threshold of the presentation). The signals for **C2** are splitted into two signals with a 2:1 ratio, for the diastereomer with the same ligands (130.7 and 129.8 ppm), the diastereomer with **L2*** at the trigonal copper atom (134.6 and 133.6 ppm) and a broad signal at 129.0 ppm, representing the other two diastereomers with mixed coordination of the ligand enantiomers at the tetragonal coordinated copper atom. After addition of ZnEt$_2$ the signals for free ligand and the various complexes remain nearly unaffected, but a new signal is detected at 123.4 ppm. For this resonance only cross signals to methine groups (4.88 and 4.53 ppm) were detected in the 2D [1]H[31]P-HMBC spectra and none in the expected peak range for transmetalated ethyl groups. Due to the missing of additional correlation signals further

assignment was not possible. With an excess of $ZnEt_2$ also a new signal at 125.0 ppm is detectable, but here also no further assignment was possible.
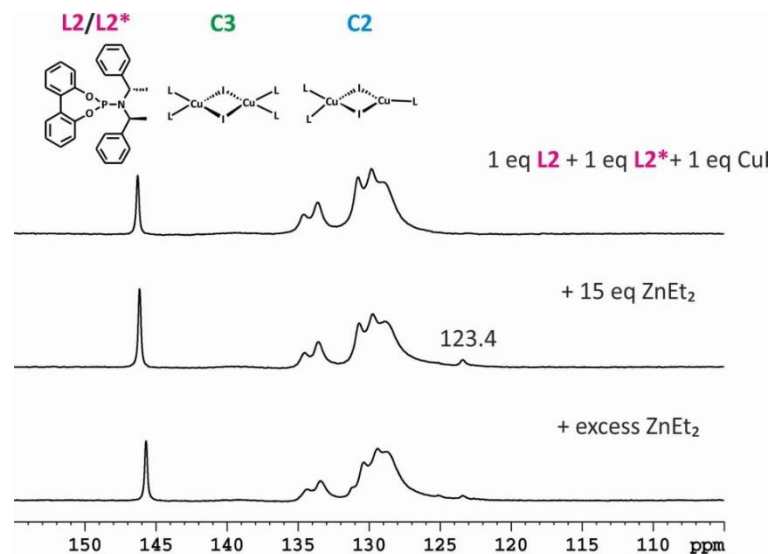
Figure SI 3.4: ^{31}P NMR spectra of 1 eq **L2**, 1 eq **L2*** and 1 eq CuI (top) with 15 eq $ZnEt_2$ (middle) and an excess $ZnEt_2$ (below) at 170 K in CD_2Cl_2. At about 146 ppm free ligand **L2/L2***, at 140 ppm **C3** (beyond threshold of the presentation) and at 135-126 ppm **C2** with different ligand arrangements occur. After addition of $ZnEt_2$ a new signal arises at 123.4 ppm, by increasing the $ZnEt_2$ amount, also a signal at 125.0 ppm is detectable.

3.7.2.3 $^{1}H^{31}P$-HMBC spectra of a 1:1 enantiomeric mixture sample with CuCl and $ZnEt_2$

In the 1D $^{1}H^{31}P$-HMBC spectra for detection of magnetization transfer via scalar coupling of a 1:1 enantiomeric mixture of **L2** and **L2*** with 1 eq CuCl and 11 eq $ZnEt_2$ signals appear at 0.91 and 0.30 ppm, corresponding to the diethylaminphosphine ligand complexes of signals I and II respectively. Furthermore a signal appear at 0.43 ppm for signal III of the 2D $^{1}H^{31}P$-HMBC spectrum. Obviously the intensity of the signals depend on the processing parameters used (see Figure SI 3.5). As window function an e-function was chosen with varying line broadening (LB), for an LB with 1.0 the signals are not really visible, with increased LB they are detected, with the best resolution with a LB of 2.0.

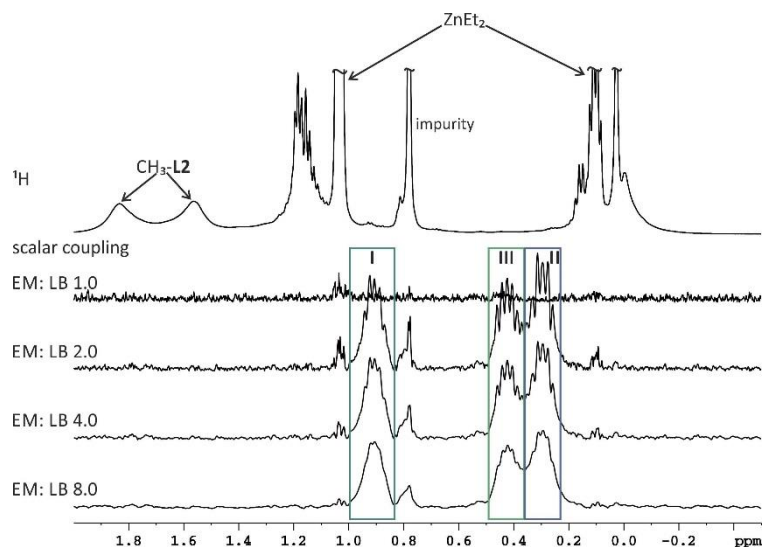**Figure SI 3.5:** ^{1}H NMR spectrum and the 1D [1]H[31]P-HMBC spectrum for magnetization transfer via scalar coupling of 1 eq **L2**, 1 eq **L2***, 1 eq CuCl and 11 eq ZnEt$_2$ with different processing parameters at 180 K in CD$_2$Cl$_2$.

3.7.2.4 Investigations of the transmetalation intermediates by Mass Spectrometry

Investigations of the transmetalation intermeditates by Mass Spectrometry were performed in cooperation with Dr. Aliaksei Putau, a former member of the Koszinowski Group at the Georg August University Göttingen. Mass spectra were recorded either at a Bruker Daltonik micrOTOF-Q II with ESI source Q-TOF mass spectrometer or at a quardupole ion trap mass spectrometer HCT with ESI, APCI and cryospray source (Bruker Daltonik). For the sample preparation the phosphoramidite copper complexes were synthesized as described above (CuI and CuCl were used as copper salt), after cooling the sample to -40-(-70) °C ZnEt$_2$ was added.

In previous measurements we were already able to detect some structural fragments of the complexes by investigations of 1:1 and 2:1 mixtures respectively of the phosphoramidite ligand **L2** with CuCl and CuBr ([**L2**$_2$Cu]$^+$ with a m/z of 941 and for the ligand two fragment peaks with m/z of 438 and 474 respectively). For most of the measurements acetonitrile was added to the solution, in order to stabilize the **L2**Cu species, afterwards also the detection of [**L2**CuMeCN]$^+$ with a m/z of 543 was possible.[20]

For better stabilization of the fragments we use THF/MeCN mixtures as solvent. Apart from the detection of the already described structural fragments, we were able to detect the complete complex species. The addition of ZnEt$_2$ to the complex mixture caused not the desired result of a detection of mixed Cu-Zn-species, which are expected for transmetalation intermediates.

2 eq **L2** + 1 eq CuI + ZnEt$_2$ in THF/MeCN:

Cation (m/z): [**L2**CuMeCN]$^+$ (543), [**L2**$_2$Cu]$^+$ (942), [**L2**$_2$Cu$_2$I]$^+$ (1133), [**L2**$_3$Cu$_2$I]$^+$ (1571), [**L2**$_4$Cu$_3$I$_2$]$^+$ (2196), [**L2**$_4$Cu$_4$I$_3$]$^+$ (2386)

Anion (m/z): CuI$_2^-$ (317)

2 eq **L2** + 1 eq CuCl + ZnEt$_2$ in THF/MeCN:

Cation (m/z): [**L2**CuMeCN]$^+$ (543), [**L2**$_2$Cu]$^+$ (942), [**L2**$_2$Cu$_2$I]$^+$ (1133), [**L2**$_3$Cu$_2$I]$^+$ (1571), [**L2**$_4$Cu$_3$I$_2$]$^+$ (2196), [**L2**$_4$Cu$_4$I$_3$]$^+$ (2386)

In the anion spectra only decomposition products of ZnEt$_2$ were observed.

3.8   Literature

[1]   T. Jerphagnon, M. G. Pizzuti, A. J. Minnaard, B. L. Feringa, *Chem. Soc. Rev.* **2009**, *38*, 1039–1075.

[2]   J. Christoffers, G. Koripelly, A. Rosiak, M. Rössle, *Synthesis* **2007**, *9*, 1279–1300.

[3]   A. Alexakis, J. E. Bäckvall, N. Krause, O. Pàmies, M. Diéguez, *Chem. Rev.* **2008**, *108*, 2796–2823.

[4]   S. R. Harutyunyan, T. den Hartog, K. Geurts, A. J. Minnaard, B. L. Feringa, *Chem. Rev.* **2008**, *108*, 2824–2852.

[5]   T. Pfretzschner, L. Kleemann, B. Janza, K. Harms, T. Schrader, *Chem. – A Eur. J.* **2004**, *10*, 6048–6057.

[6]   C. Hawner, A. Alexakis, *Chem. Commun.* **2010**, *46*, 7295–7306.

[7]   M. Shi, W. Zhang, *Adv. Synth. Catal.* **2005**, *347*, 535–540.

[8]   E. Gallo, F. Ragaini, L. Bilello, S. Cenini, C. Gennari, U. Piarulli, *J. Organomet. Chem.* **2004**, *689*, 2169–2176.

[9]   J. F. Teichert, B. L. Feringa, *Angew. Chemie Int. Ed.* **2010**, *49*, 2486–2528.

[10]   A. Alexakis, J. Frutos, P. Mangeney, *Tetrahedron: Asymmetry* **1993**, *4*, 2427–2430.

[11]   B. L. Feringa, M. Pineschi, L. A. Arnold, R. Imbos, A. H. M. De Vries, *Angew. Chemie* **1997**, *109*, 2733–2736.

[12]   A. H. M. de Vries, A. Meetsma, B. L. Feringa, *Angew. Chemie Int. Ed. English* **1996**, *35*, 2374–2376.

[13]   B. L. Feringa, R. Badorrey, D. Peña, S. R. Harutyunyan, A. J. Minnaard, *Proc. Natl. Acad. Sci. United States Am.* **2004**, *101* , 5834–5838.

[14]   S. M. W. Bennett, S. M. Brown, G. Conole, M. R. Dennis, P. K. Fraser, S. Radojevic, M. McPartlin, C. M. Topping, S. Woodward, *J. Chem. Soc. Perkin Trans. 1* **1999**, 3127–3132.

[15]   S. M. W. Bennett, S. M. Brown, A. Cunningham, M. R. Dennis, J. P. Muxworthy, M. A. Oakley, S. Woodward, *Tetrahedron* **2000**, *56*, 2847–2855.

[16]   P. K. Fraser, S. Woodward, *Chem. – A Eur. J.* **2003**, *9*, 776–783.

[17]   S. R. Harutyunyan, F. López, W. R. Browne, A. Correa, D. Peña, R. Badorrey, A. Meetsma, A. J. Minnaard, B. L. Feringa, *J. Am. Chem. Soc.* **2006**, *128*, 9103–9118.

[18]   N. Krause, *Modern Organocopper Chemistry*, WILEY-VCH Verlag GmbH, Weinheim, **2002**.

[19]   M. D. Murphy, C. A. Ogle, S. H. Bertz, *Chem. Commun.* **2005**, 854–856.

[20] H. Zhang, R. M. Gschwind, *Chem. – A Eur. J.* **2007**, *13*, 6691–6700.

[21] H. Zhang, R. M. Gschwind, *Angew. Chemie Int. Ed.* **2006**, *45*, 6391–6394.

[22] K. Schober, H. Zhang, R. M. Gschwind, *J. Am. Chem. Soc.* **2008**, *130*, 12310–12317.

[23] M. Welker, S. Woodward, L. F. Veiros, M. J. Calhorda, *Chem. – A Eur. J.* **2010**, *16*, 5620–5629.

[24] L. A. Arnold, R. Imbos, A. Mandoli, A. H. M. de Vries, R. Naasz, B. L. Feringa, *Tetrahedron* **2000**, *56*, 2865–2878.

[25] A. Alexakis, C. Benhaim, *European J. Org. Chem.* **2002**, *2002*, 3221–3236.

[26] A. Alexakis, C. Benhaim, S. Rosset, M. Humam, *J. Am. Chem. Soc.* **2002**, *124*, 5262–5263.

[27] T. Thaler, B. Haag, A. Gavryushin, K. Schober, E. Hartmann, R. M. Gschwind, H. Zipse, P. Mayer, P. Knochel, *Nat Chem* **2010**, *2*, 125–130.

[28] R. M. Gschwind, *Chem. Rev.* **2008**, *108*, 3029–3053.

[29] Z. Rappoport, I. Marek, *The Chemistry of Organocopper Compounds Part 1*, John Wiley / Sons Ltd., **2009**.

[30] T. Gärtner, R. M. Gschwind, in *Chem. Organocopper Compd.*, John Wiley & Sons Ltd., **2009**.

[31] S. H. Bertz, M. D. Murphy, C. A. Ogle, A. A. Thomas, *Chem. Commun.* **2010**, *46*, 1255–1256.

[32] K. Schober, E. Hartmann, H. Zhang, R. M. Gschwind, *Angew. Chemie Int. Ed.* **2010**, *49*, 2794–2797.

[33] P. Ernö, S. Joseph, S. Wilhelm, C. Thomas, *Strukturaufklärung Organischer Verbindungen Mit Spektroskopischen Methoden*, Springer Verlag Berlin Heidelberg, **1990**.

[34] S. H. Bertz, *J. Am. Chem. Soc.* **1990**, *112*, 4031–4032.

[35] S. H. Bertz, S. Cope, D. Dorton, M. Murphy, C. A. Ogle, *Angew. Chemie Int. Ed.* **2007**, *46*, 7082–7085.

[36] E. R. Bartholomew, S. H. Bertz, S. Cope, D. C. Dorton, M. Murphy, C. A. Ogle, *Chem. Commun.* **2008**, 1176–1177.

[37] R. M. Gschwind, M. Armbrüster, I. Z. Zubrzycki, *J. Am. Chem. Soc.* **2004**, *126*, 10228–10229.

[38] G. Federwisch, R. Kleinmaier, D. Drettwan, R. M. Gschwind, *J. Am. Chem. Soc.* **2008**, *130*, 16846–16847.

[39] F. Löhr, S. G. Mayhew, H. Rüterjans, *J. Am. Chem. Soc.* **2000**, *122*, 9289–9295.

[40]   S. Berger, S. Braun, H.-O. Kalinowski, *NMR-Spektroskopie von Nichtmetallen, Bd. 3: 31P-NMR-Spektroskopie*, Georg Thieme Verlag, Stuttgart, **1997**.

[41]   E. Hartmann, R. M. Gschwind, *Angew. Chemie Int. Ed.* **2013**, *52*, 2350–2354.

[42]   E. Hartmann, M. M. Hammer, R. M. Gschwind, *Chem. – A Eur. J.* **2013**, *19*, 10551–10562.

[43]   F. Hastreiter, Master Thesis, NMR-Spektroskopische Untersuchungen an Pd-Komplexen, Universität Regensburg, **2014**.

[44]   A. F. Holleman, E. Wiberg, N. Wiberg, *Lehrbuch Der Anorganischen Chemie*, Walter De Gruyter, Berlin, **1995**.

[45]   D. F. Evans, G. V Fazakerley, *J. Chem. Soc. A* **1971**, 182–183.

[46]   C. Elschenbroich, *Organometallchemie*, B. G. Teubner Verlag, Wiesbaden, **2008**.

[47]   R. G. Goel, A. L. Beauchamp, *Inorg. Chem.* **1983**, *22*, 395–400.

[48]   C. Koch, Master Thesis, NMR-Spektroskopische Studien Mechanistischer Schlüsselschritte in Der Cu-Katalysierten Konjugierten 1,4-Additionsreaktion Mit Dimethylzink, Universität Regensburg, **2011**.

[49]   D. Müller, M. Tissot, A. Alexakis, *Org. Lett.* **2011**, *13*, 3040–3043.

[50]   M. Kasturiah, A. Uma Ravi Sankar, B. Siva Kumar, C. Suresh Reddy, C. Naga Raju, *Chinese J. Chem.* **2009**, *27*, 408–412.

[51]   J. E. Phelps, S. B. Frawley, R. G. Peters, *Heteroat. Chem.* **2009**, *20*, 393–397.

[52]   A. Alexakis, N. Krause, S. Woodward, *Copper-Catalyzed Asymmetric Synthesis*, Wiley-VCH Verlag GmbH & Co. KGaA, Weinheim, **2014**.

[53]   "AIST: Integrated Spectral Database System of Organic Compounds (Data were obtained from the National Institute of Advanced Industrial Science and Technology (Japan))," can be found under http://sdbs.db.aist.go.jp/sdbs/cgi-bin/direct_frame_top.cgi

[54]   J. B. Johnson, R. T. Yu, P. Fink, E. A. Bercot, T. Rovis, *Org. Lett.* **2006**, *8*, 4307–4310.

[55]   M. Schinnerl, M. Seitz, A. Kaiser, O. Reiser, *Org. Lett.* **2001**, *3*, 4259–4262.

[56]   C. Bolm, J. P. Hildebrand, K. Muñiz, N. Hermanns, *Angew. Chemie Int. Ed.* **2001**, *40*, 3284–3308.

[57]   S. H. Bertz, G. Dabbagh, X. He, P. P. Power, *J. Am. Chem. Soc.* **1993**, *115*, 11640–11641.

[58]   D. Pena, F. Lopez, S. R. Harutyunyan, A. J. Minnaard, B. L. Feringa, *Chem. Commun.* **2004**, 1836–1837.

[59]   K. Schober, PhD Thesis, NMR-Investigations on Intermediates and Interactions in Transition-Metal Catalysis, University of Regensburg, **2011**.

[60]   K. Lee, M. K. Brown, A. W. Hird, A. H. Hoveyda, *J. Am. Chem. Soc.* **2006**, *128*, 7182–7184.

[61]   "Chem 605 - Structure Determination Using Spectroscopic Methods," can be found under http://www.chem.wisc.edu/areas/reich/chem605/index.htm

[62]   A. Alexakis, S. Rosset, J. Allamand, S. March, F. Guillen, C. Benhaim, *Synlett* **2001**, *2001*, 1375–1378.

[63]   F. Mutzbauer, Diploma Thesis, Umsetzung von Polypentelanionen Mit Übergangsmetallkomplexen in Flüssigem Ammoniak, Universität Regensburg, **2008**.

3.9 Submitted Manuscript

The Elusive Transmetalation Intermediate in Copper-Catalyzed Conjugate Additions: Direct NMR Detection of an Ethyl Group Attached to a Binuclear Phosphoramidite Copper Complex[*]

Abstract: Asymmetric copper-catalyzed conjugate addition reactions are a very powerful and widely applied method for the enantioselective carbon-carbon bond formation. In contrast, the structural and mechanistic insight into these famous reactions has been very limited so far. In this study for the first time a direct experimental detection of transmetalation intermediates in copper-catalyzed reactions is presented. Special combinations of ^{1}H^{31}P-HMBC spectra allow for the identification of complexes with chemical bonds between the alkyl groups and the copper complexes. For the structural characterization of these transmetalation intermediates a special approach is applied, in which samples using enantiopure ligands are compared with others using enantiomeric mixtures of ligands. For the first time the retention of the dimeric copper complex structure upon transmetalation is experimentally proven providing an intermediate with mixed trigonal/tetrahedral coordination on the copper atoms. In addition, monomeric intermediates with one ligand but none with two ligands are detected. These experimental results in combination with the well known ligand to copper ratio of 2:1 in synthetic applications allow to propose the binuclear transmetalation intermediate as reactive species in asymmetric copper-catalyzed conjugate addition reactions. This first direct experimental insight into the structure of the transmetalation intermediate is expected to support the mechanistic and theoretical understanding of this important class of reactions and to enable further synthetic development. In addition, the special NMR approach presented here for the identification and characterization of intermediates below to the detection limit of ^{1}H spectra can be applied also to other classes of catalyses.

Introduction

The asymmetric copper-catalyzed conjugate addition (ACA) reaction is one of the most powerful methods for enantioselective carbon-carbon bond formation in organic synthesis, which often combines excellent regio- and stereoselectivities, a high compatibility with many functional groups and low costs of the copper salts (for recent reviews see[1-4]). In this active research area, recent efforts considerably enlarged the scope of substrates and nucleophiles, which allow numerous syntheses of complex chiral organic compounds including e.g. biologically active and natural compounds.[1-7] However, in contrast to the great synthetic success of the ACA reaction, structural and mechanistic studies about the copper complexes and their reaction intermediates

---

Felicitas von Rekowski, Carina Koch, Ruth M. Gschwind

are very rare. Therefore, more structural information about the reaction intermediates and the enantiodiscriminating steps were claimed to be an essential prerequisite for the further development of this important class of reactions.[1,4,8]

To our knowledge, the only in depth experimental study of transmetalation intermediates in copper-mediated ACA reactions known so far, has been presented by Feringa *et al.* using a combination of copper complexes with chiral bidentate ferrocenyl-based diphosphine ligands and Grignard reagents.[9] In this brilliant study, a binuclear, halide-bridged diphosphine copper complex was reported as precatalyst based on e.g. ^{31}P NMR spectroscopic, electrochemical and kinetic investigations (Scheme 3.8 a). Performing several sophisticated indirect experimental studies, Feringa reasoned that the dimeric copper precatalyst breaks up via transmetalation with the Grignard reagent and forms a bimetallic complex, which is mononuclear in copper (Scheme 3.8 a).[9] This mixed metallic composition of the complex proposed by Feringa perfectly agrees with the core element of e.g. the famous intermetallic Knochel cuprates FGRCu(CN)ZnI.[10]

In our NMR studies of copper complexes with monodentate phosphoramidite ligands similar binuclear copper complexes were found as basic structural motif of the thermodynamic ground state of precatalysts with highly stereoselective ligands.[11,13,14] However, in solution as main species a binuclear copper complex with mixed trigonal/tetrahedral stereochemistry (see [$Cu_2X_2L_3$] in Scheme 3.8 b) was identified. At temperatures below 200 K, self-aggregation of the phosphoramidite ligands starts[15] and intermolecular interactions between free ligand and [$Cu_2X_2L_3$] induce the formation of the binuclear complex [$Cu_2X_2L_4$] corroborating the known crystal structures.[9,16] Recently, a DFT study of the reaction mechanism of ACA reactions with monodentate phosphoramidite ligands corroborated both studies.[12] As lowest energy transmetalation complexes, accessible from simplified phosphoramidite ligands, Cu(OAc) and ZnMe$_2$, monomeric zinc cuprates were identified (Scheme 3.8 c left).[17] However, starting from this monomeric zinc cuprate, reasonable energetic pathways were only accessible for π-complexes derived from the binuclear structure with mixed trigonal/tetrahedral stereochemistry (Scheme 3.8 c right).[12]
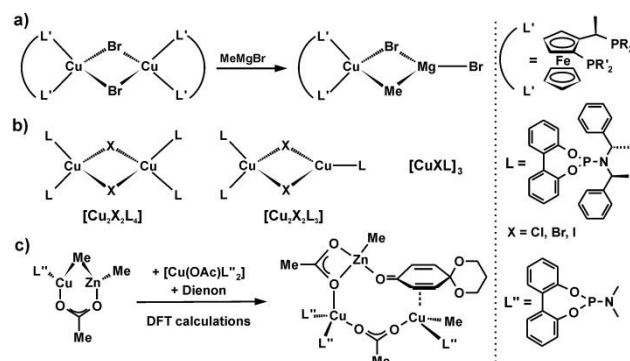
Scheme 3.8: Proposed structures of precatalysts and transmetalation intermediates: a) Monomerization and formation of a bimetallic transmetalation complex upon addition of MeMgBr,[9] b) Interconversion/coexistence of phosphoramidite copper complexes [Cu$_2$X$_2$L$_4$], [Cu$_2$X$_2$L$_3$] and [CuXL]$_3$ with [Cu$_2$X$_2$L$_3$] as proposed precatalyst of the ACA reaction,[11] c) Monomeric in Cu, but bimetallic transmetalation intermediate and a π-complex, which essentially agrees with [Cu$_2$X$_2$L$_3$] calculated theoretically.[12]

The transmetalation of an organic moiety from ZnR$_2$, RMgX or AlR$_3$ reagents is a commonly accepted step in mechanistic schemes of ACA reactions.[1,3,4,8] However, to the best of our knowledge a direct experimental detection of a transmetalated intermediate was elusive so far and information about the structure or even the stoichiometry of transmetalation complexes with ZnR$_2$ or AlR$_3$ are not available at all.[1,4]

Therefore we present in this paper an NMR spectroscopic investigation of the transmetalation reaction between phosphoramidite copper precatalyst [Cu$_2$X$_2$L$_3$] and diethylzinc. For the first time a direct experimental evidence of a transmetalation intermediate in the ACA reaction is presented. In addition, for the first time a transmetalation complex which is binuclear in copper is detected, which essentially retains the structure of the precatalytic complex [Cu$_2$X$_2$L$_3$]. Apart from this binuclear transmetalation complex, also several mononuclear copper transmetalation complexes were detected.

Results and Discussion

For the NMR spectroscopic investigation of transmetalated phosphoramidite copper complexes, a 2:1 ratio of the highly enantioselective phosphoramidite ligand **L** and CuI in CD$_2$Cl$_2$ was chosen (see Scheme 3.9). Previous investigations[11] and low temperature studies[13] showed that this model system reveals the best ^{31}P chemical shift dispersion at 180 K and the broadest temperature range for the exclusive existence of [Cu$_2$X$_2$L$_3$]. Furthermore, in CD$_2$Cl$_2$ narrow line widths were observed for the complex species.[14] From the variety of organometallic reagents ZnEt$_2$ as well as ZnMe$_2$ and ZnPh$_2$ were selected to cover a broader spectrum of transmetalation reagents. ZnEt$_2$ is broadly used in synthetic applications providing high yields and enantioselectivies,[1] the methyl groups in ZnMe$_2$ should stabilize the transmetalation intermediate, due to a lower reactivity[18,19] and phenyl groups are assumed to be more readily

transferred then alkyl groups.[18,20-23] However, for $ZnMe_2$ and $ZnPh_2$ only unspecific interactions with the copper complexes were detected (see supporting information). Therefore, in the following exclusively investigations with $ZnEt_2$ are discussed. In synthetic applications a high excess of $ZnEt_2$ with regard to the copper complex is applied (60-70 eq).[24] In order to increase the signal to noise ratio (S/N) and to enable the detection of upstream intermediates here a reduced excess of $ZnEt_2$ is used (4-20 eq compared to $[Cu_2X_2L_3]$). With commercially available solutions of $ZnEt_2$ in toluene the spectral quality was too bad to detect any transmetalation intermediates. Therefore neat $ZnEt_2$ in CD_2Cl_2 was used (for spectra and details see supporting information). Investigations in a temperature range of 170-250 K showed, that both the highest signal intensities and the highest number of intermediate species were detected at 170 and 180 K. Therefore in the following exclusively the low temperature spectra (170-180 K) are discussed.

After addition of $ZnEt_2$ to the copper complex neither in the ^1H nor in the ^{31}P NMR spectra any signals of transmetalated species could be detected. Next $^1H^{31}P$-HMBC spectra were tested, which act as a spectroscopic filter for free $ZnEt_2$ and are therefore highly sensitive to transmetalation complexes. In case of an ethyl group, transmetalated to copper, a magnetization transfer of the protons of the ethyl group via copper to the phosphorous atom of a ligand should become possible (see Scheme 3.9 on the example of $[Cu_2X_2L_3]$). Such a magnetization transfer is visible as cross signal in $^1H^{31}P$-HMBC spectra.
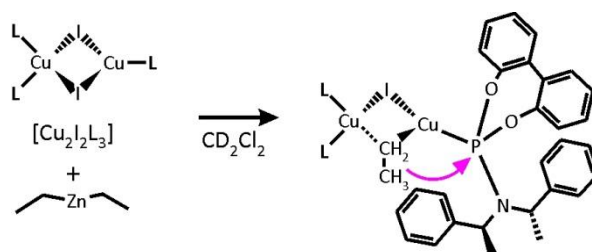
Scheme 3.9: Proposed transmetalation step of $ZnEt_2$ to $[Cu_2X_2L_3]$. In case an ethyl group and a phosphoramidite ligand are both bound to one copper atom, a $^1H^{31}P$-HMBC cross peak between those moieties (see purple arrow) should indicate a transmetalation intermediate.

The use of $^1H^{31}P$-HMBC spectra was already successfully applied in investigations of palladium-catalyzed Negishi coupling reactions.[25] However, in contrast to palladium complexes used in the previous study, the transfer of magnetization via copper is much more difficult.[26] The high quadrupole moment of $^{63/65}Cu$ provides an efficient relaxation pathway for magnetization leading to short relaxation times and broad line widths of the nuclei directly coordinated to the copper atom (see e.g. the ^{31}P line width of $[Cu_2I_2L_3]$ versus **L** in the supporting information). Therefore, especially in complexes with relevant electric field gradients, i.e. with P-, N-, or S-ligands, and structures deviating from a highly symmetrical coordination, scalar couplings across copper are usually not detectable.[26] As a result, successful experimental magnetization transfers

via copper are reported only for few examples, e.g. in $^1H^{13}C$-HMBC spectra of ^{13}C-labelled organocuprates,[27] in $^1H^{31}P$-HMBC spectra of $Me_3Cu(PPh)_2Li$[28] or $^{31}P^{31}P$-COSY spectra of complexes $[Cu_2X_2L_2]$ (X: Cl, Br; L: **L**).[8,11] On the other hand, the $^1H^{31}P$-HMBC pulse sequence acts as an isotope filter for transmetalation intermediates, eliminating all signals of free $ZnEt_2$ beside very small remaining unspecific interactions (visible between free $ZnEt_2$ and the precatalytic complex or the free ligand respectively, see below), thus even extremely small amounts of intermediates can be detected. Indeed, despite all obstacles for copper complexes described above, we were able to detect new signals of transmetalation intermediates in $^1H^{31}P$-HMBC spectra neither detectable in ^1H nor in ^{31}P NMR spectra. As a consequence, the complete identification and structural characterization of the transmetalation intermediates had to be based exclusively on $^1H^{31}P$-HMBC spectra.

First we had to produce proof of real transmetalation intermediates allowing for magnitization transfers through bonds via scalar coupling in contrast to other kinds of complexes possibly leading to cross signals through space via cross correlation (as combination of chemical shift anisotropy and dipolar interaction). Therefore, several modified 1D $^1H^{31}P$-HMBC spectra were measured (see Figure 3.28 a). These experiments were already applied successfully in investigations of H-bond networks in acylguanidin complexes and of flavoproteins.[29-31] In Figure **3.28** b a comparison of the ^1H NMR and the 1D $^1H^{31}P$-HMBC spectra is shown. For signals 2-5 (red ellipses) only signals in the HMBC and in the scalar coupling spectra were observed. These signals belong to transmetalation intermediates with a directly bound ethyl group (for assignment see below). Signal 1 and the signal at 0.95 ppm (red boxes) show the same NMR characteristic, that means ethyl groups and phosphorous atoms linked by chemical bonds, but these signals were assigned to side products, in which $ZnEt_2$ is bound to the ligand and not to copper (for details see supporting information). Unspecific interactions show signals in all three 1D $^1H^{31}P$-HMBC spectra as visible here for bulk $ZnEt_2$ (see red dashed boxes in Figure 3.28 b and for details see supporting information).
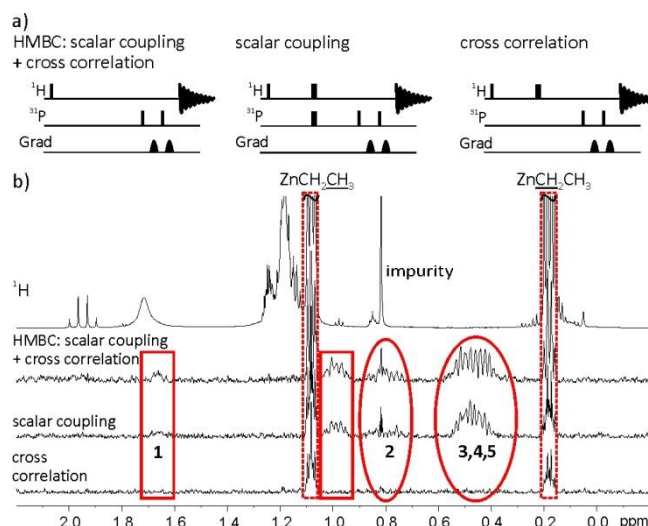
Figure 3.28: a) Pulse sequences of the 1D $^1H^{31}P$-HMBC allowing for magnetization transfers via scalar coupling and cross correlation as well as modified versions for the exclusive detection of scalar coupling or cross correlation; b) Comparison of the ^1H NMR and 1D $^1H^{31}P$-HMBC spectra of 2 eq **L**, 1 eq CuI and 7 eq ZnEt$_2$ at 230 K in CD$_2$Cl$_2$. Red ellipses and boxes indicate transfers via scalar couplings, red dashed boxes represent unspecific interactions.

The signals of the transmetalation intermediates 2-5 could be also detected in the 2D $^1H^{31}P$-HMBC spectra (see Figure 3.29 b). Their ^1H chemical shift range of 0.80-0.30 ppm is in agreement with a CH$_2$ group transmetalated to a neutral Cu(I) complex. $\delta(^1H)$ of CH$_2$ of negatively charged cuprates show upfield shifted signals (Et$_2$CuLi•LiI and Et$_2$CuLi•LiCN -0.53 and -0.54 ppm, respectively[32]), ethyl groups bound to Cu(III) low field shifted signals (e.g. Me$_3$EtCu 0.54 ppm,[33] Me$_2$EtCuPMe$_3$ 1.89 ppm, Me$_2$EtCuP(OMe)$_3$ 2.07 ppm and Me$_2$EtCu(PPh$_3$) 2.31 ppm[34]). In the ^{31}P dimension all four signals of the transmetalation intermediates are upfield shifted compared to the precatalytic copper complex by 2.9 to 7.4 ppm. This is in agreement with the upfield shifts observed for transmetalation intermediates of Grignard reagents and ferrocenyl-based diphosphine copper complexes (1.8 and 3.1 ppm).[9] Thus, to our knowledge the presented $^1H^{31}P$-HMBC data provide for the first time a direct experimental proof for transmetalation intermediates of copper complexes. The lowfield shifts of the ^1H and the upfield shifts of the ^{31}P resonances of the transmetalation intermediates relative to free ZnEt$_2$ and the precatalytic copper complex corroborate previous results of Bertz and Feringa.[9,28]

Next the structure of these transmetalation intermediates was addressed. In principle several structures of transmetalation intermediates are feasible, which are either mono- or dimeric in copper and contain one, two or three ligands as well as varying amounts of ZnEt$^+$ and I$^-$ moieties (see Figure 3.29 a). Using DFT-calculations, simplified phosphoramidite ligands, Cu(OAc) and ZnMe$_2$, Woodward and co-workers identified the monomeric zinc cuprate **A** as lowest energy structure for transmetalation intermediates.[12] Furthermore, species **A** and **C** were proposed for monomeric transmetalation intermediates with Grignard reagents described by Feringa and co-

workers.[9] Monomeric transmetalation intermediates with two ligands **D** were proposed in several reaction mechanisms due to the typical ligand to copper ratio of 2:1.[4,7,24] For the dimeric transmetalation intermediates with three ligands, structures **E-G** are possible.

To address the structure under the prerequisite that exclusively ^{1}H^{31}P-HMBC spectra can be used, a special approach has to be applied. In principle information about the number of ligands can be gained by comparing ^{1}H^{31}P-HMBC spectra of transmetalation intermediates with enantiopure phosphoramidite ligands (**L**) and such with equal amounts of enantiomeric phosphoramidite ligands (50 % **L**, 50 % **L***). Intermediates with one ligand are not affected by the use of the enantiomeric mixture of the phosphoramidite ligands, because complexes with one ligand form only enantiomers, which are not distinguishable by NMR spectroscopy (for a graphical representation see Figure 3.29 b). As a result, all complexes with one ligand appear with the same integral in both samples. In contrast, species with two or three ligands are expected to appear with reduced signal integrals of the enantiopure intermediates. In addition, new signals should arise due to formation of diastereomers with mixed ligand arrangements. For monomeric transmetalation intermediates with two ligands, one reduced signal and one new signal are expected; for dimeric structures with three ligands a pattern of one reduced and three new signals is expected (see Figure 3.29 b).
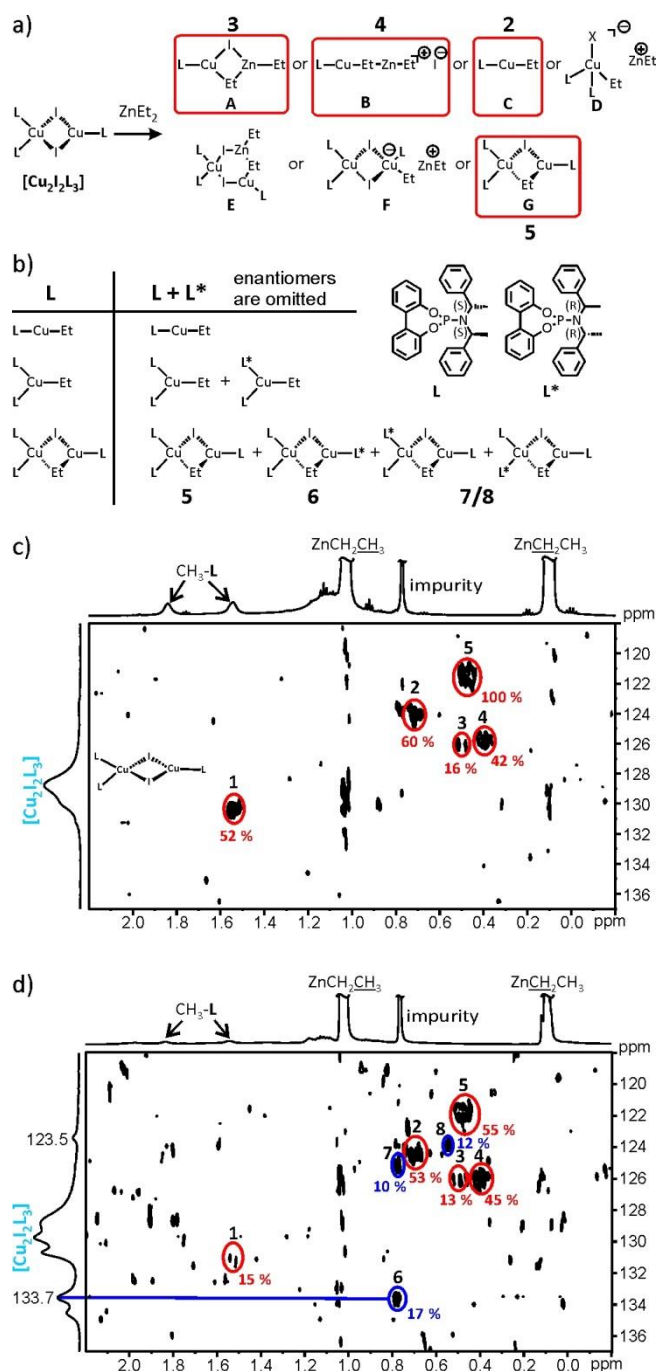
Figure 3.29: a) Possible monomeric **A-D** and dimeric transmetalation intermediates **E-G** after the addition of ZnEt$_2$ to the precatalyst [Cu$_2$I$_2$L$_3$]. The numbers indicate the signals finally assigned to these structures; b) signal distribution of the transmetalation intermediates with enantiopure ligands (**L**) and an enantiomeric mixture (**L** + **L***) including signal assignment; c) section of the 2D ^{1}H^{31}P-HMBC spectrum with 2 eq **L**, 1 eq CuI and 14.7 eq ZnEt$_2$ at 170 K in CD$_2$Cl$_2$; d) corresponding section of the 2D ^{1}H^{31}P-HMBC spectra with 1 eq **L**, 1 eq **L***, 1 eq CuI and 14.5 eq ZnEt$_2$ at 170 K in CD$_2$Cl$_2$. The signal integrals given are referenced to signal 5 of the enantiopure sample. The integrals of signals 2-4 (red) are nearly identical in both spectra indicating monomeric complexes with one ligand. In contrast signal 5 (red) diminishes and signals 6-8 arise in the enantiomeric mixture (blue) indicating a complex with three ligands. For structure assignment see a) and b) and text.

In Figure 3.29 c and Figure 3.29 d the 2D ^{1}H^{31}P-HMBC spectra of the complexes with enantiopure ligands **L** (Figure 3.29 c) and with the enantiomeric mixture of **L** and **L*** (Figure 3.29 d) are presented after addition of ZnEt$_2$. Indeed three classes of signals occur in the spectrum of the

enantiomeric ligand mixture. Signals 2-4 (red) show similar integrals within the experimental error. This indicates monomeric species with one ligand for complexes 2-4. In contrast signal 5 (red) shows around half the integral. In addition, three new signals 6-8 (blue) appear in the enantiomeric mixture. This pattern fits exactly to a dimeric structure with three ligands (see Figure 3.29 b). Furthermore, the integrals of these four intermediates 5-8 sum up to 94 %, which is strong evidence that all of these four intermediates in the enantiomeric mixture indeed originate from intermediate 5 in the enantiopure sample (100 %). This gives experimental evidence for the retention of the binuclear complex structure upon transmetalation with mixed trigonal/tetrahedral coordination on the copper atoms and excludes monomeric intermediates with two ligands. At first glance the integral distribution of signals 5-8 is puzzling, because the assumption of identical interligand interactions for **LL** and **LL*** leads to a statistical distribution of 25 % for all four diastereomers (for details see supporting information). However, previous and ongoing investigations of noncovalent interligand interactions in phosphoramidite palladium and copper complexes showed distinct preferences for special ligand combinations[35-37] and quite pronounced interligand interactions.[15,35-37] Such significant interaction preferences directly lead to non-statistical distributions as observed here. Signal 5 appearing over statistically with 55 % indicates a preference for interactions between enantiopure ligands (see Figure 3.29 d). This is also visible on a lower level in the integrals of signals 6-8 with 17 %, 12 % and 10 %, showing lower values for mixed ligand arrangements at the copper fragment with two ligands (see Figure 3.29 b).

To sum up, signals 2-4 are identified as monomeric species with one ligand and the signal and integral pattern of signals 5-8 indicate a dimeric transmetalation intermediate with three ligands.

Next the structures of the transmetalation intermediates 2-8 were refined to assign the intermediates 2-8 to the structures **A**, **B**, **C** and **E**, **F**, **G** (see Figure 3.29 a and Figure 3.29 b). Since a selective chelation of zinc versus copper is very difficult, the involvement of ZnI units was addressed by varying the amount of ZnI_2. For this purpose a high excess of ZnI_2 was added to a sample of 2 eq **L**, 1 eq CuI and 7.7 eq $ZnEt_2$ (for spectra see supporting information). With a high excess of ZnI_2 the signals of the complexes with ZnI moieties should become stronger, whereas those without ZnI moieties should decrease. In the resulting $^1H^{31}P$-HMBC, only signal 3 of a monomeric complex remained. Thus, 3 represents the only structure with a ZnI unit and was assigned to the monomeric species **A**. Signals 2 and 4 are also monomeric species (see above) but without ZnI units. They show significant differences in their proton chemical shifts as expected for species with a ZnEt unit (upfield shift of the CH_2 group) and without. Therefore, signal 4 is assigned to **B** and signal 2 to **C**. The addition of ZnI_2 also shows that no ZnI moiety is

incorporated in the complex of signal 5, which excludes structure **E**. The involvement of a halogen bridge was proven by further investigations with CuCl as copper salt. For CuI and CuCl no identical signals of transmetalation intermediates were observed in the 2D ^{1}H^{31}P-HMBC spectra (for details see supporting information). This indicated the existence of a halogen bridge in the dimeric transmetalation complex. In addition, samples with CuCl and high amounts of ZnEt$_2$ showed cuprate like structures with distinct upfield shifted signals (for details see supporting information). This pronounced chemical shift difference excludes two ethyl groups bound to one copper atom in the transmetalation intermediates discussed here. The remaining differentiation between structures **F** and **G** for signal 5 can be solved by the formation trends of the transmetalation intermediates dependent on the equivalents of ZnEt$_2$ added (see Figure 3.30). The analysis of the monomeric transmetalation intermediates with one ligand shows that **A** and **B** containing ZnEt units are preferentially formed at lower amounts of ZnEt$_2$, whereas the "final" transmetalation intermediate **C** without a ZnEt unit accumulates at higher amounts of ZnEt$_2$. Due to the fact that we used in this investigation a significantly reduced excess of ZnEt$_2$ compared to synthetic application (see above), in synthesis the preference of **C** is expected to be even more pronounced. Assuming similar trends for the formation of dimeric transmetalation intermediates as indicated by similar intensity trends of signals 2 and 5, signal 5 can be assigned to the "final" transmetalation intermediate **G** without ZnEt unit. Considering the results described above, further structural characteristics of **G** are one ethyl and one iodine bridge, and the retention of the mixed trigonal/tetrahedral coordination on the copper atoms. This structural assignment is corroborated by the number of the new appearing signals 6-8 in the enantiomeric mixture as well as by their integral pattern, representing the three possible diastereomers of **G** with mixed ligand arrangements and indicating a preference for homoligand interactions.
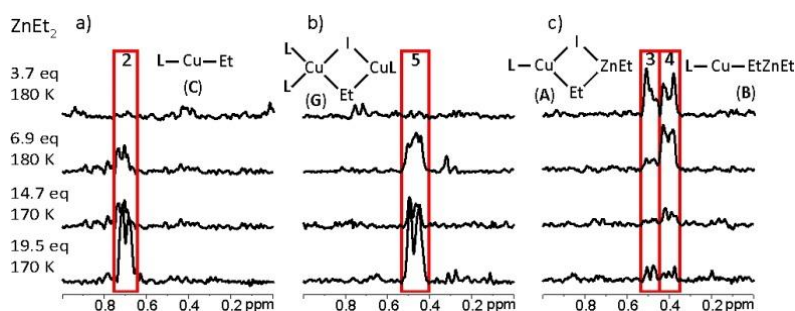

Figure 3.30: Formation trends of transmetalation intermediates with 2 eq **L**, 1 eq CuI and an increasing excess of ZnEt$_2$ (typical synthetic conditions about 60 eq. ZnEt$_2$). at 170 and 180 K in CD$_2$Cl$_2$. The 1D rows taken from the 2D ^{1}H^{31}P-HMBC spectra at the ^{31}P chemical shifts of the respective intermediates reveal intermediates 3 and 4 as precursors and 2 as well as 5 as final intermediates.

The existence of monomeric transmetalation intermediates with one ligand coordinated to copper is in agreement with results of Feringa and co-workers, who found exclusively monomeric transmetalation intermediates with one ligand as transmetalation intermediates with Grignard

reagents.[9] The structures proposed in this study are similar to **A** and **C** observed here. Monomeric intermediates with CuL_2 fragments as often proposed in reaction mechanisms were neither detected in this study nor previously by Feringa. Furthermore, here for the first time a transmetalation intermediate with a binuclear structure with mixed trigonal/tetrahedral coordination on the copper atoms is experimentally detected, which provides both an open coordination place for the enone and plenty of ligand interactions for high stereoselectivities (see studies on palladium phosphoramidite complexes for interaction schemes of phosphoramidite ligands).[36,37] Now, the question remains, whether the monomeric **C** or the binuclear **G** is the reactive transmetalation intermediate being both detected in similar amounts. So far, there are no direct experimental proofs accessible but strong indirect arguments. The most substantial argument for the binuclear complex **G** as reactive species is the well known ligand to copper ratio of 2:1 in synthetic applications. At ligand to copper ratios of 2:1, stabilizing optimal the binuclear complex with the mixed trigonal/tetrahedral coordination on copper,[13] highly enantioselective reactions can be performed.[1,8,24] At ligand to copper ratios of 1:1, stabilizing optimal the monomeric complex **C** with one ligand only considerably reduced enantioselectivities are obtained. Considering **G** as reactive species, at first glance the high enantioselectivities in the presence of nearly equal amounts of **G** and **C** are puzzling. At this point DFT-calculations of Woodward give an explanation, because in that theoretical study starting from monomeric transmetalation intermediates only suitable energetic pathways for dimeric copper complexes with mixed trigonal/tetrahedral coordination were found.[12]

Conclusions

In summary the first direct experimental detection of transmetalation intermediates in asymmetric copper-catalyzed addition reactions is presented using phosphoramidite copper complexes [$Cu_2X_2L_3$] and an excess of $ZnEt_2$. The transmetalation intermediates, which are below the detection limit in one-dimensional ^1H and ^{31}P spectra, were identified by using a special set of 1D $^1H^{31}P$-HMBC spectra separating complexes with ethyl groups chemically bound from those with unspecific interactions. For the structure characterization again a special approach was applied using samples with enantiopure ligands and samples with mixtures of enantiomeric ligands. This and experiments with CuCl, ZnI_2 and varying amounts of $ZnEt_2$ revealed two main transmetalation intermediates: one with one ethyl group and one ligand as well as for the first time a binuclear intermediate with three ligands, one ethyl group and a mixed trigonal/tetrahedral coordination on the copper atoms. Intermediates with two ligands were not observed. The well known optimal ligand to copper ratio of 2:1 in combination with theoretical calculations proposing feasible reaction pathways only for binuclear complexes and the

experimental study presented here reveal a retention of the binuclear copper complex with mixed trigonal/tetrahedral coordination in the reactive transmetalation intermediate. This first direct experimental insight into the structure of transmetalation intermediates is expected to aid the mechanistic understanding and the further synthetic development of the asymmetric copper-catalyzed conjugate addition reaction and related methods. In addition, the special NMR approach presented here to characterize the structure of reaction intermediates below the detection limit of ^{1}H and ^{31}P spectra can be also applied to other catalytic system.

References

(1)   Alexakis, A.; Backvall, J. E.; Krause, N.; Pamies, O.; Dieguez, M. *Chem. Rev.* **2008**, *108*, 2796.

(2)   Christoffers, J.; Koripelly, G.; Rosiak, A.; Roessle, M. *Synthesis* **2007**, 1279.

(3)   Hawner, C.; Alexakis, A. *Chem. Comm.* **2010,** *46*, 7295.

(4)   Jerphagnon, T.; Pizzuti, G. M.; Minnaard, A. J.; Feringa, B. L. *Chem. Soc. Rev.* **2009**, *38*, 1039.

(5)   Gallo, E.; Ragaini, F.; Bilello, L.; Cenini, S.; Gennari, C.; Piarulli, U. *J. Organomet. Chem* **2004**, *689*, 2169.

(6)   Min, S.; Wen, Z. *Adv. Synth. Catal.* **2005**, *347*, 535.

(7)   Pfretzschner, T.; Kleemann, L.; Janza, B.; Harms, K.; Schrader, T. *Chem. Eur. J.* **2004**, *10*, 6048.

(8)   Teichert, J. F.; Feringa, B. L. *Angew. Chem. Int. Ed.* **2010**, *49*, 2486.

(9)   Harutyunyan, S. R.; Lopez, F.; Browne, W. R.; Correa, A.; Pena, D.; Badorrey, R.; Meetsma, A.; Minnaard, A.; Feringa, B. L. *J. Am. Chem. Soc.* **2006**, *128*, 9103.

(10)   Knochel, P.; Singer, R. D. *Chem. Rev.* **1993**, *93*, 2117.

(11)   Zhang, H.; Gschwind, R. M. *Chem. Eur. J.* **2007**, *13*, 6691.

(12)   Welker, M.; Woodward, S.; Veiros, L. F.; Calhorda, M. J. *Chem. Eur. J.* **2010**, *16*, 5620.

(13)   Schober, K.; Zhang, H.; Gschwind, R. M. *J. Am. Chem. Soc.* **2008**, *130*, 12310.

(14)   Zhang, H.; Gschwind, R. M. *Angew. Chem. Int. Ed*. **2006**, *45*, 6391.

(15)   Schober, K.; Hartmann, E.; Zhang, H.; Gschwind, R. M. *Angew. Chem. Int. Ed.* **2010**, *49*, 2794.

(16)   Shi, W.-J.; Wang, L.-X.; Fu, Y.; Zhu, S.-F.; Zhou, Q.-L. *Tetrahedron Asymmetry* **2003**, *14*, 3867.

(17)   The change from the monodentate Br to the bidentate OAc is in accordance with the by one reduced number of ligands in the transmetalation complex.

(18)   Woodward, S. In Copper-Catalyzed Asymmetric Synthesis; Alexakis, A., Krause, N., Woodward, S., Eds.; Wiley-VCH: Weinheim, **2014**, p 3.

(19)   Lee, K.-S.; Brown, M. K.; Hird, A. W.; Hoveyda, A. H. *J. Am. Chem. Soc*. **2006,** *128*, 7182.

(20)   Bertz, S. H.; Dabbagh, G.; He, X.; Power, P. P. *J. Am. Chem. Soc.* **1993**, *115*, 11640.

(21)   Johnson, J. B.; Yu, R. T.; Fink, P.; Bercot, E. A.; Rovis, T. *Org. Lett.* **2006**, *8*, 4307.

(22)   Schinnerl, M.; Seitz, M.; Kaiser, A.; Reiser, O. *Org. Lett.* **2001**, *3*, 4259.

(23)   Bolm, C.; Hildebrand, J. P.; Muñiz, K.; Hermanns, N. *Angew. Chem. Int. Ed.* **2001**, *40*, 3284.

(24)   Alexakis, A.; Benhaim, C.; Rosset, S.; Humam, M. *J. Am. Chem. Soc*. **2002**, *124*, 5262.

(25)   Thaler, T.; Haag, B.; Gavryushin, A.; Schober, K.; Hartmann, E.; Gschwind, R. M.; Zipse, H.; Mayer, P.; Knochel, P. *Nature Chemistry* **2010**, *2*, 125.

(26)   Gschwind, R. M. *Chem. Rev.* **2008**, *108*, 3029.

(27)   Gärtner, T.; Gschwind, R. M. In The Chemistry of Organocopper Compounds; Rappoport, Z., Marek, I., Eds.; John Wiley & Sons Ltd.: Chichester, England, **2009**, p 163.

(28)   Bertz, S. H.; Murphy, M. D.; Ogle, C. A.; Thomas, A. A. *Chem Commun* **2010**, *46*, 1255.

(29)   Gschwind, R. M.; Armbrüster, M.; Zubrzycki, I. *J. Am. Chem. Soc.* **2004**, *126*, 10228.

(30)   Löhr, F.; Mayhew, S. G.; Rüterjans, H. *J. Am. Chem. Soc.* **2000**, *122*, 9289.

(31)   Federwisch, G.; Kleinmaier, R.; Drettwan, D.; Gschwind, R. M. *J. Am. Chem. Soc*. **2008**, *130*, 16846.

(32)   Bertz, S. H. *J. Am. Chem. Soc.* **1990**, *112*, 4031.

(33)   Bertz, S. H.; Cope, S.; Dorton, D.; Murphy, M.; Ogle, C. A. *Angew. Chem. Int. Ed.* **2007**, *46*, 7082.

(34)   Bartholomew, E. R.; Bertz, S. H.; Cope, S.; Dorton, D. C.; Murphy, M.; Ogle, C. A. *Chem Commun* **2008**, 1176.

(35)   Hastreiter, F. Master Thesis, University Regensburg, **2014**.

(36)   Hartmann, E.; Gschwind, R. M. *Angew. Chem. Int. Ed*. **2013**, *52*, 2350.

(37)   Hartmann, E.; Hammer, M. M.; Gschwind, R. M. *Chem. Eur. J.* **2013**, *19*, 10551.

Supporting Information

Additional NMR spectra and Information

Solvent influence on the spectra quality

The solvent used for the solution of ZnEt$_2$ has a big influence on the spectral resolution. In the ^{1}H NMR spectra of ZnEt$_2$ dissolved in different solvents, and the associated complex spectra it becomes obvious that spectral resolution is explicitly better, if no further solvent is present than the deuterated one (here CD$_2$Cl$_2$, data not shown). All in all the spectra are slightly shifted, depending on the used solvent, while the shift of free ZnEt$_2$ in CD$_2$Cl$_2$ is not as big as in the toluene solution, which is based on shielding effects of the solvents. Furthermore the commercially acquired solution contains more impurities, as the freshly prepared one. A more substantial influence is observed in the 2D ^{1}H^{31}P-HMBC spectra. In a sample with about 10 eq ZnEt$_2$ as toluene solution (Figure SI 3.6) it is not possible to detect any cross signals of transmetalation intermediates, in contrast in a sample with 6.5 eq ZnEt$_2$ in pure CD$_2$Cl$_2$ (Figure SI 3.7) detection of cross signals for transmetalated ethyl groups (red box) is possible.
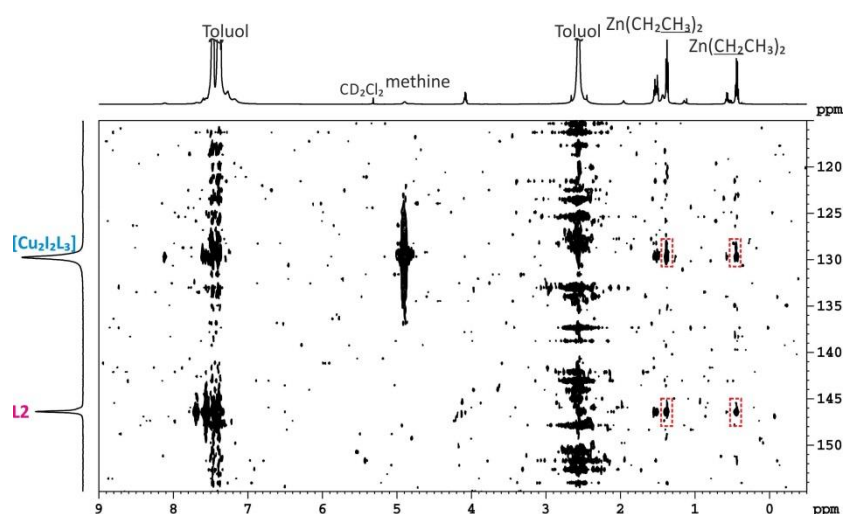

Figure SI 3.6: 2D ^{1}H^{31}P-HMBC spectrum of 2 eq **L**, 1 eq CuI and 10 eq ZnEt$_2$ (1M in toluene) at 230 K in CD$_2$Cl$_2$. The red dashed boxes represent unspecific interactions between ZnEt$_2$ and [Cu$_2$I$_2$L$_3$] and free ligand respectively.
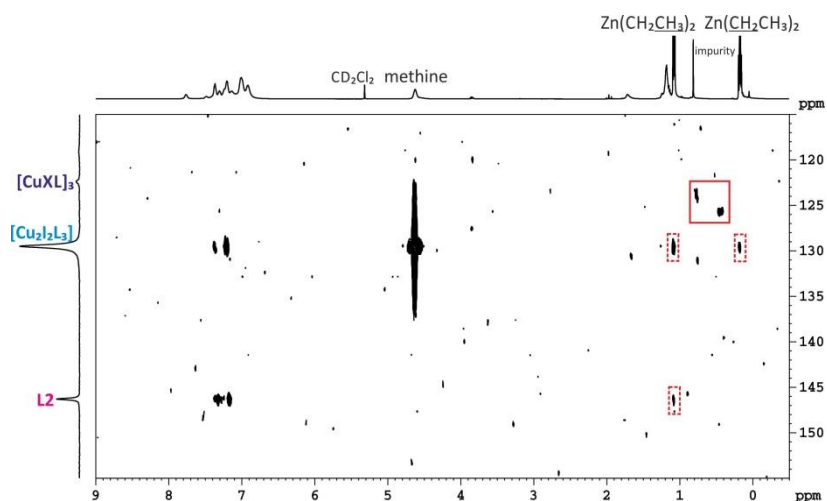
Figure SI 3.7: 2D ^{1}H^{31}P-HMBC spectra of a sample with 2 eq **L** and 1 eq CuI with 6.5 eq ZnEt$_2$ (circa 2M in CD$_2$Cl$_2$) at 230 K in CD$_2$Cl$_2$. The red boxes represent new appearing signals for transmetalation intermediates, whereas the red dashed boxes represent unspecific interactions between ZnEt$_2$ and [Cu$_2$I$_2$L$_3$] or **L**.

The red dashed boxes represent unspecific interactions. The assignment as unspecific interactions is based on further investigations using ZnMe$_2$ as organometallic reagent. Therefore ZnMe$_2$ was used as a 2M solution in toluene. In the 1D ^{1}H^{31}P-HMBC spectra (Figure SI 3.8) for the differentiation of magnetization transfer, either via scalar coupling (c) or via cross correlation (combination of chemical shift anisotropy and dipolar interaction, d), in both spectra a signal occurs at the chemical shifts of residual toluene (7.24, 7.15 and 2.34 ppm) therefore no clear identification of the transfer pathway is possible. Such a signal without clear assignment to one transfer pathway also occurs at -0.59 ppm, the chemical shift value of free ZnMe$_2$. We assume that signals occurring in spectra for both magnetization transfer pathways belong to unspecific interactions, based on strong π,π- or CH,π-interactions. From investigations with ZnEt$_2$ we knew, that a distinct amount of ZnEt$_2$ is needed before such interactions occur. In contrast for ZnMe$_2$ these interactions already occur with one equivalent. We assume that these unspecific interactions have no influence on the reaction, as the species remain (obvious by no changes in the chemical shift values).
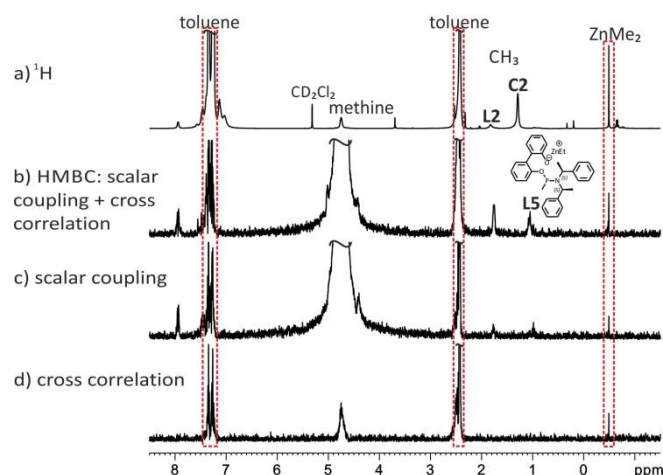
Figure SI 3.8: Comparison of ^{1}H NMR spectrum (a) and 1D ^{1}H^{31}P-HMBC spectra with both pathways (b), solely scalar coupling (c) and with only cross correlation (d) of 2 eq **L**, 1 eq CuI and 1 eq ZnMe$_2$ at 230 K in CD$_2$Cl$_2$.
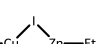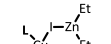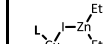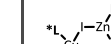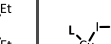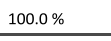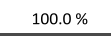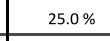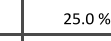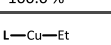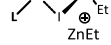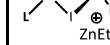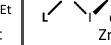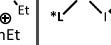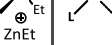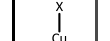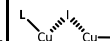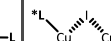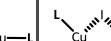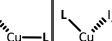
Apart from the unspecific interactions in the 1D ^{1}H^{31}P-HMBC spectra of 2 eq **L2**, 1 eq CuI and 1 eq ZnMe$_2$ signals appear at 1.76 and 1.06 ppm in the spectra for magnetization transfer via scalar coupling. The first one corresponds to the methyl group in the amine side chain of the free ligand, while the latter was identified as a ligand side product, in which one half of the biphenol backbone is cleaved and a methyl group is directly bound to the phosphorous atom.

Additional findings with CuI as copper salt

Possible ligand distributions in the proposed transmetalation intermediates

The special approach of using enantiopure and enantiomeric mixtures of the phosphoramidite ligands for complex formation was used in order to differentiate between species with different numbers of ligands coordinated. Scheme SI 3.2 represents the possible diastereomers accessible with the enantiomeric mixture and the statistical ligand distribution of the species for monomeric (**A**-**D**) and dimeric (**E**-**G**) structures. Therefore species with one ligand coordinated to the copper atom, are not affected and appear with the same integral. In contrast for species with two or three ligands, diastereomeric structures with mixed ligand arrangement are possible and therefore the signal integral is reduced. A differentiation thereby is only possible by new appearing signals in the enantiomeric mixture. For dimeric species **D** one or two new signals appear, while for the dimeric species **E**-**G** three new signals are expected, each with 25 % probability. The coordination of more than three ligands in the dimeric transmetalation intermediate would induce a more sophisticated signal pattern, but was not detected and therefore not taken into further account.

Scheme SI 3.2: Possible diastereomeric structures and statistical structure distribution in % given below each structure for the enantiopure and enantiomeric mixture of phosphoramidite ligand for complex formation for a) monomeric (**A-D**, charge is omitted for structures **B** and **D**) and b) dimeric (**E-G**) transmetalation intemediates.

<u>Addition of ZnI$_2$</u>

In order to determine if a zinc iodine unit is part of the structure of the transmetalation species a ZnI$_2$ solution was added to a sample of 2 eq **L2**, 1 eq CuI and 7.7 eq ZnEt$_2$ in order to force the equilibrium towards incorporation of zinc iodine units. Signal 3 is the only remaining signal after addition, therefore we assume that signal 3 is the only structure with a zinc iodine unit incorporated and was assigned to species **A**. All other signals disappeared with additional ZnI$_2$ and therefore we can assume that those species have no zinc iodine unit incorporated.
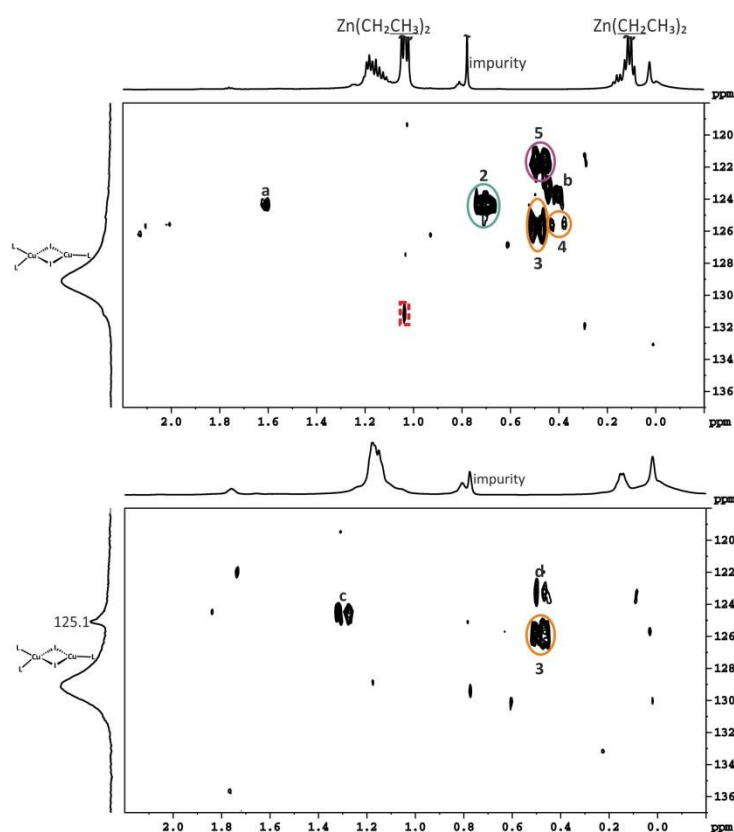
Figure SI 3.9: 2D ^{1}H^{31}P-HMBC spectra of 2 eq **L2**, 1 eq CuI and 7.7 eq ZnEt$_2$ before (top) and after (below) addition of an excess of a ZnI$_2$ solution at 180 K in CD$_2$Cl$_2$. After addition of the zinc salt solution only signal 3 remains and two new signals c and d appear.

<u>Identification of side products in CuI samples</u>

For the determination of interactions between free ligand and ZnEt$_2$ a copper free sample was prepared. Therefore 1 eq of **L2** were dissolved in 0.7 ml CD$_2$Cl$_2$ and 2.3 eq ZnEt$_2$ added. Figure SI 3.10 presents the comparison of the ^{1}H NMR spectrum (a) and the 1D ^{1}H^{31}P-HMBC spectra (b) magnetization transfer via scalar coupling and cross correlation, (c) magnetization transfer via scalar coupling, (d) magnetization transfer via cross correlation – combination of chemical shift anisotropy and dipolar interactions (the red dashed boxes represent unspecific interactions).
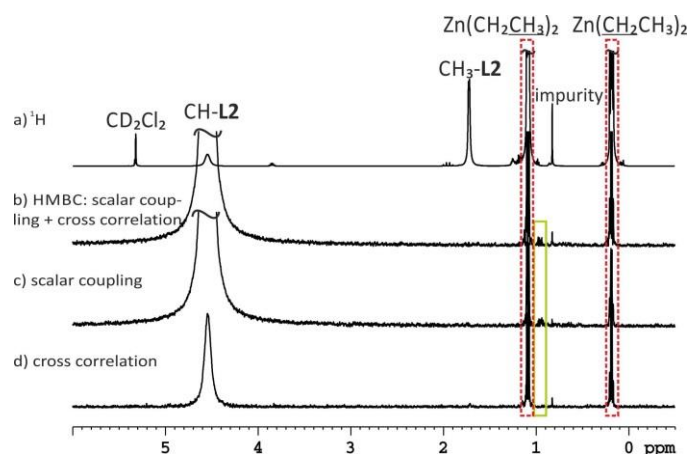
Figure SI 3.10: Comparison of the ^{1}H NMR spectrum (a) and the 1D [1]H[31]P-HMBC spectra with both pathways (b), solely scalar coupling (c) and cross correlation (d) of 1 eq **L2** and 2.3 eq ZnEt$_2$ at 230 K in CD$_2$Cl$_2$.

Obviously unspecific interactions with ZnEt$_2$ occur, due to the existence of signals in all three spectra (red dashed boxes). In contrast the signal at 0.95 ppm (light green) appears only in the scalar coupling spectra, so it corresponds to a directly transferred ethyl group. The occurrence of the signal in a copper free sample permits the assumption, that this structure plays a non-decisive role in the catalytic cycle and is a ligand-ZnEt$_2$ interaction product.

In contrast signal 1, observed in the 2D [1]H[31]P-HMBC spectra of 2 eq **L2**, 1 eq CuI with 7 or 15 eq ZnEt$_2$ (see main part), does not appear in the copper free sample. However, it was assigned to a copper complex with a ligand derivative, which has one half of the biphenol backbone opened and substituted by an ethyl group. This assignment to decomposed ligand is in analogy to the above described investigations with ZnMe$_2$. The missing of the signal in the copper free sample and the reduction of the signal integral in the enantiomeric mixture sample (see main part) supports the assumption of complex formation with decomposed ligand **L4**. With additional **L4** present in solution also mixed ligand arrangement with phosphoramidite ligands are possible, not only for [Cu$_2$I$_2$L$_3$] but also for dimeric transmetalation intermediates **E-G**. Therefore Scheme SI 3.3 presents the possible ligand arrangements in [Cu$_2$I$_2$L$_3$].
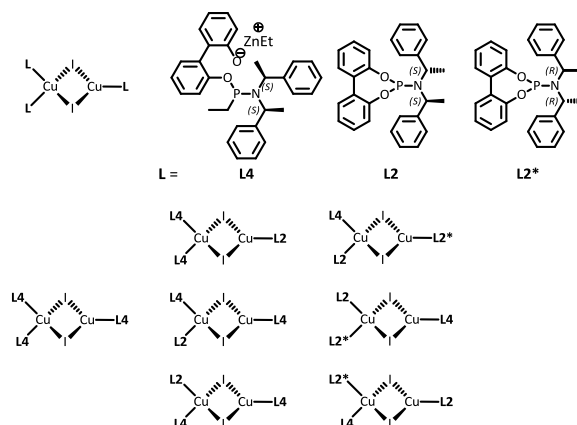
Scheme SI 3.3: Possible ligand arrangements for [Cu$_2$I$_2$L$_3$] with decomposed ligand **L4** and the two enantiomeric forms of phosphoramidite ligand **L2** and **L2*.** These ligand arrangements are also possible for dimeric transmetalation intermediates, resulting in reduced signal integrals.

Investigation with CuCl as copper salt

To investigate the salt influence on the transmetalation intermediates investigations with CuCl were performed. This salt was chosen due to high *ee*-values and excellent conversions,[3] furthermore the existence of complex species is tunable by the used ligand to salt ratio.[4] Indeed several signals were observed in the 2D ^{1}H^{31}P-HMBC spectra in a comparable shift range with those detected for transmetalation intermediates with CuI (see Figure SI 3.11 and Figure SI 3.12). Furthermore it seems plausible to assume that no identical transmetalation intermediates are formed, due to the missing of identical signals for both copper salt samples.
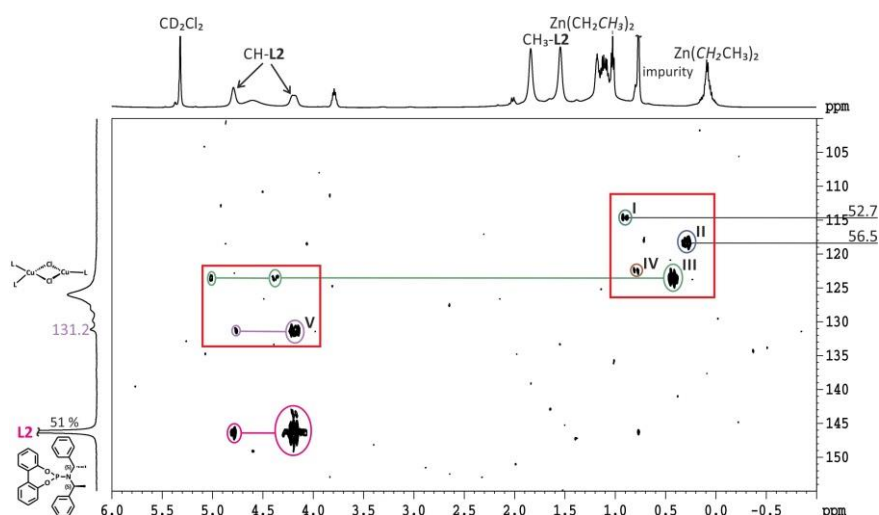
Figure SI 3.11: 2D ^{1}H^{31}P-HMBC spectra of 2 eq **L2**, 1 eq CuCl and 1 eq ZnEt$_2$ at 170 K in CD$_2$Cl$_2$. The red boxes highlight new arising signals I-V after the addition of ZnEt$_2$. The low temperature splitting of the methine signals is detected for free ligand **L2** (pink, 146.2 ppm), signal V (light purple, 131.2 ppm) and signal III (green, 123.5 ppm). The signals between 0.20 and 1.00 ppm are in agreement with the expected peak range of transmetalated ethyl groups.[5–7] Signals I and II are folded back; therefore the correct phosphorous chemical shifts are indicated. The percentage in the ^{31}P NMR spectra refers to the ligand distribution in the range of 160.0 to 100.0 ppm.
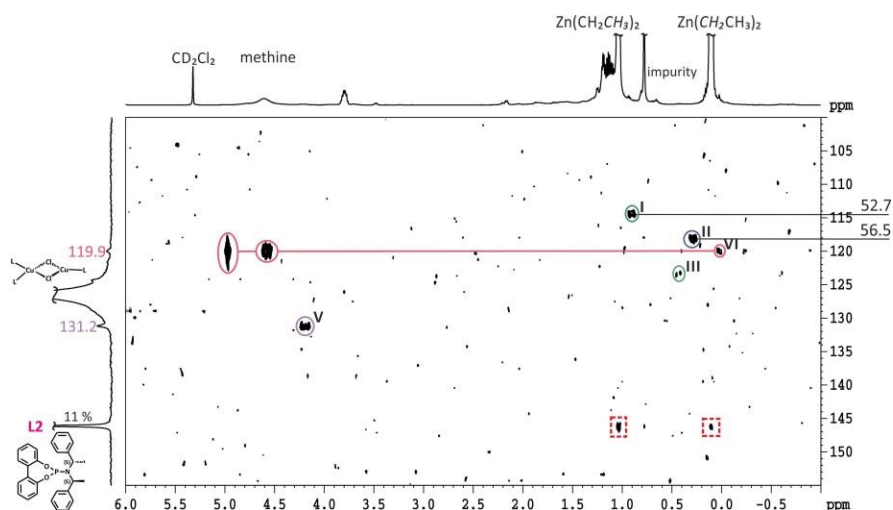
Figure SI 3.12: 2D $^1H^{31}P$-HMBC spectra of 2 eq **L2**, 1 eq CuCl and 10 eq ZnEt$_2$ at 180 K in CD$_2$Cl$_2$. Signals I-III and V were already detected with a smaller amount of ZnEt$_2$. Signal VI arises only with the higher amount of ZnEt$_2$ at a phosphorous chemical shift of 119.9 ppm, where a new signal arises in the ^{31}P NMR spectrum (light rose). Furthermore for 119.9 ppm signal splitting of the methine groups is detected. Unspecific interactions occur between free ligand and ZnEt$_2$ (red dashed boxes). Signals I and II are folded back; therefore the correct phosphorous chemical shift is indicated. The percentage in the ^{31}P NMR refers to the ligand distribution in the range of 160.0 to 100.0 ppm.

Obviously the amount of free ligand and ZnEt$_2$ present in the sample has an influence on the appearance of the species. With small amounts of ZnEt$_2$ in combination with high amounts of free ligand signals I-V appear, while with increasing amounts of ZnEt$_2$ and decreasing amounts of free ligand a further signal VI appears. In the 1D $^1H^{31}P$-HMBC spectra for signals III and VI scalar coupling signals were detected (see Figure SI 3.13) proving the transfer of an ethyl group. In order to get better spectral resolution a small spectral window (60 ppm) was chosen; therefore Signals I and II are folded back as the spectrometer has no digital filter in the indirect dimension. These signals were assigned to diethylaminophosphine ligand copper complexes. The chemical shift values (52.7 and 56.6 ppm) are in agreement with a lowfield shift for the more electron rich dialkylaminophosphine ligands ($\delta(^{31}P)$ for diethylaminophosphine ligand: 40.1 ppm in C$_6$D$_6$[8]) upon complex formation. The contrary effect to phosphoarmidite ligands (complexes appear highfield shifted) is based on different electronic properties of the phosphorous atom.
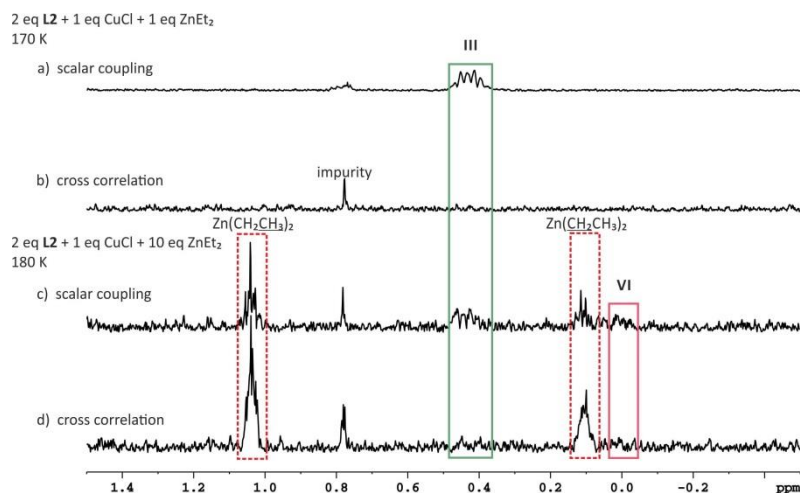
Figure SI 3.13: 1D ^{1}H^{31}P-HMBC spectra of 2 eq **L2**, 1 eq CuCl and 1 eq ZnEt$_2$ with magnetization transfer via scalar coupling (a) and cross correlation (b) at 170 K and of 2 eq **L2**, 1 eq CuCl and 10 eq ZnEt$_2$ via scalar coupling (c) and cross correlation (d) at 180 K in CD$_2$Cl$_2$. With 1 eq ZnEt$_2$ no unspecific interactions to ZnEt$_2$ (dashed red boxes) were detected. In both samples a scalar coupling signal for signal III of the corresponding 2D spectra is detectable (0.43 ppm). In the second sample, with higher amounts of ZnEt$_2$, also scalar coupling is visible for signal VI (0.03 ppm). For signals I and II spectra with scalar coupling signals are presented below.

In the 1D ^{1}H^{31}P-HMBC spectra for detection of magnetization transfer via scalar coupling of a 1:1 enantiomeric mixture of **L2** and **L2***   with 1 eq CuCl and 11 eq ZnEt$_2$ signals appear at 0.91 and 0.30 ppm, corresponding to the diethylaminphosphine ligand complexes (signals I and II respectively). Furthermore a signal appears at 0.43 ppm for signal III of the 2D ^{1}H^{31}P-HMBC spectrum. Obviously the intensity of the signals depends on the processing parameters used. As window function an e-function was chosen with varying line broadening (LB), for a LB of 1.0 the signals are hardly visible, with increased LB growing signal intensity is observed, while the best resolution is obtained with a LB of 2.0.
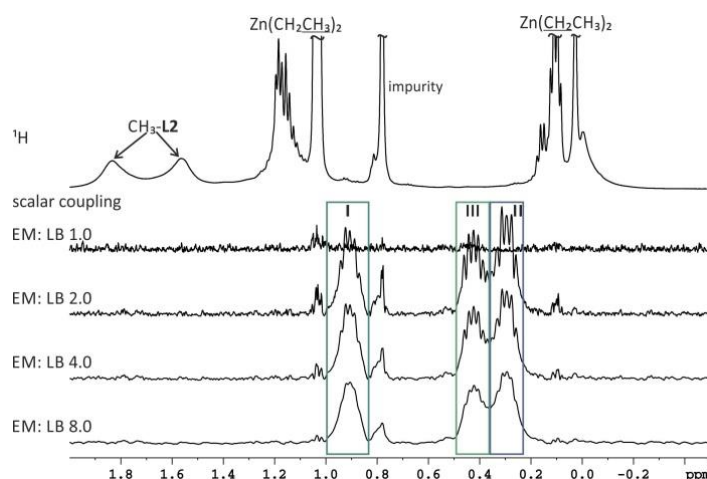
Figure SI 3.14: ^{1}H NMR spectrum and the 1D ^{1}H^{31}P-HMBC spectrum for magnetization transfer via scalar coupling of 1 eq **L2**, 1 eq **L2***, 1 eq CuI and 11 eq ZnEt$_2$ with different processing parameters.

In the 2D ^{1}H^{31}P-HMBC spectra of the enantiomeric mixture (1:1 **L2:L2***) apart from signals I-IV a new signal VII arises (data not shown), which is supposed to be a species with at least two

ligands in a mixed coordination of the ligand enantiomers. In order to force the equilibrium towards structures with a zinc chloride unit incorporated a $ZnCl_2$ solution was added, providing significant changes in the ^{31}P NMR spectrum, thereby $[Cu_2I_2L_3]$ is almost completely decomposed and ligand is released. In the 2D $^1H^{31}P$-HMBC spectra signals I and II seems to be unaffected, while signal III decreases and IV and VII vanishes totally, in contrast a new signal VIII appears, which was assigned to the free diethylaminophosphine ligand (data not shown).

In accordance with the CuI investigations a sample with a 1:1 ligand to salt ratio was prepared. In Figure SI 3.15 the 2D $^1H^{31}P$-HMBC spectrum after addition of 33 eq $ZnEt_2$ at 200 K is presented. Therein signal III is not detected, a probable explanation therefore is that the corresponding structure involves a Cu**L₂** fragment. Apart from signal VI a new signal IX appears. The ^1H chemical shift of VI and the further signal pattern enables the assignment to a cuprate like species. Signal IX was assigned to a ligand side product, in which the amine side chain is substituted by an ethyl group, due to the missing of cross signals to methine protons of the amine side chain. The signal with $\delta(^{31}P)$ 131.3 ppm (purple) is in agreement with the phosphorous chemical shift of signal V and was assigned as ligand derivative with a P-OEt group and intact amine side chain, due to existing signal splitting in low temperature spectra for the methine protons, based on reduced rotation of the C-N bond and very similar chemical shifts of the methine groups to that of the free ligand.
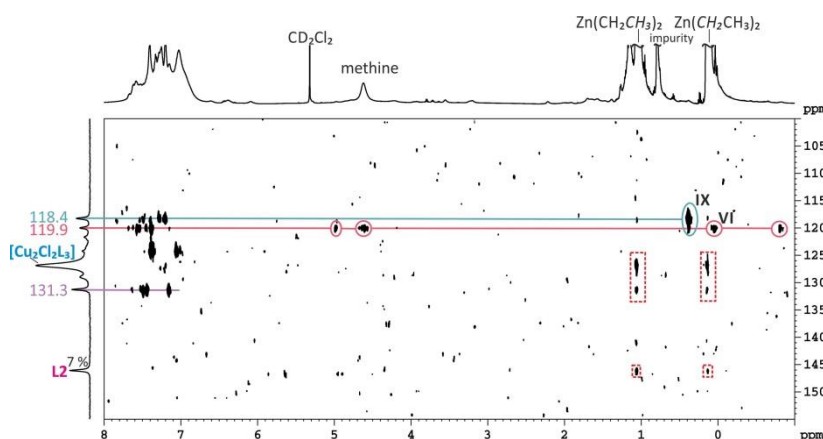
Figure SI 3.15: 2D $^1H^{31}P$-HMBC spectra of 1 eq **L2**, 1 eq CuCl and 33 eq $ZnEt_2$ after three weeks at 200 K in CD_2Cl_2. Signal VI was already detected in a sample with a 2:1 ligand to salt ratio with 11 eq of $ZnEt_2$, while signal IX appears as a new signal in the 1:1 mixture. Due to the excess of $ZnEt_2$ unspecific interactions occur to free ligand **L2**, $[Cu_2Cl_2L_3]$ and to the signal at 131.3 ppm (red dashed boxes).

Experimental Part

General Considerations

All sample preparations were performed under standard Schlenk technique under argon atmosphere and in dry solvents. CD_2Cl_2 was purchased by Deutero GmbH (99.6 %), dried with CaH_2 and was freshly distilled before use. The phosphoramidite ligands were either prepared according to reported protocols[1] or purchased by ABCR. Copper iodide was used as commercially available from Sigma Aldrich (99.999 %). Copper chloride was used as commercially available from Alfa Aesar (97 %). The solutions of the dialkylzinc reagents were freshly prepared in deuterated solvents (diethyl- and dimethylzinc in CD_2Cl_2). $ZnEt_2$ was purchased by Sigma-Aldrich (≥ 95 %) and used without further purification. $ZnMe_2$ was purchased either by ABCR (95 %) or as 2M solution in toluene by Sigma-Aldrich and used without further purification. $ZnPh_2$ was used as commercially available from Strem Chemicals or it was used as synthesized by Dipl.-Chem. Fabian Mutzbauer (AK Korber).[2] The synthesis of $ZnPh_2$ was performed from a reaction of $ZnCl_2$ and PhLi in Et_2O at 0 °C. $ZnPh_2$ was purified via distillation at 120 °C under vacuum ($5x10^{-2}$ mbar) and obtained as pure white solid. $ZnCl_2$ was recrystallized from 1,4-dioxane and dried before use. PhLi was synthesized from PhBr and Li in Et_2O under reflux. All manipulations with $ZnPh_2$ were performed in a glove box under argon atmosphere and exclusion of daylight. In the commercially available source of $ZnPh_2$ traces of benzene were detected. Investigations were performed in CD_2Cl_2.

Sample Preparation

Preparation of the phosphoramidite copper complexes

An argon flushed Schlenk tube equipped with magnetic stirring bar and septum was charged with 2 eq ligand (0.036 mmol, 15.81 mg) and 1 eq copper iodide (0.018 mmol, 3.43 mg) or copper chloride (0.018 mmol, 1.78 mg), freshly distilled solvent CD_2Cl_2 (0.6 ml) was added and the mixture stirred for 1-2 h at room temperature until a clear solution was obtained. Subsequently the samples were transferred to an argon flushed NMR tube. The samples were stored at -85 °C.

Preparation of the phosphoarmidite copper complexes – MR_x samples

To the freshly prepared phosphoramidite copper complex solution the corresponding amount of freshly prepared $ZnEt_2$ or $ZnMe_2$ solution was added at room temperature.

$ZnPh_2$: Complex preparation as describe above. A second argon flushed Schlenk tube with magnetic stirring bar and septum was charged with $ZnPh_2$ (0.09 mmol, 22.04 mg; 5-fold excess to

CuI, 10-fold excess to **C2**) and CD_2Cl_2 (0.4 mL). After stirring for 2 h, the cloudy solution of $ZnPh_2$ was transferred to the solution of the phosphoramidite copper complexes. A slightly exothermic reaction was observed upon by the condensation of CD_2Cl_2 at the upper part of the Schlenk tube. The mixture was stirred for 25 min and transferred into an argon flushed NMR tube.

NMR Data Collection and Processing

NMR spectra were recorded on a Bruker Avance DRX 600 (600.13 MHz) spectrometer equipped with a 5 mm broadband triple resonance z-gradient probe (maximum gradient strength 53.5 Gauss/cm). The temperature for all low temperature measurements were controlled by a BVTE 3000 unit. The ^{1}H chemical shifts were referenced to the residual solvent signal of CD_2Cl_2 (5.32 ppm), for the ^{31}P chemical shifts the Ξ value of an external standard was applied. NMR data were processed and evaluated with Bruker Topspin 3.1/3.2.

2D ^{1}H^{31}P-HMBC spectra: pulse program = inv4gplrndqf, relaxation delay = 6 s, mixing time = 0.05 s, NS = 128, DS = 8, TD = 16k F2 and 64 F1. 1D ^{1}H^{31}P-HMBC spectra: pulse program = gs_hmbc1D27.gf for HMBC, gs_hmbc1D25.gf for scalar coupling and gs_hmbc1D26.gf for cross correlation, relaxation delay = 6 s, NS = 1k, DS = 16, TD = 64k.

Literature:

(1)   Alexakis, A.; Rosset, S.; Allamand, J.; March, S.; Guillen, F.; Benhaim, C. *Synlett* **2001**, *2001*, 1375–1378.

(2)   Mutzbauer, F. Diploma Thesis, Umsetzung von Polypentelanionen mit Übergangsmetallkomplexen in flüssigem Ammoniak, Universität Regensburg, 2008.

(3)   Alexakis, A.; Benhaim, C.; Rosset, S.; Humam, M. *Journal of the American Chemical Society* **2002**, *124*, 5262–5263.

(4)   Zhang, H.; Gschwind, R. M. *Chemistry – A European Journal* **2007**, *13*, 6691–6700.

(5)   Bertz, S. H. *Journal of the American Chemical Society* **1990**, *112*, 4031–4032.

(6)   Bertz, S. H.; Cope, S.; Dorton, D.; Murphy, M.; Ogle, C. A. *Angewandte Chemie International Edition* **2007**, *46*, 7082–7085.

(7)   Bartholomew, E. R.; Bertz, S. H.; Cope, S.; Dorton, D. C.; Murphy, M.; Ogle, C. A. *Chem. Commun.* **2008**, 1176–1177.

(8)   Müller, D.; Tissot, M.; Alexakis, A. *Organic Letters* **2011**, *13*, 3040–3043.

4 Structure Elucidation of a Phosphoramidite Copper Complex in Tetrahydrofuran and of the Transmetalation with Trimethylaluminum
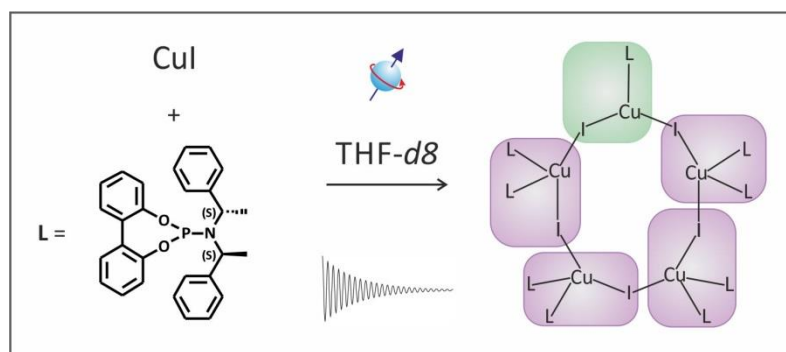
4.1 Abstract

The formation of enantioselective C-C bonds is very important for synthetic applications, a very powerful method is thereby the copper-catalyzed 1,4-addition reaction. Despite their versatile applicability only little information concerning the mechanisms and involved structures is known. Therefore we present here an NMR spectroscopic study, dealing with the precatalytic structure of phosphoramidite copper complexes in THF-*d8* and first investigations concerning the difference between normal and reverse addition order of the reagents.

4.2 Introduction

The asymmetric copper-catalyzed conjugate addition (ACA) reaction is a very powerful method for the formation of highly selective C-C bonds and their versatile applicability is described in several reviews.[1–4] Apart from diorganozinc[5–7] and Grignard[4,8] reagents also the use of triorganoaluminum reagents has been of increasing interest during the last years.[9,10] Many triorganoaluminum reagents are commercial available or accessible by simple hydro- and carboalumination reactions.[3,10] Due to higher Lewis acidity of the aluminum reagent compared to zinc reagents increased reactivity is observed, especially for the introduction of methyl groups.[10,11] Additionally better activation of the substrate is obtained, and therefore also sterically hindered enones are suitable substrates, which enables the formation of chiral quarternary centers.[10,12–14] First attempts in the use of AlR_3 compounds in ACA reactions were done by Woodward and co-workers with binaphthol heterodonor (S,O) ligands[15] and with phosphoramidite ligands by Pineschi and co-workers.[16] All in all the number of suitable ligands for addition reactions of AlR_3 is fewer as for addition reactions of diorganozinc reagents.[3,10] Despite the increasing interest of AlR_3 in synthetic application only little information concerning the mechanism is available. The only mechanistic study known is from Alexakis *et al.* describing the cleavage of the biphenol backbone of phosphoramidite ligands by the use of AlR_3 in non-coordinating solvents.[17] Nevertheless differences in the performance of the reaction are observed by different addition order of the reagents. To the best of our knowledge until now only synthetic investigations reveal a better performance of the reverse addition, where the enone is added before the organometallic reagent to the precatalytic system.[13,14,18] Due to the fact, that investigations with triorganoaluminum reagents are normally performed in coordinating solvents we present here a structure elucidation study of phosphormamidite copper complexes in THF-*d8*. Furthermore, first NMR spectroscopic investigations of the ACA reaction of $AlMe_3$ were performed, in order to determine the advantages of the reverse addition compared to the normal addition order.

4.3   Investigation of the precatalytic system

Normally we use non-coordinating solvents, like CD_2Cl_2 for our NMR spectroscopic investigations in the field of copper-catalyzed asymmetric synthesis, because separated signals are observed for the complex species in the ^{31}P NMR spectra in this solvent.[19–21] For investigations with AlR_3 non-coordinating solvents are not feasible, due to substitution of the biphenol backbone by alkyl groups, based on the high oxophilicity of the aluminum atom.[17] Therefore in synthetic applications coordinating solvents like diethylether or THF are typically used. Moreover the use of stronger coordinating solvents enables a splitting of the AlR_3 dimers, and therefore increases the reactivity of the organometallic reagent.[12] For that reason our NMR spectroscopic investigations were performed in the stronger coordinating solvent THF-*d8*. Initially the precatalytic system without organometallic reagent was investigated. In a previous study CuCl was tested as copper source in THF-*d8*, beside the trinuclear complex **C1** ([CuX**L**]$_3$) and the binuclear complex **C2** ([Cu$_2$X$_2$**L**$_3$]) with a mixed trigonal/tetrahedral coordination on the copper atoms, additional signals exist in the ^{31}P NMR spectrum without sufficient signal separation, indicating the existence of further complexes.[19,20] In order to get a better suited salt for our NMR spectroscopic studies with sharp and well separated signals for each complex species, a salt screening was performed. Therefore we solely use copper(I) salts in order to avoid severe NMR problems, due to the paramagnetic character of copper(II) salts.[20] Three copper(I) salts were tested. CuI, which is not used in synthetic application, but reveals well resolved spectra and we already got promising results in the detection of transmetalation intermediates with diorganozinc reagents (see Chapter 3.3). In addition copper thiophencarboxylate (CuTC) and tetrakis-(acetonitrile)copper(I) tetrafluoroborate ([Cu(CH$_3$CN)$_4$]BF$_4$) were tested as typically salts used in synthetic procedures.[10,12–14] For the salt dependency study we use a 2:1 ligand to salt ratio as it is normally used in synthetic protocols.[10,12–14]

In Figure 4.1 the ^{31}P and ^1H NMR spectra of 2:1 mixtures of phosphoramidite ligand **L2** and the three copper salts at 230 (a and b) and 180 K (c and d) are presented. In the ^{31}P NMR spectra for all three salts a signal for free ligand **L2** is observed (145.6 ppm at 230 K and 145.4 ppm at 180 K respectively). With CuI as salt relatively sharp signals appear at 128.8, 121.8 and 118.6 ppm in the ^{31}P NMR spectrum for complex species. Using the potentially bidentate TC anion significant broader line widths of the signals occur, these line broadening was already observed in a salt screening in CD_2Cl_2.[20] However the signal pattern is quite similar to those of a sample with CuI, signals appearing at 125.0 and 117.4 ppm. In contrast for samples containing [Cu(CH$_3$CN)$_4$]BF$_4$ as salt there is less signal separation, apart from a large signal at 125.4 ppm with a shoulder at 123.0 ppm a small one is observed at 128.8 ppm. In a previous investigation set out to

determine the structure of the precatalyst in CD_2Cl_2 Gschwind *et al.* found that the ligand to copper ratio in the complex influences the ^{31}P chemical shift, with a higher amount of ligand incorporated in the complex a stronger lowfield shift is observed.[19,20] Under the assumption that a similar behavior appears also in coordinating solvents we can assign the signal at 128.8 ppm to a complex with a ligand to copper ratio higher than 1:1, while the signal at 121.8 ppm is attributable to complex **C1** with a 1:1 ligand to salt ratio in the complex. Also the signal at 118.6 ppm has a 1:1 ligand to salt ratio or lower and is therefore in the following assigned as **C1'**, due to a stronger highfield shift. Furthermore in the ^1H NMR spectra with CuI for the first time signal separation for the methine and methyl groups of the ligand - free and coordinated in the different complex species - is observed, while the other salts generating one averaged signal for free and complexed ligands. The assignment of the methine and methyl groups to the different complex species or to free ligand is based on cross signals in 2D $^1H^{31}P$-HMBC and $^1H^1H$-COSY spectra (spectra shown in the supporting information). In the low temperature (180 K) ^{31}P NMR spectra for all three salts line broadening occurs for the complex species, due to slowed down but still remaining ligand exchange processes. Whereas the signal for free ligand becomes sharper, based on the slower exchange processes.[21] For CuI signals at 130.5, 128.4, 122.7 and 118.0 ppm are observed. In previous investigations addressing the low temperature complexes in CD_2Cl_2, we observed signal splitting into two signals for **C2** (using CuI) with an integral ratio close to 1:2, representing the two different ligand groups at the differently coordinated copper atoms.[21] In contrast, in this investigation the integral ratio for 130.5 and 128.4 ppm is different and with spectra simulations and analysis of the integrals of the signals a signal ratio of 1:8 was proven (see below). The implementation of ^1H diffusion ordered spectroscopy (DOSY) measurements enables no clear assignment of the aggregation number, as the signals were not sufficiently separated and therefore mixed values of the diffusion coefficients appear for the different complex species. Solely for **C1** ([CuX**L**]$_3$) a disaggregation of the trinuclear complex to single CuX**L** fragments was detectable in a sample with 1.3 eq **L2** and 1 eq CuI (aggregation number 0.3). The signal pattern for CuTC is again similar to CuI with signals at 127.6, 124.8, 121.0 and 116.8 ppm. With [Cu(CH$_3$CN)$_4$]BF$_4$ one broad signal appears at 124.2 ppm with pronounced shoulders at 127.9 and 122.7 ppm. With all three salts signal separation for the methine (4.83 and 4.36 ppm respectively) and methyl (1.88 and 1.68 ppm respectively) groups of the amine side chain of free ligand is observed in the ^1H NMR spectra at low temperature, due to slower rotation of the C-N bond in the amine side chain.[22] Summarizing the spectra quality and signal separation it is obvious that for investigations in THF-*d8* combinations with CuI represents the best model system for further studies.
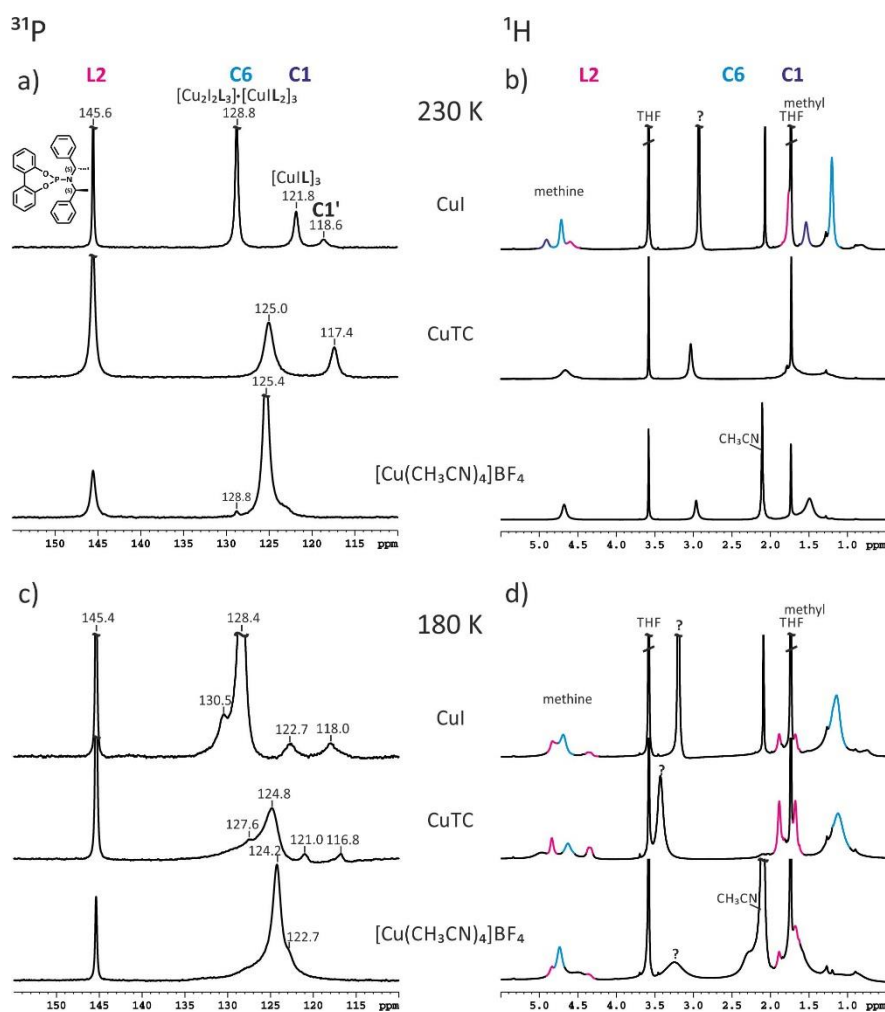
Figure 4.1: ^{31}P and ^{1}H NMR spectra of 2:1 mixtures of **L2** and three different CuX salts at 230 K (a and b) and at 180 K (c and d) in THF-*d8*. In the ^{1}H NMR spectra at 180 K (d) for all three salts signal separation for the methine and methyl groups of the amine side chain of free ligand was observed.

Having now a suitable model system in hand, further investigations for additional information concerning the complex structure was collected. Therefore two different approaches were adopted. On the one hand the ligand to salt dependent formation of the complex species was addressed and on the other hand spectra simulations of the low temperature ^{31}P NMR spectrum with CuI were used for the assignment of the unusual integral distribution of the signals at low temperatures.

For the first approach the ligand to salt ratio was varied from 1.3:1 up to 3:1. Figure 4.2 a represents the appearance of the complexes as function of the ligand to salt ratio. Ratios less or equal to 1.5:1 give **C1** as main component, with decreasing amounts of the signal at 128.8 ppm and **L2**. The existence of a small amount of **C1** also with a threefold excess of ligand compared to the copper salt point to a stabilization of this complex through the solvent. The amount of the signal at 128.8 ppm increases up to the 2:1 ratio, afterwards the amount decreases again, while the amount of free ligand increases and reaches at the 3:1 ratio a higher value than the signal at

128.8 ppm. The signal at 118.6 ppm rises up to a 2:1 ratio and is then decreasing again, ending up by nearly the same amount in the 3:1 ratio sample as in the 1.3:1 ratio sample. Due to the fact, that typically in synthetic applications a 2:1 ratio is used, we can assume that in stronger coordinating solvents the signal at 128.8 ppm represents the precatalytic species, as it appears as main species.
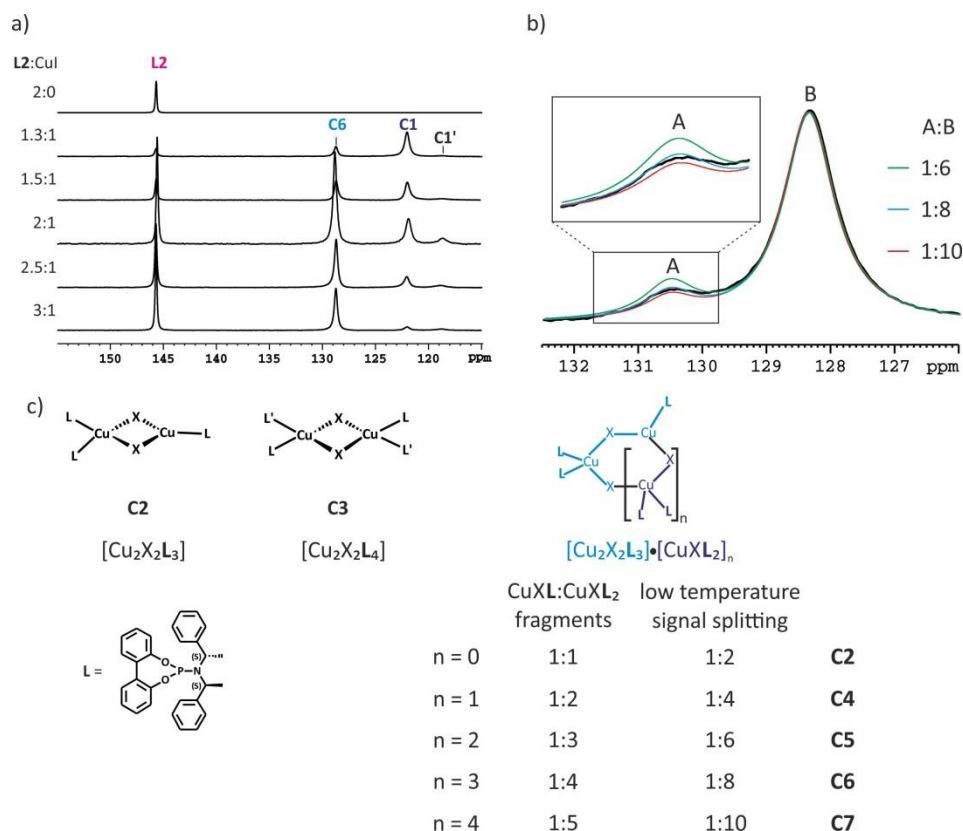
Figure 4.2: a) ^{31}P NMR spectra of **L2** and mixtures of **L2** and CuI at varying ligand to salt ratios at 230 K in THF-*d8*. b) ^{31}P NMR simulations of the superposition of signal A (130.5 ppm) and signal B (128.4 ppm) in order to assign the signal ratio at 180 K. c) Proposed structures for the complex species with the corresponding signal splitting in the low temperature ^{31}P NMR spectrum.

The second approach was to simulate the superposition of the low temperature ^{31}P NMR signals with CuI at 130.5 ppm (characterized as A in Figure 4.2 b) and 128.4 ppm (characterized as B in Figure 4.2 b), due to the unusual low temperature splitting (Figure 4.2 b).[7] Therefore the ratio between the two signals was varied and the corresponding spectra simulated. Obviously the 1:8 ratio (blue) for the two signals A (130.5 ppm) and B (128.4 ppm) is in good agreement with the experimental spectrum (black), indicating complex **C6** with one CuX**L** and four CuX**L₂** fragments (see Figure 4.2 c). Whereas a ratio of 1:6 (green), representing complex **C5** with three CuX**L₂** units and one CuX**L** unit (see Figure 4.2 c) is considerably higher as the experimental spectrum, indicating the upper limit. In contrast a ratio of 1:10 (red), building complex **C7** with five CuX**L₂**

---

[7] Simulations were performed by Carina Koch with the TOPSPIN 3.2 simulation tool DAISY.

units (see Figure 4.2 c), is distinctly below the experimental spectrum and therefore represents the lower limit. Therefore in coordinating solvents a higher amount of CuX**L₂** fragments is involved in the precatalytic complex compared to non-coordinating solvents (one CuX**L₂** fragment in the precatalytic complex **C2**). Possible complex species with various amounts of CuX**L** and CuX**L₂** fragments and their corresponding low temperature signal splitting are depicted in Figure 4.2 c. A further hint for the higher number of CuX**L₂** units is the missing of a signal for **C3** (two CuX**L₂** units) at low temperatures, which is the result of an interaction of **C2** and free ligand. Furthermore the solvent dependent stabilization of **C1** - small amounts are still observed with 3 eq **L2** - represents also a probable explanation for the existence of species containing higher numbers of CuX**L₂** units.

Next the temperature dependent interconversion of the complexes was addressed, in order to determine if the complex species show the same behavior as in CD_2Cl_2 solution. Therein **C1** only appears at temperatures above 200 K, in contrast lowering the temperature reveals apart from **C2** a further low temperature species **C3** ($[Cu_2X_2L_4]$).[21] Therefore ^{31}P NMR spectra were measured between 230 and 180 K of the 2:1 mixture (see Figure 4.3) and of the 1.3:1 and 2.5:1 mixtures (see supporting information).

In all three samples the amount of **C6** increases with lowering temperature along with signal splitting into one large signal (128.4 ppm) and a small one (130.6 ppm). Accompanied by decreasing amounts for free ligand and **C1**. In contrast to investigations in CD_2Cl_2 no formation of the thermodynamic most stable binuclear complex, with four ligands coordinated to the copper atoms (**C3**) is observed at low temperatures.[21]
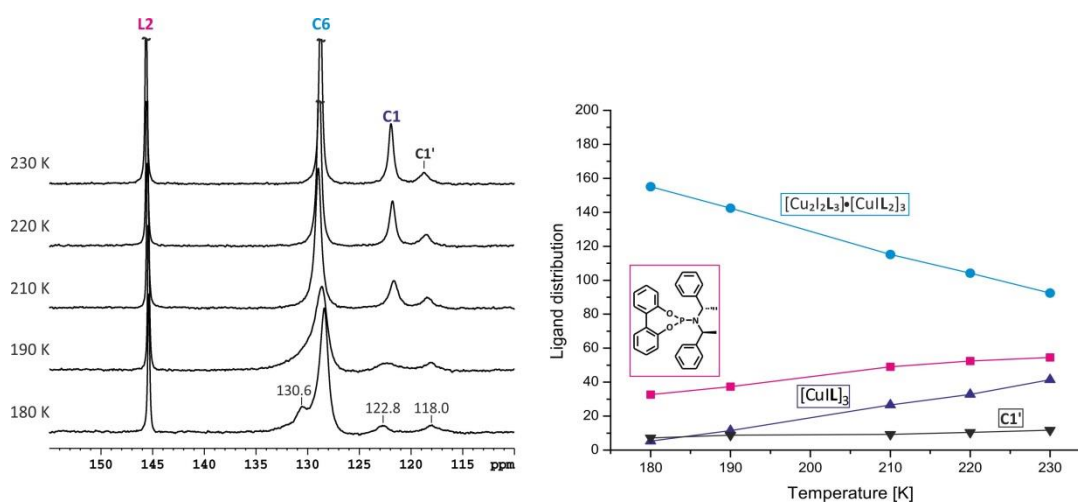
Figure 4.3: Temperature dependent ^{31}P NMR spectra of a 2:1 mixture of **L2** and CuI in THF-*d8* (left) and ligand distribution (right, normalized to 200, as two equivalents of **L2** are used, representing all ligand containing species).

The temperature dependent ligand distribution enables a detailed analysis of the signal integrals and therefore a calculation of copper containing species, indicating the possible complex species (see Figure 4.2 c). Therefore the sum of the copper containing species had to be 100 %, meaning that all copper atoms are involved in a complex. Table 4.1 represents the values for a sample with 2 eq **L2** and 1 eq CuI (for samples with 1.3 and 2.5 eq **L2** see supporting information).

Table 4.1: Temperature dependent ligand distribution in the ^{31}P NMR spectra of 2 eq **L2** and 1 eq CuI and the calculated sum of copper containing species with different ligand and copper contents in the complex species.

Temp	Ligand distribution[a]				Sum of copper containing species[b]				
	L2	C6	C1	C1'	C2	C4	C5	C6	C3
	--	--	--	--	2/3*C6	3/5*C6	4/7*C6	5/9*C6	½*C6
230 K	54.5	92.5	41.4	11.7	114.8	108.6	106.0	104.5	99.4
220 K	52.4	104.2	32.8	10.4	112.7	105.7	102.7	101.1	95.3
210 K	49.0	115.2	26.6	9.2	112.6	104.9	101.6	99.8	93.4
190 K	37.3	142.4	11.5	8.8	115.2	105.7	101.7	99.4	91.5
180 K	32.6	155.1	5.3	7.1	115.8	105.5	101.0	98.6	90.0
Average	--	--	--	--	114.2	106.1	102.6	100.7	93.9

a) Representing the integrals of the corresponding signals, normalized to 200 representing all ligand containing species (2 eq **L2** used); b) each added with corresponding integral of **C1** and **C1'**, the numerator represents the number of involved copper atoms and the denominator the number of involved ligands in the complex species.

The incorporation of further CuX**L2** fragments in the precatalytic species was proven on this calculations. The values show, that the strongest deviation from 100 % is observed for **C2** compared to complexes with a higher amount of CuX**L2** fragments (**C4**-**C6**) for each temperature (see rows in Table 4.1). Furthermore for **C2** the deviation increases with lower temperature (14.8 % at 230 K and 15.8 % at 180 K, see the column for **C2** in Table 4.1), whereas for **C4**-**C6** the deviation is getting smaller with decreasing temperature (4.5-8.6 % at 230 K and 1.0-5.5 % at 180 K, see columns for **C4**-**C6** in Table 4.1). Also **C3** (two CuX**L2** fragments, no CuX**L** fragment) was included in the calculations. At 230 K only a very small deviation of 0.6 % is observed, but at 180 K a deviation of 10 % occurs (see the column for **C3** in Table 4.1), therefore it was excluded as possible structure. Moreover for **C3** a lowfield shifted signal was expected, as observed in CD$_2$Cl$_2$ in previous investigations.[21] Altogether the analysis of the signal integrals reveal, that complex **C6** with one CuX**L** and four CuX**L2** fragments provides the smallest averaged deviation (0.7 %) from the expected 100 % for all copper containing species and was therefore proposed as structure for the precatayltic complex (128.8 ppm). The signal integral analysis and the ligand distribution corroborates the assumption of incorporation of further CuX**L2** fragments in the precatalytic copper complex **C2**. The observation of a mixed coordination of trigonal and tetrahedral coordinated copper atoms shows that the formation tendency of copper complexes with mixed copper coordination is relatively high.

The investigations of the precatalytic system in THF-*d8* demonstrates, that CuI is the best salt to use, due to well separated signals for the different complex species, both in ^{31}P and ^{1}H NMR spectra. In contrast to investigations in CD_2Cl_2 a precatalytic system **C6** with four CuX**L$_2$** units and one CuX**L** unit was proposed (precatalyst **C2** in CD_2Cl_2 has only one CuX**L$_2$** and CuX**L** unit each), based on ^{31}P NMR spectra simulations and the analysis of the signal integrals of temperature dependent ligand distributions of copper containing species. The incorporation of further CuX**L$_2$** fragments can be explained by a solvent dependent stabilization of the **C1** complex, as it is also visible in small amounts in a sample with a 3:1 ligand to salt ratio and also at low temperature. All in all a precatalyst is built which is polynuclear in copper (here five copper atoms are involved), while the copper atoms appear with mixed trigonal/tetrahedral coordination.

4.4 Investigation of a 2:1 mixture of L2 and CuI and their transmetalation intermediates with AlMe₃

For addition reactions with trialkylaluminum reagents the outcome and conversion of the reaction is strongly influenced by the order of addition of the reagents.[13,18] Alexakis and co-workers reported in a study concerning the improvement of experimental conditions, that better results were obtained if first the enone (cyclopent-2-enone) is added to the precatalyst and then the organoaluminum reagent, especially for sterically demanding substrates.[13,14] Similar results were obtained by Chan *et al.* they use copper complexes of bidentate phosphite ligands for addition reactions of triethylaluminum to cyclopent-2-enone.[18] This order of addition is the so called reverese addition, in contrast to the normal addition where the organoaluminum reagent is added before the enone. The higher reactivity of the reverse addition is probably based on the formation of more reactive copper clusters[13] and a precoordination of the enone to the copper complex.

In order to determine and elucidate the differences between these two addition pathways both were investigated by NMR spectroscopy for a catalytic system consisting of a chiral phosphoramidite ligand **L2** and CuI as copper salt. For the enone cyclohexenone (Cy) was used, because it was successfully introduced in ACA reactions of AlR_3[10] and various π-complexes were already identified by Bertz and Ogle in investigations concerning the mechanisms in organocopper chemistry[23] and by Gschwind and co-workers.[24,25] For the trialkylaluminum reagent we selected $AlMe_3$ which is often used in synthetic protocols with good yields and enantioselectivities.[10,12–15] Furthermore compared to the higher homolog $AlEt_3$ only one signal for the methyl group is observed in the ^1H NMR spectrum, in a range where no signals for the ligands are observed, whereas the signals for the ethyl groups often are in the same chemical shift range as the methyl groups of the ligand amine side chain (see investigations with $ZnEt_2$ Chapter 3.3). Furthermore as described above AlR_3 dimers are splitted into monomeric structures by the use of THF as solvent.

4.4.1 Reverse Addition

In order to investigate the reaction intermediates occurring in the reverse addition of enones and organoaluminum reagents a sample of 2 eq **L2**, 1 eq CuI and 5 eq cyclohexenone was prepared and investigated by NMR spectroscopy. In Figure 4.4 the ^{31}P NMR spectra before and after addition of the enone to the preactalytic system are presented. After the addition no significant changes occur. Also in the ^1H NMR spectrum beside the signals for Cy no new signals appear (data not shown).
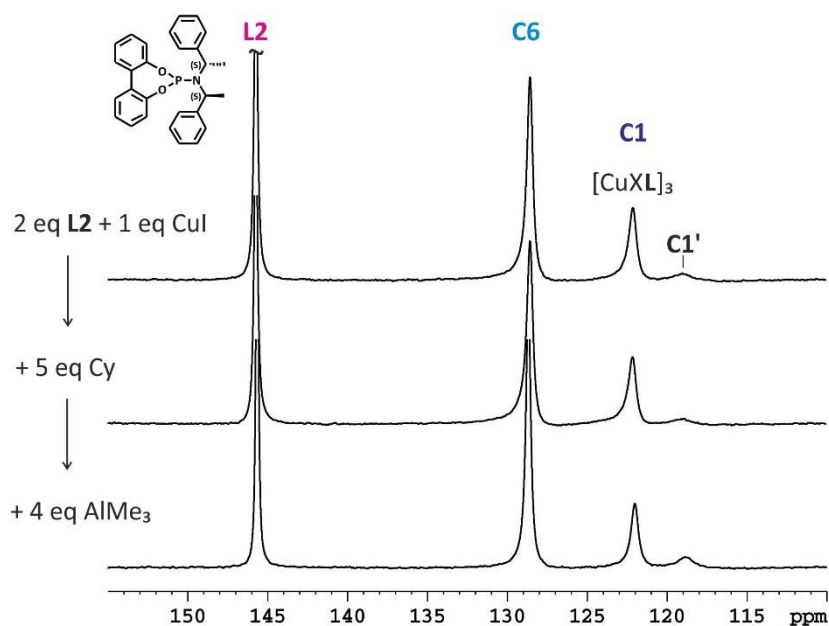
Figure 4.4: ^{31}P NMR spectra of 2 eq **L2** and 1 eq CuI (top), after addition of 5 eq cyclohexenone Cy (middle) and after addition of 4 eq AlMe$_3$ (below) at 230 K in THF-*d8*. No significant changes appear in the integral intensity of **L2**, **C6**, **C1** and **C1'**.

Copper complexes are expected to precoordinate an enone by the formation of a copper-π-complex. These copper-π-complexes were already described in various NMR spectroscopic investigations (see Figure 4.5).[23–25] For example Gschwind and co-workers detected π-complexes with various substituted cyclohexenone derivatives, which were stable for days in diethyl ether, by conventional low temperature NMR measurements. The substitution of the cyclohexenone is necessary to stabilize the π-complexes, by reducing the reaction rate in diethyl ether. Furthermore substitution is possible in position 3 and 4 as well as in position 6 of cyclohexenone.[24,25] In contrast Bertz and Ogle were able to detect a π-complex of unsubstituted cyclohexenone and commonly used Gilman reagents (Me$_2$CuLi·LiI or Me$_2$CuLi·LiCN) in THF-*d8* by using rapid injection NMR methods.[23] The double bond of the enone is a highly sensitive monitor for the formation of π-complexes, because the protons and carbon atoms of the double bond are strongly highfield shifted in the ^{1}H and ^{13}C NMR spectra (for example cyclohexenone has a ^{1}H chemical shift at 5.90 ppm and a ^{13}C chemical shift at 130.1 ppm for C$_2$, which is shifted 2.13 ppm to highfield in the ^{1}H NMR spectrum and 52.7 ppm to highfield in the ^{13}C NMR spectrum in a π-complex, a considerably stronger effect appears to C$_3$, which is shifted 3.82 ppm to highfield in the ^{1}H NMR spectrum and 90.1 ppm in the ^{13}C NMR spectrum upon π-complex formation[23]).
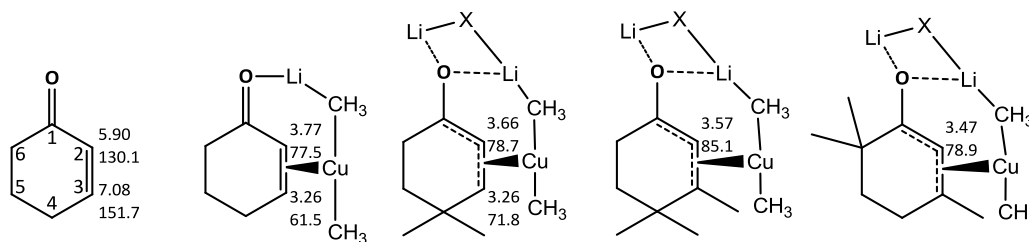
Figure 4.5: Copper-π-complexes of cyclohexenone at 173 K in THF-*d8*[23] and various substituted cyclohexenone derivatives at 180 and 170 K respectively in diethyl ether[24,25] with the ^{1}H and ^{13}C chemical assignment of the protons and carbon atoms of the double bond (C_2 and C_3).

Although the double bond is such a sensitive monitor, the HSQC spectrum of the investigated reaction mixture (2 eq **L2**, 1 eq CuI and 5 eq Cy) provides no signal which can be assigned to a π-complex. This missing of a signal can have several reasons. First of all it is literature known, that the conversion of the reaction in THF is a little bit lower as in diethyl ether, even if the *ee*-values are not strongly influenced.[12] This solvent dependence is in agreement with investigations of the conjugate addition reaction in which the reaction rate is reduced, due to the existence of solvent separated ion pairs in THF,[25–29] while in diethyl ether dimeric or oligomeric contact ion pairs exist, which are able to react faster.[28,29] Therefore investigations in diethyl ether are normally performed with substituted enones in order to slow down the reaction and enabling the detection of cuprate enone π-complexes by NMR spectroscopy.[26,30] Among the experimental parameters also our NMR spectrometer equipment makes it difficult to detect π-complexes, due to the missing of a rapid injection unit under inert atmosphere.

Nevertheless AlMe3 was added to the reaction mixture. In the ^{31}P NMR spectrum in turn no significant changes occur (see Figure 4.4 below). In Figure 4.6 time-dependent ^{1}H NMR spectra after addition of the organoaluminum reagent are presented. Apart from the signals of Cy (green) and AlMe3 new signals appear in the range of 5.00-4.40, 2.45-1.85 and 1.10-0.75 ppm (purple boxes). The disappearance of the cyclohexenone signals and the appearance of new signals imply successful product formation. The slower reaction is based on lower temperature as those described in synthetic protocols, there full conversion is obtained after 18 h at -30 °C, with increased temperature the reaction is faster with a small drop in the *ee*-values.[12] The large time intervals between the ^{1}H NMR spectra are based on 2D measurements, therefore a detailed kinetic investigation is missing until now and probably can give further information concerning the formation tendencies of the involved intermediates. Also reducing the temperature might be a possible strategy to detect the participating reaction intermediates.
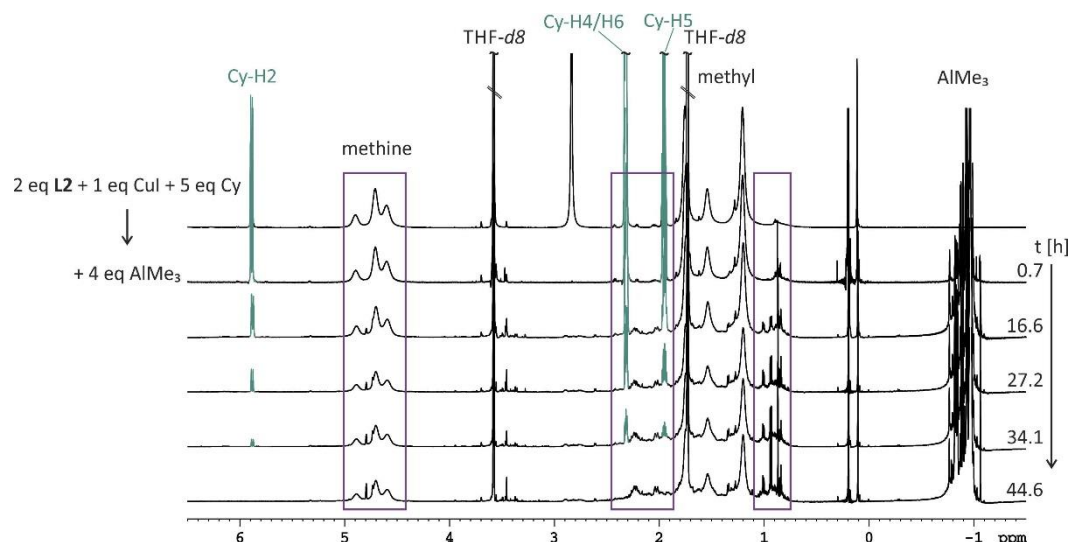
Figure 4.6: Time-dependent ^{1}H NMR spectra of a 2:1 mixture of **L2** and CuI with reverse addition of 5 eq Cyclohexenone and 4 eq AlMe$_3$ in THF-*d8* at 230 K. The signals for Cy decrease (green), while some new signals arise (purple boxes) representing product formation.

With [1]H[1]H-NOESY (see Figure 4.7) and [1]H[1]H-COSY (see Figure 4.8) spectra it was possible to identify two signal sets. The first one is assigned to the precursor of the product, representing an enol form with the organometallic reagent coordinated to the oxygen atom (blue line). The coordination of the organometallic reagent was proven by a NOE signal between 4.79 and -0.82 ppm. The first signal was assigned to the methine group of the double bond (C$_2$) and shows further NOE contacts to 2.21 and 0.94 ppm, which were identified as the methine proton and the introduced methyl group at C$_3$ of the cyclohexenone, due to the appearing [1]H[1]H-COSY pattern. The structure and the signal assignment of this product precursor are shown in Figure 4.8. This structure assumption is in good agreement with previous investigations concerning the reaction of ZnMe$_2$.[31] The second signal set has partially similar ^{1}H chemical shifts, with NOE contacts starting from 4.73 to 2.89, 2.03, 1.01 and -0.83 ppm (purple line). The main difference to the product precursor is the signal at 2.89 ppm, which gives a signal in the [1]H[1]H-COSY spectrum to 4.73 ppm (the methine signal at C$_2$). A further significant difference is that also the signal at -0.83 ppm, which is assigned to a methyl group of the organoaluminum reagent, gives a NOE pattern to 2.03 and 1.01 ppm, whereas for the product precursor no NOE contacts were obtained starting from the methyl group of the organoaluminum moiety. A clear structure assignment was not possible for the second species, but we assume that both the enone and the trimethylaluminum reagent are involved, probably another product precursor conformation exist. In order to get a detailed insight in the structure further investigations are necessary.
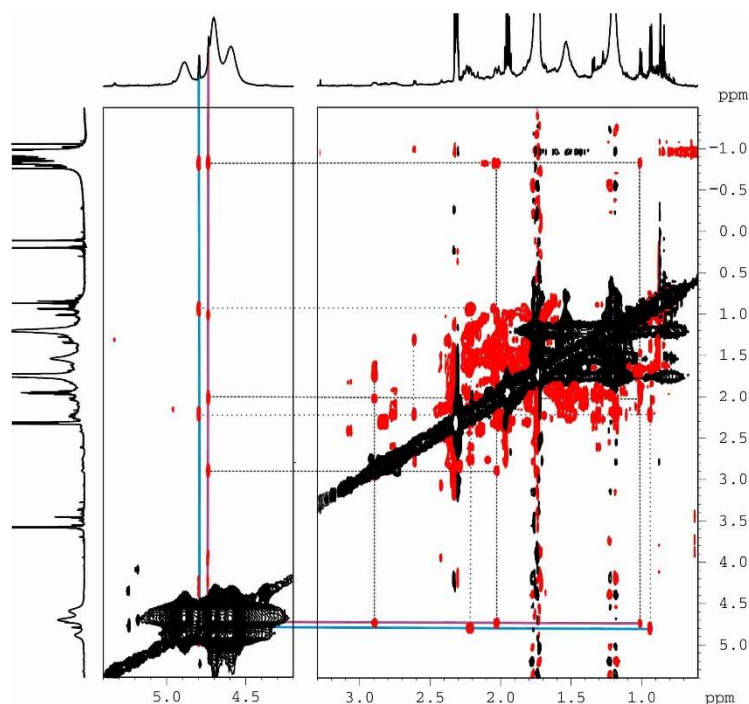
Figure 4.7: ^{1}H^{1}H- NOESY spectrum of a 2:1 mixture of **L2** and CuI with reverse addition of 5 eq Cyclohexenone and 4 eq AlMe$_3$ in THF-*d8* at 230 K. The blue line represents NOE contacts of 4.79 ppm and the purple one of 4.73 ppm respectively.
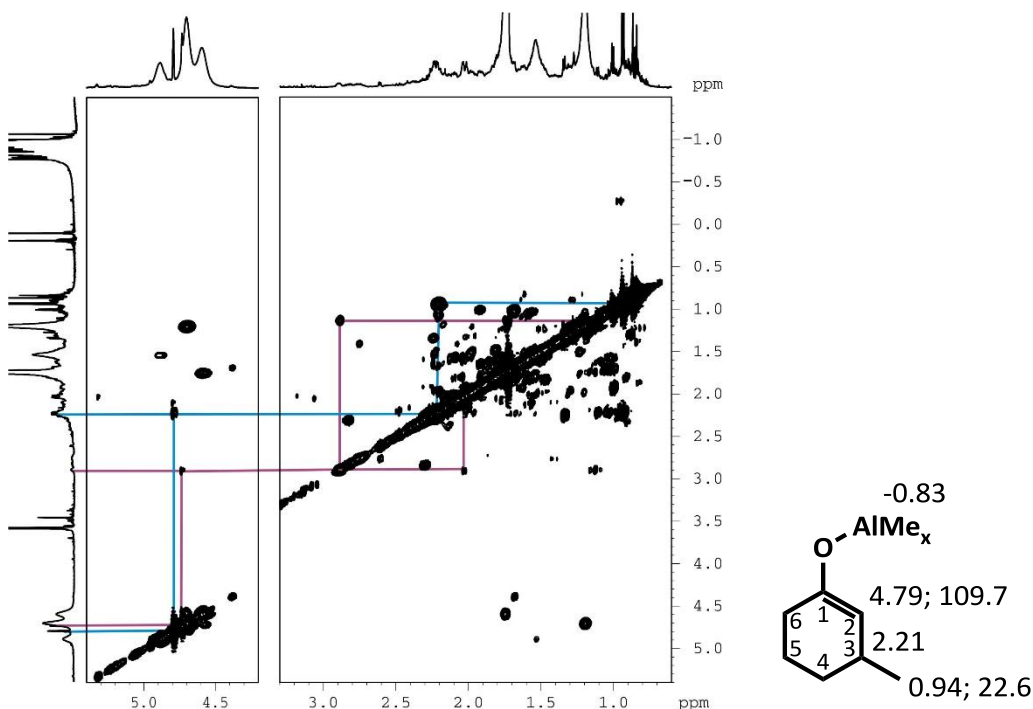
Figure 4.8: ^{1}H^{1}H-COSY spectrum of a 2:1 mixture of **L2** and CuI with reverse addition of 5 eq Cyclohexenone and 4 eq AlMe$_3$ in THF-*d8* at 230 K. The blue line represents the COSY pattern for the signal at 4.79 ppm, assigned to the product precursor, structure see on the right, and the purple line shows the COSY pattern for the signal at 4.73 ppm.

In the reverse addition reaction until now no information for a higher reactive copper cluster was obtained and only in the reaction mixture with all reagents, significant differences appear in the spectra compared to the precatalytic system. With ^{1}H NMR, ^{1}H^{1}H-NOESY and ^{1}H^{1}H-COSY

spectra it was possible to identify two species, which have quite similar signal sets. One of them was identified as the product in an enol form with the organoaluminum reagent coordinated to the oxygen. For the other one a detailed structural assignment is still missing, and therefore further investigations are necessary.

4.4.2 Normal Addition

In contrast to the reverse addition in the normal addition first the organometallic reagent is added to the prepared precatalytic system and afterwards the substrate (enone). In this addition order it is expected that a transmetalation of the organic moiety from the organometallic reagent to the copper complex occurs. A transmetalation using organoaluminum reagents is supposed to work better compared to ZnR_2, because the M-O bond energy is higher, implying a stronger thermodynamic driving force for additions to carbonyl substrates (M-O bond energies: with AlR_3 418 kJ mol^{-1} and with ZnR_2 381 kJ mol^{-1}).[9,32] In addition based on the higher Lewis acidity a better activation of the substrate is possible.[3] For the NMR spectroscopic investigation of this order of addition samples with phosphoramidite ligand **L2** and CuI as copper salt in a 2:1 ratio were prepared.

After the addition of $AlMe_3$ no significant changes appear in the ^{31}P NMR spectrum (Figure 4.9), the missing of new signals in the ^{31}P NMR spectrum for transmetalated intermediates is already known from our investigations with diorganozinc reagents (see Chapter 3.3). Based on our promising results in the detection of transmetalation intermediates with diorganozinc reagents by 1D and 2D $^1H^{31}P$-HMBC spectra, we also tested this NMR approach for the investigation of the transmetalation step with $AlMe_3$. Although the transmetalation should be easier[9,32] and several attempts for increasing the spectral quality were performed no signal was obtained which can be attributed to a transmetalation intermediate, neither in the 2D nor in the 1D $^1H^{31}P$-HMBC spectra, for the differentiation of magnetization transfers via scalar coupling or cross correlation. This missing of signals and therefore detection of a transmetalation intermediate probably are based on the lower reactivity in THF compared to diethyl ether.[12,25] Therefore further investigations in diethyl ether represent a promising strategy to solve this problem. Furthermore the enhanced spectrometer equipment which is now available at our working group (AVANCE III HD console and a cryo probe prodigy) probably simplifies the detection of elusive reaction intermediates.
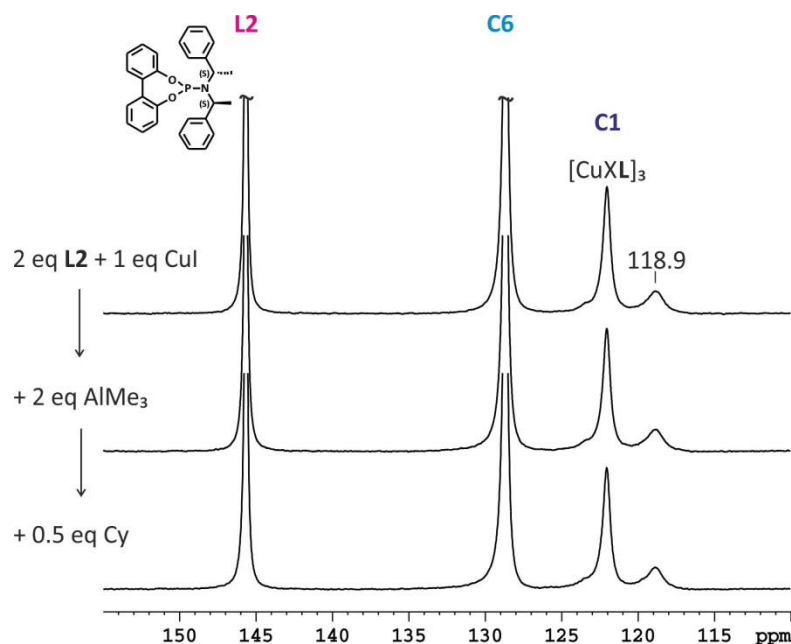
Figure 4.9: ^{31}P of 2 eq **L2** and 1 eq CuI (top), after addition of 2 eq AlMe$_3$ (middle) and after addition of 0.5 eq cyclohexenone Cy (below) at 230 K in THF-*d8*. There appear no significant changes in the integral intensity of **L2**, **C6**, **C1** and the signal at 118.9 ppm. Probably the amounts of AlMe$_3$ and Cy are too low.

Despite no changes appear in the ^{31}P NMR spectrum after AlMe$_3$ addition cyclohexenone was added to the reaction mixture. In turn, no changes appear in the ^{31}P NMR spectrum (see Figure 4.9 below), and also in the ^{1}H^{31}P-HMBC spectra no variations were observed. But the two signal sets for the product precursor and the similar substance by ^{1}H^{1}H-NOESY and ^{1}H^{1}H-COSY measurements were obtained, therefore successful product formation is observed (data not shown).

Up to now it is not possible to determine the reason for the better performance of the reverse addition order in synthetic applications, because with both the normal and reverse addition order identical products were obtained by the investigation of the complete reaction mixture. A differentiation between the formation rates is not possible, due to missing of identical kinetic investigations. Furthermore such a detailed kinetic study is difficult to perform, as equal time intervals, both for sample preparation and determination of the spectrometer parameters (e. g. temperature equilibration and time required for tuning and shimming) and identical or similar reagent concentrations are needed.

4.5 Conclusion

This NMR spectroscopic study was performed in order to investigate the mechanism of copper-catalyzed 1,4-addition reactions of organoaluminium reagents and to find an explanation for the better conversions and reaction outcome in synthetic protocols using the reverse addition order of enone before organoaluminum reagents instead of the normal addition. Therefore first of all the precatalytic complex was investigated in coordinating solvent (THF-*d8*), because reactions with AlMe$_3$ in non-coordinating solvents reveal a substitution of the biphenol backbone of the ligand by alkyl groups, due to the high oxophilicity of aluminum. However a polynuclear precatalytic complex with four CuX**L$_2$** fragments and one CuX**L** fragment was proposed in which the mixed trigonal/tetrahedral coordination of the copper atoms still remains, indicating a preferred formation of complexes with mixed coordination. This unexpected structure, with an increased number of CuX**L$_2$** fragments compared to coordinating solvents (one CuX**L** and one CuX**L$_2$** fragment), was corroborated by simulations of the low temperature ^{31}P NMR spectra and analysis of the temperature dependent complex formation and their signal integrals. Next, the two different reaction pathways of normal and reverse addition were addressed. In both addition orders (normal and reverse) two product species were identified, although a stabilization and detection of the involved intermediates by investigation of the single addition steps was not yet possible. The first one was assigned to a product precursor with an existing coordination of the organoaluminum reagent to the oxygen atom. In contrast for the second species we propose from the different observations, that also both the enone and the organoaluminum reagent are involved, due to ^{1}H^{1}H-COSY and ^{1}H^{1}H-NOESY coupling patterns. The most probable explanation for missing of signals both for copper-π-complexes and transmetalation intermediates is the reduced reactivity in THF-*d8*. A copper-π-complex is assumed to be formed if enone is added to a copper complex first (reverse addition order), in contrast transmetalation intermediates are commonly accepted if an organometallic reagent is added to a copper complex first (normal addition order). Therefore the most promising approaches for the detection of those intermediates are to use diethyl ether as solvent and the use of substituted cyclohexenone derivatives.

4.6 Supporting Information

4.6.1 Experimental Part

4.6.1.1 General Considerations

All sample preparations were performed under standard Schlenk technique under argon atmosphere and in dry solvents. CD_2Cl_2 (99.6 %) was purchased by Deutero GmbH, dried with CaH_2 and freshly distilled before use. THF-*d8* (99.5 %) was purchased by Deutero GmbH, dried with sodium/benzophenone and freshly distilled before use. The phosphoramidite ligands (≥ 99.0 %) were purchased by ABCR and used without further purification. Copper iodide was used as commercially available from Sigma Aldrich (99.999 %). The solutions of the trimethylaluminum reagent were freshly prepared in deuterated solvent (THF-*d8*). Therefore the organometallic reagent (0.5 mL) was solved in 2 mL solvent. $AlMe_3$ was purchased by ABCR (98 %) and used without further purification. Investigations were performed in THF-*d8* and CD_2Cl_2.

4.6.1.2 Sample Preparation

4.6.1.2.1 Preparation of the Phosphoramidite Copper Complexes

An argon flushed Schlenk tube equipped with magnetic stirring bar and septum was charged with 2 eq ligand (0.036 mmol, 15.81 mg) and 1 eq copper salt (0.018 mmol, CuI: 3.43 mg, CuTC: 3.43 mg, $[Cu(CH_3CN)_4]BF_4$: 5.66 mg), freshly distilled solvent THF-*d8* (0.6 ml) was added and the mixture stirred for 1-2 h at room temperature until a clear solution was obtained. Subsequently the samples were transferred to an argon flushed NMR tube. The samples were stored at -85 °C. For the ligand to salt dependent complex formation with CuI same sample preparations was used:

Ligand to CuI ratio	Amount ligand		Amount CuI	
	[mmol]	[mg]	[mmol]	[mg]
1.3:1	0.023	10.27	0.018	3.43
1.5:1	0.027	11.86	0.018	3.43
2:1	0.036	15.81	0.018	3.43
2.5: 1	0.045	19.77	0.018	3.43
3:1	0.054	23.72	0.018	3.43

4.6.1.2.2   Inverse addition order of Cyclohexenone and AlMe$_3$

The precatalytic mixture was prepared as described above. After cooling the sample to -50 °C the cyclohexenone was added and the corresponding spectra measured. AlMe$_3$ was added at temperatures between -30 and -75 °C.

4.6.1.2.3   Normal addition order of AlMe$_3$ and Cyclohexenone

The precatalytic mixture was prepared as described above. After cooling the sample to temperatures between -30 and -75 °C AlMe$_3$ was added and the corresponding spectra measured. Cyclohexenone was added at -30 or -50 °C.

4.6.1.3   NMR Data Collecting and Processing

NMR spectra were recorded on a Bruker Avance DRX 600 (600.13 MHz) spectrometer equipped with a 5 mm broadband triple resonance z-gradient probe (maximum gradient strength 53.5 Gauss/cm). The temperature for all low temperature measurements were controlled by a BVTE 3000 unit. The ^{1}H chemical shifts were referenced to the residual solvent signal of CD$_2$Cl$_2$ or TMS, for the ^{31}P chemical shifts the Ξ value was applied. NMR data were processed and evaluated with Bruker Topspin 3.1.

^{1}H: relaxation delay = 4.0 s, acquisition time = 1.1-7.8 s, SW 12-14 ppm, TD = 16k, NS 1-32; ^{31}P: relaxation delay = 2.5 s, acquisition time = 0.03-0.14 s, SW = 60-260 ppm, TD = 4K, NS = 512-1k; ^{1}H^{31}P-HMBC: relaxation delay = 6 s, mixing time = 0.04 s, TD = 16k F2 and 64 F1, DS = 8, NS = 128; ^{1}H^{1}H-COSY: relaxation delay = 4 s, acquisition time = 0.29 F2 and 0.02 F1, SW = 12 ppm, TD = 4k F2 and 256 F1, NS = 32; ^{1}H^{1}H-NOESY: relaxation delay = 5 s, mixing time = 0.7 s, acquisition time = 0.29 F2 and 0.02 F1, SW = 12 ppm, TD = 4k F2 and 256 F1, DS = 16, NS = 16.

4.6.2   Additional NMR spectra and Information

4.6.2.1   Signal Assignment to the Different Complex Species

For the first time separated signals appear in the ^{1}H NMR spectrum for the methine and methyl groups of free and complexed ligand with CuI as salt in THF-*d8*. The assignment of the methine groups to the different complex species, as well as to free ligand was possible by 2D ^{1}H^{31}P-HMBC spectra. Therein cross signals were detected for **C1** between 4.89 and 121.9 ppm and for **C6** between 4.71 and 128.9 ppm at 230 K (Figure SI 4.1). The low temperature spectrum at 180 K (Figure SI 4.2) shows only one cross signal between 4.35 and 145.4 ppm, representing one of the methine groups of the amine side chain of free ligand.
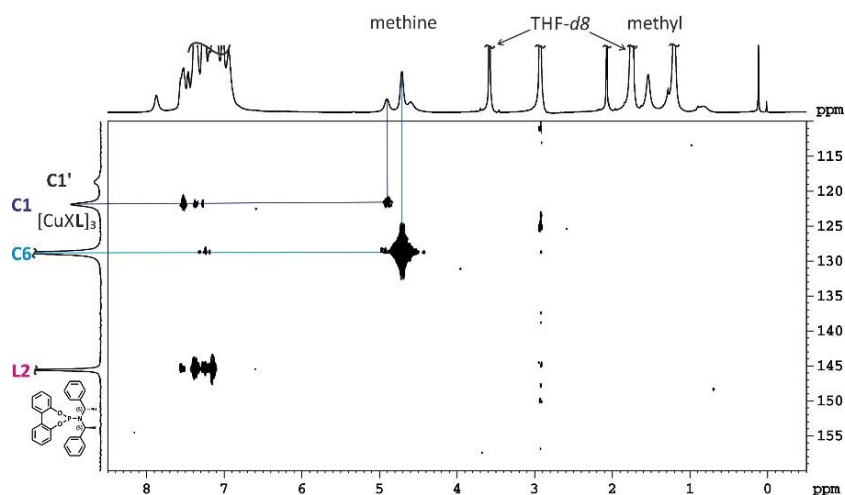
Figure SI 4.1: 2D ^{1}H^{31}P-HMBC spectrum of 2 eq **L2** and 1 eq CuI at 230 K in THF-*d8*.
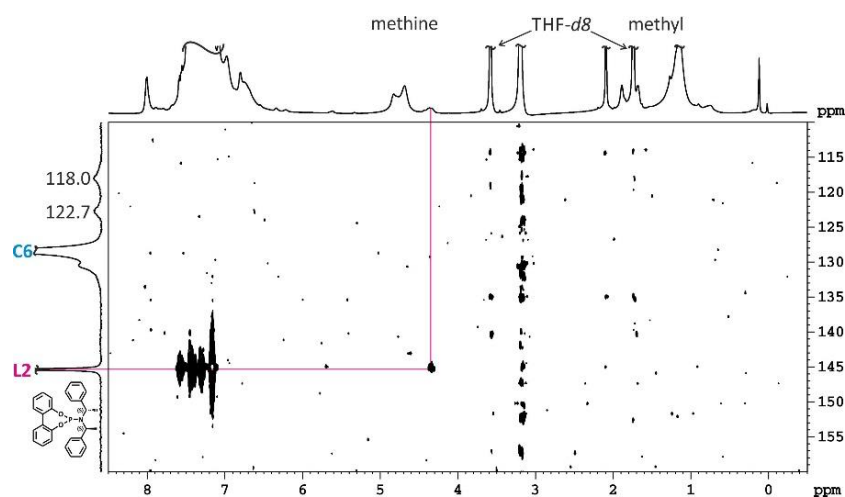
Figure SI 4.2: 2D ^{1}H^{31}P-HMBC spectrum of 2 eq **L2** and 1 eq CuI at 180 K in THF-*d8*.

The corresponding methyl groups were identified by ^{1}H^{1}H-COSY measurements. At 230 K (see Figure 4.8 in the main part) cross signals were obtained at 4.89 to 1.54 ppm, attributable to **C1**, between 4.71 and 1.19 ppm representing **C6** and for free ligand **L2** between 4.61 and 1.76 ppm. The signal of the methyl group of **L2** is superimposed by one of the THF-*d8* resonances. In contrast the low temperature spectrum (180 K, Figure SI 4.3) shows only cross signals for **C6** (blue) and for free ligand (pink). The signal splitting for the methine and methyl groups of free ligand is visible, due to decelerated rotation of the C-N bond of the amine side chain at low temperatures. The missing of signals for **C1** is based on the temperature dependent existence of the complexes and therefore **C1** only exist at higher temperatures or rather too broad signals and signal overlap exists. The signal between 5.30 and 2.04 ppm represents a not identified impurity.
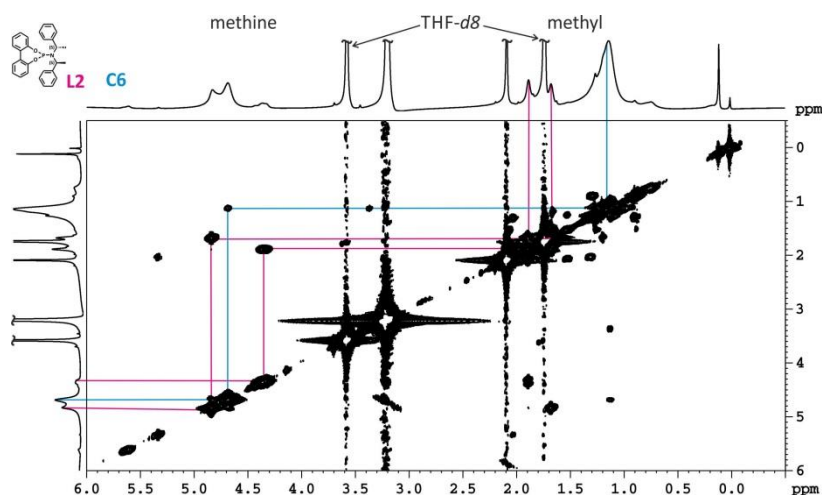
Figure SI 4.3: [1]H[1]H-COSY spectrum of 2 eq **L2** and 1 eq CuI at 180 K in THF-*d8*.

4.6.2.2 Investigation of Temperature Dependent Complex Formation

Figure SI 4.4 represents a comparison of the ^{31}P NMR spectra of a 1.3:1 mixture of **L2** and CuI in a temperature range of 230-180 K (left). The amount of **C1** and free ligand decreases with lowering the temperature, while the amount of **C6** increases. Due to the fact that the amount of **C1** accumulates with this ratio also at low temperatures still **C1** exists, but at 200 K distinct reduction occurs. The interconversion of the complexes is shown by the temperature dependent ligand distribution (right).
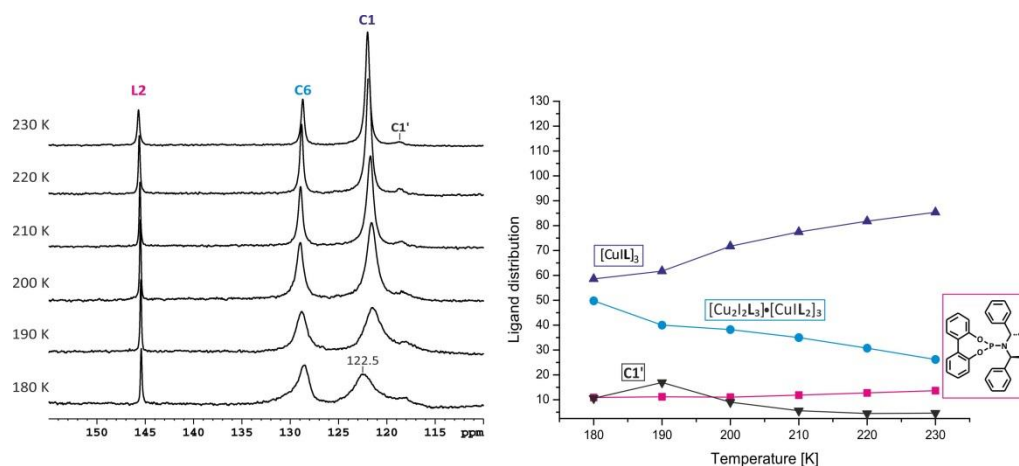
Figure SI 4.4: Temperature dependent ^{31}P NMR spectra of a 1.3 eq **L2** and 1 eq CuI (left) and the temperature dependent ligand distribution (right, normalized to 130, as 1.3 equivalents of **L2** are used, representing all ligand containing species).

With the 2.5:1 ratio (Figure SI 4.5) the interconversion becomes clearer; there a quite high amount of **C6** appears at 230 K, which increases by lowering the temperature. The interconversion of **C1** and **L2** into **C6** is visible in the ligand distribution presentation (right). There the decrease of both is in agreement with the increase of **C6**.
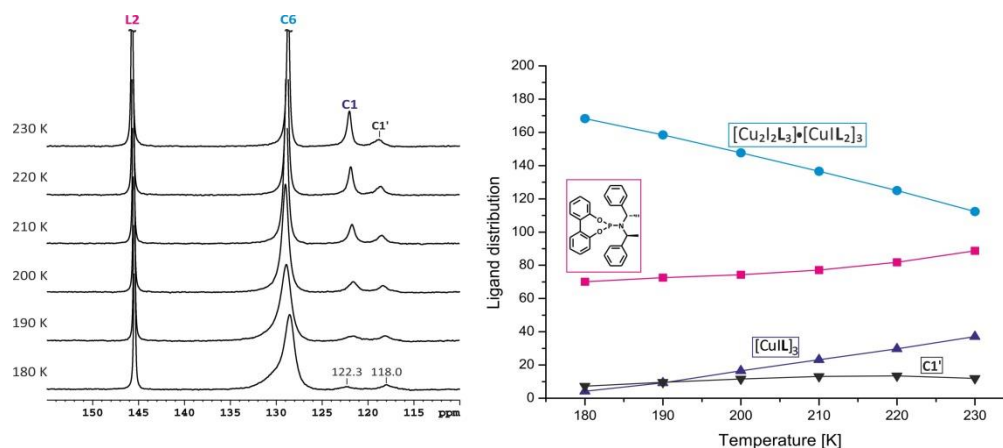
Figure SI 4.5: Temperature dependent ^{31}P NMR spectra of 2.5 eq **L2** and 1 eq CuI (left) and the temperature dependent ligand distribution (right, normalized to 250, as 2.5 equivalents of **L2** are used, representing all ligand containing species).

For both samples an analysis of the signal integrals of the temperature dependent complex formation was performed in analogy to the 2:1 sample described in the main part. Therefore for each mixture the ligand distribution in a temperature range of 180-230 K was investigated. With these values it is possible to calculate the sum of copper containing species and to receive an estimate for the possible complex species (for structures see main part Figure 4.2). Therefore the sum of the complex species with copper had to be 100 %, meaning that all copper atoms are involved in a complex. This assumption is also in samples with reduced and increased ligand to salt ratios better fulfilled with higher amounts of ligand and copper in the complex structure (see blue marked values in Table SI 4.1 and Table SI 4.2). Furthermore the same temperature dependent effects as in the 2:1 sample, described in detail in the main part, are observed.

Table SI 4.1: Temperature dependent ligand distribution in the ^{31}P NMR spectra of 1.3 eq **L2** and 1 eq CuI and the calculated sum of copper containing species with different ligand and copper contents in the complex species.

	Ligand distribution[a]				Sum of copper containing species[b]				
Temp	**L2**	**C6**	**C1**	**C1'**	**C2**	**C4**	**C5**	**C6**	**C3**
	--	--	--	--	2/3*128.8	3/5*128.8	4/7*128.8	5/9*128.8	½*128.8
230 K	13.7	26.2	85.4	4.7	107.6	105.8	105.1	104.7	103.2
220 K	12.8	30.8	81.8	4.5	106.8	104.8	103.9	103.4	101.7
210 K	11.9	35.0	77.5	5.6	106.4	104.1	103.1	102.5	100.6
200 K	11.1	38.2	71.7	9.1	106.3	103.7	102.6	102.0	99.9
190 K	11.2	40.0	61.7	17.0	105.4	102.7	101.6	100.9	98.7
180 K	10.9	49.8	58.6	10.6	102.4	99.1	97.7	96.9	94.1
Average	--	--	--	--	105.8	103.4	102.3	101.7	99.7

a) Representing the integrals of the corresponding signals, normalized to 130 representing all ligand containing species (1.3 eq **L2** used); b) each added with corresponding integral of **C1** and **C1'**, the numerator represents the number of involved copper atoms and the denominator the number of involved ligands in the complex species.

Table SI 4.2: Temperature dependent ligand distribution in the ^{31}P NMR spectra of 2.5 eq **L2** and 1 eq CuI and the calculated sum of copper containing species with different ligand and copper contents in the complex species.

Temp	Ligand distribution[a]				Sum of copper containing species[b]				
	L2	**C6**	**C1**	**C1'**	**C2**	**C4**	**C5**	**C6**	**C3**
	--	--	--	--	**2/3*128.8**	**3/5*128.8**	**4/7*128.8**	**5/9*128.8**	**½*128.8**
230 K	88.7	112.3	37.1	11.9	123.9	116.4	113.2	111.4	105.2
220 K	81.8	125.0	29.7	13.5	126.5	118.2	114.6	112.6	105.7
210 K	77.1	136.6	23.2	13.1	127.4	118.3	114.4	112.2	104.6
200 K	74.3	147.7	16.5	11.6	126.6	116.7	112.5	110.2	102.0
190 K	72.6	158.5	9.3	9.6	124.6	114.0	109.5	107.0	98.2
180 K	70.1	168.3	4.2	7.3	123.7	112.5	107.7	105.0	95.7
Average	--	--	--	--	125.4	116.0	112.0	109.7	101.9

a) Representing the integrals of the corresponding signals, normalized to 250 representing all ligand containing species (2.5 eq **L2** used); b) each added with corresponding integral of **C1** and **C1'**, the numerator represents the number of involved copper atoms and the denominator the number of involved ligands in the complex species.

4.6.2.3 Investigation with Dimethylaminephosphine Ligand

Apart from phosphoramidite ligands phosphinamine ligands were successfully used in asymmetric conjugate addition reactions (ACA) with alkenylalanes yielding good to excellent enantioselectivities.[13,33–35] The structure differs from the phosphoramidite ligands. They have an amine side chain, but instead of the biaryl ring system they have two alkyl groups bound to the phosphorous atom, therefore they are more electron rich.[36] Furthermore Alexakis and co-workers showed that biphenol- or binapthol-based phosphoramidite ligands react with AlMe$_3$ in non-coordinating solvents by substitution of the backbone with methyl groups, and that these dimethylaminephosphine ligands are the active ligand in CD$_2$Cl$_2$.[17] We were able to confirm the existence of dimethylaminephosphine ligands in non-coordinating solvents. In contrast to the observations of Alexakis with the free ligand,[17] we use the precatalytic mixture of phosphoramidite ligand **L2** and CuI. After the addition of AlMe$_3$ significant changes appear in the ^{31}P NMR spectrum. The signals for free ligand (145.0 ppm) and **C2** (130.0 ppm) decreases drastically and a new signal arises at 20.1 ppm. This resonance is not in agreement with published values of Alexakis,[17] therefore the dimethylaminephosphine ligand was synthesized and investigated separately. In the ^{31}P NMR spectra of pure ligand a signal appears at 12.7 ppm, which is in accordance with the reported resonance of 13.0 ppm by Alexakis.[17] Due to the fact that in the phosphoramidite sample also the copper salt is present, we add CuI to the dimethylaminephosphine ligand. In turn significant differences are visible in the ^{31}P NMR spectrum, a broad signal appears at 20.6 ppm, and this line broadening is a hint for complex formation. Besides the broad signal a significant narrower signal occurs at 16.4 ppm, which is probably a shifted signal of free ligand (lowfield shift of 3.7 ppm). Next, AlMe$_3$ was added to the complex mixture and besides the signals of the complex mixture a new signal appears at

34.0 ppm, attributable to the dimethylaminephosphine ligand in presence of an excess of AlMe$_3$, already reported by Alexakis (35 ppm).[17]
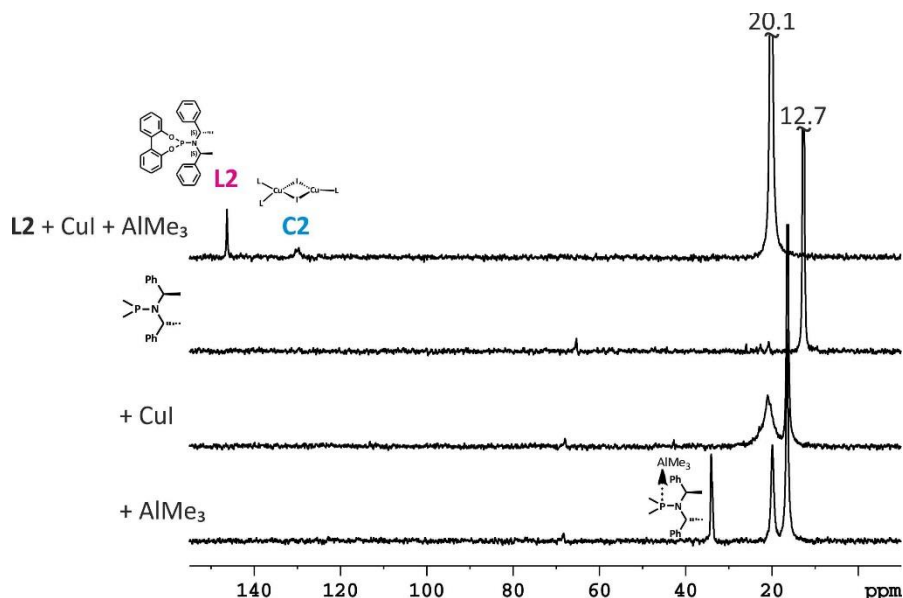
Figure SI 4.6: ^{31}P NMR spectra of 2 eq **L2**, 1 eq CuI and AlMe$_3$ at 230 K in CD$_2$Cl$_2$ and of dimethylaminophosphine ligand before and after addition of CuI and AlMe$_3$ at 230 K in CD$_2$Cl$_2$.

With these measurements we were able to assume that the signal at 20.1 ppm in the phosphoramidite ligand sample corresponds to a copper complex of the dimethylamine-phosphine ligand, as it is in agreement with the broad signal at 19.8 ppm detected in the dimethylaminephosphine ligand/CuI sample. In contrast to phosphoramidite ligands the copper complex is lowfield shifted compared to free ligand. This is based on the different electronic properties of the two ligand classes. Phosphoramidite ligands are strong π-acceptors,[37] therefore they can easily take electron density of the copper atom, and distribute it on their biaryl ring system. In contrast the phosphinamine ligands are already electron rich,[36] hence they cannot take as much electron density of the copper atom, and furthermore due the alkyl groups they are not able to distribute the electron density.

The 2D [1]H[31]P-HMBC spectrum (Figure SI 4.7) of the phosphoramidite sample with CuI and AlMe$_3$ in CD$_2$Cl$_2$ reveals different signal patterns for the signals at 20.1 and 33.5 ppm respectively.
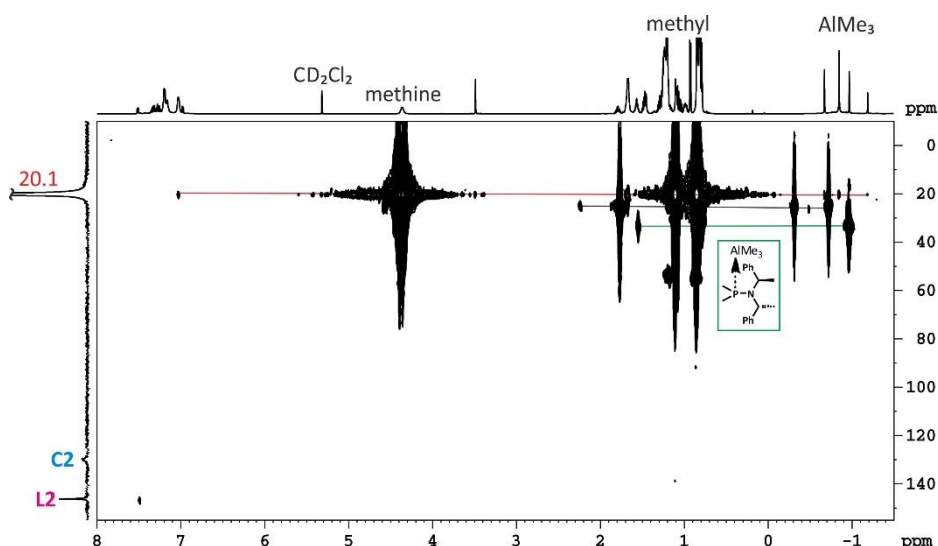
Figure SI 4.7: 2D ^{1}H^{31}P-HMBC spectrum of 2 eq **L2**, 1 eq CuI and AlMe$_3$ at 230 K in CD$_2$Cl$_2$. The green line (33.5 ppm) represents the dimethylaminephosphine ligand in presence of an excess of AlMe$_3$ and the red line (20.1 ppm) represents the copper complex of diemethlyaminephosphine ligand with AlMe$_3$.

The signal at 33.5 ppm (green line), which is attributed to the dimethylaminephosphine ligand with an excess of AlMe$_3$, shows cross signals to 1.54 and -0.95 ppm. The first one represents the methyl group at the phosphorous atom, while the second one are methyl groups bound to the aluminum atom. In contrast for the signal at 20.1 ppm (red line), supposed to be a complex of the dimethylaminephosphine ligand, cross signals to 7.03, 4.38, -0.65, -0.84 and -1.18 ppm appear. The existence of cross signals to an aromatic proton and the methine protons reveals that an intact amine side chain is involved in the structure. The existence of three signals for methyl groups bound to aluminum is probably explained by different chemical environments for the three methyl groups bound to aluminum, due to their position in the complex species.

Dialkylaminephosphine ligands were supposed by Alexakis to be the active ligand species if AlMe$_3$ is used in non-coordinating solvents. Therefore copper complexes of these ligands in CD$_2$Cl$_2$ were investigated. Thereby one copper complex was identified in which the methyl groups at the aluminum atom have different chemical environments and therefore give three separated signals. Whereas the ligand in presence of an excess of AlMe$_3$ reveals only one signal to methyl groups bound to aluminum. This effect is probably based on steric hindrance in the complex species.

4.7 Literature

[1]   T. Jerphagnon, M. G. Pizzuti, A. J. Minnaard, B. L. Feringa, *Chem. Soc. Rev.* **2009**, *38*, 1039–1075.

[2]   J. Christoffers, G. Koripelly, A. Rosiak, M. Rössle, *Synthesis* **2007**, *9*, 1279–1300.

[3]   A. Alexakis, J. E. Bäckvall, N. Krause, O. Pàmies, M. Diéguez, *Chem. Rev.* **2008**, *108*, 2796–2823.

[4]   S. R. Harutyunyan, T. den Hartog, K. Geurts, A. J. Minnaard, B. L. Feringa, *Chem. Rev.* **2008**, *108*, 2824–2852.

[5]   A. Alexakis, J. Frutos, P. Mangeney, *Tetrahedron: Asymmetry* **1993**, *4*, 2427–2430.

[6]   B. L. Feringa, M. Pineschi, L. A. Arnold, R. Imbos, A. H. M. De Vries, *Angew. Chemie* **1997**, *109*, 2733–2736.

[7]   A. H. M. de Vries, A. Meetsma, B. L. Feringa, *Angew. Chemie Int. Ed. English* **1996**, *35*, 2374–2376.

[8]   B. L. Feringa, R. Badorrey, D. Peña, S. R. Harutyunyan, A. J. Minnaard, *Proc. Natl. Acad. Sci. United States Am.* **2004**, *101* , 5834–5838.

[9]   A. Alexakis, N. Krause, S. Woodward, *Copper-Catalyzed Asymmetric Synthesis*, Wiley-VCH Verlag GmbH & Co. KGaA, Weinheim, **2014**.

[10]   A. Alexakis, V. Albrow, K. Biswas, M. d'Augustin, O. Prieto, S. Woodward, *Chem. Commun.* **2005**, 2843–2845.

[11]   P. von Zezschwitz, *Synthesis (Stuttg).* **2008**, *2008*, 1809–1831.

[12]   M. d'Augustin, L. Palais, A. Alexakis, *Angew. Chemie Int. Ed.* **2005**, *44*, 1376–1378.

[13]   M. Vuagnoux-d'Augustin, A. Alexakis, *Chem. – A Eur. J.* **2007**, *13*, 9647–9662.

[14]   M. Vuagnoux-d'Augustin, S. Kehrli, A. Alexakis, *Synlett* **2007**, *2007*, 2057–2060.

[15]   P. K. Fraser, S. Woodward, *Chem. – A Eur. J.* **2003**, *9*, 776–783.

[16]   M. Pineschi, F. Del Moro, V. Di Bussolo, F. Macchia, *Adv. Synth. Catal.* **2006**, *348*, 301–304.

[17]   C. Bournaud, C. Falciola, T. Lecourt, S. Rosset, A. Alexakis, L. Micouin, *Org. Lett.* **2006**, *8*, 3581–3584.

[18]   L. Su, X. Li, W. L. Chan, X. Jia, A. S. C. Chan, *Tetrahedron: Asymmetry* **2003**, *14*, 1865–1869.

[19]   H. Zhang, R. M. Gschwind, *Angew. Chemie Int. Ed.* **2006**, *45*, 6391–6394.

[20]   H. Zhang, R. M. Gschwind, *Chem. – A Eur. J.* **2007**, *13*, 6691–6700.

[21]   K. Schober, H. Zhang, R. M. Gschwind, *J. Am. Chem. Soc.* **2008**, *130*, 12310–12317.

[22]   K. Schober, E. Hartmann, H. Zhang, R. M. Gschwind, *Angew. Chemie Int. Ed.* **2010**, *49*, 2794–2797.

[23]   S. H. Bertz, S. Cope, M. Murphy, C. A. Ogle, B. J. Taylor, *J. Am. Chem. Soc.* **2007**, *129*, 7208–7209.

[24]   W. Henze, T. Gärtner, R. M. Gschwind, *J. Am. Chem. Soc.* **2008**, *130*, 13718–13726.

[25]   T. Gärtner, W. Henze, R. M. Gschwind, *J. Am. Chem. Soc.* **2007**, *129*, 11362–11363.

[26]   S. H. Bertz, C. M. Carlin, D. A. Deadwyler, M. D. Murphy, C. A. Ogle, P. H. Seagle, *J. Am. Chem. Soc.* **2002**, *124*, 13650–13651.

[27]   R. M. Gschwind, P. R. Rajamohanan, M. John, G. Boche, *Organometallics* **2000**, *19*, 2868–2873.

[28]   M. John, C. Auel, C. Behrens, M. Marsch, K. Harms, F. Bosold, R. M. Gschwind, P. R. Rajamohanan, G. Boche, *Chem. – A Eur. J.* **2000**, *6*, 3060–3068.

[29]   W. Henze, A. Vyater, N. Krause, R. M. Gschwind, *J. Am. Chem. Soc.* **2005**, *127*, 17335–17342.

[30]   K. Nilsson, T. Andersson, C. Ullenius, A. Gerold, N. Krause, *Chem. – A Eur. J.* **1998**, *4*, 2051–2058.

[31]   C. Koch, Master Thesis, NMR-Spektroskopische Studien Mechanistischer Schlüsselschritte in der Cu-Katalysierten Konjugierten 1,4-Additionsreaktion Mit Dimethylzink, Universität Regensburg, **2011**.

[32]   S. Woodward, *Tetrahedron* **2002**, *58*, 1017–1050.

[33]   L. Palais, A. Alexakis, *Chem. – A Eur. J.* **2009**, *15*, 10473–10485.

[34]   C. Hawner, K. Li, V. Cirriez, A. Alexakis, *Angew. Chemie Int. Ed.* **2008**, *47*, 8211–8214.

[35]   D. Müller, C. Hawner, M. Tissot, L. Palais, A. Alexakis, *Synlett* **2010**, *2010*, 1694–1698.

[36]   D. Müller, M. Tissot, A. Alexakis, *Org. Lett.* **2011**, *13*, 3040–3043.

[37]   J. F. Teichert, B. L. Feringa, *Angew. Chemie Int. Ed.* **2010**, *49*, 2486–2528.

5 NMR Spectroscopic Investigation of Rhodium-Catalyzed 1,2- and 1,4-Addition Reactions of Trimethylaluminum
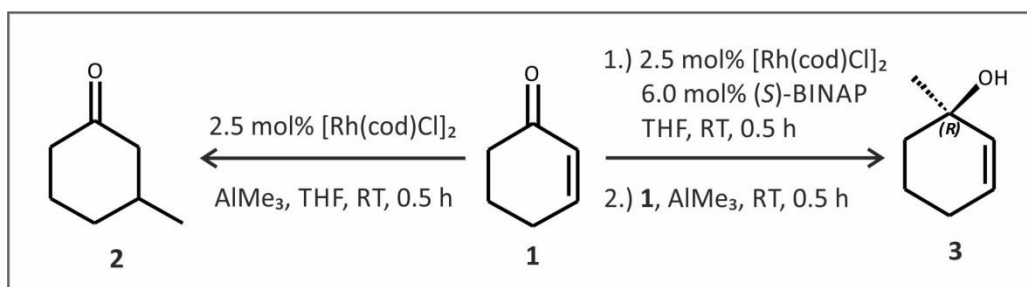

The investigation of this reaction was performed in close collarboration with

Dr. Andreas Kolb (Marburg).

5.1 Introduction

Over the last decades an increasing interest has been observed in the field of asymmetric transition metal-catalyzed C-C bond forming reactions. Thereby especially complexes of the late transition metals ruthenium,[1,2] rhodium,[3–6] palladium,[7,8] copper[9–13] and only recently gold[14,15] are often reported in literature. In 1998 Hayashi published the first example of a rhodium-catalyzed reaction.[3] Since then the rhodium-catalyzed addition of boronic acids as well as other organometallic reagents has developed as a powerful reaction in organic synthesis.[16] Besides addition reactions also a variety of other transformations are catalyzed, for example hydrogenations,[17] CH-activations or allylic substitution reactions.[18] Due to the fact that rhodium-catalyzed reactions can be performed with water as a co-solvent and even as sole solvent, the development of environmentally benign processes might be possible.[6] This is nowadays very important in the case of sustainability and green chemistry.[19] In 2007 von Zezschwitz and co-workers published a 1,4- or 1,2-addition reaction of trimethylaluminum to cyclohexenone, depending on the used rhodium catalyst (see Scheme 5.1).[20] With the achiral [Rh(cod)Cl]$_2$ complex the expected product of a 1,4-addition reaction is obtained (see Scheme 5.1 left, cod: 1,5-cyclooctadiene), whereas the attempt of performing an enantioselective reaction by use of the *in situ* prepared complex [Rh(BINAP)Cl]$_2$ results in an unexpected highly selective 1,2-addition reaction (see Scheme 5.1 right).[20] In general the asymmetric conjugate 1,4-addition reaction is already very well researched and established in synthetic procedures.[10,11,21,22] Hayashi and co-workers were able to elucidate the mechanism of a rhodium-catalyzed 1,4-addition reaction of phenylboronic acid to cyclohexenone, by identification of the involved intermediates step by step in ^{31}P NMR spectra.[23] In contrast the 1,2-addition reaction is addressed to a much lesser extent, even if the received chiral allylic alcohols build a very important structural motif in several target molecules and enables the formation of additional stereocenters, due to stereoinduction of the hydroxyl group.[24,25] Besides that, transformations with ketones and especially conjugated enones need harsher reaction conditions contrary to aldehydes, e. g. nucleophiles with higher reactivity and stronger stereodiscriminating catalysts.[24]
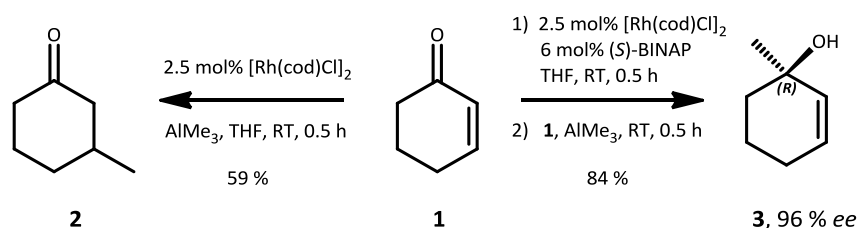
Scheme 5.1: Rhodium-catalyzed 1,4- and 1,2 addition reaction of trimethylaluminum to cyclohexenone **1**.[20]

The previous describe rhodium-catalyzed 1,2-addition reaction of trimethlyaluminium to cyclohexenone[20] was improved further.[24] The addition of a silver salt enables the decrease of the catalyst loading (5 mol% Rh without silver salt, reduction to 1 mol% Rh with silver salt). Furthermore the scope of applicable organoaluminum reagents ($AlMe_3$) was extended to DABCO-$(AlMe_3)_2$ (DABCO: 1,4-diazobicyclo[2.2.2]octane), an air-stable alternative and to $ArAlMe_2$, enabling the transfer of aryl groups. With these optimizations a variety of substituted cycloalkenones can be transformed into the corresponding allylic alcohols. Additionally, first mechanistic informations were obtained by ^{31}P NMR spectroscopy and GC analysis.[24] In order to get further insight into the reaction mechanism of the 1,2-addition advanced NMR spectroscopic investigations were performed in collaboration with Andreas Kolb a former member of the working group of Prof. P. von Zezschwitz. Therefore two diphosphine rhodium complexes were prepared and investigated by NMR spectroscopy. Additionally first test reactions with $AlMe_3$ were performed, in order to determine the involved reaction intermediates in this unexpected rhodium-catalyzed 1,2-addition reaction.

5.2 Investigation of Rhodium Complexes

First of all a suitable model system for NMR spectroscopic investigations had to be found beyond the synthetically applied systems. Therefore in accordance with our investigations in the field of copper-catalyzed addition reactions (see Chapter 4.3 and references [26–28]) the precatalytic system was investigated initially. For the precatalytic system either the diphosphine ligands (S)-BINAP or (R)-Tol-BINAP were used in combination with [Rh(cod)Cl]$_2$ to form the corresponding dimeric rhodium complex (see Scheme 5.2).

(S)-BINAP   [Rh(BINAP)Cl]$_2$

(R)-Tol-BINAP   [Rh(Tol-BINAP)Cl]$_2$
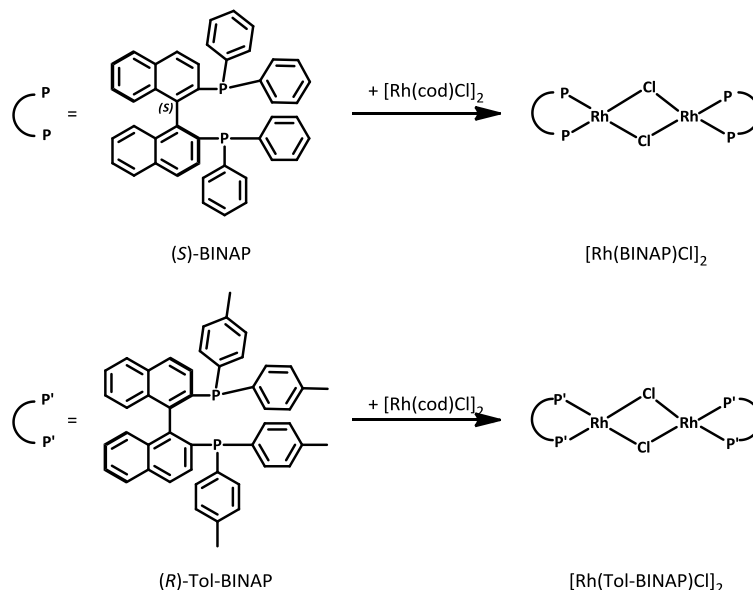
Scheme 5.2: Formation of a dimeric rhodium complex with (S)-BINAP and (R)-Tol-BINAP as ligand and [Rh(cod)Cl]$_2$ as salt (BINAP: 2,2'-Bis(diphenylphosphino)-1,1'-binaphthyl, Tol-BINAP: 2,2'-Bis(di-p-tolylphosphino)-1,1'-binaphthyl, cod: 1,5-cyclooctadiene).

The BINAP ligands were chosen, as other tested mono- and bidentate ligands (e. g. PPh$_3$, P(nBu)$_3$, dppe, dppb and diop) provided almost no transformation in synthesis.[20] The rhodium salt was used as it reveals quite high yields and excellent ee-values in the reaction, the best solvent is THF, because in other ethereal solvents reduced yields are observed, whereas non-ethereal solvents, like toluene induce several background reactions.[20] Although the reaction is performed with quite high amounts of catalysts, and a reduction is only possible by the addition of silver salts,[24] first investigations were performed without this additive, in order to investigate first of all why the enantioselective 1,2-addition reaction occurs instead of the 1,4-addition reaction.

5.2.1 Investigation of Rhodium BINAP Complexes

In synthetic applications normally a 2.4:1 ligand to salt ratio is used for complex formation.[20] Therefore for our NMR spectroscopic investigations the same ratio was used for sample preparation for better comparability. Figure 5.1 shows a comparison of the ^{31}P NMR spectra of

(*S*)-BINAP (top) and of the expected dimeric rhodium complex (below). In the ^{31}P NMR spectra a signal at -15.4 ppm occurs for the free ligand due to slight ligand excess and a small signal appears at 25.4 ppm assigned to the oxidized ligand. After addition of the rhodium salt, and thereof complex formation a doublet appears at 48.6 ppm with a $^1J_{Rh,P}$ coupling constant of 195.8 Hz, which is in good agreement with literature known values for corresponding rhodium complexes of 49.7 ppm with 197 Hz[23] and 50.0 ppm with 196 Hz.[29] Along with the signals for free and oxidized ligand and the dimeric complex two not yet identified signals appear at 24.3 and -15.0 ppm. These chemical shift values are very similar to those of free and oxidized ligand.
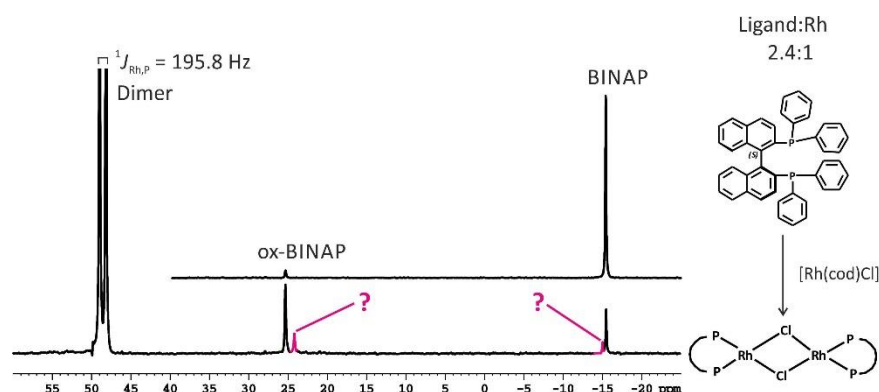
Figure 5.1: ^{31}P NMR spectra of (*S*)-BINAP (top) and of 2.4 eq (*S*)-BINAP and 1 eq [Rh(cod)Cl]$_2$ (below) at 300 K in THF-*d8*.

Also in the ^{1}H NMR spectra successful complex formation was detected, by the observation of signals for free cod at 5.50 and 2.33 ppm (see Figure 5.2). In the aromatic region beside signals for free ligand and the dimeric complex species several small signals appear, for which a clear assignment was not yet possible. Furthermore in the aliphatic region between 3.00 and 0.50 ppm several small signals appear which are partially already observed in the spectra of free ligand. This signals indicating that the ligand and probably also the rhodium salt used are not sufficiently pure for the detection of small signals of the occurring intermediates, especially for 2D spectra. Furthermore, we knew from our mechanistic studies in the field of copper-catalyzed 1,4-addition reactions that for example the signals of transmetalation intermediates occur in very tiny amounts close to the detection limit (see Chapter 3.3), this can also be expected for rhodium-catalyzed reactions. Thus, minimizing the impurities in the sample and therefore the number of detected signals in the ^{1}H NMR spectra are supposed to distinctly improve the probability of signal detection for further investigations.
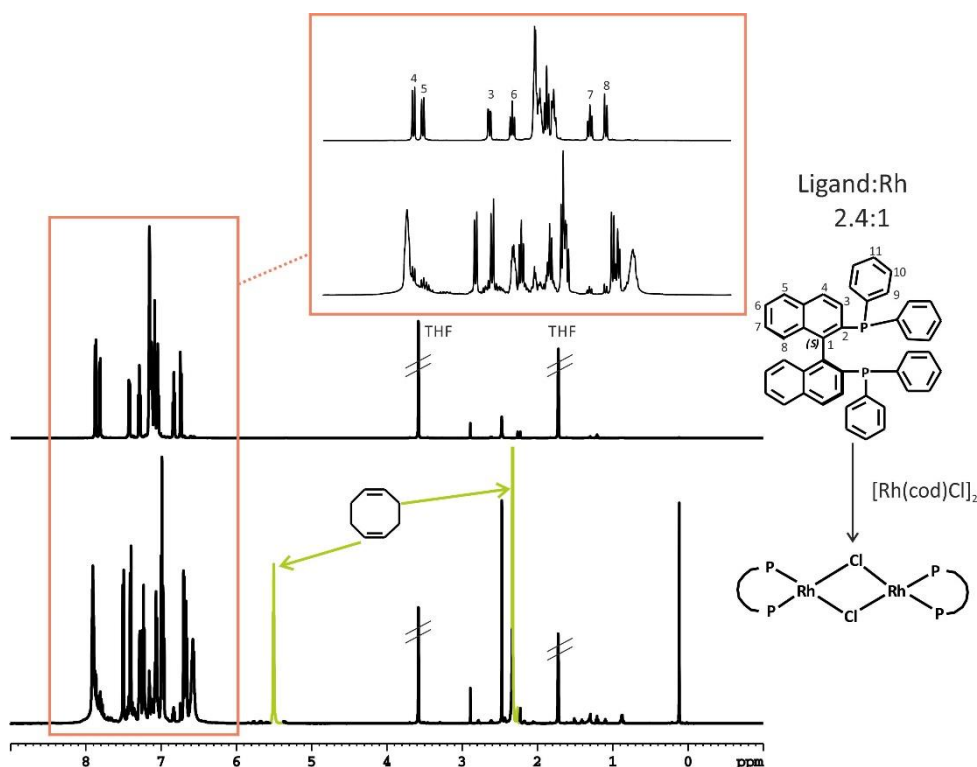
Figure 5.2: ^{1}H NMR spectra of (*S*)-BINAP (top) and of 2.4 eq (*S*)-BINAP and 1 eq [Rh(cod)Cl]$_2$ at 300 K in THF-*d8*.

Despite these limitations concerning the sample purity, first attempts were conducted to add AlMe$_3$ to this precatalytic mixture. Upon the applied organoaluminium reagents (e. g. AlMe$_3$, DABCO-(AlMe$_3$)$_2$ as well as ArAlMe$_2$)[24] AlMe$_3$ was chosen, as the simplest ^{1}H NMR spectra are observed with only one resonance for the methyl groups. In the ^{31}P NMR spectra no big changes were observed, and also in the ^{1}H NMR spectra no new signals appear, despite the AlMe$_3$ signal (data not shown). Measuring ^{1}H NMR spectra after about three hours reveals new signals in the region of AlMe$_3$, but it cannot be excluded that they stem from decomposition reactions of free AlMe$_3$ due to residual oxygen in the solution. The fact that the BINAP ligand possesses only aromatic protons, and therefore a spy signal is missing, which probable can give further insight in the involved structures revealed that complexes with BINAP ligands are not the best model system to use. Therefore the toluene substituted derivative was tested.

5.2.2 Investigation of Rhodium Tol-BINAP Complexes

As an alternative ligand toluene substituted BINAP (Tol-BINAP) ligand was chosen, because the methyl groups of the toluene substituents are expected to gain further insight in the involved structures, as it can act as a spy signal and furthermore the aromatic region is not as crowded as with unsubstituted BINAP. Therefore a sample of 2 eq (*R*)-Tol-BINAP and 1 eq [Rh(cod)Cl]$_2$ in THF-*d8* was prepared. The reduced amount of ligand was used, in order to minimize the signals of remaining free ligand in the sample. In Figure 5.3 the ^{31}P NMR spectra of free (*R*)-Tol-BINAP at

300 K (top) and of the corresponding complexes at 300 K (middle) and at 270 K (below) are presented. In the ^{31}P NMR spectrum of the complex mixture three doublets **1-3** appear (53.7, 47.8 and 46.8 ppm) with $^1J_{Rh,P}$ coupling constants of 200.0, 199.2 and 194.8 Hz assigned to dimeric rhodium complexes. In addition, small signals were observed for oxidized (25.3 ppm) and free (-16.7 ppm) ligand. The chemical shift values and the coupling constants of signals **1-3** are in good agreement with values known for dimeric complex species (dimeric rhodium complex with BINAP: $\delta^{31}P$ = 49.2 ppm, $^1J_{Rh,P}$ = 195 Hz[30]). Moreover monomeric complexes can be excluded, as they appear stronger highfield shifted at about 25.0 ppm and with smaller coupling constants of about 145 Hz.[29,30] At 300 K signal **1** appears in very tiny amounts close to the detection limit, whereas signals **2** and **3** have a signal ratio of 1:1.9. By cooling the sample (270 K) the signal ratio of **2:3** increases to 1:5.4 and also signal **1** increases slightly, while the amount of free ligand decreases. Therefore complex **3** is built with a distinct preference, compared to **1** and **2**, which is further increased at lower temperatures. In order to gain further detailed information concerning the formation tendencies of this three dimeric complexes, the variation of the ligand to salt ratio, as well as additional low temperature measurements appear to be promising approaches and were already applied successfully in the structure elucidation of phosphoramidite copper complexes.[27,28]
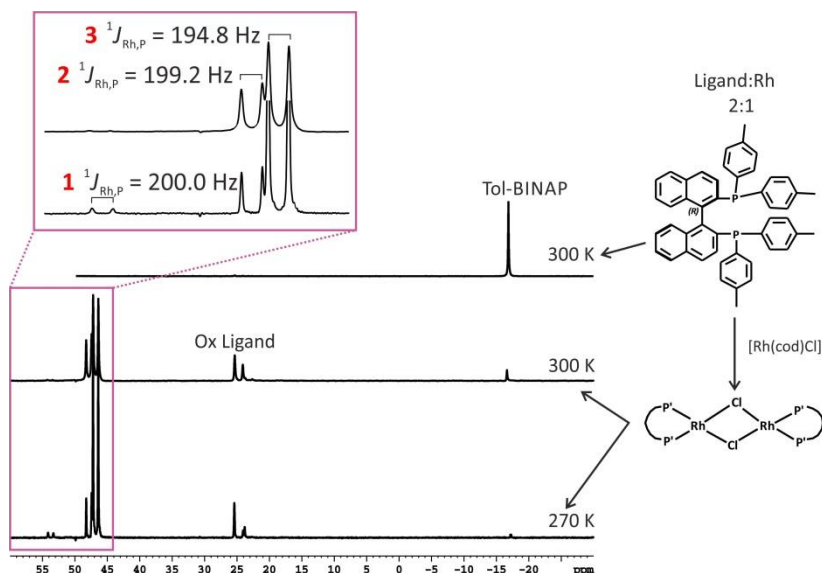
Figure 5.3: ^{31}P NMR spectra of (*R*)-Tol-BINAP at 300 K (top) and of 2 eq (*R*)-Tol-BINAP and 1 eq [Rh(cod)Cl]$_2$ at 300 K (middle) and at 270 K (below) in THF-*d8*.

In the ^{1}H NMR spectra of (*R*)-Tol-BINAP and the corresponding complex mixture, again successful complex formation was detected, by the signals for free cod. In combination with $^1H^{31}P$-HMBC spectra the methyl groups of the toluene substituent were detected at 2.06 and 1.94 ppm.

Beside them a small signal appears at 1.93 ppm (colored pink in Figure 5.4), these three signals have a signal ratio of 2:2:1. But also here several small signals of impurities are observed.
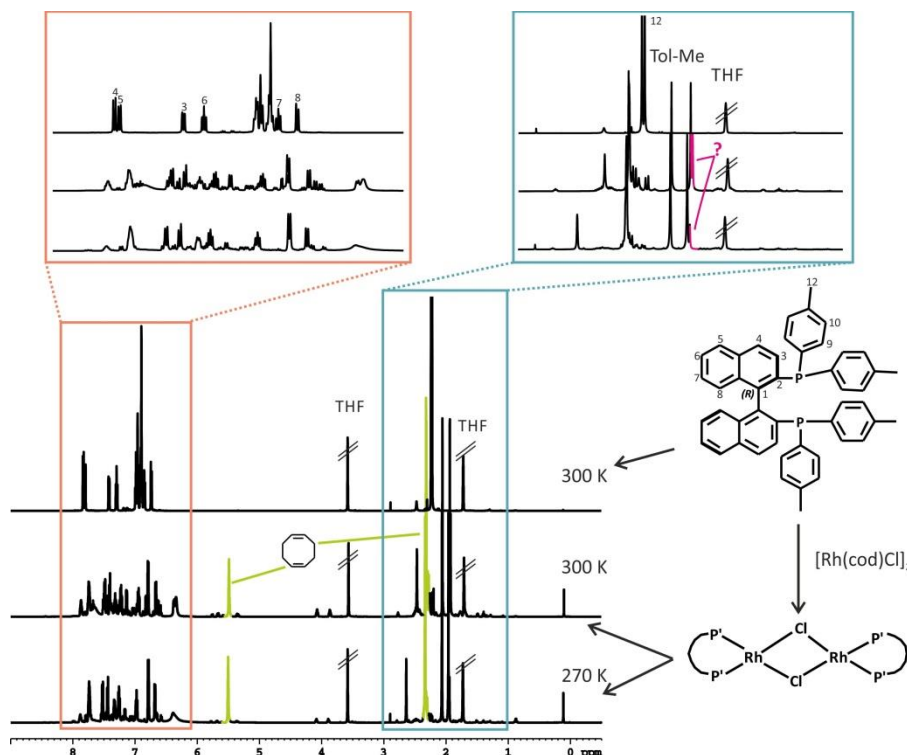
Figure 5.4: ^{1}H NMR spectra of (*R*)-Tol-BINAP at 300 K (top) and of 2 eq (*R*)-Tol-BINAP and 1 eq [Rh(cod)Cl]$_2$ at 300 K (middle) and at 270 K (below) in THF-*d8*.

After the addition of the organometallic reagent to the complex mixture distinct changes appear in the ^{31}P NMR spectrum. In Figure 5.5 the time dependent ^{31}P NMR spectra after addition of AlMe$_3$ are shown. Several new signals are observed which can be divided into three groups. First of all one increasing signal is detected at 42.3 ppm. Also in the range of oxidized ligand a variation of the signals occurs, this might be explained by the formation of small amounts of monomeric complexes (normally observed at about 25 ppm in the ^{31}P NMR spectrum). Monomeric rhodium complexes were already observed in ^{31}P NMR spectra as main species, if a silver salt is added to the solution for optimization of the 1,2-addition reaction.[24] All in all compared to the main species **3** (at 46.7 ppm), which increases during time the new appearing signals are quite small. However it was not possible until today to determine, if these structures are important for the mechanism or the results of decomposition reactions. Interestingly the signal for free Tol-BINAP vanishes and a new one appears highfield shifted at -18.8 ppm which gives a cross signal to -1.03 ppm in the 2D [1]H[31]P-HMBC spectrum (data not shown). Therefore a possible explanation would be an interaction of ligand and AlMe$_3$. Such an interaction has to be addressed in further investigations of rhodium free samples. Therefore a promising approach would be the measurement of modified 1D [1]H[31]P-HMBC spectra, in order to differentiate

between magnetization transfers via chemical bonds (scalar coupling) or through space (cross correlation as combination of chemical shift anisotropy and dipolar interactions). With these spectra we already were able to propose several transmetalation intermediates in copper-catalyzed 1,4-addition reactions, but until now did not tested it for rhodium-catalyzed reactions.
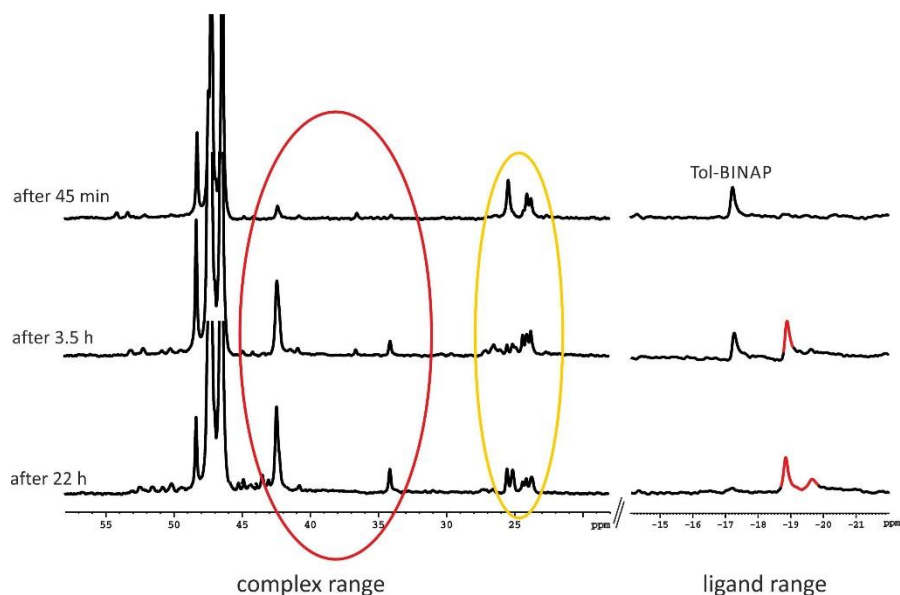
Figure 5.5: Time dependent ^{31}P NMR spectra of 2 eq (*R*)-Tol-BINAP and 1 eq [Rh(cod)Cl]$_2$ after addition of 2.8 eq AlMe$_3$ at 270 K in THF-*d8*.

Although the first promising results were obtained upon addition of AlMe$_3$ to a (*R*)-Tol-BINAP rhodium complex further investigations are necessary, both for the search of the best suited modelsystem and for the next step, the transmetalation. Additional detailed information concerning the precatalytic complex, and therefore the model system is accessible, by variation of the ligand to salt ratio, temperature dependent ^{31}P NMR spectra and variation of the rhodium salt. Furthermore with the Tol-BINAP ligand diffusion ordered spectroscopy (DOSY) could turn out as powerful tool, due to the methyl groups, appearing in a chemical shift range with sufficient signal separation to other signals, and the less crowded aromatic region probably provide also sufficient signal separation for DOSY measurements.

5.3 Conclusion and Outlook

In asymmetric transition metal-catalyzed C-C bond forming reactions, rhodium is apart from copper and palladium a typically used transition metal. Thereby since the first example of rhodium-catalyzed addition reactions of phenylboronic acids by Hayashi and co-workers in 1998 several further transformations, for example hydrogenations, CH-activations and several others were determinted to work with rhodium. In 2007 von Zezschwitz and co-workers found that a highly enantioselective 1,2-addition reaction is observed by the use of [Rh(BINAP)Cl]$_2$ as catalyst, cyclohexenone as substrate and AlMe$_3$ as organometallic reagent, instead of the expected 1,4-addition reaction. Due to the fact, that the resulting chiral allylic alcohols are a very important structural motif in several target molecules and enable the formation of further stereocenters due to stereodiscriminating effects of the hydroxyl group we started to investigate the corresponding mechanism in collaboration with the group of von Zezschwitz by advanced NMR spectroscopy. Thereby we found that Tol-BINAP ligands are better suited ligands for NMR spectroscopic investigations instead of unsubstituted BINAP ligands, because of a less crowed aromatic region and better signal separation in there, as well as the methyl group of the toluene substituent is accessible as a spy signal, which can reveal further insight in the participating structures. With [Rh(cod)Cl]$_2$ as salt three dimeric rhodium complexes were observed, with one having a distinct formation preference appearing in high amount, whereby the other two occur in smaller amounts. Further investigation of the formation tendencies of these dimeric complexes is possible by variation of the ligand to salt ratio and further spectra at lower temperature. Nevertheless, several small signals appear in the spectra, indicating a not sufficient purity of the ligand and rhodium salt, which is very problematic for the detection of intermediates in very tiny amounts. Therefore, further optimization of the model system, e. g. the rhodium salt, should be performed first, to be sure to use the best suited model system. The approach of varying the ligand to salt ratios and usage of several copper salts was already successfully applied in our working group to get detailed information concerning phosphoramidite copper complexes. Although first observations reveal new appearing signals in the ^{31}P NMR spectra upon addition of organometallic reagent, still further investigations are necessary to gain detailed insight into the mechanism and to determine if this species are important for the mechanism or caused by decomposition reactions. Furthermore, apart from the synthetically approaches, also ^{103}Rh NMR spectroscopy and ^{31}P^{103}Rh-HMQC spectra appear to be a very promising and powerful tool for the mechanism investigation. The theory and application of transition metal NMR spectroscopy (especially ^{57}Fe, ^{103}Rh, ^{187}Os and other quadrupole nuclei) were investigated by von Philipsborn.[31,32] Transition metal NMR

spectroscopy is very sensitive to changes in the coordination sphere of the metal and also to steric or electronic perturbations, due to the broader range of the chemical shift compared to ^{1}H or ^{13}C (about 12000 ppm for ^{103}Rh) and represents directly the center of the interested structure.[33] In order to use ^{103}Rh NMR spectroscopy as a powerful analytical tool, a distinct knowledge of the influence of the steric and electronic properties of a complex series on the ^{103}Rh chemical shift is necessary. Therefore several neutral rhodium complexes with mono- and bidentate diphosphine ligands, as well as cationic rhodium complexes with bidentate diphosphine ligands were already investigated NMR spectroscopically.[29] Therefore also in the investigation of the mechanism of the unexpected, highly enantioselective 1,2-addition reaction described here the use of ^{103}Rh NMR spectroscopy offers a promising approach.

5.4 Supporting Information

5.4.1 Experimental Part

5.4.1.1 General Considerations

All sample preparations were performed under standard Schlenk technique under argon atmosphere and in dry solvent. Investigations were performed in THF-*d8*, which was purchased by Deutero GmbH (99.5 %), dried with Na/benzophenone and freshly distilled before use. The (*S*)-BINAP and (*R*)-Tol-BINAP ligands were purchased by Sigma Aldrich and used without further purification (≥ 94 %). [Rh(cod)Cl]$_2$ was used as commercially available from Alfa Aesar (98 %). Trimethylaluminum was purchased as 2.6M solution in hexane by Sigma-Aldrich and used without further purification.

5.4.1.2 Sample Preparation

5.4.1.2.1 Preparation of the diphosphine rhodium complexes

An argon flushed Schlenk tube equipped with magnetic stirring bar and septum was charged with diphosphine ligand and [Rh(cod)Cl]$_2$, freshly distilled solvent THF-*d8* (0.6 ml) was added and the mixture stirred for 1 h at room temperature. The red brown solution was transferred into an argon flushed NMR tube.

Ligand to [Rh(cod)Cl]$_2$ ratio	Amount ligand		Amount [Rh(cod)Cl]$_2$	
	[mmol]	[mg]	[mmol]	[mg]
2:1 (BINAP)	0.036	22.42	0.018	8.87
2.4:1 (BINAP)	0.036	22.42	0.015	7.40
2:1 (Tol-BINAP)	0.036	20.36	0.018	8.87
	0.030	20.36	0.015	7.40

5.4.1.2.2 Preparation of the diphosphine rhodium complexes – AlMe$_3$ samples

To the freshly prepared diphosphine rhodium complex the corresponding amount of AlMe$_3$ solution (5-20 μl of a 2.6M solution in hexane) was added.

5.4.1.3 NMR Data Collecting and Processing

NMR spectra were recorded on a Bruker Avance DRX 600 (600.13 MHz) spectrometer equipped with a 5 mm broadband triple resonance z-gradient probe (maximum gradient strength 53.5 Gauss/cm). The temperature for all low temperature measurements were controlled by a BVTE 3000 unit. The ^{1}H chemical shifts were referenced to the residual solvent signal of THF-*d8*,

for the ^{31}P chemical shifts the Ξ value was applied. NMR data were processed and evaluated with Bruker Topspin 3.1.

[1]H: relaxation delay = 4 s, acquisition time = 1.1-4.6 s, SW = 12 ppm, TD 16k, NS = 1-32; [31]P: relaxation delay = 2.5 s, acquisition time = 0.04 s, SW 80-200 ppm, TD 4k, NS 1-2k; [1]H[31]P-HMBC: pulse program = inv4gplrndqf, relaxation delay = 6 s, mixing time = 0.04 s, NS = 128, DS = 8-16, TD = 16k F2 and 64 F1.

5.5 Literature

[1]   A. Grabulosa, A. Mannu, A. Mezzetti, G. Muller, *Journal of Organometallic Chemistry* **2012**, *696*, 4221–4228.

[2]   T. Naota, H. Takaya, S.-I. Murahashi, *Chemical Reviews* **1998**, *98*, 2599–2660.

[3]   Y. Takaya, M. Ogasawara, T. Hayashi, M. Sakai, N. Miyaura, *Journal of the American Chemical Society* **1998**, *120*, 5579–5580.

[4]   T. Hayashi, K. Yamasaki, *Chemical Reviews* **2003**, *103*, 2829–2844.

[5]   K. Yoshida, T. Hayashi, in *Modern Rhodium-Catalyzed Organic Reactions* (Ed.: P. A. Evans), Wiley-VCH, Weinheim, **2005**, pp. 55–77.

[6]   K. Fagnou, M. Lautens, *Chemical Reviews* **2002**, *103*, 169–196.

[7]   K. Ohmatsu, M. Ito, T. Kunieda, T. Ooi, *Nat Chem* **2012**, *4*, 473–477.

[8]   K. Kikushima, J. C. Holder, M. Gatti, B. M. Stoltz, *Journal of the American Chemical Society* **2011**, *133*, 6902–6905.

[9]   N. Krause, *Modern Organocopper Chemistry*, WILEY-VCH Verlag GmbH, Weinheim, **2002**.

[10]   A. Alexakis, J. E. Bäckvall, N. Krause, O. Pàmies, M. Diéguez, *Chemical Reviews* **2008**, *108*, 2796–2823.

[11]   T. Jerphagnon, M. G. Pizzuti, A. J. Minnaard, B. L. Feringa, *Chem. Soc. Rev.* **2009**, *38*, 1039–1075.

[12]   T. Thaler, P. Knochel, *Angewandte Chemie* **2009**, *121*, 655–658.

[13]   R. Šebesta, *ChemCatChem* **2013**, *5*, 1069–1071.

[14]   A. Pradal, P. Y. Toullec, V. Michelet, *Synthesis* **2011**, *2011*, 1501–1514.

[15]   S. Sengupta, X. Shi, *ChemCatChem* **2010**, *2*, 609–619.

[16]   J. Christoffers, G. Koripelly, A. Rosiak, M. Rössle, *Synthesis* **2007**, *9*, 1279–1300.

[17]   P. Etayo, A. Vidal-Ferran, *Chem. Soc. Rev.* **2013**, *42*, 728–754.

[18]   P. A. Evans, Ed., *Modern Rhodium-Catalyzed Organic Reactions*, Wiley-VCH, Weinheim, **2005**.

[19]   P. Anastas, N. Eghbali, *Chem. Soc. Rev.* **2010**, *39*, 301–312.

[20]   J. Siewert, R. Sandmann, P. von Zezschwitz, *Angewandte Chemie International Edition* **2007**, *46*, 7122–7124.

[21] J.-X. Ji, A. S. C. Chan, in *Catalytic Asymmetric Synthesis* (Ed.: I. Oijama), John Wiley & Sons, Hoboken, **2010**, pp. 439–495.

[22] K. Yoshida, T. Hayashi, in *Modern Rhodium-Catalyzed Organic Reactions* (Ed.: P. A. Evans), Wiley-VCH, Weinheim, **2005**, pp. 55–77.

[23] T. Hayashi, M. Takahashi, Y. Takaya, M. Ogasawara, *Journal of the American Chemical Society* **2002**, *124*, 5052–5058.

[24] A. Kolb, W. Zuo, J. Siewert, K. Harms, P. von Zezschwitz, *Chemistry – A European Journal* **2013**, *19*, 16366–16373.

[25] A. Lumbroso, M. L. Cooke, B. Breit, *Angewandte Chemie International Edition* **2013**, *52*, 1890–1932.

[26] H. Zhang, R. M. Gschwind, *Angewandte Chemie International Edition* **2006**, *45*, 6391–6394.

[27] H. Zhang, R. M. Gschwind, *Chemistry – A European Journal* **2007**, *13*, 6691–6700.

[28] K. Schober, H. Zhang, R. M. Gschwind, *Journal of the American Chemical Society* **2008**, *130*, 12310–12317.

[29] A. Fabrello, C. Dinoi, L. Perrin, P. Kalck, L. Maron, M. Urrutigoity, O. Dechy-Cabaret, *Magnetic Resonance in Chemistry* **2010**, *48*, 848–856.

[30] T. Ohshima, H. Tadaoka, K. Hori, N. Sayo, K. Mashima, *Chemistry – A European Journal* **2008**, *14*, 2060–2066.

[31] W. von Philipsborn, *Pure & Appl. Chem.* **1986**, *58*, 513–528.

[32] W. von Philipsborn, *Chem. Soc. Rev.* **1999**, *28*, 95–105.

[33] J. M. Ernsting, S. Gaemers, C. J. Elsevier, *Magnetic Resonance in Chemistry* **2004**, *42*, 721–736.

6 ORGANOCATALYTIC DIMERIZATION OF NITROALKENES TO ENYNES
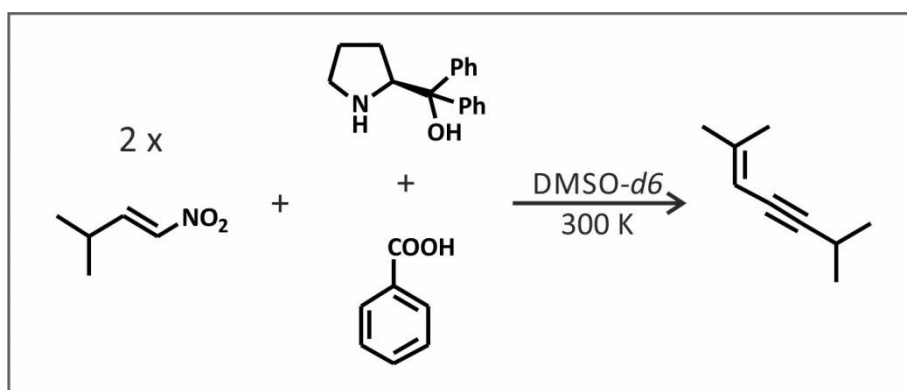
NMR spectroscopic investigations on the reactions of **2** and **4** were performed in close collaboration with Dr. Markus Schmid.

6.1   Introduction

Nitroalkenes are a very powerful and widely used Michael acceptor species in organocatalyic transformations. They possess not only very high electrophilicities ("super-electrophiles"),[1] but also nucleophilic reactivity is known in Baylis-Hillman reactions with tertiary amines. Due to this simultaneous reactivity as α-nucleophile and as β-electrophile they are often called a synthetic chameleon.[2,3] The diversity of application of nitroalkenes is thereby based on the nitro group and their possible transformation into several functional groups, only to mention a few: reduction to amine,[4] Nef reaction[5] as well as nucleophilic displacement.[6] In contrast, in presence of bases nitroalkanes typically act as α-nuclephiles, e. g. in the Henry reaction (addition to carbonyl compounds) or addition to electron-poor alkenes.[7,8] In this context, special mention should be made of the addition of nitroalkanes to nitroalkenes forming 1,3-dinitro compounds, which in turn are valuable synthetic building blocks.[3] Furthermore this reaction is promoted by the use of bases,[9] ammonium bifluorides,[10] bifunctional amine-thioureas[11,12] or Cinchona alkaloids.[13] However, the chameleon-like properties of nitroalkenes can also be a possible explanation for their high tendency of polymerization[1,7] under basic conditions and for the formation of nitroalkene dimers as side products in the formation reaction of β-nitronitriles in presence of cyanide.[3] A further important structural motif are conjugated enynes, as they can be found in several natural products, ligands for transition metal complexes, antitumor drugs and also in synthons and intermediates of organic chemistry (e. g. metathesis reactions, Bergman cyclization or Paulson reactions).[14] Typically transition metal catalysis gain access to enynes, a very powerful method is for example the palladium-catalyzed Sonogashira coupling of alkenes and alkynes.[15] Until now, to the best of our knowledge, enyne formation by direct connection of two carbon atoms via a triple bond is not known and also an organocatalytic transformation is not yet reported. In the last years, catalysis with small organic molecules evolves as the third pillar in asymmetric synthesis, besides biocatalysis and metal catalysis.

Nitroalkenes are often used as substrates in organocatalytic reactions, because they can react both as α-nucleophile and as β-electrophile simultaneously. However, until now no detailed studies concerning the dimerization or oligomerization of nitroalkenes in presence of amines is observed, although the high tendency of nitroalkenes to build polymers is known.[1,7] Previous investigations in our working group showed that nitroalkenes react to enynes in presence of an amine catalyst.[16] Therefore here our ongoing results of this unexpected reaction are presented.

6.2   Results and Discussion

In previous investigations Markus Schmid found that the reaction of nitropentene **1** and propionaldehyde catalayzed by diphenylprolinol **C3** does not provide the expected Michael addition product, although **1** was consumed.[16] A test reaction of **1** with 100 mol% of the catalyst and reaction monitoring by ^{1}H NMR spectroscopy, as well as 2D NMR spectroscopic measurements indicating unexpectedly the 3-nonen-5-yne **10** as main product of the reaction. Apart from **10** also some intermediates were accessible by the use of L-proline **C5** as catalyst, due to slower reaction. Thereby a catalyst nitroalkene adduct and a nitroalkene dimer was obtained by 2D NMR spectroscopy.[16] In Scheme 6.1 the observed reaction of **1** to **10** and the used catalysts **C1**-**C5** are presented, thereby **C1** (equimolar mixture of diphenylprolinol **C2** and benzoic acid) provides the best results.[16]
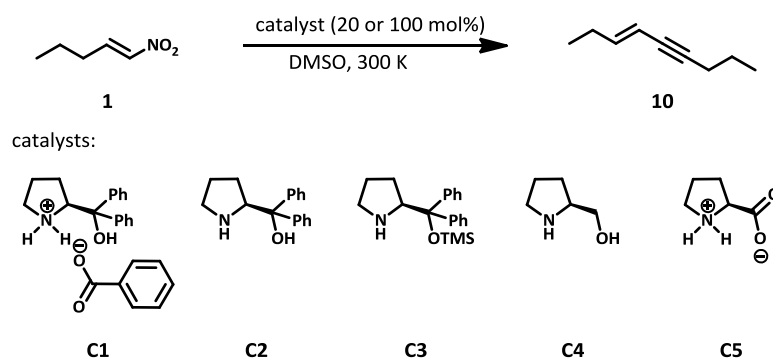
Scheme 6.1: Investigated reaction of nitropentene **1** to enyne **10** and catalysts **C1**-**C5** used, thereby **C1** provides the best results.

This reaction represents an unprecedented organocatalytic formation of enynes by dimerization of nitroalkenes. In order to determine if there exist a general applicability of this reaction or if it is an exceptional reaction of **1**, several methyl substituted nitroalkenes **2** and **3**, as well as some nitrostyrene derivatives **4** and **5** (see Scheme 6.2) have been synthesized according to literature known procedures[17–19] and investigated as possible substrates for this extraordinary reaction with catalyst **C1** (equimolar mixture of diphenylprolinol and benzoic acid), as this catalyst provides the best results in the reaction of **1**.
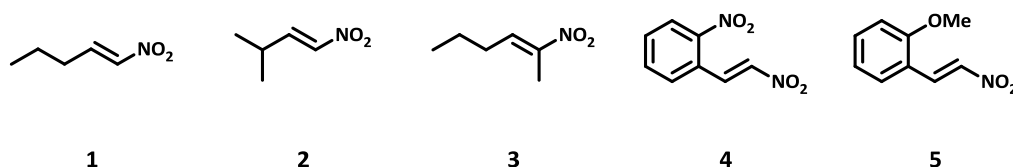
Scheme 6.2: Linear nitroalkenes **1**-**3** and aromatic nitroalkenes **4** and **5** were synthesized according to literature known procedures[17–19] for the investigation of the substrate scope.

Thereby **2**[17,20] was used, as the predicted enyne should possess improved stabilization, due to inductive effects of the methyl groups. Whereas **3**[18,21] can gain further insight into the involved structures in the mechanism, due to the different substitution pattern. With nitrostyrene derivatives **4**[17,23] and **5**[17] detailed information concerning the influence of the electronic properties on enyne formation can be obtained, due to the electron withdrawing and releasing substituents. Notwithstanding the literature known procedures, only nitroalkenes **2** and **4** were achieved in sufficient purity for kinetic investigations and are therefore discussed in the following as possible substrates for homo and hetero coupling reactions. The applicability and further purification of the other nitroalkenes is now ongoing work in our group as subject of a further PhD thesis.

6.2.1 Homo coupling

In order to increase the substrate scope of homo coupling of nitroalkenes to the corresponding enynes first **2** (100 mM) and **C1** (equimolar mixture of diphenylprolinol and benzoic acid, each 50 mM) were mixed at room temperature in DMSO-*d6* (see Figure 6.1). With **2** due to inductive effects of the branched methyl groups a stabilization of the enyne should be observed and therefore faster conversion of **2** to **11**. For monitoring of the reaction progress ^{1}H NMR spectra were recorded. Despite the assumed stabilization a similar reaction profile as for **1** was observed (compare the reaction profiles in Figure 6.1 b and c). Thereby first the catalyst nitroalkene adduct **Int3** was detected and afterwards the nitroalkene dimer **Int4** was formed. The amount of **Int3** is lower as with the non-branched substrate **1** but in turn the amount of **Int4** is higher. That implies, that the attack of the second nitroalkene molecule by **Int3** is accelerated due to substitution, as **Int3** is completely vanished after 1.5 hours (see Figure 6.1 b), in contrast with unsubstituted nitroalkene **1** the corresponding **Int1** vanishes after about 3 hours (see Figure 6.1 c[16]). However **Int4** is subsequently transformed into the enyne **11** with a slightly increased, but still comparable rate as for the conversion of **1**. Therefore this reaction step is not influenced by substitution. The successful formation of **11** and the similar reaction profile to **1** inducing that aliphatic α- and β-unbranched nitroalkenes are suitable substrates in this exceptional reaction of enyne formation.

Figure 6.1: a) Investigated reaction of nitro-isopentene **2** (100 mM) and catalyst **C1** (each 50 mM) in DMSO-*d6*. b) Reaction profile of a mixture of **2** (100 mM) and **C1** (each 50 mM) in DMSO-*d6*. c) Reaction profile of a mixture of **1** and **C1** in DMSO-*d6* (nitropentene **5** is omitted).[16] c) ^{1}H chemical shift assignment for the two intermediates **Int3** and **Int4** and the enyne product **11**.

In order to gain further insight in the involved structures nitro-β-nitrostyrene **4** was mixed with **C1** at room temperature in DMSO-*d6* (see Figure 6.2). Among the nitrostyrene derivatives **4** and **5**, **4** is the more electrophilic one. Moreover with these nitrostyrene derivatives a shift of the double bond from the α,β- to the β,γ-position is not feasible as it is observed typically in the nitro alkene dimer intermediates (see for example **Int4** in Figure 6.1 b), due to the aromatic ring. This means, that also the enyne structural characteristic is not possible to be formed, and therefore this substrates represent a dead end reaction on the level of the intermediates. The reaction progress was again controlled by ^{1}H NMR spectra. In combination with [1]H[1]H-COSY, [1]H[13]C-HSQC and [1]H[13]C-HMBC measurements **12** was proposed as a possibly formed product, representing a nitroalkene dimer with a non-shifted double bond and the typical formed connection between the C_α of one nitroalkene molecule to the C_β of the second nitroalkene molecule. Furthermore the nitro group of the second molecule appears as the aci-nitro tautomer. Apart from **12** a second not yet identified product was observed with a similar kinetic profile. Therefore further investigations of the aromatic nitroalkenes are necessary to elucidate the involved structures.
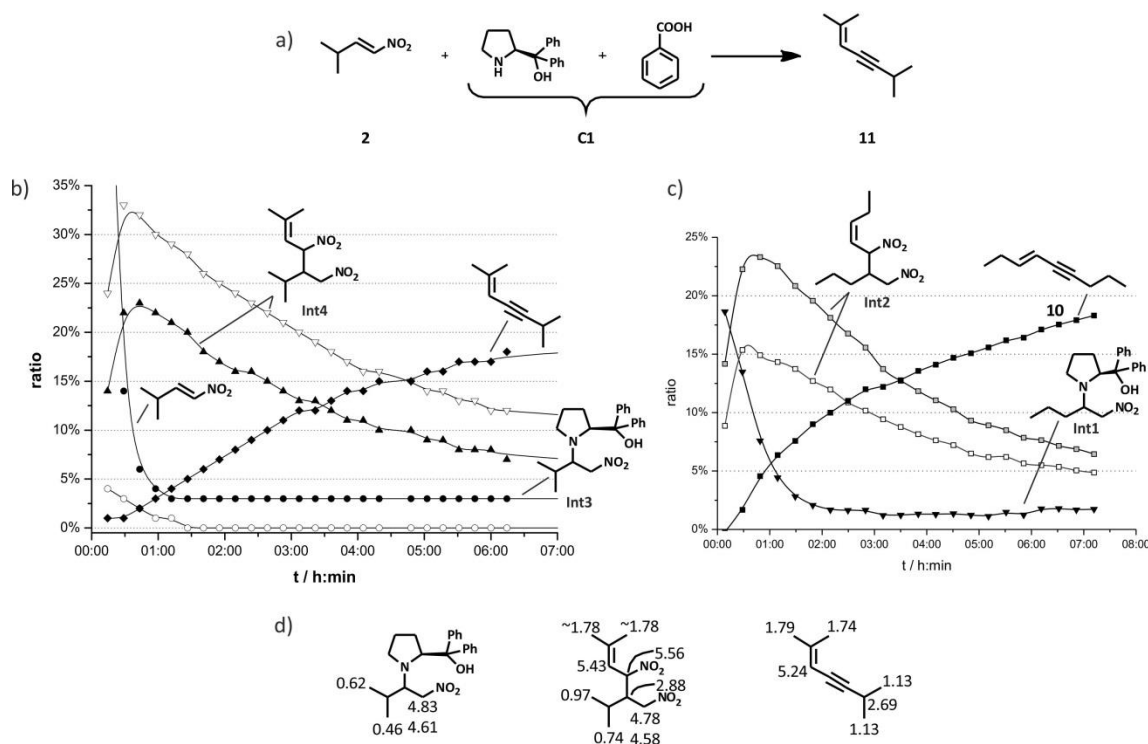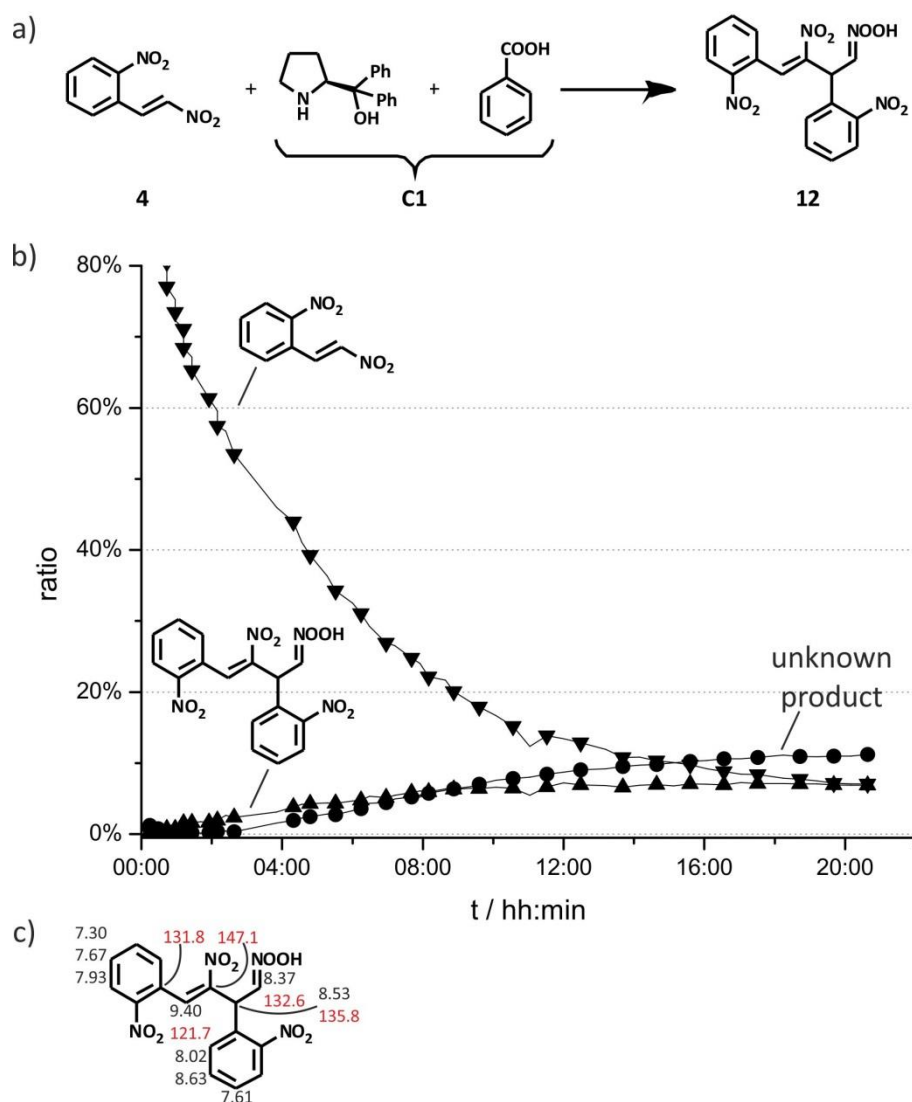
Figure 6.2: a) Investigated reaction of nitro-β-nitrostyrene **6** (100 mM) and catalyst **C1** (each 50 mM) in DMSO-*d6*. b) Reaction profile of a mixture of **6** and **C1** in DMSO-*d6* and c) ^{1}H and [13]C (red) chemical shift assignment for the proposed product **12**.

The substrate scope for homo coupling reactions of nitroalkenes to the corresponding enynes was extended to aliphatic α- and β-unbranched nitroalkenes. Whereas the use of aromatic nitroalkenes has to be investigated further.

6.2.2 Hetero coupling

Nevertheless, due to the promising results observed in organocatalytic homo coupling of nitroalkenes, producing enynes, we were also interested if this reaction also enables a hetero coupling of different nitroalkenes in order to obtain unsymmetrical substituted enynes.[16] Such a cross coupling should become possible, as one of the nitroalkenes reacts exclusively as the electrophilic and the other as the nucleophilic reaction partner (for mechanistic details see below). This is based on the fact, that the C-C double bond of the nucleophilic reaction partner is shifted from the α,β-position to the β,γ-position, and therefore nitroalkenes for which such a

shift is unfavoured react exclusively as the electrophilic reaction partner. Typical electrophilic nitroalkenes are the nitrostyrene derivatives **4** and **5**. In a first attempt nitro-β-nitrostyrene **4** (50 mM) was used, as it represents the most electrophilic one in the series, as potential reaction partner for **2** (50 mM) with catalyst **C1** (each 50 mM) at room temperature in DMSO-*d6* (see Figure 6.3). The progress of the reaction was again monitored by ^{1}H NMR spectroscopy. Indeed, the cross coupled enyne **13** is observed, but the conversion is significant slower as in the corresponding homo coupling reactions. In contrast the mixed nitroalkene dimer **Int5** is detected in similar amounts and with a comparable reaction profile as **Int4** (not detected here) of the homo coupling reaction of **2**. The catalyst nitroalkene adduct **Int3** is observed with almost doubled life time compared to homo coupling reaction of **2** (see Figure 6.1 b). A part of the used nitro-β-nitrostyrene **4** was transformed to **12**, the product of the homo coupling reaction of nitroalkene **4** and is therefore no longer applicable for the cross coupling reaction. This side reaction reached after 6 hours saturation, as the yield remains constant.
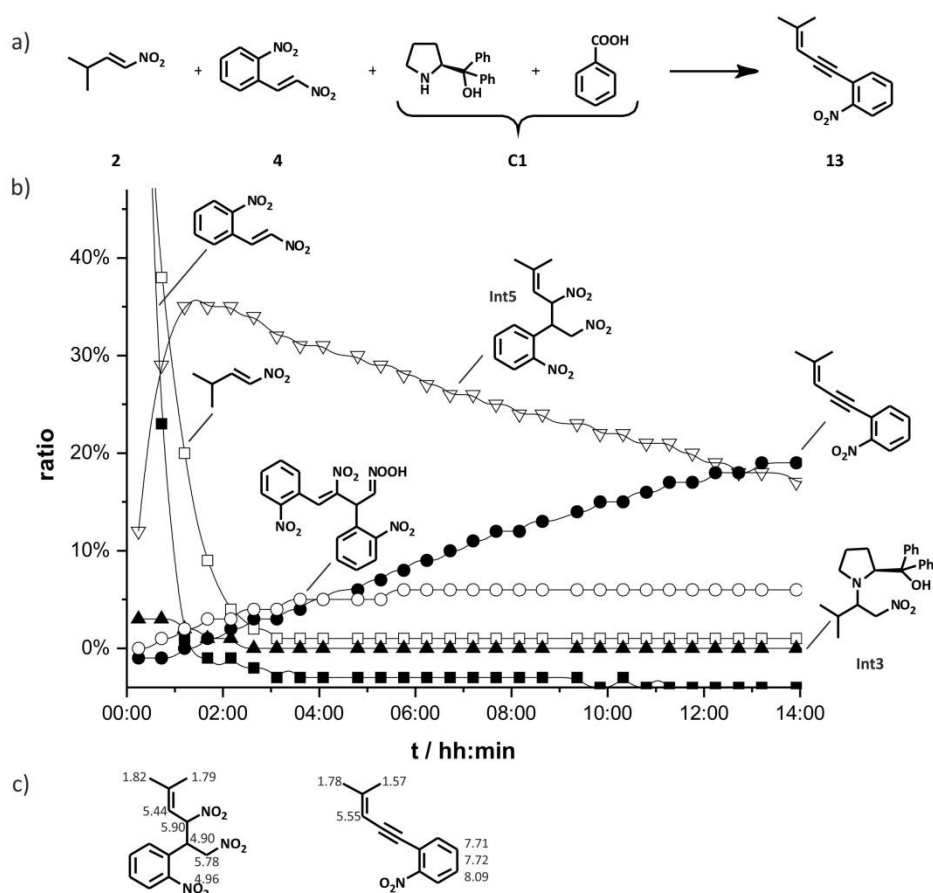
Figure 6.3: a) Investigated cross coupling reaction between nitroisopentene **2** (50 mM) and nitro-β-nitrostyrol **4** (50 mM) with catalyst **C1** (each 50 mM) in DMSO-*d6* and b) reaction profile of a mixture of **2**, **4** and **C1** in DMSO-*d6*. c) ^{1}H chemical shift assignment of **Int5** and the cross coupled enyne **13**.

The successful detection of the cross coupled enyne **13** extended this unprecedented organocatalytic transformation also to hetero coupling reactions of nitroalkenes. Nevertheless,

the first attempt of this reaction was performed without optimized conditions, which is certainly needed for further improvement, especially in order to eliminate contributions of the homo coupling reaction (e. g. side product **12**).

6.2.3 Mechanistic Proposal

The here obtained results of homo and hetero coupling reactions of nitroalkenes producing enynes, proof the previous assumed Baylis-Hillman-type nitroalkene dimerization as first steps in the mechanism of the organocatalytic enyne formation.[16] Scheme 6.3 represents the proposed mechanism. Thereby a nucleophilic attack of the secondary amine catalyst on the highly electrophilic β-carbon atom of the nitroalkene appears first, resulting in the formation of the catalyst nitroalkene adduct (**Int1** in Figure 6.1 c, and **Int3** in Figure 6.1 b and Figure 6.3 b). Next, deprotonating of the catalyst nitroalkene adduct in α-position to the nitro group, enables a further nucleophilic attack of the electrophilic β-carbon atom of a second nitroalkene molecule, forming a catalyst nitroalkene nitroalkene adduct. Subsequent catalyst elimination and rebuilding of the C-C double bond, shifted one position compared to the starting material, indicating the formation of the deconjugated β,γ-unsaturated nitroalkene dimer (see **Int2** in Figure 6.1 c, **Int4** in Figure 6.1 b and **Int5** in Figure 6.3 b). The preferred formation of deconjugated tautomers is known for nitroolefines and increased by alkyl substitution in α- or β-position.[24] Furthermore, identical regiochemical observations were described for DBU-induced Baylis-Hillman reactions using nitroalkenes (DBU: 1,8-diazabicylco[5.4.0]undec-7-ene),[25] for tetramethylguanidine-catalyzed Michael addition of α,β-unsaturated nitroalkenes to electron deficient olefins (e. g. α,β-unsaturated ketons, esters, nitriles and sulfones)[8] and for amine base-mediated addition reactions of α,β-unsaturated nitroalkenes to aldehydes.[8]
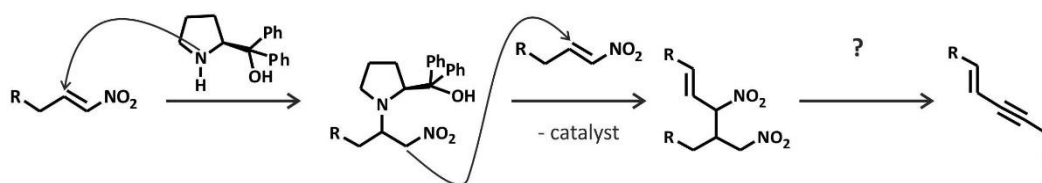
Scheme 6.3: Proposed mechanism for the proline-catalyzed enyne formation.

Nevertheless the transformation of the nitroalkene dimer to the corresponding enyne is still not yet clear and is addressed in a further PhD thesis in our working group. Until now we can exclude the previous assumed fragmentation along with the release of nitromethane and nitrous acid.[16] However detailed mechanistic investigations are ongoing.

6.3 Conclusion

In general we present here the first organocatalytic formation of enynes by homo and hetero dimerization of nitroalkenes. Additionally, this reaction presents the first metal free access to enynes known until today. Furthermore, to the best of our knowledge this is the first transformation reported, which connects two carbon atoms by direct formation of a triple bond. For this unprecedented organocatalytic reaction a mechanism was proposed partially. Thereby, we assume that a C-C bond is formed between the α-nucleophilic and the β-electrophilic positions of two nitroalkene molecules, induced by the amine base catalyst, providing a nitroalkene dimer. In the next step the nitroalkene dimer is transformed to the corresponding enyne, this step is not yet fully understood and addressed in a further PhD thesis in our working group. Nonetheless, this first promising results obtained in the NMR spectroscopic investigation of this unprecedented reaction should offer sufficient incentive to optimize the reaction conditions and to gain further insight into the involved mechanism. Moreover, this reaction indicates a new application of nitroalkenes and enables a completely new approach to enynes.

6.4   Experimental Part

6.4.1   General Considerations

All sample preparations were performed in DMSO-*d6* at room temperature. Therefore 100 mM of the nitroalkene (for cross coupling reactions for each substrate 50 mM were used) were mixed with 100 mM of the catalyst (an equimolar mixture of diphenylprolinol and benzoic acid, each 50 mM). The catalyst and benzoic acid were used as commercially available. The nitroalkenes were prepared according to literature known procedures (nitropentene **1**,[17] nitro-isopentene **2**,[17] nitrohexene **3**,[18] nitro-β-nitrostyrene **4**,[17] and methoxy-β-nitrostyrene **5**[19].

6.4.2   NMR Data Collecting and Processing

NMR spectra were recorded on a Bruker Avance DRX 600 (600.13 MHz) spectrometer equipped with a 5 mm broadband triple resonance z-gradient probe (maximum gradient strength 53.5 Gauss/cm). The temperature was controlled by a BVTE 3000 unit. The ^{1}H and ^{13}C chemical shifts were referenced to the residual solvent signal of DMSO-*d6*. NMR data were processed and evaluated with Bruker Topspin 3.1.

^{1}H: relaxation delay = 3 s, acquisition time = 2.1 s, SW = 12 ppm, TD = 32k, NS = 8; ^{1}H^{13}C-HMBC: relaxation delay = 2 s, mixing time = 0.7 s, TD = 4k F2 and 512 F1, DS = 16, NS = 16; HSQC = relaxation delay = 2 s, TD = 4k F2 and 256 F1, DS = 16, NS = 8; ^{1}H^{1}H-NOESY: relaxation delay = 3 s, mixing time = 0.7 s, acquisition time = 0.3 s F2 and 0.02 s F1, SW = 12 ppm, TD = 4k F2 and 256 F1, DS = 16, NS = 16; ^{1}H^{1}H-COSY: relaxation delay = 2 s, acquisition time = 0.3 s F2 and 0.04 s F1, SW = 12 ppm, TD = 4k F2 and 256 F1, NS = 4.

6.5 Literature

[1]   D. Seebach, A. K. Beck, D. M. Badine, M. Limbach, A. Eschenmoser, A. M. Treasurywala, R. Hobi, W. Prikoszovich, B. Linder, *Helvetica Chimica Acta* **2007**, *90*, 425–471.

[2]   G. Calderari, D. Seebach, *Helv. Chim. Acta.* **1995**, *68*, 1592–1604.

[3]   J. C. Anderson, A. J. Blake, M. Mills, P. D. Ratcliffe, *Organic Letters* **2008**, *10*, 4141–4143.

[4]   R. C. Larock, in *Comprehensive Organic Transforamtions* (Ed.: R.C. Larock), Wiley-VCH, New York, **2010**.

[5]   H. W. Pinnick, *Org. React.* **1990**, *38*, 655–792.

[6]   R. Tamura, A. Kamimura, N. Ono, *Synthesis* **1991**, 423.

[7]   R. Ballini, G. Bosica, D. Fiorini, A. Palmieri, M. Petrini, *Chemical Reviews* **2005**, *105*, 933–972.

[8]   N. Ono, I. Hamamoto, A. Kamimura, A. Kaji, R. Tamura, *Synthesis* **1987**, *1987*, 258–260.

[9]   M.-P. D. Alcántara, F. C. Escribano, A. Gómez-Sánchez, M. J. Diánez, M. D. Estrada, A. López-Castro, S. Pérez-Garrido, *Synthesis* **1996**, *1996*, 64–70.

[10]   T. Ooi, S. Takada, K. Doda, K. Maruoka, *Angewandte Chemie International Edition* **2006**, *45*, 7606–7608.

[11]   X.-Q. Dong, H.-L. Teng, C.-J. Wang, *Org. Lett.* **2009**, *11*, 1265–1268.

[12]   C. Rabalakos, W. D. Wulff, *J. Am. Chem. Soc.* **2008**, *130*, 13524–13525.

[13]   J. Wang, H. Li, L. Zu, W. Jiang, W. Wang, *Adv. Synth. Catal.* **2006**, *348*, 2047–2050.

[14]   G. Gervasio, P. J. King, D. Marbello, E. Sappa, *Inorg. Chim. Acta* **2003**, *350*, 215–244.

[15]   K. Sonogashira, Y. Tohda, N. Hagihara, *Tetrahedron Letters* **1975**, *16*, 4467–4470.

[16]   M. Schmid, PhD Thesis, NMR Spectroscopic Investigations on Aminocatalysis: Catalysts and Intermediates, Conformations and Mechanisms, University of Regensburg, **2011**.

[17]   B. M. Trost, C. Müller, *Journal of the American Chemical Society* **2008**, *130*, 2438–2439.

[18]   J. Hübner, J. Liebscher, M. Pätzel, *Tetrahedron* **2002**, *58*, 10485–10500.

[19]   S. Batra, Y. S. Sabnis, P. J. Rosenthal, M. A. Avery, *Bioorganic & Medicinal Chemistry* **2003**, *11*, 2293–2299.

[20]   G. Kumaran, G. H. Kulkarni, *Synthesis* **1995**, *1995*, 1545–1548.

[21]   P. Mikesell, M. Schwaebe, M. DiMare, R. D. Little, *Acta. Chem. Scand.* **1999**, *53*, 792–799.

[22]   P. J. Black, G. Cami-Kobeci, M. G. Edwards, P. A. Slatford, M. K. Whittlesey, J. M. J. Williams, *Org. Biomol. Chem.* **2006**, *4*, 116–125.

[23]   G. Kumaran, G. H. Kulkarni, *Tetrahedron Letters* **1994**, *35*, 9099–9100.

[24]   G. Hesse, R. Hatz, H. König, *Liebigs Ann. Chem.* **1967**, *709*, 79–84.

[25]   R. Ballini, L. Barboni, G. Bosica, D. Fiorini, E. Migini, A. Palmieri, *Tetrahedron* **2004**, *60*, 4995–4999.

7 SUMMARY

In recent years, there has been an increasing demand for enantiopure compounds, for example for chiral fine chemicals, pharmaceuticals, agrochemicals or in material science. Thereby the use of asymmetric catalysis and especially transition metal catalysis emerges as advantageous, due to cheap and prochiral starting materials. Thereby the enantioselective copper-catalyzed conjugate addition reaction evolves as one of the most powerful and widely used methods for the formation of carbon-carbon bonds resulting in high yields and enantioselectivities. In recent years impressive results were obtained in extending the copper catalytic system, by the development of new classes of ligands, copper sources and reaction parameters, but also the substrate scope and the spectrum of organometallic reagents was enlarged. Apart from that, in the past decade tremendous scientific progress was observed in the field of asymmetric organocatalysis. Independent of the kind of catalysis often a lack of knowledge of the involved mechanisms exists. Yet, a sophisticated understanding of these mechanisms is necessary to optimize the existing technologies and to enable the development of further catalytic systems adjusted to the required conditions.

This thesis has investigated mainly the mechanism of copper-catalyzed 1,4-addition reactions of organometallic reagents to α,β-unsaturated enones by NMR spectroscopic methods. Thereby particular attention was paid to the transmetalation of an alkyl group of the organometallic reagent to the copper catalyst, which is a well-accepted step in mechanistic presentations but an experimental prove was not accesssible so far. Structure elucidation of copper complexes in solution, especially with NMR spectroscopy is a very challenging research area, because their structural properties (e. g. high quadrupole moment of copper, tendency to form self-aggregates, existence of averaged sets of signals for complexed and free ligands, with small differences in the chemical shifts, due to intra- and interligand exchange processes, as well as a high sensitivity towards the synthetic conditions used) make it difficult to apply standard NMR approaches, which are generally used for small molecules. Therefore, the best investigated copper systems are organocuprates, but for copper complexes used in asymmetric catalysis nearly no information concerning the structures is accessible. For this reason we present here a model system for copper catalysis based on binuclear phosphoramidite copper complexes and a special NMR approach, so far only used for detection of H-bond networks, with which it was possible to detect transmetalation intermediates below the detection limit of one-dimensional ^{1}H and ^{31}P NMR spectra. For the first time a direct experimental proof of different monomeric

and dimeric transmetalation intermediates is observed for reactions of diethyl zinc and binuclear phosphoramidite copper complexes with a mixed trigonal/tetrahedral coordination of the copper atoms. The assignment to transmetalation intermediates is exclusively based on modified 1D ^{1}H^{31}P-HMBC spectra enabling the differentiation of magnetization transfers via chemical bonds (transmetalation) and through space (unspecific interaction), because no signals were observed in the 1D ^{1}H and ^{31}P NMR spectra and therefore standard NMR approach of proton-based 2D measurements is not accessible. Normally, a HMBC transfer in non-symmetrical copper complexes is not possible, due to the high quadrupole moment of copper. Furthermore a special approach of enantiopure and enantiomeric mixtures of the phos-phoramidite ligands has to be applied for structure identification, which causes different signal integrals for species with one, two or three ligands. The combination of these special approaches and experiments with CuCl, ZnI$_2$/ZnCl$_2$ and different amounts of ZnEt$_2$ revealed two main transmetalation intermediates, a monomeric one with one ligand and one ethyl group and for the first time a dimeric one with three ligands, an ethyl and an iodine bridge as well as retention of the mixed trigonal/tetrahedral coordination of the binuclear phosphoramidite copper complex. The coexistence of monomeric and dimeric transmetalation intermediates side by side deviates from previous investigations of Feringa and contradicts previous proposals of Woodward, which were both investigating a similar catalytic system. However, neither in this study nor previous results of Feringa reveals an evidence of a monomeric species with two ligands coordinated to the copper atom, although those structures are often proposed in mechanistic schemes. The results of this experimental study indicate in combination with the typically used 2:1 ligand to salt ratio and theoretical calculations (assuming possible reaction pathways solely for binuclear copper complexes) that in the reactive transmetalation intermediate retention of the coordination of the copper atoms of the precatalytic complex appears. This direct NMR spectroscopically detection of transmetalation intermediates enables an improved understanding of the mechanism and promote further synthetic development of this important kind of reaction. In addition, the special NMR approach used here for the detection and characterization of intermediates beyond the detection limit in 1D ^{1}H and ^{31}P NMR spectra can also be applied to other catalytic systems.

These current results of the transmetalation step of copper-catalyzed 1,4-addition reactions will serve as a base for future studies, addressing the next step in the proposed mechanism - the addition of the substrate (enones). Due to the fact, that the signals of transmetalation intermediates are close to the detection limit and all attempts to detect a phosphoramidite copper-π-complex failed until now, the only possibility to increase the probability of signal

detection for the next mechanistic step is to increase the interaction sites between substrate and copper complex with simultaneous reduction of the energy differences. Therefore a suitable model system of precatalytic complex and substrate with optimized interaction sites, should be found based on our experiences in the field of inter- and intraligand interactions in phosphoramidite palladium complexes and simplified DFT-calculations, which is subject of a further PhD thesis in the working group.

A further study was performed to determine the structure of the precatalytic copper complex in coordinating solvents, addressing the sensitivity of copper complexes to the conditions used. The application of coordinating solvents is especially important for investigations of the mechanism occurring with organoaluminum compounds as potential transmetalation reagents. Otherwise cleavage of the biphenol backbone of the phosphoramidite ligands is observed in non-coordinating solvents, due to the high oxophilicity of the aluminum atom. This study has found that generally in coordinating solvents the precatalytic complex tend to incorporate a higher number of CuX**L$_2$** fragments as in non-coordinating solvents. Typically in non-coordinating solvents a binuclear copper complex with a mixed trigonal/tetrahedral coordination of the copper atoms is observed, consisting of one CuX**L$_2$** fragment and one CuX**L** fragment. In contrast, in coordinating solvents a polynuclear copper complex with four CuX**L$_2$** fragments and one CuX**L** fragment is indicated. There the mixed coordination of the copper atoms is still present, indicating a high preference of those mixed coordinations. This unexpected, increased number of CuX**L$_2$** fragments in the precatalytic complex in coordinating solvents is corroborated by simulations of the low temperature ^{31}P NMR spectra and a detailed analysis of the temperature dependent ligand distribution in the different copper containing species. This project was also undertaken to evaluate the differences between normal and inverse addition order of trimethylaluminum reagents, visible in synthetic observations. However, until now product formation was observed, but the stabilization and detection of the involved intermediates was not possible.

Another part of the thesis dealt with preliminary NMR spectroscopic investigations of an unexpected but highly enantioselective rhodium-catalyzed 1,2-addition reaction of trimethyl-aluminum to cyclohexenone producing chiral allylic alcohols, which are a very important structural motif in organic chemistry. However, this study showed that rhodium complexes with Tol-BINAP ligands are better suited as unsubstituted BINAP ligands for NMR spectroscopic investigations because of the methyl group and a less crowded aromatic region. Nevertheless, some difficulties appear e. g. existence of different dimeric rhodium complexes and the spectra

show several impurities, based on the ligand or rhodium salt used. The variation of the ligand to salt ratio and application of several rhodium salts can possibly provide remedy and therefore further optimize the used model system.

Apart from transition metal-catalyzed asymmetric reactions mechanistic elucidations of the first organocatalytic formation of enynes by the dimerization of nitroalkenes in presence of an amine base catalyst were performed. Thereby the aim was to prove previous results in our working group and to extend the substrate scope. This unprecedented reaction reveals both homo coupled (symmetrically substituted) and hetero coupled (unsymmetrically substituted) enynes. This reaction delivers a new synthetic route to the important structural motif of enynes.

In conclusion this thesis predominantly deals with NMR spectroscopic investigations of the mechanism of transition metal-catalyzed conjugate addition reactions. In particular the direct experimental detection of transmetalation intermediates is anticipated to aid the mechanistic understanding and to support further synthetic developments in the field of copper-catalyzed ACA reactions. The structural insight into these transmetalation intermediates and to the precatalytic copper complex in coordinating solvents delivers explanations for the high sensitivity of this class of reaction to the parameters (e. g. solvent, temperature or copper salt) used. Furthermore, the complex structure of the precatalyst seems to be essential for the catalysis, as a dimeric transmetalation intermediates with remaining mixed trigonal/tetrahedral coordination of the copper atoms is observed. Thus, no exclusive monomerization of the transmetalation intermediates is observed as postulated by Feringa and theoretical calculations of Woodward. This results are a further example for the high sensitivity to the parameters and conditions used, indicating that it is not possible to determine one general structure for transmetalation intermediates, but different structures can appear depending on the ligand and transmetalation reagent used. Furthermore a new approach for structure elucidation in transitiom metal-catalyzed reactions was obtained, which can also be applied to further catalytic systems.

8 ZUSAMMENFASSUNG

In den letzten Jahren hat sich ein erhöhter Bedarf an enantiomerenreinen Verbindungen, die vor allem in der Synthese von Feinchemikalien für Arzneistoffe oder Agrochemikalien, aber auch in Materialwissenschaften verwendet werden herauskristallisiert. Durch die Verwendung von günstigen und prochiralen Edukten zeichneten sich die asymmetrische Katalyse und im Besonderen die Übergangsmetallkatalyse als ein hervorragendes Werkzeug für die Synthese dieser wichtigen Verbindungen aus. Dabei entwickelte sich, unter den unzähligen chemischen Reaktionen die enantioselektive kupferkatalysierte konjugierte Additionsreaktion zu einer der leistungsstärksten und einer der am häufigsten angewendeten Methoden bezüglich der Knüpfung hoch enantioselektiver Kohlenstoff-Kohlenstoffbindungen mit hohen Ausbeuten und Enantioselektivitäten. Zudem wurden in den letzten Jahren zahlreiche Bestrebungen unternommen das kupferkatalytische System zu erweitern, dies erfolgte unter anderem durch die Entwicklung neuer potentieller Ligandklassen, Kupferquellen und Reaktionsbedingungen, sowie der Erweiterung des Spektrums an Substraten und Organometallverbindungen. Zusätzlich wurde in dem letzten Jahrzehnt vermehrt Augenmerk auf Entwicklungen im Bereich der organokatalystischen asymmetrischen Katalyse gelegt. Das detaillierte Wissen über die Struktur der beteiligten Verbindungen ist unabhängig von der Art der Katalyse in vielen Fällen noch unvollständig. Dennoch ist die genaue Kenntnis der Strukturen unabdingbar, um weiter Fortschritte in der Weiterentwicklung von bestehenden Technologien und der Entwicklung neuer Katalysatorsysteme, abgestimmt auf die benötigten Bedingungen, erzielen zu können.

Diese Arbeit konzentriert sich überwiegend auf die Untersuchung des Mechanismus der kupferkatalysierten 1,4-Additionsreaktion von Organometallverbindungen an α,β-ungesättigte Enon-Verbindungen mittels NMR-Spektroskopie. Das Hauptaugenmerk lag dabei auf dem Transmetallierungsschritt, der die Übertragung des organischen Restes der Organometallverbindung auf den Kupferkomplex darstellt. Dieser Schritt ist in mechanistischen Darstellungen zwar allgemein akzeptiert, jedoch konnte bislang kein direkter experimenteller Beweis gefunden werden. Die Strukturaufklärung von Kupferkomplexen in Lösungen, gestaltet sich insbesondere mittels NMR-Spektroskopie schwierig, da die Sturktureigenschaften der Komplexe (u. a. hohes Quadrupolmoment von Kupfer, hohe Tendenz zur Bildung von Aggregaten, Überlagerung der Signale für freien und komplexierten Liganden, auf Grund von inter- und intramolekularen Ligandaustauschprozessen, aber auch hohe Sensitivität gegenüber den verwendeten Bedingungen) erschweren die Anwendbarkeit der typischen NMR-Methoden für kleine Moleküle.

Das am besten untersuchte System stellen dabei die Organocuprate dar, im Gegensatz ist nur sehr wenig Information zu den Strukturen der Kupferkatalysatoren in asymmetrischen Katalysen bekannt. Aus diesem Grund stellen wir hier ein Modellsystem, basierend auf Phosphoramidit-Kupferkomplexen, für kupferkatalytische Reaktionen und einen besonderen Ansatz zur Detektion von Intermediatsignalen unter dem Detektionslimit von 1D ^{1}H und ^{31}P Spektren vor, der bislang nur für die Detektion von H-Brücken-Netzwerken verwendet wurde. In dieser Arbeit konnte nun zum ersten Mal ein experimenteller Nachweis für monomere und dimere Transmetallierungsintermediate der Reaktion von Diethylzink mit einem binuklearen Phosphoramidit-Kupferkomplex, mit gemischter trigonaler/tetraedrischen Koordination der Kupferatome gefunden werden. Die Zuordnung der Transmetallierungsintermediate erfolgte dabei ausschließlich über die Messung modifizierter 1D ^{1}H^{31}P-HMBC Spektren, die eine Unterscheidung zwischen Magnetisierungstransfers über chemische Bindungen (Trans-metallierung) und über den Raum (unspezifische Wechselwirkungen) ermöglichen, da weder im ^{1}H noch im ^{31}P Spektrum Signale detektierbar waren und somit die üblichen ^{1}H basierten 2D Messungen für die Strukturafuklärung nicht anwendbar waren. In der Regel ist die Aufnahme und Detektion von HMBC Transferen in nicht symmetrischen Kupferkomplexen sehr schwierig auf Grund des hohen Quadrupolmoments von Kupfer. Der Strukturidentifizierung liegt ebenfalls eine ausgefallene Vorgehensweise zu Grunde, dabei wurden neben enantiomerenreinen Mischungen der Phosphoramidit-Liganden auch Mischungen der beiden Ligandenantiomeren für die Komplexbildung verwendet, dies ermöglicht eine Differenzierung von Verbindungen, die ein, zwei oder drei Liganden an das Kupferatom koordiniert haben anhand der Signalintensität und den damit einhergehenden Integralen. Die Kombination dieser besonderen Ansätze und weiterer Experimente mit CuCl, ZnI$_2$/ZnCl$_2$ und unterschiedlicher Mengen an Diethylzink ermöglichten die Identifizierung zweier Haupttransmetallierungsintermediate. Eines davon liegt mono-mer mit einer Ethylgruppe und einem Liganden vor, während das zweite Intermediat zum ersten Mal eine dimere Struktur mit drei Liganden, je einer Ethyl- und Iodid-Brücke, sowie der Retention der gemischten trigonalen/tetraedrischen Koordination der Kupferatome des binuk-learen Kupferkomplexes aufweist. Die gleichzeitige Existenz von monomeren und dimeren Transmetallierungsintermediaten widerspricht früheren Ergebnissen und Annahmen von *Feringa* und *Woodward*. In Einklang mit früheren Ergebnissen von *Feringa* ist jedoch, dass keine Transmetallierungsintermediate mit zwei Liganden detektiert werden konnten, obwohl diese häufig in Mechanismen postuliert werden. Die Ergebnisse dieser experimentellen Studie weisen darauf hin, dass in dem reaktiven Transmetallierungsintermediat eine Retention der Ko-ordination der Kupferatome des Präkatalysators vorliegt. Dies ist in Übereinstimmung mit dem

typischen 2:1 Ligand-zu-Salz-Verhältnis und theoretischen Rechnung, die einen energetisch möglichen Reaktionsweg nur für binukleare Komplexe annehmen. Die direkte NMR-spektroskopische Detektion von Transmetallierungsintermediaten ermöglicht ein verbessertes Verständnis des zugrunde liegenden Mechanismus und fördert weitere synthetische Entwicklungen. Zusätzlich kann dieser besondere NMR-Ansatz zur Detektion von Intermediat-signalen unter dem Detektionslimits der ^{1}H und ^{31}P NMR Spektren auch auf weitere katalytische Systeme angewendet werden.

Die derzeitigen Erkenntnisse bezüglich des Transmetallierungsschrittes in kupferkatalysierten 1,4-Additionsreaktionen dienen als Grundlage für weitere Studien, die den nächsten Schritt des postulierten Mechanismus – die Addition des Substrates (Enon) – adressieren. Da bereits die Signale der Transmetallierungsintermediate sehr nahe am Detektionslimit liegen und bis jetzt sämtliche Versuche der Detektion von Phosphoramidit-Kupfer-π-Komplexen fehlgeschlagen sind, ist die einzige Möglichkeit die Intermediate für die Detektion zu stabilisieren eine Optimierung der Wechselwirkungsflächen zwischen Substrat und Kupferkomplex, bei gleichzeitiger Reduktion der Energieunterschiede. Hierfür muss zunächst ein geeignetes Modellsystem aus Präkatalysator und Substrat mit optimierten Wechselwirkungsflächen gefunden werden. Um dies zu erreichen soll auf unsere Erfahrungen aus dem Bereich von Inter- und Intra-Ligand-Wechselwirkungen in Phosphoramidit-Palladium-Komplexen, sowie auf einfache DFT-Rechnungen zurückgegriffen werden, dies wird nun im Rahmen einer weiteren Doktorarbeit in dem Arbeitskreis fortgeführt.

In einer weiteren Studie wurde die Struktur des präkatalytischen Kupferkomplexes in koordinieren Lösungsmitteln untersucht, um einen näheren Einblick bezüglich der hohen Sensitivität gegenüber den verwendeten Bedingungen zu bekommen. Die Verwendung von koordinierenden Lösungsmitteln ist besonders dann unumgänglich, wenn Mechanismus Studien von Transmetallierungsreaktionen mit Organoaluminiumverbindungen durchgeführt werden sollen. Auf Grund der hohen Oxophilie von Aluminium kommt es in nicht koordinierenden Lösungsmitteln zu einer Abspaltung des Biphenolrückgrats der Phosphoramidit-Liganden. Die hier vorliegende Untersuchung hat gezeigt, dass der Präkatalysator in koordinierenden Lösungsmitteln eine höhere Affinität für den Einbau von CuX**L**$_2$ Einheiten zeigt, als in nicht koordinierenden Lösungsmitteln. In nicht koordinierenden Lösungsmitteln tritt ein binuklearer Präkatalysator-Komplex mit je einer CuX**L**$_2$ und CuX**L** Einheit auf. Dahingegen wird für koordinierende Lösungsmittel ein polynuklearer Komplex mit vier CuX**L**$_2$ und einer CuX**L** Einheit postuliert, interessanterweise bleibt dabei die gemischte trigonale/tetraedrische Koordination der Kupferatome erhalten, was auf eine bevorzugte Ausbildung gemischter Koordinationen

hindeutet. Diese unerwartet hohe Anzahl an CuX**L₂** Einheiten konnte durch Spektren Simulationen und einer detaillierten Analyse der Signalintegrale der unterschiedlichen Kupferenthaltenen Spezies bestätigt werden. Mit Hilfe dieses Projekts sollten zudem die unterschiedlichen Reaktionsverläufe der normalen und reversen Additionszugabe von Trimethylaluminium, wie sie bereits in synthetischen Anwendungen beobachtet wurden, erläutert werden. Bislang konnte in beiden Reaktionswegen Produktbildung detektiert werden, jedoch war eine Stabilisierung und Detektion der beteiligten Intermediate nicht möglich.

Ein weiteres Kapitel dieser Arbeit befasst sich mit vorbereitenden NMR-spektroskopischen Untersuchungen einer unerwarteten, aber hochenantioselektiven Rhodiumkatalysierten 1,2-Additionsreaktion von Trimethylaluminium an Cyclohexenon. Dabei entstehen chirale Allylalkohole, die ein wichtiges Strukturmotiv in der Organischen Chemie darstellen. Diese Studie zeigte, dass Toluol-substituierte BINAP-Liganden die bessere Wahl für NMR-spektroskopische Untersuchungen darstellen, auf Grund der Methylgruppe und dem nicht so stark überlagerten Aromaten Bereich. Jedoch traten einige Schwierigkeiten bezüglich der Reinheit der Edukte und eine Vielzahl an dimeren Rhodium Komplexen auf. Abhilfe kann dabei voraussichtlich durch die Variation von Ligand-zu-Salz-Verhältnissen und die Verwendung weiterer Rhodium Salze geschaffen werden und somit eine weitere Optimierung des Modelsystems erzielt werden.

Neben Übergangsmetallkatalysierten asymmetrischen Reaktionen wurden auch Mechanismus Studien der ersten organokatalytischen Bildung von Eninen durch Dimerisierung von Nitroalkenen in Gegenwart eines Aminbase-Katalysators durchgeführt. Ziel war es dabei frühere Ergebnisse unserer Arbeitsgruppe zu bestätigen und die Anwendung auf weitere Substrate auszuweiten. Diese ungewöhnliche Reaktion ermöglicht beides, sowohl die Synthese homo-gekoppelter (symmetrisch substituierte) als auch hetero-gekoppelter (unsymmetrisch substituierte) Enine. Somit konnte ein neuer Zugang zu dem wichtigen Strukturmotiv der Enine gefunden werden.

Zusammenfassend handelt diese Arbeit überwiegend von der NMR-spektroskopischen Untersuchung der Mechanismen in Übergangsmetallkatalysierten konjugierte Additions-reaktionen. Insbesondere kann durch die direkte experimentelle Detektion von Transmetallier-ungsintermediaten ein besseres Verständnis des Mechanismus geschaffen werden und somit die synthetische Entwicklung auf dem Gebiet der kupferkatalysierten asymmetrischen konjugierten Additionsreaktionen vorangetrieben werden. Die erzielten Einblicke in die Struktur der Transmetallierungsintermediate und des Präkatalysators in koordinierenden Lösungsmitteln können künftig eine mögliche Erklärung für die hohe Sensitivität dieser Reaktion gegenüber den

verwendeten Reaktionsbedingungen (z. B. Lösungsmittel, Temperatur oder Kupfersalz) liefern. Zudem scheint es, dass die komplexe Struktur des Präkatalysators essentiell für die Katalyse ist, da ein dimeres Transmetallierungsintermediat mit gleichbleibender gemischter trigonaler/tetraedrischer Koordination erhalten wird. Somit tritt in der hier gezeigten Studie keine exklusive Monomerisierung der Transmetallierungsintermediate auf, wie sie experimentell von Feringa und Woodwards theoretischen Rechnungen postuliert wurde. Diese Ergebnisse stellen ein weiteres Beispiel für die hohe Sensitivität gegenüber den Reaktionsbedingungen dar, dies deutet zudem darauf hin, dass es nicht möglich ist eine generelle Stuktur für Transmetallierungsintermediate zu bestimmen, sondern, dass unterschiedliche Strukturen auftreten, ahängig von verwendeten Ligand und Transmetallierungsreagenz. Basierend auf diesem neuen Ansatz zur Strukturuntersuchung von Übergangsmetallkatalysiertenreaktionen können nun auch weitere katalytische Systeme untersucht werden.

Ich erkläre hiermit, dass ich die vorliegende Arbeit ohne unzulässige Hilfe Dritter und ohne Benutzung anderer als der hier angegebenen Hilfsmittel angefertigt habe. Die aus anderen Quellen direkt oder indirekt übernommenen Daten und Konzepte sind unter Angabe des Literaturzitats gekennzeichnet.

Diese Arbeit wurde bisher weder im In- noch im Ausland in gleicher oder ähnlicher Form einer anderen Prüfungsbehörde vorgelegt.

Regensburg, den 15.05.2014